Rethinking the Light Water Reactor Fuel Cycle

by
Evgeni Shwageraus
B.Sc., Nuclear Engineering,
Ben Gurion University of the Negev, Israel (1997)
M.Sc., Nuclear Engineering,
Ben Gurion University of the Negev, Israel (2001)

Submitted to the Department of Nuclear Engineering
in partial fulfillment of the requirements for the degree of
DOCTOR OF PHILOSOPHY
at the
MASSACHUSETTS INSTITUTE OF TECHNOLOGY
September 2003

Signature of Author_____
Department of Nuclear Engineering
September 8, 2003

Certified by _____
Mujid S. Kazimi (thesis supervisor)
TEPCO Professor of Nuclear Engineering

_____
Dr. Pavel Hejzlar (thesis supervisor)
Principal Research Scientist

Accepted by _____
Jeffrey A. Coderre
Chairman, Department Committee on Graduate Students

Rethinking the Light Water Reactor Fuel Cycle

by
Evgeni Shwageraus

Submitted to the Department of Nuclear Engineering
on September 8, 2003, in partial fulfillment of
the requirements for the degree of
Doctor of Philosophy

ABSTRACT

The once through nuclear fuel cycle adopted by the majority of countries with operating commercial power reactors imposes a number of concerns. The radioactive waste created in the once through nuclear fuel cycle has to be isolated from the environment for thousands of years. In addition, plutonium and other actinides, after the decay of fission products, could become targets for weapon proliferators. Furthermore, only a small fraction of the energy potential in the fuel is being used. All these concerns can be addressed if a closed fuel cycle strategy is considered offering the possibility for partitioning and transmutation of long lived radioactive waste, enhanced proliferation resistance, and improved utilization of natural resources. It is generally believed that dedicated advanced reactor systems have to be designed in order to perform the task of nuclear waste transmutation effectively. The development and deployment of such innovative systems is technically and economically challenging. In this thesis, a possibility of constraining the generation of long lived radioactive waste through multi-recycling of Trans-uranic actinides (TRU) in existing Light Water Reactors (LWR has been studied.

Thorium based and fertile free fuels (FFF) were analyzed as the most attractive candidates for TRU burning in LWRs. Although both fuel types can destroy TRU at comparable rates (about 1150 kg/GWe-Year in FFF and up to 900 kg/GWe-Year in Th) and achieve comparable fractional TRU burnup (close to 50a/o), the Th fuel requires significantly higher neutron moderation than practically feasible in a typical LWR lattice to achieve such performance. On the other hand, the FFF exhibits nearly optimal TRU destruction performance in a typical LWR fuel lattice geometry. Increased TRU presence in LWR core leads to neutron spectrum hardening, which results in reduced control materials reactivity worth. The magnitude of this reduction is directly related to the amount of TRU in the core. A potential for positive void reactivity feedback limits the maximum TRU loading. Th and conventional mixed oxide (MOX) fuels require higher than FFF TRU loading to sustain a standard 18 fuel cycle length due to neutron captures in Th232 and U238 respectively. Therefore, TRU containing Th and U cores have lower control materials worth and greater potential for a positive void coefficient than FFF core. However, the significantly reduced fuel Doppler coefficient of the fully FFF loaded core and the lower delayed neutron fraction lead to questions about the FFF performance in reactivity initiated accidents.

The Combined Non-Fertile and UO_2 (CONFU) assembly concept is proposed for multi-recycling of TRU in existing PWRs. The assembly assumes a heterogeneous structure where about 20% of the UO_2 fuel pins on the assembly periphery are replaced with FFF pins hosting TRU generated in the previous cycle. The possibility of achieving zero TRU net is demonstrated. The concept takes advantage of superior TRU destruction performance in FFF allowing minimization of TRU inventory. At the same time, the core physics is still dominated by UO_2 fuel allowing maintenance of core safety and control characteristics comparable to all-UO_2. A comprehensive neutronic and thermal hydraulic analysis as well as numerical simulation of reactivity initiated accidents demonstrated the feasibility of TRU containing LWR core designs of various heterogeneous geometries. The power peaking and reactivity coefficients for the TRU

containing heterogeneous cores are comparable to those of conventional UO_2 cores. Three to five TRU recycles are required to achieve an equilibrium fuel cycle length and TRU generation and destruction balance. A majority of TRU nuclides reach their equilibrium concentration levels in less than 20 recycles. The exceptions are Cm246, Cm248, and Cf252. Accumulation of these isotopes is highly undesirable with regards to TRU fuel fabrication and handling because they are very strong sources of spontaneous fission (SF) neutrons. Allowing longer cooling times of the spent fuel before reprocessing can drastically reduce the SF neutron radiation problem due to decay of Cm244 and Cf252 isotopes with particularly high SF source. Up to 10 TRU recycles are likely to be feasible if 20 years cooling time between recycles is adopted. Multi-recycling of TRU in the CONFU assembly reduces the relative fraction of fissile isotopes in the TRU vector from about 60% in the initial spent UO_2 to about 25% at equilibrium. As a result, the fuel cycle length is reduced by about 30%. An increase in the enrichment of UO_2 pins from 4.2 to at least 5% is required to compensate for the TRU isotopics degradation.

The environmental impact of the sustainable CONFU assembly based fuel cycle is limited by the efficiency of TRU recovery in spent fuel reprocessing. TRU losses of 0.1% from the CONFU fuel reprocessing ensure the CONFU fuel cycle radiotoxicity reduction to the level of corresponding amount of original natural uranium ore within 1000 years.

The cost of the sustainable CONFU based fuel cycle is about 60% higher than that of the once through UO_2 fuel cycle, whereas the difference in total cost of electricity between the two cycles is only 8%. The higher fuel cycle cost is a result of higher uranium enrichment in a CONFU assembly required to compensate for the degradation of TRU isotopics and cost of reprocessing. The major expense in the sustainable CONFU fuel cycle is associated with the reprocessing of UO_2 fuel. Although reprocessing and fabrication of FFF pins have relatively high unit costs, their contribution to the fuel cycle cost is marginal as a result of the small TRU throughput. Reductions in the unit costs of UO_2 reprocessing and FFF fabrication by a factor of two would result in comparable fuel cycle costs for the CONFU and conventional once through cycle. An increase in natural uranium prices and waste disposal fees will also make the closed fuel cycle more economically attractive. Although, the cost of the CONFU sustainable fuel cycle is comparable to that of a closed cycle using a critical fast actinide burning reactor (ABR), the main advantage of the CONFU is the possibility of fast deployment, since it does not require as extensive development and demonstration as needed for fast reactors. The cost of the CONFU fuel cycle is projected to be considerably lower than that of a cycle with an accelerator driven fast burner system.

Thesis Supervisor:	Mujid S. Kazimi
Title:	TEPCO Professor of Nuclear Engineering Director, Center for Advanced Nuclear Energy Systems (CANES)
Thesis Supervisor:	Pavel Hejzlar, ScD
Title:	Principal Research Scientist; Program Director, Advanced Reactor Technology Program, Center for Advanced Nuclear Energy Systems (CANES)

Acknowledgments

I would like to express my sincere gratitude to my thesis supervisors, Professor Mujid S. Kazimi and Dr. Pavel Hejzlar for their guidance, help, and support throughout my stay at MIT.

The help of Professor Michael J. Driscoll and Dr. Edward E. Pilat on various subjects covered in this thesis was invaluable and greatly appreciated.

Special thanks to Professor Kenneth Czerwinski and Dr. Pradip Saha for their advice and insightful comments.

I gratefully acknowledge the help of Mr. Dandong Feng in performing thermal hydraulic calculations with VIPRE computer code and the help of Dr. Zhiwen Xu and Dr. Yun Long on a variety of technical issues.

Numerous discussions with my friends and colleagues Vaclav Dostal, Dr. Jacoppo Saccheri, Dr. Antonino Romano, and Pete Yarski, although not necessarily related to this thesis, comprised an essential part of its evolution.

My studies at MIT would be impossible without countenance and encouragement of my former Professor Alex Galperin at Ben-Gurion University of the Negev, Israel and Dr. Michael Todosow at Brookhaven National Laboratory who believed that I could make it from the very beginning.

I dedicate this thesis to my wife Noga, and my children Netta and Yoav. I thank them all for their boundless love, support, and sacrifices that they made in all these years. I thank all my relatives and friends for their help and just for being there when I and my family needed them.

This work was partially supported by the Idaho National Engineering and Environmental Laboratory through the NERI and LDRD projects and by the Argonne National Laboratory through the Advanced Fuel Cycle Initiative project of the US DOE.

Table of Contents

List of Figures

List of Tables

Abbreviations for Organizations

AECL	Atomic Energy of Canada Limited (Canada)
ANL	Argonne National Laboratory (US)
BNFL	British Nuclear Fuels, Ltd. (UK)
BNL	Brookhaven National Laboratory (US)
CANES	Center for Advanced Nuclear Energy Systems (MIT)
DOE	Department of Energy (US)
EPRI	Electric Power Research Institute (US)
ERDA	Energy Research and Development Administration (US)
GA	General Atomics (US)
GE	General Electric (US)
IAEA	International Atomic Energy Agency
INEEL	Idaho National Engineering & Environmental Laboratory (US)
JAERI	Japan Atomic Energy Research Institute (Japan)
KAERI	Korea Atomic Energy Research Institute (Republic of Korea)
LANL	Los Alamos National Laboratory (US)
NEA	Nuclear Energy Agency (OECD)
NRC	Nuclear Regulatory Commission (US)
OECD	Organization for Economic Co-operation and Development
ORNL	Oak Ridge National Laboratory (US)
TEPCO	Tokyo Electric Power Co., Inc. (Japan)

Nomenclature

a/o	atom percent
ABR	Actinide Burner Reactor
ADS	Accelerator Driven System
AFCI	Advanced Fuel Cycle Initiative
ALMR	Advanced Liquid Metal-cooled Reactor
ALWR	Advanced Light Water Reactor
An	actinides
APA	Advanced Plutonium Assembly
ATW	Accelerator Transmutation of Waste
BOC	Beginning of Cycle
BOL	Beginning of Life
BOP	Balance of Plant
BP	Burnable Poison
BW	boron reactivity worth
BWR	Boiling Water Reactor
CANDU	Canada Deutrium Uranium reactor
CERCER	ceramic fuel particle dispersed in a ceramic matrix
CERMET	ceramic fuel particle dispersed in a metallic matrix
CF	Capacity Factor
CHF	Critical Heat Flux
CMS	Core Management System
COE	Cost of Electricity
CONFU	Combined Non-Fertile and UO_2 assembly
CR	Conversion Ratio
CZP	Cold Zero Power
D&D	Decommissioning and Decontamination
DDC	Distributed Doppler Coefficient
DNBR	Departure from Nucleate Boiling Ratio
EFPD	Effective Full Power Day
EFPY	Effective Full Power Year
EOC	End of Cycle
EOL	End of Life

FBR	Fast Breeder Reactor
FCC	Fuel Cycle Cost
FFF	Fertile free fuel
FP	fission product
FTC	Fuel Temperature Coefficient
GT-MHR	Gas Turbine-Modular Helium Reactor
H/HM	Hydrogen to Heavy Metal Atom Ratio
HFP	Hot Full Power
HLW	High-Level Waste
HM	Heavy Metal
HTGR	High Temperature Gas-cooled Reactor
HZP	Hot Zero Power
IFBA	Integrated Fuel Burnable Absorber
IFR	Integral Fast Reactor
IHM	Initial Heavy Metal
LLFP	Long lived fission products
LMFBR	Liquid Metal Fast Breeder Reactor
Ln	Lanthanides
LOCA	Loss of Coolant Accident
LOFA	Loss of Flow Accident
LRM	Linear Reactivity Model
LWR	Light Water Reactor
MA	Minor actinides
MCNP	Monte Carlo N-Particle Transport Code
MCODE	MCNP-ORIGEN DEpletion Program
MDNBR	Minimum Departure from Nucleate Boiling Ratio
METMET	Metallic fuel in metallic matrix
MOX	Mixed Oxide (UO_2 and PuO_2) fuel
MTC	Moderator Temperature Coefficient
MTIHM	Metric Ton Initial Heavy Metal
MWd/kgIHM	MWd per kg IHM, equivalent to GWD per MTIHM
NFC	Nuclear Fuel Cycle
NU	Natural Uranium
O&M	Operation and Maintenance

ORIGEN	Oak Ridge Isotope GENeration and Depletion Code
PCI	Pellet-Cladding Interaction
pcm	percent milli ρ, (10^{-5} Δk/k)
ppm	part per million
PUREX	Pu-U recovery by extraction process
PWR	Pressurized Water Reactor
R&D	Research and Development
RCCA	Rod Cluster Control Assembly
REA	Rod Ejection Accident
RG Pu	Reactor Grade Plutonium
RIA	Reactivity initiated accident
SF	Spontaneous Fission
SLFP	Short lived fission products
SSP	Solid solution pellet (homogeneous)
SWU	Separative Work Unit
TBP	Tri-butyl phosphate
TRU	Trans-uranic elements
TRUEX	Trans-uranic elements recovery by extraction process
UREX	Uranium recovery by extraction process
v/o	volume percent
VIPRE	Versatile Internals and Component Program for Reactors; EPRI
Vm/Vf	Moderator to Fuel volume ratio
w/o	weight percent
WG Pu	Weapon Grade Plutonium

Chapter 1. Introduction

1.1. Background

Nuclear energy is an integral part of the global energy market. Today, it is the largest non-polluting energy source. Almost 17% of the world's electricity is generated from 444 nuclear reactors as of December 31 2002 [Nuclear News, 2003]. Six different reactor types are currently in service, but only two contribute to power generation considerably (Figure 1.1.1). These are the Pressurized Water Reactors (PWR) and the Boiling Water Reactors (BWR) together referred to as Light Water Reactors (LWR). Presently, 262 PWRs supply 236,236 MWe, while 93 BWRs contribute 81,071 MWe. Most of the reactor units under construction are also of LWR-type. The LWRs dominate the current nuclear electricity market with total power share of almost 90% due to their well developed technology and the extensive experience accumulated over many years of safe and reliable operation.

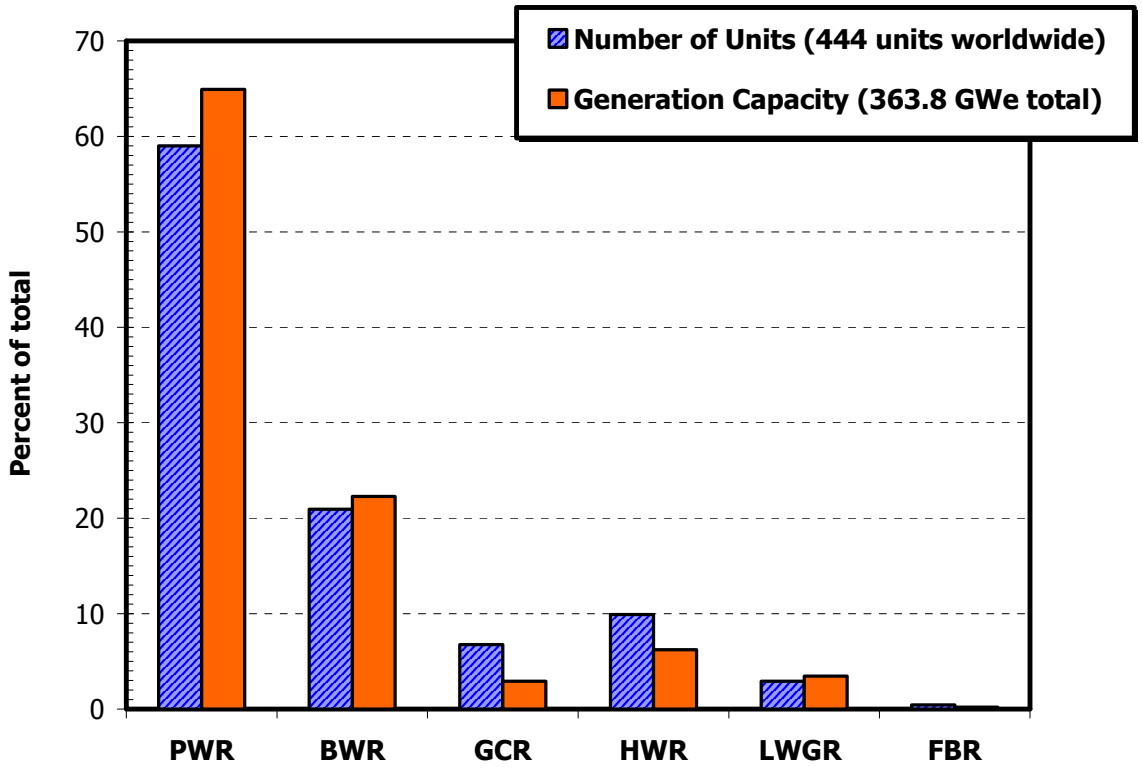

Figure 1.1.1. Reactors in operation by type and their generation capacity in 2002.

The majority of existing commercial power reactors operate in a once-through fuel cycle in which the nuclear fuel, after its discharge from the core, is destined for long-term geological storage.

Such a strategy raises a number of potential concerns. Radioactive isotopes in the spent nuclear fuel (SNF) have to be isolated from the environment for hundreds of thousands of years before their activity decays below the level of the natural uranium ore that was originally used for manufacturing of the fuel. As a result, sophisticated engineering barriers must be designed in order to prevent the release of long lived radioactive isotopes in the spent fuel from leaking into the environment. The design of such barriers is both scientifically and economically challenging. The main design challenge is associated with uncertainties that are large in numbers and in their magnitude relative to the long term behavior of the materials comprising the engineering barrier and to the variation in local environmental conditions (such as climate, geology, hydrology etc.) over periods of time well beyond the range of certainty of prediction of any existing scientific model. Moreover, the models that attempt to predict the evolution of the nuclear waste package and its content with time are difficult to assess and verify because of extremely long time periods involved. These uncertainties make the regulatory and legislative processes related to repository design and construction particularly challenging.

Proliferation resistance of the spent nuclear fuel is an additional concern. The Pu in the SNF shortly after its discharge from the reactor is largely protected by the high levels of radiation originating from the decay of fission products (FP). In geologic storage of the SNF, the FP will decay in a few hundreds of years to the levels at which the Pu becomes accessible more easily. Therefore, the repository might become an attractive target for nuclear proliferators within a few hundreds of years after its closure. Although sufficient barriers against potential Pu diversion will still exist even after FP decay, the general public concern over nuclear proliferation issues may trigger a decision to explore alternative fuel cycles that would avoid long term storage of weapons usable materials.

Similar to fossil fuels such as natural gas, coal, and oil, uranium is not an inexhaustible resource. In the once through fuel cycle, only about 0.5% of the potential energy content of the original uranium ore (or about 5% of the enriched uranium energy content) is recovered. If the SNF from the once through fuel cycle is stored in an irretrievable geological repository, this energy potential cannot be reclaimed. Currently however, the relative costs of natural uranium

and SNF reprocessing do not favor Pu recovery and use as a fuel to enhance the utilization of natural resources.

At the same time, sustainable development is a major goal of modern society. The recently issued roadmap for Generation IV nuclear energy systems [DOE/Generation IV International Forum, 2002] clearly recognizes this fact. According to the Gen IV roadmap, sustainable development implies improved utilization of natural resources extending their availability to future generations. The advantage of nuclear power for the global environment as a non-polluting energy source is particularly emphasized. Moreover, in a sustainable economy, the environmental impact of the future nuclear energy system fuel cycles must be minimized both in the long and in the short terms. Therefore, allowing accumulation of long lived radioactive materials in the environment and wasteful management of natural resources is irresponsible towards future generations and contradicts the principles of sustainable development.

Finally, the planning, construction, and approval of the long term geological repository, as proved to be in the case of the United States, is a rather costly and time consuming process. In addition, any repository has a limited storage capacity. In the US, for example, the existing 44,000 metric tons of SNF are increasing at a rate of about 2,000 MT/year which would fill up the statutory capacity of the planned geological repository at Yucca Mountain site by the year 2015. Re-licensing of the repository for increased capacity or construction of a second one will be required thereafter even if no new nuclear plants are built in that period. In the likely scenario of expanding global nuclear power generation in the next few decades, the availability and construction costs of SNF geological repositories may become a major issue facing a large public opposition.

In summary, the currently employed once through fuel cycle strategy leads to

- accumulation of nuclear material in the environment that represents a long term radiological threat
- proliferation concerns due to growing stockpile of Pu which would be potentially accessible after the decay of fission products
- regulatory and safety uncertainty due to scientific and engineering challenges in modeling of the long term waste package behavior in the repository
- poor utilization of natural resource which is inconsistent with sustainable economic development goals

- additional costs associated with limited geological storage capacity in the case of an expanding nuclear power economy.

1.2. Transmutation Strategies Review

Once through fuel cycle options

Some of the issues listed above can be partially addressed within the constraints of the once trough fuel cycles through a number of potential strategies. The most straight forward approach is to increase fuel burnup. A recent analysis of the high burnup fuel strategies [Xu Z., 2003] revealed notable positive impact of the high burnup on the spent fuel characteristics e.g. SNF volume and decay heat per unit energy produced. High burnup however does not improve the natural uranium utilization if higher enrichment is required to achieve it.

Introduction of thorium into the once through LWR fuel cycle through heterogeneous seed-blanket core arrangements [Wang D., 2003], [Todosow M., et al., 2002] can also reduce short term decay heat generation and spent fuel mass and volume by up to 50% in comparison with conventional UO2 once through fuel cycle.

High burnup also enhances proliferation resistance of the fuel cycle. Increasing the burnup of conventional UO_2 fuel from currently common 50 MWd/kg to 100 MWd/kg may reduce the Pu production rate by about 35% [Xu Z., 2003]. Also, higher fractions of even Pu isotopes (Pu238, 240, 242) in the discharged fuel lead to increased spontaneous fission neutrons background which prevents manufacturing of a reliable nuclear weapon. In addition, elevated heat generation due to high concentration of Pu238 would cause degradation of conventional high explosives required to trigger the Pu based nuclear explosive device. Utilization of thorium in the seed-blanket once through fuel cycle reduces Pu generation rate by a factor of 2 to 3 in comparison with conventional UO_2 fuel cycle [Wang D., 2003], [Todosow M., et al., 2002].

Reactor systems based on the “Breed and Burn” (B&B) concept [Feinberg S.M. et al., 1958], [Yu K. et al., 2002] have particularly high uranium utilization potential. In the Breed and Burn

reactor, the uranium in the fresh fuel feed does not require any enrichment. At the same time, very high burnup levels can be achieved through the core arrangements with dedicated regions where Pu can be effectively bred and the regions where Pu generated in former region can be effectively fissioned [Ficher G.J. et al., 1979]. However, B&B concept employs fast spectrum to provide effective breeding of Pu. As a result, Pu in the spent fuel is rich in Pu239 isotope (over 80% of total Pu [Yarsky P., 2003]) which raises significant proliferation concerns.

As discussed above, selected issues of the once through fuel cycle can be addressed via extended fuel burnup. However, the extent of these benefits is limited by the fuel performance with respect to its ability to withstand radiation damage and exposure to severe reactor operating conditions for long periods of time. Alternative fuel designs such as coated TRISO particles suggested for use in advanced gas cooled reactors (Pebble Bed Modular Reactor – PBMR [Koster A. et al., 2003] and Gas Turbine-Modular Helium Reactor - GT-MHR [LaBar M. P., 2002]) can maximize the benefits of the high burnup in the once through fuel cycle.

Partitioning of the spent nuclear fuel

Recycling of the SNF is the ultimate approach to diminishing the concerns over the nuclear waste in the once through fuel cycle to a considerable extent. Even after irradiation, the major part of the fuel is uranium (Figure 1.2.1). Uranium is practically non radioactive and if separated from the rest of the irradiated fuel constituents with adequate efficiency can be stored as a low level waste (LLW) or reintroduced into the fuel cycle. This would allow a major reduction in volume of the SNF and enhance the effective storage capacity of geological repository.

Pu constitutes about 1% of the SNF. It can be used as fuel virtually in any type of reactor. Recycling plutonium in LWRs is a common practice in Europe, Russia, and Japan. Other countries also consider Pu recovery and develop SNF reprocessing technologies and infrastructure for that purpose. Typically, recovered Pu is mixed with depleted or natural uranium in UO2-PuO2 mixed oxide (MOX) form. Currently, the spent MOX fuel assemblies are not reprocessed. Nevertheless, even single path Pu recycling results in significant improvement in natural uranium utilization and proliferation resistance characteristics [Pellaud B., 2002].

Fission products typically amount to less than 4% of the spent fuel but most of them are stable or very short lived. Only about 0.4% of the fission products are of a significant importance (Figure 1.2.1). Relatively short lived Cs137 and Sr90 are responsible for most of the decay heat production in the first few decades after fuel discharge from the reactor. Separation of Cs and Sr from the spent fuel constituents for dedicated storage would practically eliminate the heat load management issue in the repository design. The activity of all fission products collectively decreases below the level of natural uranium ore required to manufacture the initial fuel in a few hundreds of years (Figure 1.2.2).

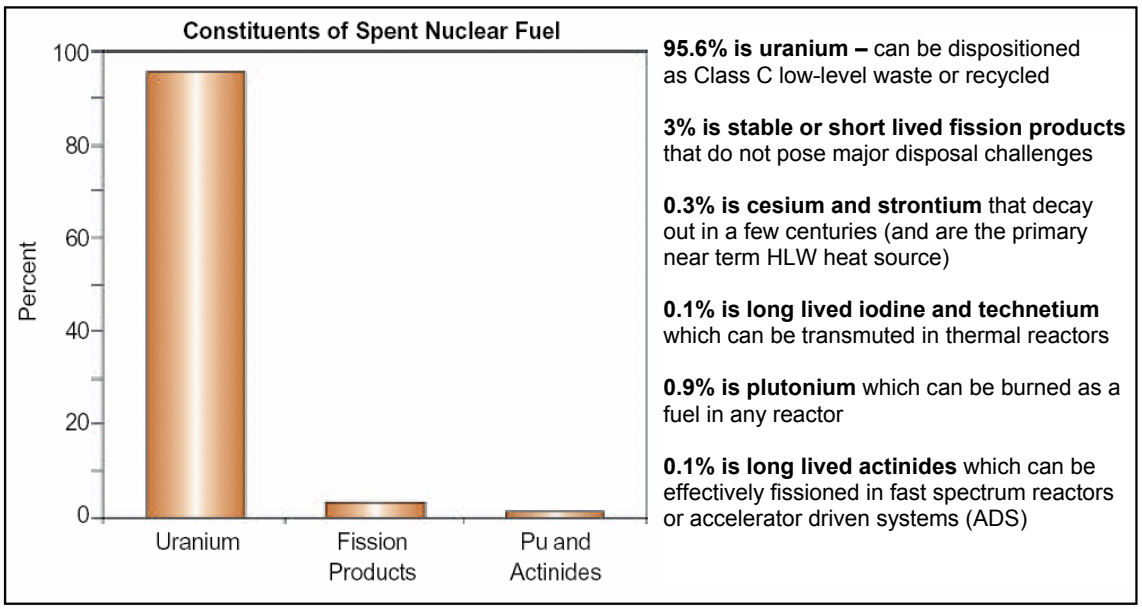

Figure 1.2.1. Typical composition of the spent nuclear fuel [DOE/NE, 2003].

Long lived fission products (LLFP) I129 and Tc99 represent a small fraction of the SNF (about 0.1%). These isotopes were identified as significant contributors to the long term radiation dose from the repository due to their high solubility in water [Van Tuyle G.J., 2001]. However, Tc99 and I129 can be transmuted to short lived isotopes if subjected to epithermal neutron flux. A number of studies showed the possibility of Tc99 and I129 transmutation in both thermal and fast spectrum reactors [Brusselaers P. et al., 1996], [Krivitsky I. and Kochetkov A. L., 2000], [Hejzlar P. et al., 2001]. The consensus on whether fast or thermal spectrum systems are more efficient with regards to LLFP transmutation has not yet been reached and different LLFP transmutation concepts are still under investigation. The factors affecting the best concept choice are: transmutation rates, achievable burnup fractions, available technologies, and the effects of LLFP

transmutation targets on other performance characteristics of transmutation system. A transmutation system of any type will require increased fissile inventory or external neutron source to compensate for the parasitic neutron absorption in the targets containing LLFP.

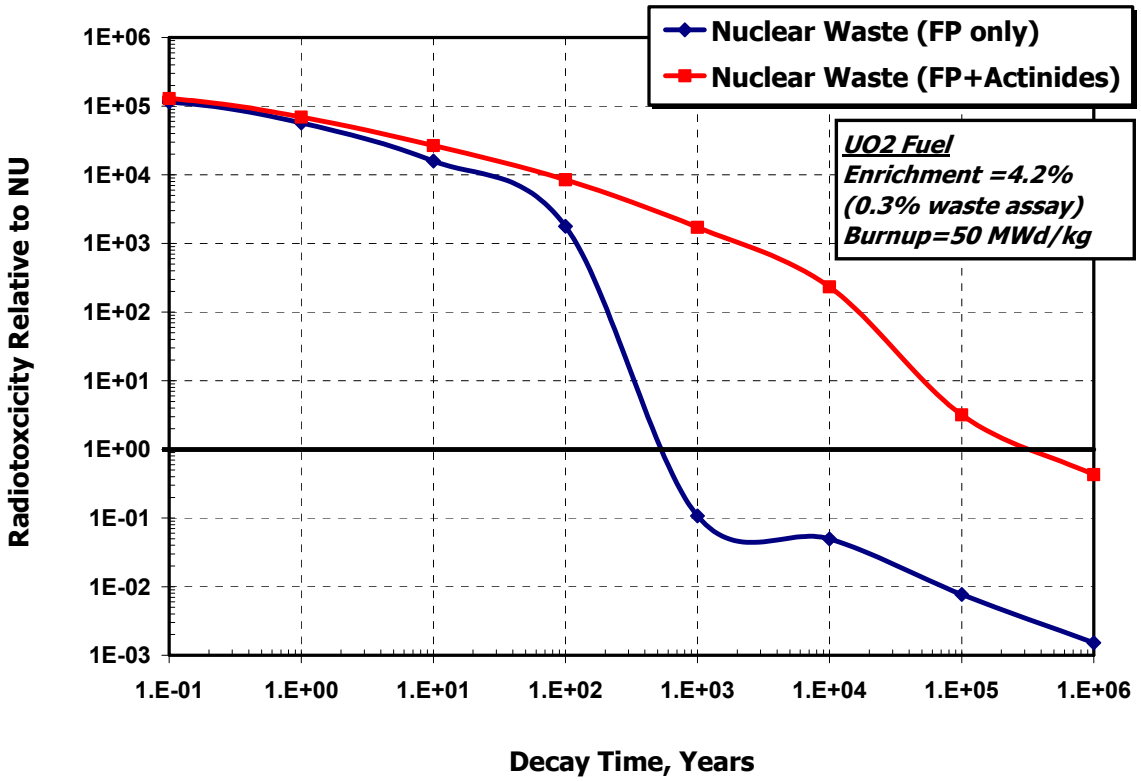

Figure 1.2.2. SNF Radiotoxicity for ingestion as function of time after discharge.

Only about 0.1% of the spent fuel is minor actinides (MA). Some of them are very long lived. In the repository, Pu and MA (also regarded as Transuranic elements – TRU) are responsible for most of the radiotoxicity of the SNF after decay of the fission products in the period between 1000 and 1M years after discharge (Figure 1.2.2). In the countries practicing fuel reprocessing, the high level radioactive waste, including MA and all the fission products, is incorporated in chemically stable host matrix (typically vitrified in glass). Only such vitrified waste is intended for geological storage. This fuel cycle strategy alone allows

- major reduction in volume of high level nuclear waste (by about 40% in France)
- improvement in uranium utilization through single path Pu recycling as MOX fuel
- enhancement of proliferation resistance characteristics of the fuel cycle due to degradation of Pu isotopic vector [Pellaud B., 2002]

However, some of the fuel cycle issues mentioned earlier remain open. The HLW conditioning into more compact and chemically stable form does not necessarily imply safer repository in the long term because long lived radioactive materials will be still present in the environment. Moreover, most of the potential fuel energy still remains un-recovered. Finally, proliferation resistance improvement due to less attractive Pu isotopics after its recycling may be offset by the increased proliferation risks due to the mere fact of Pu separation during SNF reprocessing which creates more opportunities for its diversion [Lowenthal M.D., 2002].

Transmutation strategies

Reduction in radiotoxicity of the nuclear waste intended for geological storage is clearly the most important goal for sustainable economic development and relying heavily on nuclear power as major non-polluting energy source. The objective is to reduce the nuclear waste radiotoxicity to a level below that of the uranium ore from which it originated within the time frame that engineering barriers preventing radioactive materials from leaking into the environment can be designed with high degree of reliability (less than 1000 years [DOE/NE, 2003], [OECD/NEA, 2002]).

Long lived radioactive nuclides can be transmuted to short lived or stable nuclides via neutron capture or fission reactions. By fissioning the actinides from the SNF the following goals can be achieved. Long lived nuclides are converted to generally short lived fission products reducing the long term radiotoxicity. Potentially weapons usable material (mainly Pu) is eliminated reducing proliferation risks. Finally, valuable energy potential is recovered extending uranium resources.

Numerous studies have been conducted on various options for radioactive waste transmutation since 1980's. None of them was realized primarily due to economic factors. The suggested transmutation systems can be categorized as presented in Table 1.2.I. Each of the categories is discussed below in some details. Figure 1.2.3 schematically shows the proposed transmutation concepts.

Table 1.2.I. Technology options for transmutation systems and fuel cycles.

System feature	*Proposed options*
Neutron spectrum	Fast, thermal, combination of two
Type of coolant	Water, gas (CO_2, He), Liquid metal (Pb, Pb-Bi, Na)
Type of fuel	Metallic, Oxide, Nitride, combined (CERMET, CERCER)
Fuel matrix	Fertile free, Th, UO_2 (MOX)
Neutron source	Critical, Accelerator driven (ADS)
Fuel cycle	Once through deep burndown, closed with multi-recycling
Recycling reactors	Single tier, multi-tier system
Nuclides intended for transmutation	Pu, Pu + MA, Pu + MA + LLFP
Transmutation target type	Homogeneous (mixed with fuel), Heterogeneous targets

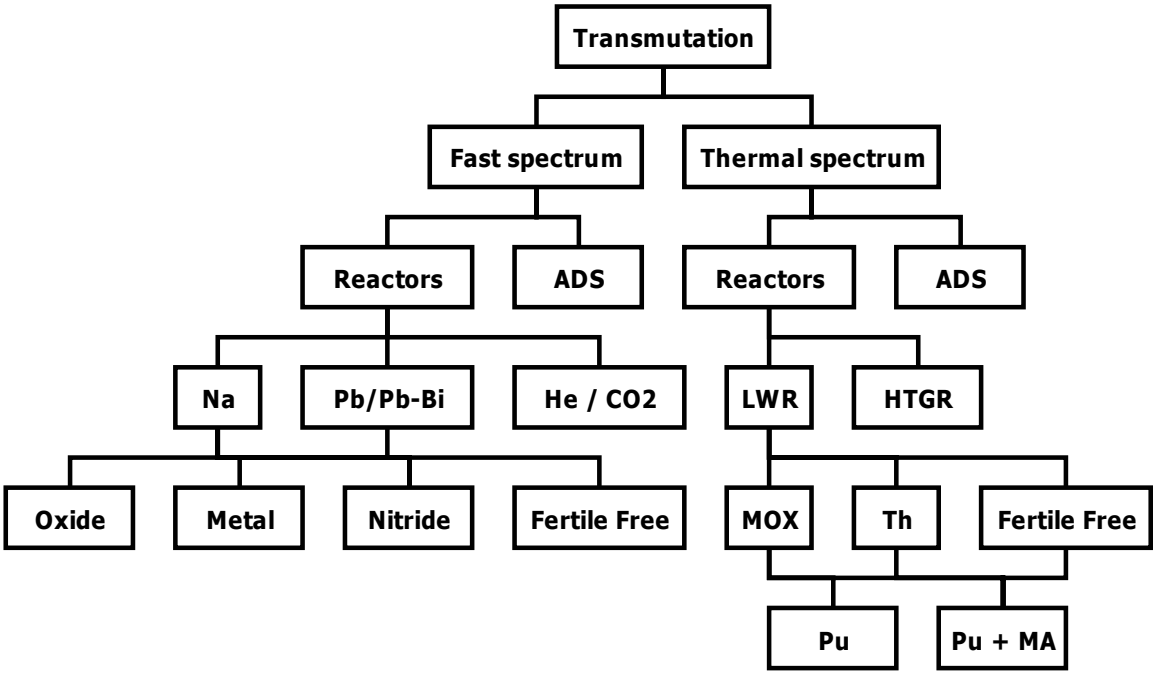

Figure 1.2.3. Transmutation system concepts

Fast vs. thermal spectrum systems

It is generally acknowledged that a fast neutron spectrum is more advantageous than a thermal spectrum with regards to TRU transmutation [Wiese H.W., 1998] simply because of the fact that fast neutrons are capable of inducing fission in almost all actinides while thermal neutrons can induce fission in only about half of them. This feature of the fast spectrum leads to better neutron economy. In the thermal spectrum system, neutrons are required first to convert some of the actinides to fissile nuclides by neutron capture and only then destroy them by fission. Moreover, the capture to fission cross-section ratio is comparable in magnitude for most of the nuclides in the fast spectrum which prevents buildup of higher MA isotopes (e.g. Cm) [Salvatores M., 2002].

The effectiveness of TRU transmutation in thermal reactors can be argued by the fact that MAs have large absorption cross sections in thermal spectra. In such spectra, the conversion of MAs by neutron capture to fissile nuclides can be very rapid. The high fission cross sections of the fissile isotopes in thermal spectra in turn allow their fast and effective destruction. In addition, the absolute magnitude of the thermal spectrum cross sections for neutron absorption is 200-300 times larger than those for fast neutrons. Thus, at a given power level a thermal spectrum system requires a significantly smaller actinide inventory, even though fast systems operate at higher neutron flux levels than thermal systems. This ultimately implies that thermal spectrum systems will discharge a smaller amount of minor actinides for reprocessing and, therefore, potentially reduce reprocessing costs. However, this is to be evaluated against particular designs of both the manufacturing and reprocessing facilities. For example, pyrochemical reprocessing and advanced fuel fabrication techniques [Wade D.C. et al., 1988] or on-line fuel reprocessing for the molten salt fuel systems [Vergnes J. et al., 2002] may offer significant benefits with respect to the economics of waste transmutation.

In the case of LWRs, the introduction of TRU into the core may reduce the requirements for burnable absorbers. The neutrons captured in even-even TRU nuclides which cannot be directly fissioned by thermal neutrons are not lost as in the case of burnable poison but transmuted to useful fissile nuclides. Careful choice of TRU amount and elemental composition can reduce the reactivity swing of the core to an extent where burnable absorbers would no longer be needed. The possibility of using TRU as a “fertile” poison in long-life reactor cores is demonstrated in [Peryoga Y. et al., 2002].

Additionally, a comparison of fast and thermal systems with equal TRU destruction rates and driven by external neutron source reported in [Bowman C.D., 2001] shows that equilibrium inventories of all the actinides including Cm are considerably smaller for the thermal system due to the higher effective cross-sections. Furthermore, the reduced Pu inventory also reduces the proliferation potential of the fuel cycle.

Coolant and fuel choice

The neutron spectrum of the system largely drives the choice of the coolant which by itself has a minor impact on transmutation capabilities of the system. The fast systems are limited to liquid metal (Na, Pb) or gas (He, CO_2) coolants (Figure 1.2.3). All three technologies: sodium, lead, and gas-cooled reactors are promising concepts and they were chosen for development as candidates for future nuclear energy systems by the Generation IV roadmap committee [DOE/Generation IV International Forum, 2002]. Considerable research activities are currently in progress throughout the world aiming at the development of lead or lead-bismuth eutectic cooled reactor systems for waste transmutation. Pb-Bi coolant offers a number of safety advantages over Na, while much more operating experience is available for Na cooled systems. A number of commercial as well as small scale research Na cooled fast reactors have been operated throughout the world. Transmutation of Pu and MA in sodium cooled fast reactors was successfully demonstrated by several studies [Hill R.N., 1995], [Kuraishi H. et al., 2001]. The experience with lead cooled reactors originates in the Russian navy propulsion program. The development of commercial power Pb (or Pb-Bi) cooled reactor (BREST concept) is also actively pursued in Russia [Orlov V.V., 2003]. Lead can effectively serve as a coolant and as a spallation neutron source in accelerator driven systems (discussed below). A number of Pb/Pb-Bi cooled critical fast reactor concepts were proposed and analyzed revealing a high potential for transmutation of TRU [Kuznetsov V.V. et al., 1995], [Hejzlar et al., 2001], [Romano A. et al., 2002].

He or CO_2 gas can be used as a coolant in either fast or thermal systems typically in combination with a graphite moderator. The conventional light water cooled reactors and their potential for waste transmutation is the main subject of this thesis and will be discussed later.

A number of factors dictate the choice of the fuel form. The ideal transmuter fuel should combine the following features.

- minimal generation of secondary actinides
- neutronic features allowing optimal spectrum for transmutation while maintaining safe operation characteristics
- high burnup capabilities
- simple and economic handling and reprocessing
- good thermal and mechanical properties that would promote reactor safety

A recent review of fertile free fuel candidates for transmutation of actinides in various reactor types has been conducted at MIT [Long Y. et al., 2003].

Critical vs. external neutron source driven systems

The presence of significant quantities of MA in a fast spectrum core particularly in combination with fertile free matrix fuel leads to degradation of feedback coefficients and inferior transient behavior of the reactor. Some of the safety features of fast spectrum TRU transmutation systems can be significantly improved if they are designed as subcritical systems driven by external neutron source. The concept of Accelerator Transmutation of Waste (ATW) was originally conceived in Los Alamos Nation Laboratory [Bowman C.D. et al., 1992] and it is presently actively advocated by C. Rubia [Carminati F. et al., 1993]. In this concept, the neutrons that drive a sub-critical reactor are produced through spallation process. The beam of accelerated to high energy protons impacts typically heavy metal target and initiates a cascade of secondary lower energy neutrons and some protons. Some neutrons are produced via direct collisions with the nuclei of the target while the majority are produced as excited target nuclei get rid of their excess energy by “boiling off” additional neutrons. In such a process, up to 30 neutrons can be produced per one 1GeV incident proton.

Sub-critical accelerator driven systems (ADS) enable the design of reactor cores that would otherwise be very challenging to operate. In addition, the external neutron source allows the control neutronic reactivity by adjustment of proton beam current which eliminates the concerns over prompt critical power excursion accidents and need for burnable absorbers. However, it does introduce a concern about accelerator beam overpower. In addition, ADS systems are still

susceptible to Loss of Flow (LOFA) and Loss of Heat Sink (LOHS) accidents and therefore require additional measures to assure their safety.

Moreover, the technology for the design of large accelerators and for their coupling with the reactor requires extensive development to improve the overall system reliability, capacity factors, and reduce the development and deployment costs. A 1999 DOE review of the US Accelerator Transmutation of Waste (ATW) program concluded that operation of an ATW prototype or demonstration unit might take as long as 20 years to implement and would cost as much as $11 billion. Full implementation of ATW in the United States for treating civilian spent nuclear fuel would require several decades and could cost hundreds of billions of dollars [Bresee J.C., 2003].

Production of electricity and improved resource utilization can partially offset the costs related to ADS technology. In addition, thermal spectrum molten salt fueled ADS, as pointed out in [Bowman C.D., 2000], may require up to 4 times smaller accelerator due to reduced neutron leakage and reduced reactivity control requirements which would also facilitate better economic performance of ADS.

On the other hand, critical fast spectrum systems with carefully designed safety features may appear to be more favorable candidates for TRU transmutation as they can potentially provide comparable to ADS transmutation capabilities but at lower cost and with greater reliability due to utilization of more mature technologies [Hejzlar et al., 2003], [Romano A., et al., 2002].

Fuel Cycles

The proposed fuel cycles for transmutation of waste differ in several respects. Depending on the main goal of transmutation Pu or Pu, MA, and LLFP can be considered. Suggested fuel cycle strategies also included single path with maximized deep burndown of TRU or multi-recycling of Pu and MA in one or multi-tier systems. Several examples of the proposed fuel cycles are presented in Figure 1.2.4.

The concern over growing Pu stockpile from commercial LWR spent nuclear fuel in addition to significant quantities of weapons grade (WG) Pu from dismantled nuclear warheads [Albright D. et al., 1997] resulted in extensive research effort aiming at the reduction of the excess amounts

of Pu. Numerous studies initiated by the US DOE confirmed the possibility of disposition of reactor grade (RG) and WG Pu in the form of mixed PuO_2-UO_2 oxide fuel in all major currently existing reactor types: [Westinghouse Electric Co., 1994] and [Combustion Engineering Inc., 1994] for PWRs, [GE Nuclear Energy, 1994] for BWRs, and [AECL Technologies Inc., 1996] for Canadian heavy water reactors (CANDU). Thorium and fertile free fuel matrices appear to be more effective for Pu burning than MOX because no secondary Pu is generated. Possibility of Pu burning in fertile free matrix fuel in PWRs peripheral assemblies and achieving the sustainable Pu inventory was demonstrated by [Chodak P., 1996]. The full fertile free fuel loaded PWR core for disposition of RG and WG Pu was analyzed in [Kasemeyer U. et al., 1998] and shown to be feasible.

RG and WG plutonium disposition using thorium based fuels has been widely studied as well. For example, potential feasibility of burning WG and RG Pu are discussed in [Lombardi C. et al., 1999] and [Phlippen P.W. et al., 2000]. They addressed several issues of reactor control and safety as well as issues concerning multi-recycling of Pu. Alternative fuel design for more efficient thorium assisted Pu disposition in PWRs based on Seed-Blanket fuel assembly concept was proposed and discussed in [Galperin A. et al., 1998]. Feasibility of using Th-Pu fuel in high conversion BWRs is discussed in [Downar T. et al., 2000]. Various other reactor systems such as High Temperature Gas-cooled Reactors [Ruetten H.J., 2000b] and fast spectrum reactors [Tommasi J. et al., 1998] with Pu-Th fuel were also suggested and examined. These studies showed that thorium based fuels can efficiently perform the task of RG and WG plutonium stockpile reduction while maintaining acceptable safety and control characteristics of the reactor systems studied. However, no significant improvement in the spent fuel repository characteristics can be achieved through single path Pu burning in thorium matrix [Reutten H.J., 2000a].

The recent and most comprehensive transmutation systems and fuel cycle strategy studies were reported in [OECD/NEA, 2002] as a part of a joint nuclear waste partitioning and transmutation effort by OECD member countries and in [Van Tuyle G.J., 2001] in the framework of formerly Advanced Accelerator Application (AAA) program sponsored by the US DOE. The most significan findings of these studies are summrized in [Finck P., 2002]. In both studies, the main goal of waste transmutation was the reduction of radiological impact of nuclear waste on the repository and surrounding environment to the extent that very long term storage would no longer be needed. The tradeoffs between single path burndown and multi-recycling as well as advantages and drawbacks of the single tier versus multi-tier approaches are discussed.

Once Through Fuel Cycle

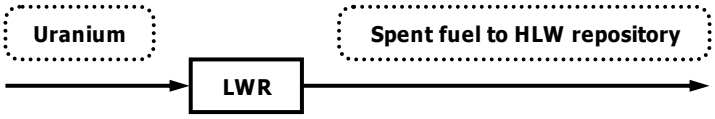

LWR Recycle

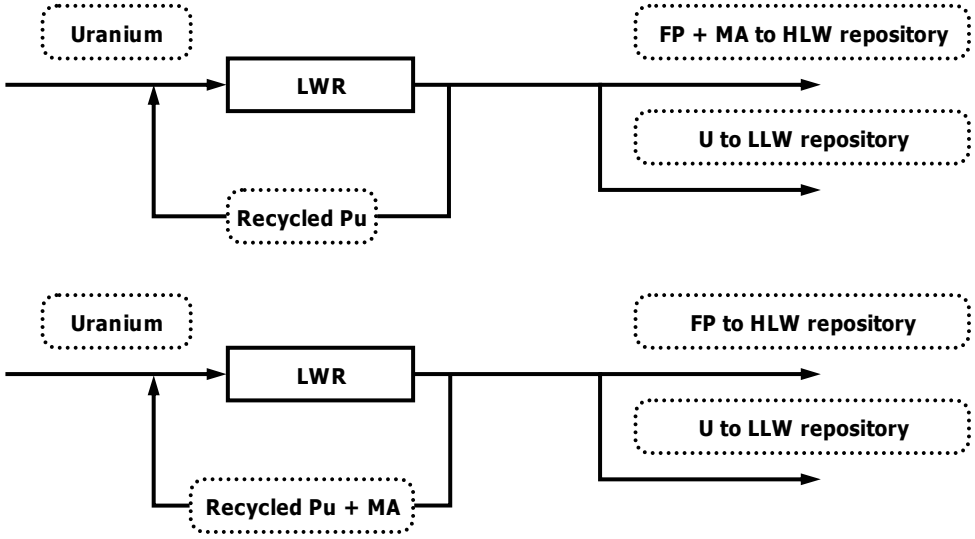

Multi-Tier Recycle

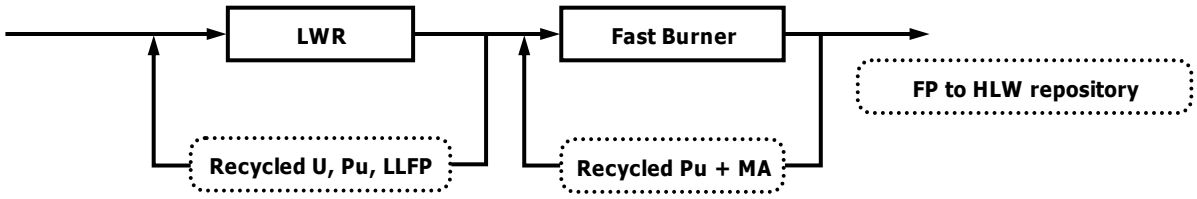

Figure 1.2.4. Examples of Fuel Cycles

In the multi-tier approach [Hill R.N. et al., 2002], Pu in the form of MOX is recycled once or multiple times in existing LWRs or advanced gas cooled reactors to achieve major TRU mass reduction using conventional technologies and therefore maximizing the economic benefits. While in the second tier, small amounts of residual Pu, MA, and LLFP are burnt in fast reactors or ADS via multiple recycling to the extent required to achieve the radiotoxicity reduction goal.

The single tier system considered in [OECD/NEA, 2002] was self supporting fast reactor system with closed fuel cycle and zero net generation of TRU. This strategy implies a distant future scenario where the entire fleet of nuclear reactors is of the described type.

The single path burndown fuel cycle strategy suggests reprocessing of the existing LWR spent fuel and subsequent once through deep burnup of Pu or TRU in various transmuter systems. For example, GT-MHR was proposed for disposition of Russian WG Pu and is said to achieve a destruction efficiency of up to 90% of fissile Pu per path [Kodochigov N., 2002]. However, none of the single path transmuter systems can achieve the degree of TRU destruction sufficient enough to satisfy the radiotoxicity reduction criteria (Figure 1.2.5 [Van Tuyle G.J., 2001]). This conclusion is consistent with the findings elaborated later in this thesis.

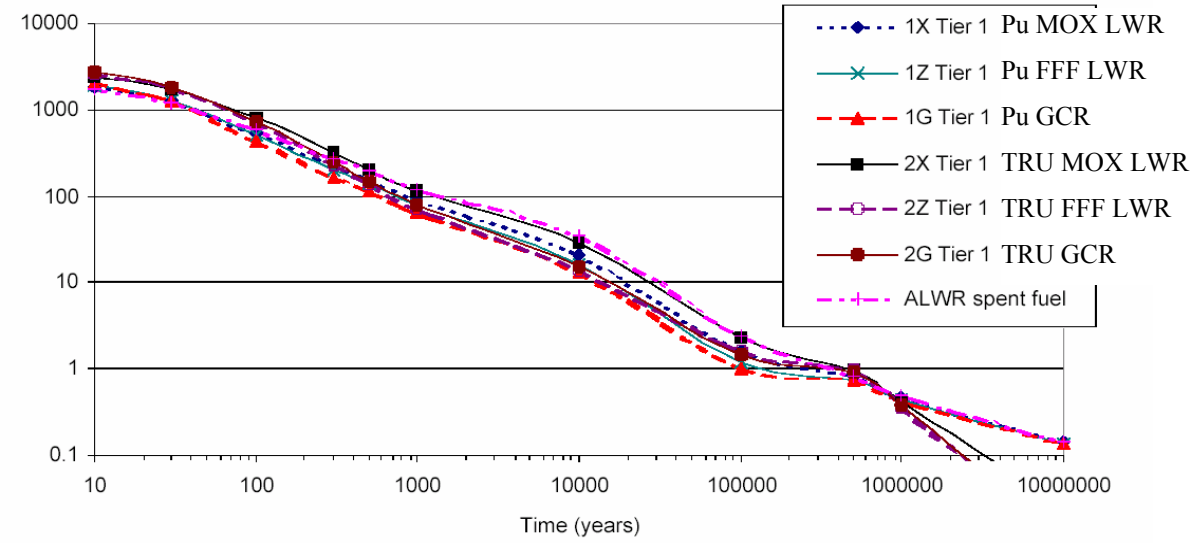

Figure 1.2.5. Radiotoxicity relative to NU ore for the single path burdown scenario [Van Tuyle G.J., 2001].

Additionally, both OECD and AAA studies came to a common conclusion that in principle, all analyzed fuel cycle options are capable of achieving the radiological and TRU mass reduction goal provided that multi-recycling of TRU with relative losses to the waste stream of less than 0.1% can be achieved.

Multi-recycling strategies to constrain generation of Pu and TRU in LWRs were also recently studied by several groups. Advanced Pu Assembly (APA) concept [Puill A. et al., 2001]

was proposed and possibility of Pu inventory stabilization in PWRs was confirmed. The APA combines large annular internally cooled fertile free fuel pins containing Pu and standard UO_2 fuel pins as shown in Figure 1.2.6.

Such a configuration allows effective Pu consumption through high moderator to fuel volume ratio in Pu bearing region and fertile free matrix. Annular geometry also helps to accommodate high power peaking in Pu pins. However, APA cannot be combined with conventional assemblies in the same PWR core because of the differences in thermal hydraulic designs.

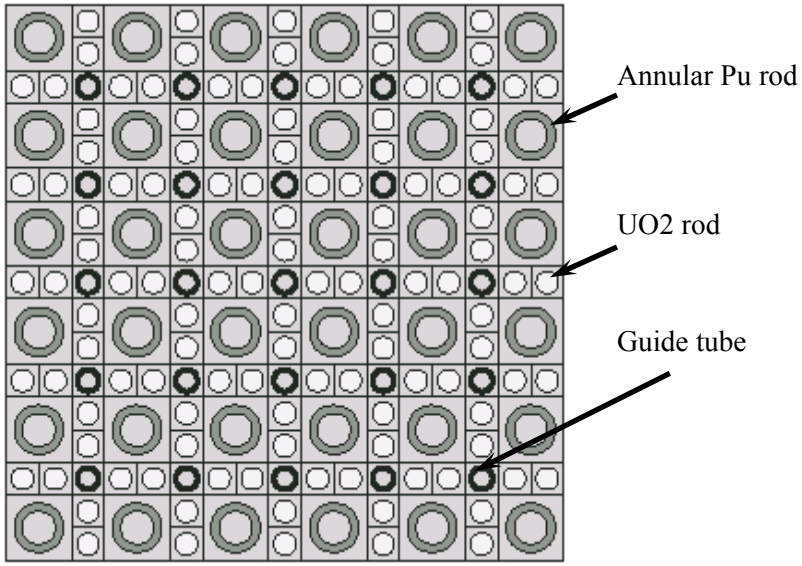

Figure 1.2.6. Advanced Plutonium Assembly [Puill A. et al., 2001]

The alternative CORAIL assembly concept [Aniel S. et al., 2001] was proposed. All fuel pins in the CORAIL assembly have identical geometry. However, the pins on the assembly periphery contain Pu or TRU [Taiwo T. A. et al., 2002] in the MOX form. The availability of existing technology for reprocessing and fabrication of MOX fuel is the main advantage of the CORAIL concept. The equilibrium TRU concentrations in the CORAIL fuel cycle are relatively high (about 36 kg per assembly) due to the presence of fertile U238 which results in additional TRU generation and therefore deteriorates TRU destruction efficiency.

TRU recycling in thorium based PWR fuel was studied recently [Todosow M. et al., 2002]. The analysis showed that for Th based fuel options equilibrium TRU inventory can also be achieved. However, re-enrichment of recovered from the fuel uranium is required to maintain constant fuel cycle length.

1.3. Thesis Objectives and Scope

The main objective of this thesis is to develop an innovative fuel cycle for Light Water Reactors (LWRs) featuring the lowest possible impact on the environment from the radioactive constituents in a spent nuclear fuel. The current analysis attempts to evaluate the potential of LWRs to manage the radioactive waste they produce in a sustainable mode. The technical feasibility of such an operation mode would offer more affordable solution to the once through fuel cycle problems due to the possible utilization of the existing reactors and technologies.

A major constraint on this study, therefore, is complete compatibility of the sustainable fuel cycle with the current generation of LWRs. Namely, all reactor core operation and safety characteristics must remain comparable to those of the reactor operating on a conventional once through fuel cycle.

The present effort examines two major fuel cycle strategies that can be applied to the existing fleet of LWRs without an immediate requirement to develop additional transmutation system technologies such as advanced fast reactors or ADS. The fuel cycle strategies studied are

- once through burndown of TRU in LWR systems alone but with several alternative fuel types
- TRU multi-recycling scenario based on the most efficient with respect to TRU transmutation potential fuel option

The additional goals of this thesis as they are addressed in the following chapters are

- to identify the fuel form which is most effective for transmutation of TRU in LWRs and at the same time allows one to maintain acceptable reactor safety and operation characteristics
- to evaluate the effect of once trough burndown scenario on the waste performance characteristics in the repository

- to evaluate the neutronic feasibility of achieving the equilibrium with respect to TRU generation state by multiple recycling of TRU from the spent fuel
- to evaluate the effect of the sustainable fuel cycle with zero net TRU generation on the repository
- to identify and address the potential challenges associated with multi-recycling of TRU in LWRs
- to perform economic analysis of the sustainable LWR fuel cycle and compare it with conventional once through fuel cycle and alternative two-tier system of LWR and Advanced fast spectrum Actinide Burner Reactor (ABR).

1.4. Foreseen Technical Challenges Associated with TRU Recycling

As discussed earlier, TRU transmutation in thermal spectrum reactors and in particular in LWRs imposes a number of potential design challenges.

Some of the MA have relatively small cross-sections for neutron absorption even in thermal spectrum in addition to relatively long half lives. As a result, these nuclides (typically Cm244, Cm246, Cm247, Cm248, and Cf252) require relatively long time and high concentrations to saturate in the thermal spectrum. Furthermore, changes in TRU isotopic vector with burnup and with the number of TRU recycles result in degradation of TRU transmutation efficiency, shorten the fuel cycle length, and lead to increased TRU loading requirements.

A harder neutron spectrum, as a result of increased TRU concentration in the core and changes in TRU isotopic composition, may lead to positive void reactivity coefficient. This would ultimately limit the maximum TRU concentration. Lower worth of the core reactivity control materials is also expected as a result of the neutron spectrum hardening.

The effective delayed neutron fraction (β_{eff}) is expected to be smaller for TRU containing LWR core because practically all Pu and MA isotopes have lower β_{eff} than U235 in conventional LWR core. The change in the fuel and moderator temperature reactivity feedbacks and prompt neutrons lifetime decrease are probable additional consequences of the harder neutron spectrum. As a result, some of the core safety criteria may be violated during the reactor response to rapid reactivity initiated transients.

Finally, the increased concentrations of TRU nuclides in the fuel cycle would complicate the fuel handling, reprocessing, and fabrication due to increase levels of radiation. Some of the higher MA nuclides mentioned above in particular Cm244, Cm246, Cm248, and Cf252 have relatively high branching ratio to spontaneous fission (SF). The neutrons released in SF process are very hard to shield so that accumulation of SF neutrons emitting nuclides would aggravate the TRU containing fuel handling and fabrication problem. Additionally, the TRU separation based on the aqueous reprocessing techniques may not be suitable for the reprocessing of fuels with high TRU concentrations. The organic solvents used for separation of TRU from the fission products degrade rapidly when exposed to high radiation or elevated temperatures caused by the decay of TRU. As a result, non-aqueous separation techniques based on pyrochemical or pyrometallurgical reprocessing may be required.

1.5. Thesis Organization

This thesis consists of ten chapters. The first chapter briefly introduced the problematic issues associated with once-through fuel cycle such as accumulation of long lived radioactive waste, proliferation resistance, and poor utilization of natural resources. Then, short overview of the suggested in the past solutions and strategies was presented. The possibility of addressing the most important once through fuel cycle issues using exclusively the existing LWRs was proposed and justified. The list of potential associated technical challenges was subsequently presented.

The evaluation of neutronic performance of the two most promising cycles, with respect to the TRU destruction capabilities, fuel matrix candidates is presented in Chapters 2 and 3 focusing on thorium oxide and fertile free fuel matrices respectively. TRU destruction rates and TRU residual fractions in the spent fuel are the main parameters of interest in the discussion. The reactivity feedback coefficients and soluble boron reactivity worth are also reported as primary indicators of practical fuel design feasibility.

Chapter 4 compares the evaluated thorium oxide and fertile free fuel options in terms of their repository performance characteristics in a once through burndown scenario aiming at the reduction of existing TRU stockpile and at constraining future TRU generation. The performance

of reference once-trough fuel cycle and mixed oxide (MOX) based fuel is also reported for the comparative assessment.

Since fertile free fuel showed superior performance in terms of TRU burning capabilities, it was chosen as the best option for the evaluation of sustainable fuel cycle with zero net production of TRU. In Chapter 5, a heterogeneous Combined Non-fertile and UO_2 (CONFU) fuel assembly concept is introduced. The possibility of achieving an equilibrium state with respect to TRU inventory and fuel cycle length is demonstrated.

Chapter 6 addresses feasibility issues of practical CONFU assembly based core design. 3-dimensional whole core neutronic simulation results are reported for a number of considered design alternatives including micro- and macro-heterogeneous CONFU assembly design options, fully fertile free TRU containing core, and the reference PWR UO_2 fueled core. The analysis is focused on the evaluation of the core power peaking factors, cycle length, reactivity coefficients, and control rods and soluble boron reactivity worth. The performed thermal hydraulic analysis aiming at the evaluation of MDNBR margin for analyzed cases is also reported.

The dynamic behavior of the cores containing TRU in response to the reactivity initiated accidents is analyzed in Chapter 7. A simple computer model created for such an assessment is described and the results of the simulations are presented. Additional concerns related to loss of coolant accident (LOCA) in TRU containing cores are discussed in some details.

Chapter 8 presents the results of environmental hazard characteristics of the sustainable LWR fuel cycle. Some practicality issues related to possibility of the fuel cycle infrastructure facilities to handle multi-recycling of TRU are discussed. The decay heat, photon, and neutron doses from spontaneous fission of TRU are reported as a function of the number of TRU recycle paths. A brief review of the existing and prospective TRU reprocessing options is also presented.

In Chapter 9, the results of the fuel cycle cost and the total cost of electricity estimations for the sustainable LWR based fuel cycle are compared with those of the once-through reference cycle and with alternative (LWR and fast actinide burner reactor) double strata fuel cycle.

Finally, Chapter 10 summarizes the main findings and conclusions of this thesis.

Chapter 2. Fuel Choice for Actinide Transmutation in LWRs

An LWR fuel cycle aiming at the reduction of waste burden must take advantage of innovative fuel materials capable of producing less TRU than currently employed UO_2 fuel. Pu and MA are products of the neutron capture reactions in uranium. Naturally, to facilitate the objective of improving the long term characteristics of the nuclear waste, the amount of uranium present in the fuel has to be minimized. However, in addition to reduced TRU generation, the innovative fuel materials have to fulfill several other requirements.

- Be able to provide high burnup. Thus, new fuel materials should have better or comparable to UO_2 performance under irradiation.
- The properties of new fuel materials should be such that the fuel design will have adequate heat removal capabilities in order to maintain or improve the thermal margin of the existing LWRs operating at their nominal power and during accident conditions.
- If recycling of the TRU is considered, the fuel matrix should be relatively easy to handle in order to reduce reprocessing costs. On the other hand, if the once-through TRU burning strategy is employed, the fuel matrix should provide good capabilities for fission product and actinide retention for a very long term.
- Innovative fuel materials must be chemically compatible with light water coolant and the cladding and have acceptable performance under irradiation with respect to the release of fission gas, swelling, and degradation of their thermal and mechanical properties.

In light of these considerations, we examine two base fuel matrix materials: thorium dioxide (ThO2 – thoria) and neutronicaly inert fertile free matrices. Capabilities of both fuel options with respect to TRU destruction efficiencies and rates were evaluated along with some feasibility assessment of practical designs. Finally, both fuel matrix material options are compared to each other and to the conventional way of burning TRUs which is based on the existing uranium-plutonium mixed oxide (MOX) technology.

2.1. Thorium Based Fuels

If introduced into the LWR fuel cycle, thorium as a primary fertile material in the core has a good potential for reducing the TRU generation simply due to its lower than uranium position in the periodic table. Longer neutron capture and decay chains have to take place in thorium to result in Pu or MA isotopes. However, significant quantities of U233 and long lived radioactive Pa231 generated in a thorium fuel mitigate this advantage. U233 is a valuable fissile isotope that, if recycled, can improve fuel utilization and due to its continuous generation from the thorium can increase fuel burnup and reduce core reactivity swing during a fuel cycle. At the same time, U233 is a weapons usable material with relatively low spontaneous neutron source. Thus, its accumulation reduces attractiveness of the thorium based fuel cycle from the proliferation resistance standpoint. Addition of natural or depleted uranium to the fuel for the sake of limiting U233 concentration in uranium below the weapons usability limit will result in increased TRU generation.

Although Th232 has a lower resonance integral than U238 its response to the fuel temperature increase (Doppler broadening) is greater, which results in a more negative fuel temperature reactivity coefficient than that of the uranium fuel – a desirable feature in case of transients with rapid reactivity increase. At the same time, the smaller delayed neutron fraction of U233 than of U235 has a negative effect on reactivity initiated accidents. This is particularly important for the Th-TRU mixtures where β_{eff} is considerably smaller than that of the uranium fuel all through the in-core residence time.

In the fuel performance area, thoria is found slightly more advantageous than UO_2. ThO_2 thermal conductivity is slightly higher than that of UO_2 at comparable temperatures in addition to about 500 °C higher melting point [Oggianu S.M. et al.,] (Table 2.1.I).

In ThO_2 compound, thorium has its highest possible and the only oxidation state +4, which makes it very stable and almost chemically inert [Belle J. et al., 1984]. Therefore, thoria is expected to be a very durable waste form for the spent fuel. If the fuel recycling strategies are considered, however, reprocessing of the thoria fuel is somewhat complicated for the same reason and therefore it is expected to be more expensive than reprocessing of UO_2 fuel. The presence of U232 isotope inevitably generated in Th fuel primarily as a result of (n,2n) reaction in U233 may further complicate reprocessing and add to its cost. U232 decay chain products emit highly

penetrating hard γ radiation which will require additional shielding and remote handling of the fuel. This complication is less critical if TRU recycling in conjunction with use of ThO_2 matrix is desired because TRUs other than U232 are likely to dominate the γ and neutron radiation doses and will require remote handling as well.

The heavy metal density in thorium oxide is slightly lower than in uranium oxide which is additional disadvantage (Table 2.1.I).

Table 2.1.I. Physical properties of some nuclear fuel materials, [CRC Press, 2000]

	U	UO_2	Pu	PuO_2	Th	ThO_2
Melting point, °C	1135	2827	639	2390	1750	3390
Phase change, °C	660				1400	
Theoretical density, g/cm^3	18.9	10.96	19.8	11.50	11.7	10.00
Thermal Conductivity at 600 °C, W/cm-°C	0.42	0.045			0.45	0.057

Finally, the interest in breeder reactor technologies including Th cycle in 1960's and 1970's resulted in accumulation of significant experience and produced a vast knowledge database covering different aspects of thorium fuel cycle [Lung M. et al., 1997]. This knowledge and experience can be effectively put in use should the interest in thorium cycle in connection with TRU burning be renewed.

The focus of this section is on establishing the practical limits for Pu and MA burning efficiency and on the feasibility of thorium based fuel in PWRs. The main parameters of interest are the rate of total Pu and MA destruction and residual fraction of trans-uranic nuclides (TRU) in discharged fuel. The former parameter is, effectively, the number of kilograms of TRU that are burnt per unit energy produced by the fuel. The latter parameter indicates the amount of TRU that will have to be recycled or disposed of in the nuclear waste repository.

The fuel composition (relative amounts of Th, Pu, MA and U in the fuel) and lattice geometry will affect both of these indices: the burning efficiency and rate of TRU destruction. Therefore, the study reported here consists of several parts. First, homogenous reactor grade PuO2-ThO2 mixtures are studied covering a wide range of possible compositions and geometries. Then, the effect of the addition of a small amount of natural uranium to the fuel was investigated. This option is important for the once-through TRU burning scenario where the discharged fuel will be sent directly to the repository. In this case, U233 generated from Th232 has to be

isotopically diluted (denatured) in order to eliminate potential nuclear proliferation threats. Next, MAs were also considered as part of the fuel and the efficiency and destruction rates of Pu, MA and total TRU were investigated.

The PWR fuel lattice allows a certain degree of freedom in optimizing the fuel to moderator ratio. This ratio defines the degree of neutron moderation and, therefore, absorption and fission reaction rates in different HM nuclides in the fuel. For that reason, a scoping study was carried out to evaluate the effect of the fuel lattice geometry on Pu and MA destruction performance for each fuel composition considered.

Heterogeneous core geometries may be beneficial if Pu and MA can be concentrated in separate fuel assemblies in the core allowing more flexibility in fuel lattice optimization and fuel management schemes. Therefore, the potential of heterogeneous core configuration to burn Pu or MA more efficiently was also explored on the basis of two dimensional 2x2 assemblies colorset segment. Figure 2.1.1 schematically depicts the topology of all investigated cases.

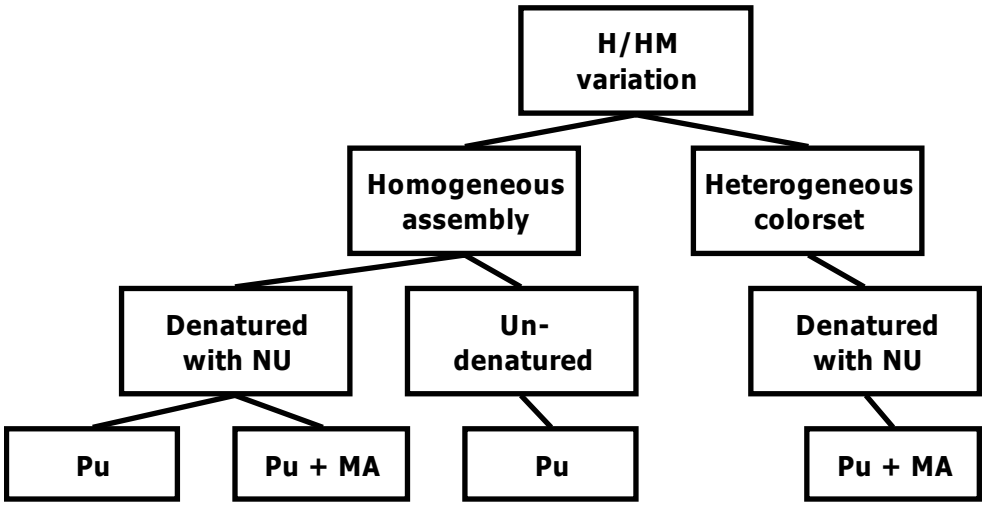

Figure 2.1.1. Topology of investigated cases.

Finally, feasibility of utilization of TRU-loaded thorium based fuels in the current generation of PWRs was studied by a comparative analysis of the reactivity coefficients and soluble boron worths for a number of realistic TRU-Th cases, typical MOX and conventional all-U fuel. In current PWRs, only moderate changes in the fuel assembly configuration are possible in order to

optimize fuel performance parameters. Additionally, denaturing of bred U233 is a required constraint for a practical design. In light of these two considerations, only denatured cases with H/HM ratios between the reference case and the reference +40% case were evaluated in terms of reactor operational characteristics.

2.1.1. Benchmark of Computational Tools

The first step in this investigation was the assessment of computational tools and data libraries available for neutronic analysis of TRU transmutation options. These include the CASMO-4 Fuel Assembly Burnup Code [Edenius M. et al., 1995] and MCODE [Xu Z. et al., 2002] – an MCNP4C and ORIGEN2 coupling code. Two benchmarks– a pin cell and a fuel assembly having a repeating typical PWR lattice are evaluated.

Pin Cell Benchmark

The first benchmark calculations were performed using CASMO-4 and MCODE for homogeneously mixed PuO_2-ThO_2 fuel in PWR pin-cell and fuel assembly geometries. The fuel composition included 95.5 weight % of Th and 4.5 weight % of reactor grade Pu. The fuel composition, geometry and parameters for the benchmark runs were chosen to be identical to those used in a benchmarking task performed within the framework of IAEA Coordinative Research Program (CRP) on "Potential of Thorium-based Fuel Cycles to Constrain Plutonium and to Reduce the Long-Lived Waste Toxicity" [Ruetten H.-J. et al., 2000]. This benchmark was performed by the CRP participants from 8 different countries. Each participating team used its own computational tools and data libraries. None of the teams used either CASMO-4 or MNCP-ORIGEN type computer codes.

The PWR pin-cell geometry and operating conditions used for the first part of the benchmark are shown in Figure 2.1.1.1. Detailed materials composition for each zone can be found in [Ruetten H.-J. et al., 2000] and [MacDonald P. et al., 2002].

The task of this benchmark was to calculate the fuel burnup at a constant power (21.1 kW/m) as a function of time, without using any burnable poison for reactivity control. The following parameters were calculated for a burnup of 0, 30, 40 and 60 MWd / kg of iHM: neutron

multiplication (k_{inf}), total neutron flux, average energy per fission, residual amount of plutonium, fraction of fissile plutonium, amount of generated minor actinides, and amount of bred U233.

Selected results of the PWR pin cell benchmark obtained from CASMO-4 and MCODE are compared with IAEA CRP results in Tables 2.1.1.I through 2.1.1.III. The fuel criticality is predicted with reasonable accuracy by all codes. The results for the average energy per fission, average neutron flux, Pu isotopes destruction rate as well as build-up of U233 and minor actinides are also in a good agreement, as documented in [MacDonald P. et al., 2002].

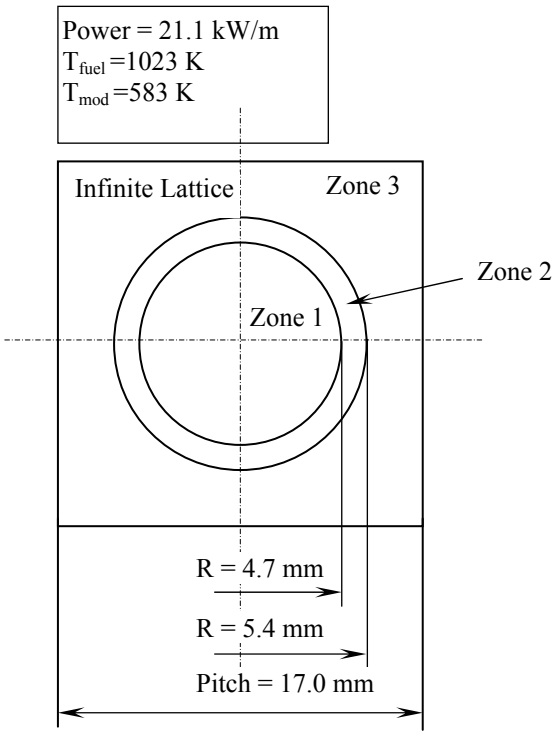

Figure 2.1.1.1 Reference Pin Cell Geometry.

Since the details about the codes used by other participants were not available to us, the discussion of the possible reasons behind the differences will be focused on CASMO4 versus MCODE results. The discrepancy in k_{inf} ranges between about 2% Δρ at BOL to about 5% at EOL. The BOL criticality predicted by CASMO4 is slightly higher than that predicted by MCODE and other codes. CASMO4-calculated reactivity, versus MCODE results, is higher even though the fuel temperature used in MCODE was lower than the fuel temperature of 1023K defined in the benchmark. Note that the cross-section data for fuel nuclides used in MCODE

calculations were available only at the temperature of 900K. The reasons for this discrepancy most likely lie in the different libraries used in MCODE and CASMO4, as discussed below.

Table 2.1.1.I. Infinite Medium Neutron Multiplication Factor as a Function of Burnup

Burnup(MWd/kg)	0.0	30	40	60
Germany	1.136	0.908	0.862	0.810
Russia	1.123	0.915	0.876	0.838
China	1.131	0.913	0.868	0.824
Korea	1.118	0.910	0.870	0.830
India	1.112	0.889	0.851	0.822
USA	1.110	0.911	0.873	0.832
Japan	1.135	0.921	0.881	0.841
Netherlands	1.125	0.925	0.887	0.848
CASMO4 (MIT)	1.142	0.915	0.870	0.824
MCODE (MIT)	1.121± 0.0014	0.916±0.0013	0.874±0.0012	0.837±0.0012

Table 2.1.1.II. Residual Amount of Plutonium (Pu / Pu initial) as a Function of Burnup

Burnup (MWd/kg)	0.0	30	40	60
Germany	1.00	0.42	0.29	0.13
Russia	1.00	0.43	0.31	0.16
China	1.00	0.40	0.28	0.12
Korea	1.00	0.41	0.28	0.14
India	1.00	0.41	0.29	0.14
USA	1.00	0.43	0.30	0.16
Japan	1.00	0.43	0.31	0.16
Netherlands	1.00	0.43	0.31	0.16
CASMO4 (MIT)	1.00	0.43	0.30	0.16
MCODE (MIT)	1.00	0.43	0.31	0.16

Table 2.1.1.III. Bred U233 Fraction (U233 / Pu initial fissile) as a Function of Burnup

Burnup(MWd/kg)	0.0	30	40	60
Germany	0.00	0.37	0.44	0.50
Russia	0.00	0.40	0.47	0.53
China	0.00	0.39	0.45	0.51
Korea	0.00	0.41	0.48	0.54
India	0.00	0.40	0.47	0.51
USA	0.00	0.41	0.48	0.54
Japan	0.00	0.38	0.44	0.50
Netherlands	0.00	0.41	0.48	0.54
CASMO4 (MIT)	0.00	0.36	0.42	0.47
MCODE (MIT)	0.00	0.38	0.44	0.50

The slope of the criticality curve calculated by CASMO4 is steeper than that obtained by MCODE. There are two reasons for this disagreement:

1. Differences in the number of fission products and actinides tracked in MCODE. One hundred fission products and 29 actinides were tracked in the MCODE calculation while about two hundred fission products and over 35 actinides were considered in the CASMO4 depletion calculations.
2. Differences in libraries between these two codes. MCODE utilized primarily ENDF-VI cross-section data. CASMO4 cross-section data are based on data files JEF-2.2 and ENDF/B-VI that are processed by NJOY-91.91 to generate libraries in 70 energy groups in CASMO4 format.

Also to be noted is that CASMO4 has higher recoverable energy per fission than ORIGEN2.1 but exhibits faster burnup rate, i.e. against the expectations based on fission energy difference. Thus, the effect of differences in fission products and cross sections is more important than the differences in recoverable energy per fission.

PWR Lattice Calculations

This part of the benchmark was performed in order to assure the capability of CASMO-4 and MCODE computer codes to manage assembly level 2D transport calculations with fuel depletion. As in the first part of the benchmark, the results obtained with CASMO-4 and MCODE will be compared to the results obtained by the participants of the IAEA Coordinative Research Program.

The calculations were performed for a 17x17 PWR fuel assembly with octant symmetry. The assembly included 25 water hole positions without guide tubes. The assembly cans were not considered. The calculations were carried out at a constant specific power of 37.7 kW/kg of initial HM and with zero buckling. The assembly and fuel pin geometry as well as the material compositions are described in details in [Ruetten H.-J. et al., 2000] and [MacDonald P. et al., 2002].

The task of the second part of the benchmark was to compare the following parameters: criticality as a function of burnup between 0 and 60 MWd/kg, fuel composition as a function of burnup (Major actinides), local pin-by-pin power distribution, moderator temperature coefficient (MTC) for 0 and 60 MWd/kg, Doppler coefficient (DC) for 0 and 60 MWd/kg, and soluble boron worth (BW) for 0 and 60 MWd/kg.

Select results are compared in Tables 2.1.1.IV through 2.1.1.V and in Figure 2.1.1.2. Detailed description of the benchmark results can be found in [MacDonald P. et al., 2002]. The criticality predictions by different codes agree within about 2.5% at the BOL and within 3.5% at 60 GWd/t. The results obtained from both CASMO4 and MCODE fall within this range of uncertainty. The BOL eigenvalue predicted by CASMO4 is slightly higher (by 1.7%) than that predicted by MCODE. Although, the fuel temperature was the same in both codes' models (900K), the trend of higher reactivity prediction by CASMO4 at BOL and lower reactivity prediction at EOL remained the same as in the pin cell benchmark. The reasons for the differences are the same as discussed above for the unit cell calculations.

As in the pin cell benchmark task, the same number of nuclides (100 fission products and 29 actinides) was tracked in MCODE depletion calculations. All fuel pins in the MCNP (MCODE) assembly model were defined as a single material. Thus, the effects of local neutron flux differences on burnup of individual pins could not be fully accounted for. Despite this simplification, the agreement in the fuel isotopics prediction between MCODE, CASMO4 and IAEA benchmark results is plausible since the differences in neutron flux within the assembly are small.

Table 2.1.1.IV. Infinite Medium Neutron Multiplication Factor versus Burnup.

Burnup, MWd/kg	Russia	Japan	Korea	India	Israel	CASMO (MIT)	MCODE (MIT)
0	1.1890	1.1987	1.1734	1.2076	1.1956	1.2035	1.1836 ± 0.0013
0.5	1.1569	1.1670	1.1384	1.1736	1.1643	1.1721	-
20	1.0298	1.0521	1.0123	1.0372	1.0290	1.0360	1.0233 ± 0.0013
40	0.9147	0.9527	0.9057	0.9104	0.9119	0.9115	0.9124 ± 0.0011
60	0.8315	0.8657	0.8310	0.8294	0.8314	0.8188	0.8318 ± 0.0011

Water								
1.071 1.068 1.066 1.075	1.025 1.019 1.022 1.015			xxxx xxxx xxxx xxxx	Russia Japan Korea Israel			
1.069	1.013			xxxx	CASMO			
1.059 1.068 1.067 1.076	1.014 1.02 1.023 1.016	1.015 1.021 1.025 1.018						
1.069	1.016	1.016						
Water	1.068 1.068 1.067 1.075	1.072 1.071 1.071 1.078	Water					
	1.069	1.069						
1.063 1.066 1.065 1.074	1.016 1.018 1.023 1.015	1.009 1.023 1.027 1.02	1.084 1.084 1.084 1.091	1.08 1.068 1.085 1.074				
1.066	1.014	1.018	1.083	1.0744				
1.072 1.061 1.061 1.069	1.013 1.014 1.019 1.011	1.005 1.019 1.024 1.017	1.08 1.085 1.085 1.092	1.122 1.107 1.124 1.124	Water			
1.063	1.011	1.015	1.083	1.115				
Water	1.053 1.051 1.053 1.06	1.058 1.054 1.057 1.064	Water	1.099 1.081 1.098 1.1	1.049 1.045 1.049 1.055	0.963 0.965 0.968 0.964		
	1.055	1.059		1.095	1.051	0.966		
1.051 1.021 1.026 1.034	0.979 0.977 0.985 0.98	0.98 0.978 0.987 0.981	1.033 1.024 1.03 1.036	0.973 0.976 0.982 0.976	0.922 0.941 0.932 0.931	0.91 0.915 0.904 0.904	0.886 0.899 0.883 0.884	
1.033	0.981	0.986	1.032	0.980	0.935	0.912	0.891	
0.925 0.929 0.925 0.926 0.928	0.924 0.925 0.923 0.921 .0927	0.921 0.925 0.923 0.921 0.927	0.93 0.929 0.924 0.924 0.930	0.922 0.921 0.914 0.914 0.919	0.907 0.91 0.897 0.897 0.906	0.889 0.901 0.883 0.885 0.892	0.889 0.896 0.869 0.876 0.886	0.876 0.898 0.895 0.872 0.880

Figure 2.1.1.2. Pin-by-pin Relative Power Distribution in PWR Fuel Assembly at 60 MWd/kg

Table 2.1.1.V. Reactivity Coefficients (× 10^4) for 0 and 60 MWd/kg.

	0 MWd/kg			60 MWd/kg		
	MTC	DC	BW	MTC	DC	BW
Russia	-3.500	-0.280	-0.380	-1.500	-0.360	-1.100
Japan	-2.696	-0.283	-0.341	-0.969	-0.378	-0.864
Korea	-3.774	-0.319	-0.394	-2.928	-0.453	-1.070
Israel	-3.333	-0.292	-0.400	-1.142	-0.477	-1.119
CASMO	-3.768	-0.235	-0.403	-2.544	-0.359	-1.175

Reactivity coefficients were calculated only with CASMO4 because it has built-in capabilities for reactivity parameter calculations. Therefore, it was used for these purposes in this study. Pin-by-pin power distribution calculated with MCODE was performed for the BOL only since the computational time required for the depletion calculation of each fuel pin within the assembly is large for the currently available computer hardware. The agreement on the pin-by-pin power distribution prediction was found to be very good. All codes identified the hot fuel pin at the same location at BOL. The discrepancy in pin power prediction at EOL for different pin locations is between 5 and 10%.

The BOL values of reactivity coefficients are in reasonable agreement. Some discrepancies in reactivity coefficients predictions were observed at EOL. These discrepancies may be attributed to different Pu isotope concentrations. However, the trend of change with burnup is predicted correctly by all the computer codes.

In summary, the performed benchmark calculations confirm that CASMO4 and MCODE are suitable for scoping studies of thorium – plutonium based fuel designs. They predict reasonably well the criticality and composition of the fuel and their results fall within the uncertainties of other codes used by the participants in the IAEA international benchmark. The CASMO4 computer code can also be used for estimation of the fuel reactivity coefficients with a reasonable degree of confidence. However, careful evaluation of the accuracy of different computational tools for fuel design with large loadings of MA has yet to be performed. It should also be noted that the accuracy of currently available nuclear data for MA nuclides is limited to a considerable extent. For example, the differences in thermal cross-sections of some MAs between major nuclear data files can range up to 30% [M. Delpech et al. 1996]. In addition, multi level spatial homogenization and collapsing of energy groups performed by typical deterministic codes to

calculate region average cross-sections may lead to inaccuracies in some heterogeneous geometry cases. In such cases, benchmarking of computational tools is particularly important.

2.2. Neutronic Assessment of Thorium Fuel

All burnup and criticality calculations in this study were performed using the CASMO4 fuel assembly burnup computer code [Edenius et al. 1995], which uses a 70 energy group neutron cross-section library.

The burnup calculations were performed for a fuel pin cell geometry of a typical PWR. The reference fuel pin cell geometry and operating parameters used in the calculations are summarized in Table 2.2.I.

Table 2.2.I Reference Pin-Cell Geometry and Operating Parameters.

Fuel pellet diameter, mm	8.192
Gap thickness, mm	0.082
Outer Cladding diameter, mm	9.500
Lattice Pitch, mm	12.6
Fuel temperature, K	900
Coolant temperature, K	583
Power density, kW/l	104
Reference H/HM ratio	3.64

The effect of differences in the neutron energy spectrum was studied by changing the hydrogen to heavy metal atom ratio (H/HM). Different H/HM ratios were simulated by varying water density in the fuel pin cell of fixed reference geometry. For the purposes of the current study, this approach of varying H/HM can be considered neutronically equivalent to other more realistic options as demonstrated in [Xu Z. et al., 2002]. The H/HM ratios were varied in a wide range from about 0.002 to about 70. All fuel compositions analyzed in this study are summarized in Table 2.2.II.

In cases with zero MA loading, the isotopic composition of the Pu vector that was used is shown in Table 2.2.III. This composition corresponds to Pu in the spent fuel from a typical LWR,

using all-U fuel with initial U-235 enrichment of 4.5% and irradiated to about 50 MWd/kg, immediately after discharge. Four different initial Pu loadings of 7, 9, 11 and 15w/o relative to total HM in the fuel (cases 1 through 4 in Table 2.2.II) were analyzed to cover the whole range of possible fuel cycle lengths.

In Cases 5 through 8 in Table 2.2.II, 15w/o of natural uranium was added to the initial Pu-Th fuel composition in order to assure that the uranium proliferation index in the discharged fuel is smaller than 0.12. The uranium proliferation index is defined as: [Forsberg C.W. et al., 1999]

$$\frac{\text{Weight of } {}^{233}\text{U} + 0.6 \times \text{Weight of } {}^{235}\text{U}}{\text{Total Weight of Uranium}} < 0.12 \qquad (2.2.1)$$

The initial Pu and MA isotopic composition of the Pu-MA-Th fuel (Cases 9 through 11 in Table 2.2.II) is shown in Table 2.2.IV. This composition corresponds to the isotopics of 4.2% enriched conventional UO_2 fuel irradiated to 50 MWd/kg and then decayed for 10 years. Three different loadings of TRU in Th were studied, again, to cover a broad range of possible fuel cycle lengths. In the reference fuel pin cell geometry these three fuel compositions will result in 12, 18 and 36 months operating cycle lengths respectively.

In this part of the study, the amount of natural uranium added for denaturing of bred U233 was chosen to be about 20% relative to the amount of thorium in the fuel. It was assumed that all MAs in the fuel have the chemical form of $(MA)O_2$ with densities equal to the theoretical density of PuO_2.

Core leakage was neglected in these scoping studies and the reactivity limited single batch burnup (BU_1) and fuel cycle length were estimated by calculating the burnup at which kinf of the fuel equals unity. The discharge fuel burnup was estimated using a 3-batch linear reactivity model [Driscoll M.J. et al., 1990], as $1.5 \times BU_1$.

Table 2.2.II. Summary of Studied Fuel Compositions

Fuel Comp.	Description	Th, w/o	Natural Uranium, w/o	Pu, w/o	MA w/o	Isotopic vector
1	Pu-Th unden.	93.0	-	7.0	-	Table 2.2.III
2	Pu-Th unden.	91.0	-	9.0	-	Table 2.2.III
3	Pu-Th unden.	89.0	-	11.0	-	Table 2.2.III
4	Pu-Th unden.	85.0	-	15.0	-	Table 2.2.III
5	Pu-Th den.	78.0	15.0	7.0	-	Table 2.2.III
6	Pu-Th den.	76.0	15.0	9.0	-	Table 2.2.III
7	Pu-Th den.	74.0	15.0	11.0	-	Table 2.2.III
8	Pu-Th den.	70.0	15.0	15.0	-	Table 2.2.III
9	Pu-MA-Th den.	63.58	13.54	19.82	3.05	Table 2.2.IV
10	Pu-MA-Th den.	61.89	13.18	21.60	3.32	Table 2.2.IV
11	Pu-MA-Th den.	58.51	12.47	25.15	3.87	Table 2.2.IV
12	MOX	-	93.00	7.00	-	Table 2.2.III
13	All-U	-	100 (4.5% ^{235}U)	-	-	-

Table 2.2.III Initial Pu Isotopic Composition in Th - Pu Fuel

Isotope	Weight %
Pu-238	2.88
Pu-239	54.60
Pu-240	21.15
Pu-241	15.30
Pu-242	6.06

Table 2.2.IV. Initial Pu Isotopic Composition in Pu-MA-Th Fuel

Isotope	Weight %
U-234	0.0001
U-235	0.0023
U-236	0.0019
U238	0.3247
Np-237	6.641
Pu-238	2.7490
Pu-239	48.6520
Pu-240	22.9800
Pu-241	6.9260
Pu-242	5.0330
Am-241	4.6540
Am-242m	0.0190
Am-243	1.4720
Cm-242	0.0000
Cm-243	0.0050
Cm-244	0.4960
Cm-245	0.0380
Cm-246	0.0060

The Doppler reactivity coefficient (DC), Moderator temperature coefficient (MTC), Void coefficient (VC) and Soluble Boron Worth (BW) were calculated for the compositions 5 through 11 in Table 2.2.II at 3 different H/HM ratios and at 3 time points: beginning (BOL), middle (MOL) and end (EOL) of fuel irradiation. In order to simulate close to realistic operating reactor conditions, all reactivity coefficients were calculated assuming that the soluble boron concentrations are 1000 ppm, 500 ppm, and 0 ppm at BOL, MOL, and EOL respectively.

The reactivity coefficients were calculated as follows.

$$MTC = \frac{\Delta K}{K_1 \times K_2 \times \Delta T_m} \tag{2.2.2}$$

where ΔT_m is the moderator temperature difference between two moderator temperatures T_1 and T_2 and K_1 and K_2 are infinite medium neutron multiplication factors corresponding to temperatures T_1 and T_2, respectively.

$$DC = \frac{\Delta K}{K_1 \times K_2 \times \Delta T_f} \tag{2.2.3}$$

where ΔT_f is fuel temperature difference between two fuel temperatures T_1 and T_2.

$$VC = \frac{\Delta K}{K_1 \times K_2 \times \Delta V} \tag{2.2.4}$$

where ΔV is the difference between two coolant void fractions V_1 and V_2.

$$BW = \frac{\Delta K}{K_1 \times K_2 \times \Delta C} \tag{2.2.5}$$

where ΔC is boron concentration difference in ppm.

RESULTS: Pu-Th cases

One of the most important characteristics of the fuel designed for Pu disposition is the Pu destruction rate; namely, the number of kilograms of Pu destroyed per unit energy produced by the fuel. Figure 2.2.1 shows Pu destruction rates normalized per 1 GWeYear for both the denatured and undenatured cases. The Pu destruction rate is relatively insensitive to the Pu loading and to the H/HM ratio in the neighborhood of the reference H/HM value.

The rate of Pu destruction for low Pu loadings at low H/HM ratios (in the epithermal energy spectra region) exhibits an increase since the fuel cycle length in this region is relatively short (Figure 2.2.2) whereas fissile Pu239 burns out rather rapidly at the beginning of fuel irradiation, increasing total Pu destruction rate. Although high Pu destruction rates in this H/HM region can be achieved, very low fuel cycle length and, thus, frequent reprocessing makes these cases impractical and uneconomical. In contrast, the rate of Pu destruction for the fuel with high Pu loading monotonically decreases as H/HM ratio decreases (Figure 2.2.1). In this case, the energy derived from fission of U233 is substantial due to effective breeding in the epithermal and fast spectra. The initial Pu loading is high enough to sustain core criticality until a significant amount of U233 is generated. As a result, the Pu destruction rate is reduced because of the competition between neutron absorption in Pu and U233, although high burnup, in general, results in deeper Pu burning as shown in Figure 2.2.3. However, the calculated achievable burnup is an overestimate since neutron leakage was not considered. Additionally, due to the harder neutron spectrum, leakage is expected to be higher in Pu containing cores than in all-U core.

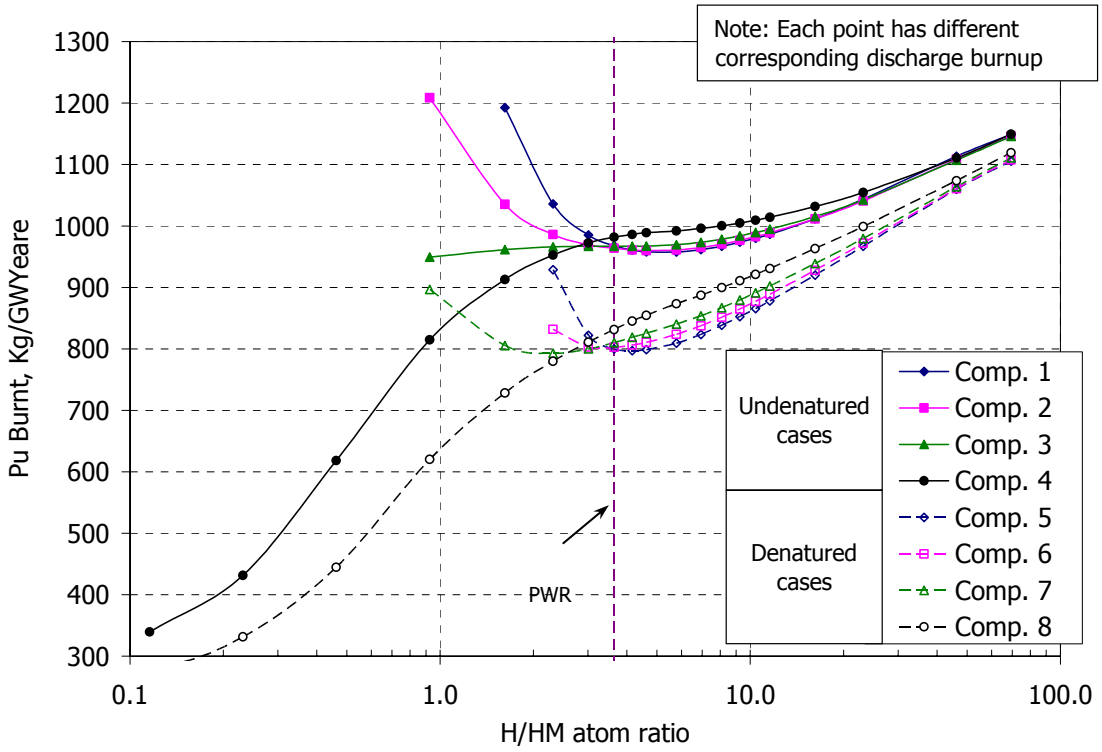

Figure 2.2.1 Energy Normalized Pu Destruction Rate

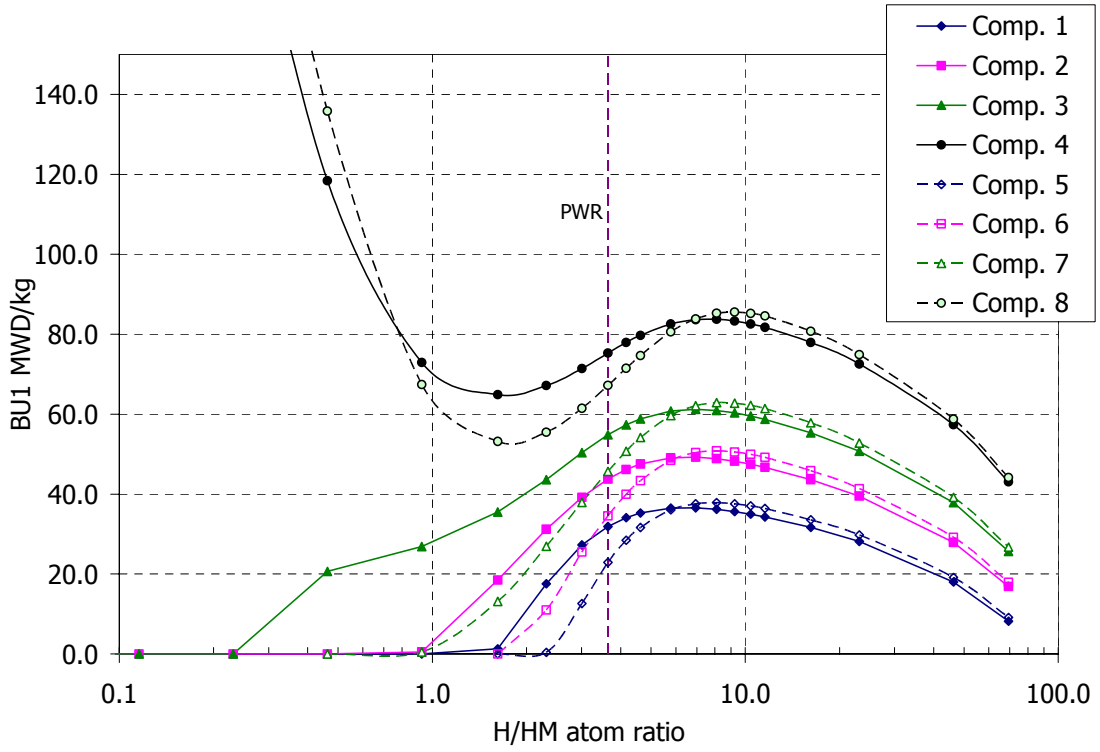

Figure 2.2.2. Reactivity Limited Burnup (BU1) vs. H/HM Ratio

Figure 2.2.3 also suggests that significantly deeper Pu burning (that is, lower fraction of residual Pu in discharged fuel) in a PWR core cannot be attained by the variation of H/HM ratio. However, there is an improvement from 67% up to 75% in destroyed Pu fraction by increasing the H/HM ratio from 3.64 to about 7 for undenatured fuel compositions (cases 1 through 4 in Table VII). Nevertheless, at high H/HM in a given core volume, the total initially loaded Pu will be smaller.

Addition of uranium to the fuel decreases the Pu destruction rate as expected. Figure 2.2.1 illustrates this fact. At the reference H/HM ratio point, the addition of 15w/o of natural uranium reduces the rate of Pu destruction by about 20%, although this relative reduction in the destruction rate becomes smaller for "wetter" than reference fuel lattices. Even at the reference H/HM, 50% Pu destruction is possible.

At the reference H/HM ratio, denaturing can almost double the amount of residual Pu (Figure 2.2.3). However, at higher than reference H/HM ratios, the difference between the denatured and undenatured cases becomes smaller and even vanishes for highly over-moderated lattices. This is partially due to the fact that denatured cases in the over-moderated region achieve slightly higher burnup due to the higher BOL reactivity and more efficient consumption of Pu. Furthermore, the conversion of Th232 to U233 is more efficient while the breeding of Pu239 from U238 is less efficient in a well thermalized spectrum due to a higher thermal absorption but lower resonance integral for Th232 than for U238. Additionally, the sensitivity of the residual Pu fraction to H/HM ratio is notably greater for denatured cases than for undenatured cases. An increase of H/HM from the reference value to about 10 can reduce the residual Pu fraction nearly by a factor of 2.

Changing the H/HM to such a high values is probably impractical in conventional PWRs. For the fixed core power and volume, an increase in H/HM through the variation of fuel pin diameter or total number of pins would mean a displacement of fuel on the expense of moderator and lead to either higher fuel temperature or heat flux to coolant. Increasing the H/HM should be done in way that would minimize the reduction in fuel loading per unit volume of the core. Using annular fuel pellets or annular internally cooled fuel is preferable to increasing the pitch to diameter ratio because it allows to keep fuel temperature and MDNBR within acceptable limits. In such case, the local fuel burnup will become a limiting factor if the cycle length is preserved.

Figure 2.2.4 shows the uranium proliferation index as a function of H/HM for denatured cases. Addition of 15 w/o of natural uranium seems to be enough to assure the proliferation resistance of uranium in discharged fuel for most of the calculated cases. In fact, the uranium proliferation index decreases with H/HM which indicates that the amount of natural uranium can be reduced for wetter fuel lattices, which also improves Pu burning performance.

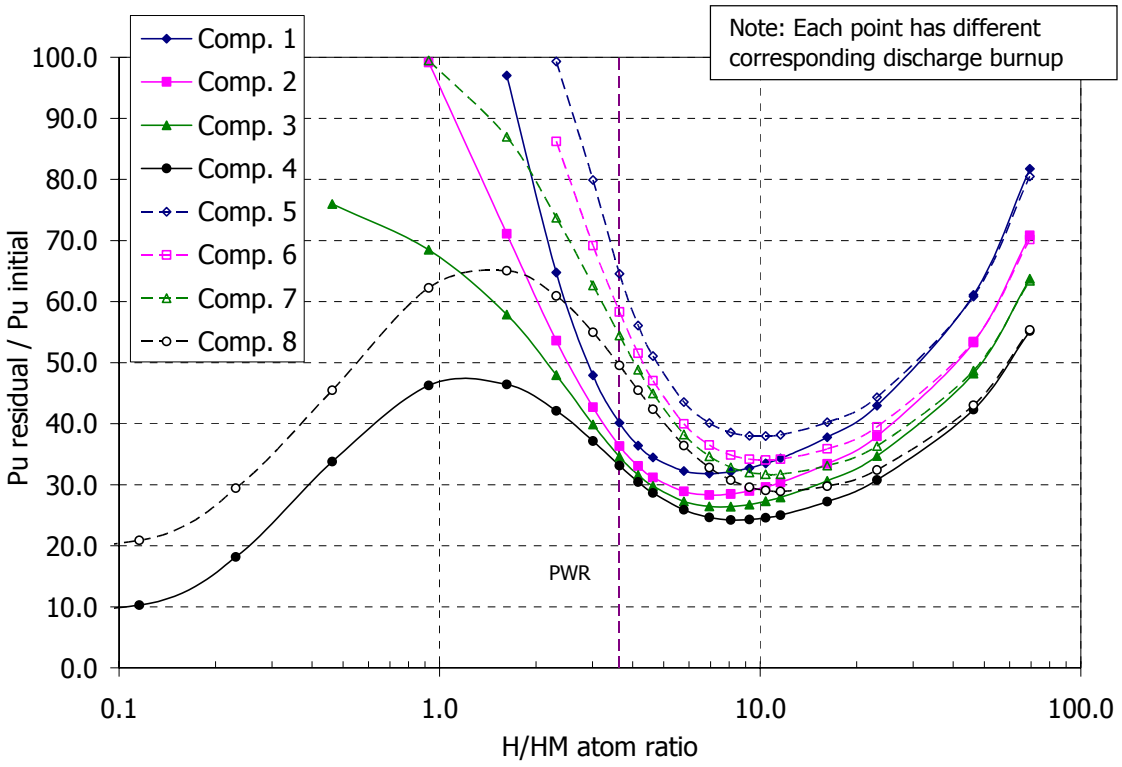

Figure 2.2.3. Residual Pu Fraction

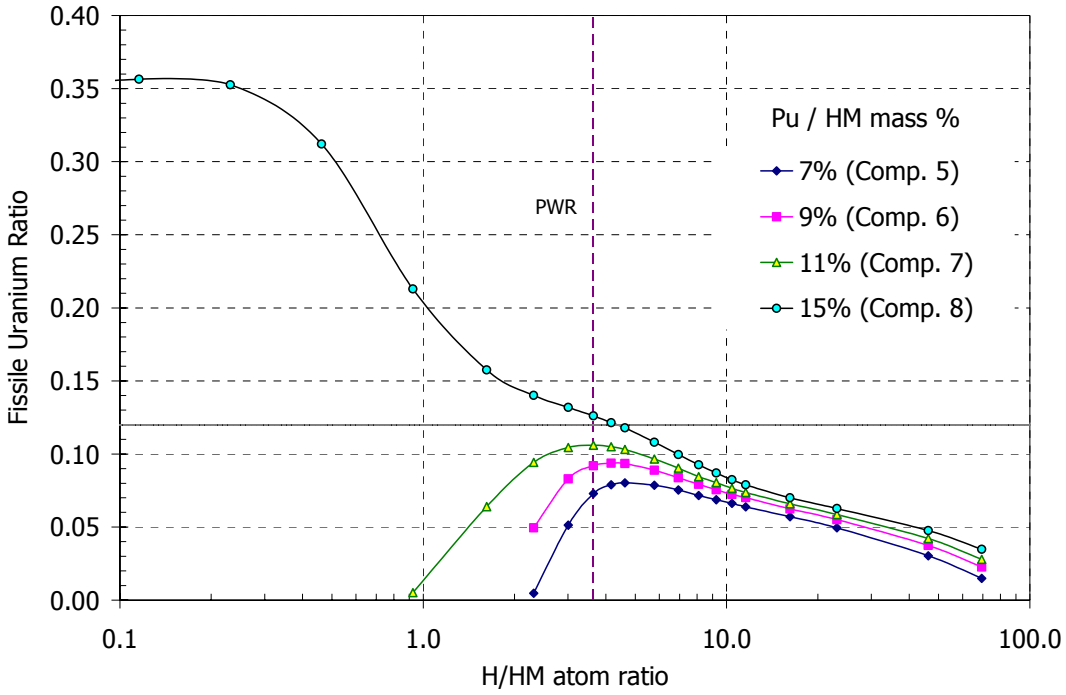

Figure 2.2.4 Uranium Proliferation Index

RESULTS: Pu-MA-Th cases

The potential of TRU destruction is an important feature of innovative fuel designs which can help the effort to reach sustainable fuel cycles. Only systems that utilize fuel which burns more TRU than originally loaded have the ability to reach an equilibrium state in a completely closed fuel cycle with zero net generation of TRUs.

Thorium based fuels used for disposition of Pu and MA, although they do not create a new generation of Pu and MA, produce noticeable amounts of actinides originating from Th232. The most valuable nuclide for the sustainable closed fuel cycle scenario is U233. It typically constitutes over 90% of all Th chain isotopes. It has a large thermal fission cross-section; thus, it can be efficiently recycled. However, small amounts of other Th chain nuclides are long lived and radioactive. For example minute quantities of U-232 can significantly complicate fuel reprocessing and fabrication because of the presence of strong γ-emitters in its decay chain [Laughter M. et al., 2002]. Therefore, in a once-through actinide destruction cycle, with the main objective being to maximize the consumption of TRU per path, Th chain nuclides have to be

included in the total balance of actinides discharged to the repository. In such TRU burndown scenario, the presence U232 would attribute to intrinsic protection of the spent fuel from being a potential target for nuclear proliferators.

Figure 2.2.5 reports TRU destruction rates normalized per 1 GWeYear for 3 different initial TRU loadings that in the reference PWR fuel pin cell geometry will result in 12, 18 and 36 month fuel cycle lengths (Figure 2.2.6), assuming 3 batch fuel management and typical PWR specific power. In this part of the study we report the TRU destruction rates and their residual amounts with and without including the Th chain nuclides in the total balance, since both indices are of interest.

The following observations can be made.

- The TRU destruction rates monotonically increase with increasing H/HM ratio over the whole investigated range of fuel lattice geometries. Therefore, it is always beneficial to keep H/HM as high as possible from the TRU destruction rate viewpoint.

- The destruction rates of TRU without Th chain nuclides are not sensitive to the initial TRU loading.

- The contribution of Th chain nuclides to total TRU destruction rate varies with H/HM and initial TRU loading. This variation originates in the fact that the efficiency of U233 buildup depends on H/HM as well as on other actinide inventories.

Figure 2.2.7 shows the MA-only contribution to the total TRU destruction rate. As can be observed, the actual reduction in MA inventory can be achieved only for highly over-moderated lattices if Th chain nuclides are included in the balance. If Th chain nuclides are not considered, the reduction of MA inventory is possible with a rate of about 100 kg per GWeYear. This rate appears to be remarkably insensitive to the initial TRU inventory and H/HM ratio in the range of practical interest (from 1 to 10).

The fraction of residual TRU in spent fuel not including Th chain nuclides is shown in Figure 2.2.8. The data plotted in Figure 2.2.8 suggests that the reference pin cell geometry is highly unfavorable from the effectiveness of TRU destruction standpoint. Higher initial TRU loadings

are preferable as they result in deeper TRU burnout for H/HM ratios close to the reference one. However, this difference vanishes as H/HM approaches 10. The maximum theoretically achievable degree of TRU burnout is about 50% of initial loading at H/HM of about 11.

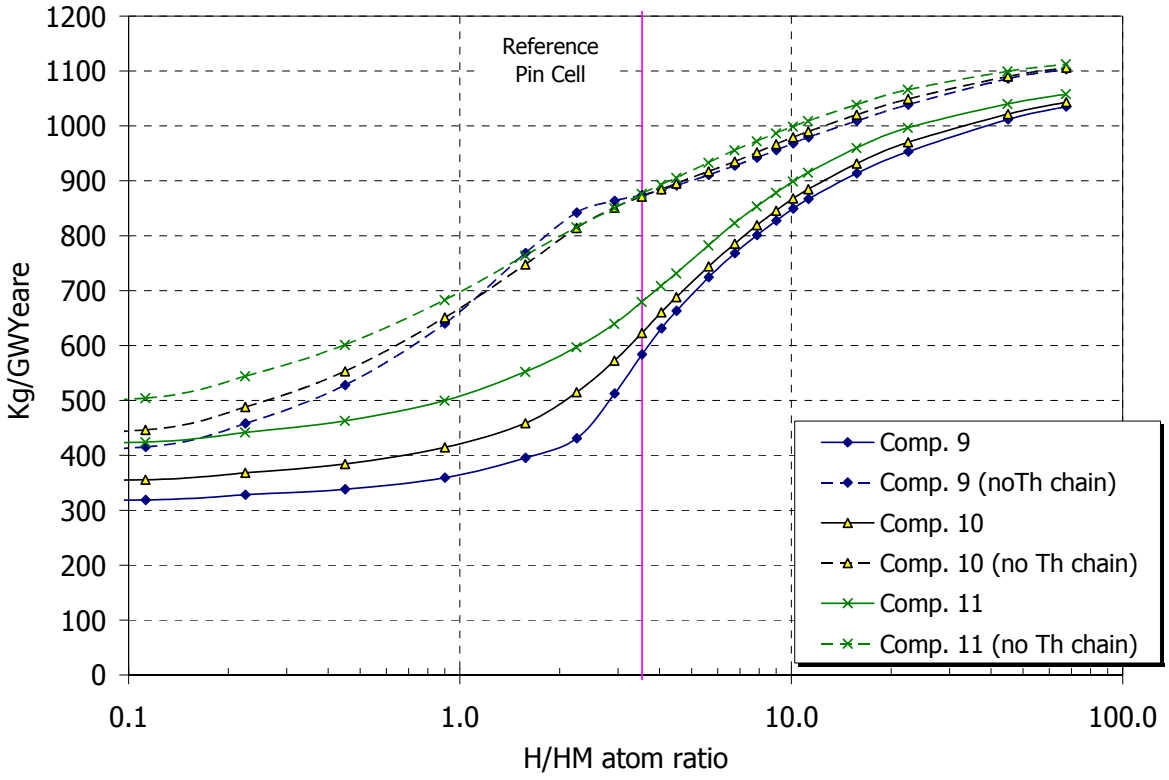

Figure 2.2.5. Energy Normalized TRU Destruction Rate

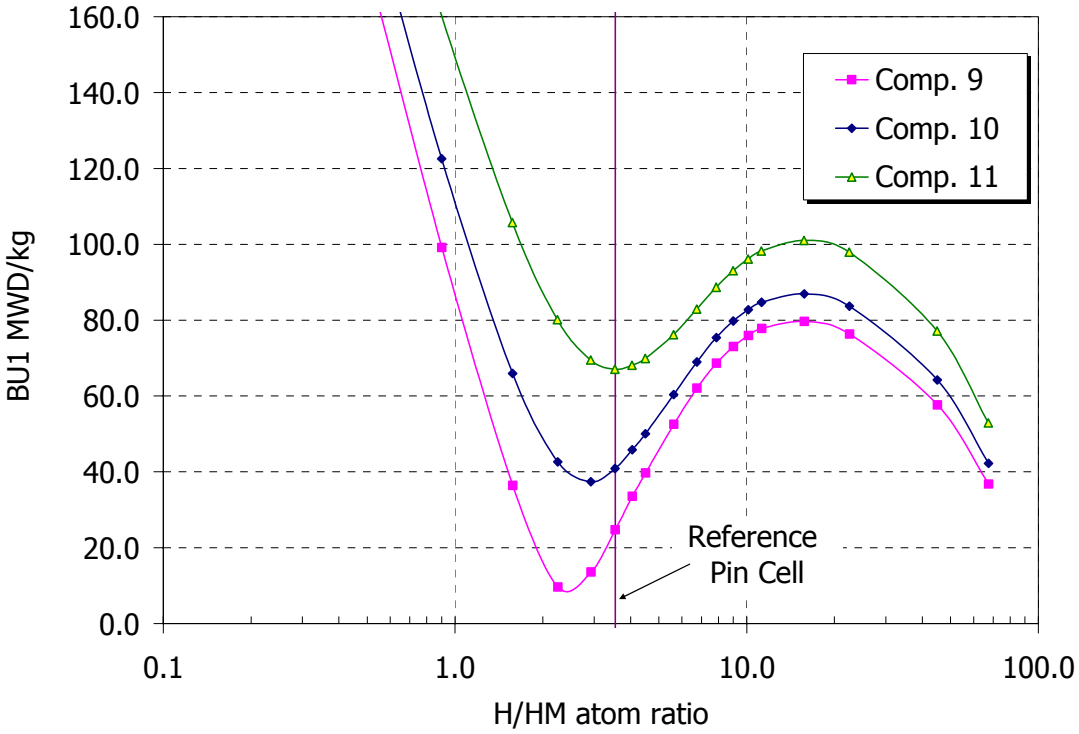

Figure 2.2.6. Reactivity Limited Burnup (BU1) vs. H/HM Ratio

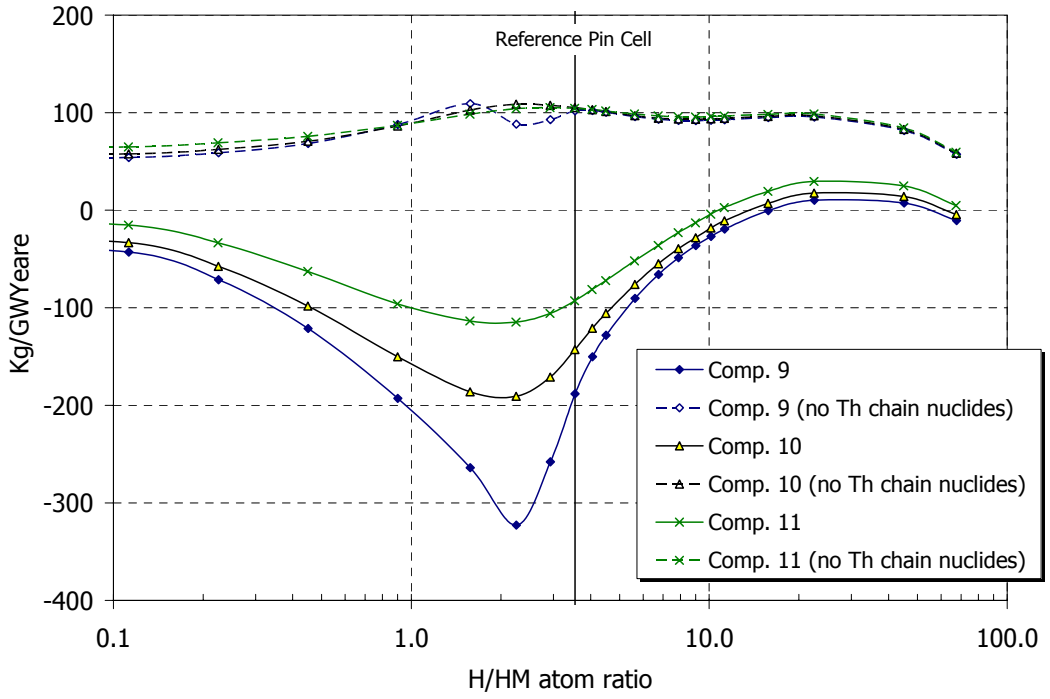

Figure 2.2.7. Energy Normalized MA destruction Rate

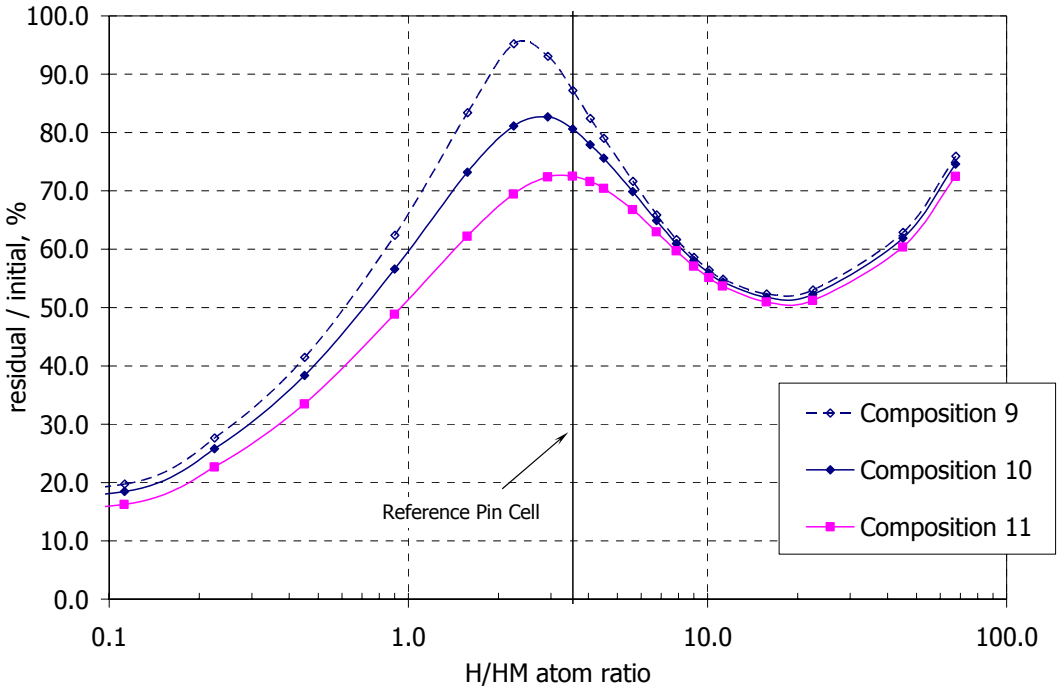

Figure 2.2.8. Residual Fraction of TRU (No Th chain nuclides)

RESULTS: Reactivity Coefficients

The results presented above suggest that higher than reference H/HM ratios are preferable for effective Pu destruction. Therefore, the reactivity coefficients were evaluated at H/HM values ranging from the reference PWR fuel pin cell to reference + 40% H/HM.

All reactivity coefficients were calculated on the basis of a pin cell geometry. Core average reactivity coefficients would be somewhat different as the core is uaually composed of fuel assemblies with different accumulated burnup. The pin cell based calculations, however, can be used for comparison of different fuel designs with different compositions and H/HM ratios against the reference UO_2 fuel evaluated on the same basis.

Selected reactivity coefficients as well as soluble boron worth calculations are summarized in Table 2.2.V. All fuel compositions presented in Table 2.2.V correspond to the 18 months cycle length currently widely accommodated by the nuclear industry.

MOX fuel provides somewhat stronger Doppler fuel temperature reactivity feedback (DC) than all-U fuel, while Pu-Th fuel has even more negative DC than MOX. Wetter lattices yield slightly less negative DC than the reference one due to the lower epithermal flux, nevertheless, Pu-Th fuel in a wetter lattice has still more negative DC than the reference All-U fuel.

Strongly negative DC is beneficial for transients associated with fuel temperature increase as it provides prompt negative reactivity feedback, however it results in larger reactivity insertion in startup and shutdown scenarios. Stronger DC may also be a disadvantage in the reactor's response to sudden cooldown scenarios, such as a steam generator depressurization event.

Calculated Moderator temperature and Void coefficients (MTC and VC respectively) for Th based fuels are negative and exhibit smaller variation with burnup than All-U and MOX fuel. The absolute values of MTC and VC of Pu-Th cases are close to those observed for typical MOX fuel while Pu-MA-Th fuels have MTC and VC values close to those of the All-U case. The calculated values of MTC and VC are consistent with those previously reported in [Lombardi C. et al., 199] and [Phlippen P.W. et al., 2000]. The effect of increased H/HM ratio is not particularly significant for Th based cases. All reactivity coefficients stay negative over the entire investigated range of H/HM values.

Table 2.2.VI shows an example of the BOL reactivity control requirements and soluble boron worth (BW) for a number of calculated cases. The BOL whole core excess reactivity was estimated assuming a 3 batch core with linear burnup-reactivity dependence for each batch. 3% of $\Delta\rho$ was allowed for leakage. No burnable poisons were considered. The BW of partially burned batches was assumed to be equal to the fresh batch BW, which is a conservative assumption since BW, generally, increases with the burnup due to depletion of fissile nuclides and therefore softer spectrum.

Although Pu-Th and Pu-MA-Th fuels require much smaller initial excess reactivity to control, the soluble boron worth is much smaller than that of the All-U fuel. As a result, the soluble boron concentrations required to control the initial excess reactivity are comparable to All-U fuel and in some cases considerably higher. Increasing the loading of TRUs in Th based fuels leads to harder neutron spectra and, therefore, lower soluble boron worth. Higher than reference H/HM increases neutron moderation and, as a result, increases soluble boron worth.

In general, the relatively hard neutron spectrum in all TRU containing fuels necessitates that special attention be devoted to the design of reactor control. Utilization of enriched boron or gadolinium in control rods or as a burnable poison might be necessary to satisfy reactor safety criteria for Th-TRU fuel designs.

Table 2.2.V Reactivity Coefficients: Selected Results

Dopler Coefficient, pcm/K							
Comp. No.	Description	Reference H/HM			Reference + 40% H/HM		
		BOL	MOL	EOL	BOL	MOL	EOL
6	Pu-Th den.	-4.32	-4.65	-5.04	-3.43	-3.78	-4.22
9	Pu-MA-Th den.	-2.98	-3.02	-3.15	-2.63	-2.80	-3.02
12	MOX	-2.92	-3.09	-3.20	-2.36	-2.57	-2.70
13	All-U	-2.20	-2.93	-3.33	-1.82	-2.31	-2.75
Moderator temperature Coefficient, pcm/K							
6	Pu-Th den.	-49.05	-58.68	-73.47	-38.91	-50.40	-66.73
9	Pu-MA-Th den.	-18.53	-17.69	-23.40	-29.57	-33.17	-44.86
12	MOX	-40.63	-54.65	-73.78	-32.37	-46.92	-66.39
13	All-U	-22.17	-51.62	-77.79	-2.21	-26.00	-50.07
Void Coefficient, pcm/%void							
6	Pu-Th den.	-128.0	-156.8	-198.3	-104.8	-142.9	-190.4
9	Pu-MA-Th den.	-42.8	-41.4	-51.7	-70.8	-85.3	-115.8
12	MOX	-104.8	-145.3	-200.7	-86.0	-130.8	-190.8
13	All-U	-62.5	-145.7	-228.0	-10.8	-83.5	-164.8
soluble boron worth, pcm/ppm							
6	Pu-Th den.	-1.95	-2.28	-3.02	-2.82	-3.60	-5.15
9	Pu-MA-Th den.	-1.05	-1.03	-1.24	-1.73	-1.90	-2.24
12	MOX	-1.96	-2.37	-2.76	-2.88	-3.70	-4.85
13	All-U	-4.80	-5.22	-6.23	-6.65	-8.15	-11.90

Table 2.2.VI. Soluble Boron Requirements for Reactivity Control at BOL

Reference H/HM					
Fuel Comp.	Description	K-inf (BOL), Pin cell	Core Average reactivity (BOL), pcm	SB worth pcm/ppm	ppm needed for control
5	Pu-Th den.	1.119	4098	-2.41	1699
6	Pu-Th den.	1.146	5183	-1.95	2664
7	Pu-Th den.	1.170	6136	-1.66	3703
8	Pu-Th den.	1.216	7849	-1.24	6322
9	Pu-MA-Th den.	1.062	1533	-1.05	1456
10	Pu-MA-Th den.	1.078	2281	-0.97	2358
11	Pu-MA-Th den.	1.109	3672	-0.81	4525
12	MOX	1.206	7473	-1.96	3804
13	All-U	1.380	12953	-4.80	2698
Reference H/HM × 1.4					
5	Pu-Th den.	1.195	7092	-3.41	2080
6	Pu-Th den.	1.216	7858	-2.82	2788
7	Pu-Th den.	1.235	8501	-2.42	3512
8	Pu-Th den.	1.269	9631	-1.92	5022
9	Pu-MA-Th den.	1.100	3289	-1.73	1903
10	Pu-MA-Th den.	1.111	3765	-1.62	2320
11	Pu-MA-Th den.	1.133	4680	-1.41	3324
12	MOX	1.275	9829	-2.88	3415
13	All-U	1.440	14528	-6.65	2185

It was also found that prompt neutron lifetime is significantly smaller than that of all-U fuel and comparable to MOX fuel values. More importantly, the effective delayed neutron fractions of Pu-Th fuel are smaller than the values for all-U by about a factor of two and smaller than MOX fuel values at EOL by more than a factor of 1.5, as shown in Table 2.2.VII. Smaller β_{eff} is a major challenge for the cores fully loaded with Th-Pu fuel and the feasibility of reactor controllability under such low β_{eff} requires further investigation. In addition, small reactivity worth of the control materials and low β_{eff} values in Pu-Th containing PWR cores may lead to much higher reactivity in dollars vested in control rods and soluble boron in comparison with conventional UO2 and

MOX cores, which is a potential concern in reactivity initiated accidents. Smaller effective delayed neutron fraction is the consequence of the smaller delayed neutron yield of Pu239 and U233 in comparison to that of U235 and smaller fast fission contributions from Th232, which has a higher delayed neutron yield than U238. Denatured Pu-Th fuels (cases 5 through 9 in Table 2.2.II) have slightly more favorable β_{eff} values than undenatured Pu-Th fuels (cases 1 through 4 in Table 2.2.II) because of the fast fission contribution from U238.

The prompt neutron lifetime values indicate significantly faster reactor kinetics in comparison with All-U, MOX and even with Pu-Th cases. More importantly, the effective delayed neutron yield is below 0.003 for all calculated Pu-MA compositions which challenges the reactor core behavior in reactivity initiated accidents.

Table 2.2.VII Effective Delayed Neutron Yield (β_{eff}) × 10^3

	H/HM Ratio					
	Reference			Reference + 20%		
Composition	BOL	MOL	EOL	BOL	MOL	EOL
1 (Pu – unden.)	2.98	2.76	2.46	2.99	2.84	2.42
2 (Pu – unden.)	3.00	2.81	2.39	3.00	2.89	2.36
3 (Pu – unden.)	3.01	2.77	2.41	3.01	2.88	2.44
4 (Pu – unden.)	3.02	2.74	2.41	3.02	2.86	2.45
5 (Pu – den.)	3.14	3.07	2.85	3.13	3.01	2.81
6 (Pu – den.)	3.14	2.96	2.75	3.13	3.01	2.76
7 (Pu – den.)	3.15	2.95	2.71	3.14	2.98	2.76
8 (Pu – den.)	3.15	2.89	2.62	3.14	2.95	2.70
9 (Pu-MA-den.)	2.63	2.57	2.53	2.69	2.65	2.63
10 (Pu-MA-den.)	2.66	2.58	2.51	2.68	2.63	2.60
11 (Pu-MA-den.)	2.62	2.50	2.43	2.65	2.58	2.55
12 (All-U)	7.23	5.49	4.80	7.20	5.54	4.81
13 (MOX)	4.01	4.10	4.15	3.92	4.06	4.15

2.3. Analysis of Heterogeneous Fuel Geometries

Heterogeneous Pu-MA-Th fuel assembly geometries offer some potential advantages over the homogeneous Pu-MA-Th fuels. Assuming that Pu and MA come as separate streams from the separation process, the relative amounts of Pu and MA in the fuel can be varied so that most of the Pu can be concentrated in one type of fuel assemblies while all of the MA can be concentrated in another type of assemblies. Therefore, for each assembly type, the fuel lattice can be optimized to a certain degree for preferential destruction of either Pu or MA. Additionally, different fuel management schemes can be applied to the fuel assemblies containing different relative amounts of Pu and MA. As a result, assembly types that required to reach higher burnup (and, therefore, higher TRU destruction efficiency) can reside in the core for larger number of cycles than other types of fuel assemblies.

An assessment of these potential advantages for an equilibrium core containing heterogeneous fuel configurations were performed with the CASMO-4 computer code that allows 2D transport and burnup calculations of 2x2 segment ("colorset") of fuel assemblies of different types. A schematic diagram of such 2x2 colorset of fuel assemblies is shown in Figure 2.3.1.

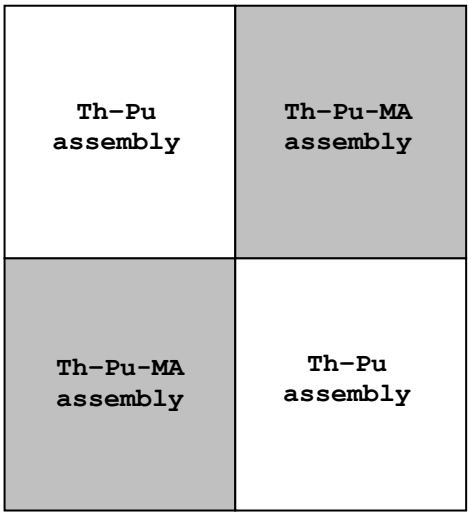

Figure 2.3.1. Example of CASMO 2x2 colorset layout.

The analysis of heterogeneous fuel configurations was performed through variation of fuel composition (Pu:MA:Th ratio) and variation of lattice H/HM ratio for each assembly type and the destruction efficiencies and destruction rates for Pu and MA averaged over the entire colorset

were examined. At the same time, a number of constraints were imposed in order to ensure feasibility of realistic designs:

- Pu content in Pu-MA-Th assembly is large enough to provide colorset pin-power peak of less than 1.2
- Variation of fuel pin diameter in H/HM optimization is in the range of ± 20 % of the reference one
- Colorset average Pu to MA ratio is the same for all calculated cases and the TRU isotopic vector used is as presented in Table 2.2.IV.
- Colorset average TRU loading is selected to provide average colorset discharge burnup corresponding to fuel cycle length of about 18 months assuming 3 batch reloading scheme for both types of fuel assemblies comprising the colorset.

The results of this preliminary analysis show that no significant improvements in TRU destruction efficiencies or destruction rate can be achieved with heterogeneous fuel configurations via lattice optimization under the imposed constraints. The residual fraction of MA in the heterogeneous colorset never exceeded the corresponding value of homogeneous fuel of the same composition if simultaneous discharge of the entire colorset is assumed. This is due to relatively low power fraction generated by the Pu-MA-Th assemblies. However, above 50% of MA can be potentially destroyed (not including U233 and other Th chain nuclides) if Pu-MA-Th assemblies are driven to 100 MWd/kg burnup due to less frequent than Pu-Th assemblies refueling.

Although the Pu-MA-Th assemblies exhibit very flat reactivity behavior during irradiation, the heterogeneous cores have higher power peaking factors than homogeneous cores due to the fact that Pu-MA-Th assemblies are sub-critical during the entire irradiation period.

The calculated colorset average reactivity coefficients are comparable to those of the homogeneous Th-Pu-MA assembly. However, small local β_{eff} in MA containing assemblies in the colorset may challenge the fuel performance in control rod ejection accident. The effect of small β_{eff} will be offset to some extent by slightly more negative Doppler coefficient than in the reference UO_2 case.

Additionally, feasibility of fuel designs with high loadings of MA may be limited by fuel handling and fuel material performance issues because of the increased γ-radioactivity and He generation in the fuel due to α-decay of relatively short lived MA (primarily Cm-242 that is produced by neutron captures in Am-241 and subsequent β-decay of Am-242).

Finally, for the heterogeneous fuel types discussed above, proliferation resistance of the fuel cycle is somewhat compromised by the fact that the Pu is separated from the MA during certain stages of the cycle and, therefore, is less self-protected.

2.4. Chapter Summary

In this chapter, potential limits for the efficiency of Pu and MA destruction in Th based fuels of PWRs are discussed. The primary focus was on two performance indices: the rate of TRU destruction and residual fraction of TRU relative to initial TRU loading.

The performed benchmark calculations confirmed that CASMO4 and MCODE are suitable for scoping studies of thorium – TRU based fuel designs. They predict reasonably well the criticality and composition of the fuel within the uncertainties of cross-section data libraries.

The results showed that Th based fuel designs can be effectively used to reduce existing stockpiles of TRU in PWRs and, theoretically, can be part of a sustainable closed fuel cycle system with zero net generation of TRUs.

The reasonably achievable rate of Pu destruction in Th based fuel is about 1000 kg of TRU destroyed per 1 GWeYear, while up to 50% of initially loaded Pu can, theoretically, be destroyed per path. The addition of MA to Pu and Th reduces the rate of destruction by about 10%.

Denaturing of generated U233 with natural uranium degrades the efficiency of Pu destruction. However, denaturing is required only for the once-through fuel cycle. In that case, denaturing reduces Pu destruction rates by approximately 20%. The difference in the destruction rate and the residual Pu fraction between the denatured and undenatured cases decreases for wetter than reference lattices.

The calculated reactivity coefficients and their comparison with MOX and All-U fuel indicate the potential feasibility of Th based fuels utilization for transmutation of TRU in PWRs.

Somewhat wetter fuel lattices than present PWRs are favorable from the TRU destruction efficiency and reactivity control perspectives. Pu and MA containing Th based fuels have significantly harder neutron spectra than for typical all-U fuel, which reduces control materials worth and imposes additional requirements on the design of reactor control features.

It was found that heterogeneous fuel configurations, with fuel assemblies having different relative amounts of Pu and MA, are not capable of improving TRU destruction capabilities beyond those of the more simple homogeneous fuels. However, the option of choosing different fuel management schemes for different assembly types provides additional flexibility to destroy preferentially Pu or MA via variation of in-core residence time for each type of the assemblies.

Chapter 3. Fertile-Free Fuel

Generation of TRUs in the fuel can be effectively constrained if the fertile isotope U238 is substituted partially or completely by a neutronically inert fertile free matrix material.

Numerous studies carried out in the past have shown that the Reactors Grade (RG) and Weapons Grade (WG) Pu can be effectively burned in the fertile-free fuels (FFF) while maintaining comparable to current generation PWRs the reactivity control and safety characteristics of the fuel. ([U. Kasemeyer et al. 1998], [Baldi S. et al. 2001], [Lombardi C. et al. 1999] and others)

Pu or TRU can be either mixed homogeneously with or dispersed as micro-size particles in the inert matrix. The dispersed micro-particles approach provides additional flexibility in the choice of matrix materials. The matrix and the micro-particle materials can be separately chosen so that in combination they will provide good mechanical and chemical stability, radiation damage resistance, compatibility with the cladding material and water coolant in addition to good thermal properties and low parasitic neutron absorption. The matrix material has also to be chemically stable in the nuclear waste repository environment, at the same time it should preferably allow a simple and inexpensive reprocessing.

The focus of this section is mainly on a preliminary neutronic evaluation of the TRU containing FFFs. In particular, $MgAl_2O_4$ (Spinel) was chosen as a primary host matrix material and Yttria Stabilized Zirconia (YSZ) was chosen to be a part of the micro-spheres composition in order to enhance the irradiation and mechanical stability of the fuel particles. The dispersed micro particles structure allows confining the radiation damage to the fuel particles themselves and protecting the host matrix. The detailed arguments promoting the choice of these inert materials to be used in the current study are described in the Section 3.2. The development of FFF matrix materials requires significant amount of research and experimental work. The effect of different inert matrix materials on the neutronic performance is expected to be small because low cross-section for interaction with neutrons is one of the major requirements for the matrix material choice.

As in the previous section discussing the thoria based fuel, a series of benchmark calculations were performed for the fertile-free fuel using available computational tools in order

to evaluate their capability to handle non-conventional fuel designs with large loadings of TRUs. Then, TRU destruction rates and residual fractions of Pu and MA in the spent fuel were calculated for various fuel geometries and compositions. In addition, reactivity feedback coefficients were calculated for a number of cases to assess the feasibility of using FFFs in the current generation of PWRs.

3.1. Benchmark of Computational Tools

The CASMO4 computer code was used for evaluation of the fertile free fuels. This section addresses two primary concerns regarding the capabilities of CASMO4 to predict with a reasonable accuracy the criticality and nuclides evolution with burnup of the fuel micro particles dispersed in the inert matrix.

- The CASMO4 utilizes 70 energy groups cross-sections library that were generated using the typical LWR energy spectrum. In the fuel with large loadings of Pu and MA, the neutron energy spectrum tends to be much harder than generally encountered in a conventional LWR. In addition, the 70 group library may not be sufficient to reflect the resonance structure differences of TRU nuclides which typically have minor contribution to total neutron absorption but which can be significant for the cases with high TRU loading and especially in FFF case. Therefore, a cross-section library with a larger number of energy groups might be needed to produce accurate results for TRU containing fuel designs.

- CASMO4 cannot explicitly handle heterogeneous structure of the fuel pellet. Therefore, only homogeneously mixed fuel and matrix materials in a solid fuel pellet can be modeled. The additional level of heterogeneous structure in the dispersed particle fuel creates an additional resonance self-shielding effect, which would be completely neglected in the CASMO4 calculations. The magnitude of this effect depends on the particle's size, composition and relative number densities of the matrix and the fuel.

Three fuel pin cell burnup calculations were performed in order to assess the effect of using 70 group cross-section library and the effect of the double heterogeneous structure on criticality and the isotopes evolution predicted by the CASMO4 code.

In the first case, the fuel micro sphere geometry was explicitly modeled in MCNP4C [Briemsmeister J. 2000]. The fuel pin cell geometry is schematically presented in Figure 3.1.1. The fuel micro particles were arranged in a simple cubic lattice with a total fraction of 30 v/o occupied by the fuel particles. All of the fuel particles had an identical diameter of about 150 μm. This particle size is close to the optimal one in terms of the mechanical and thermal properties of the fuel as well as its ability to sustain radiation damage [Long Y. et al., 2003],[Yuan Y. et al., 2001]. The burnup calculations were performed using the MCODE [Xu Z. et al., 2002] – MCNP-ORIGEN linkage utility program. The ENDF-BVI based continuous energy cross-sections set was used for the MCNP calculations. The number of neutron histories in the Monte-Carlo simulation was chosen so that the sufficient number of collision events had occurred in nearly every fuel micro particle in order to ensure that the double-heterogeneous self-shielding effect is represented correctly.

In the second case, the MCODE calculation was repeated for the fuel pin cell of identical geometry and materials composition except for the fact that in this case the fuel particles (TRUs and YSZ) and the Spinel matrix were homogeneously smeared over the entire fuel pellet volume.

Finally, the homogeneously mixed fuel (TRU, YSZ and Spinel) case identical to the second one was calculated with CASMO4.

Figure 3.1.2 reports the results of the criticality prediction by MCODE and CASMO4 for the three calculated cases. The difference in k_∞ between the homogeneous and heterogeneous cases calculated with the MCODE is on the order of a fraction of a percent. At a number of data points the difference is larger than the statistical error. This suggests that k_∞ value is somewhat higher in the heterogeneous case than in the homogeneous case although in general the overall double-heterogeneity effect is small. In the case of UO2 TRISO micro particles used in Pebble-bed gas cooled reactors [Koster A. et al., 2003], the effect of double heterogeneity is appreciable [Lebenhaft J.R et al., 2002]. The observed small magnitude of this effect in the current benchmark case can be attributed to the small fuel particle size and relatively low concentrations of the fertile resonance nuclides in contrast to conventional UO_2 fuel with its large concentration of U238. Another reason could be the fact that the total resonance absorption in the fissile and fertile nuclides changes by a similar factor due to additional self-shielding introduced by the double-heterogeneous geometry so that the overall criticality of the system changes only marginally. The confirmation of these assumptions requires additional investigation.

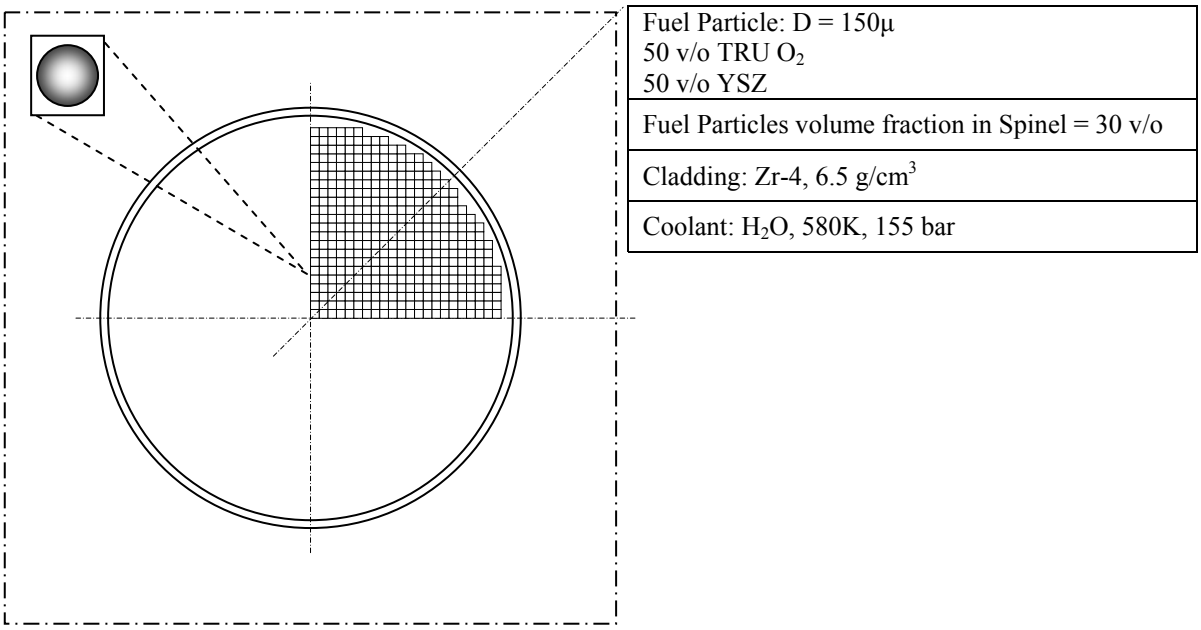

Figure 3.1.1 Double-Heterogeneous Fuel Pin Cell Geometry

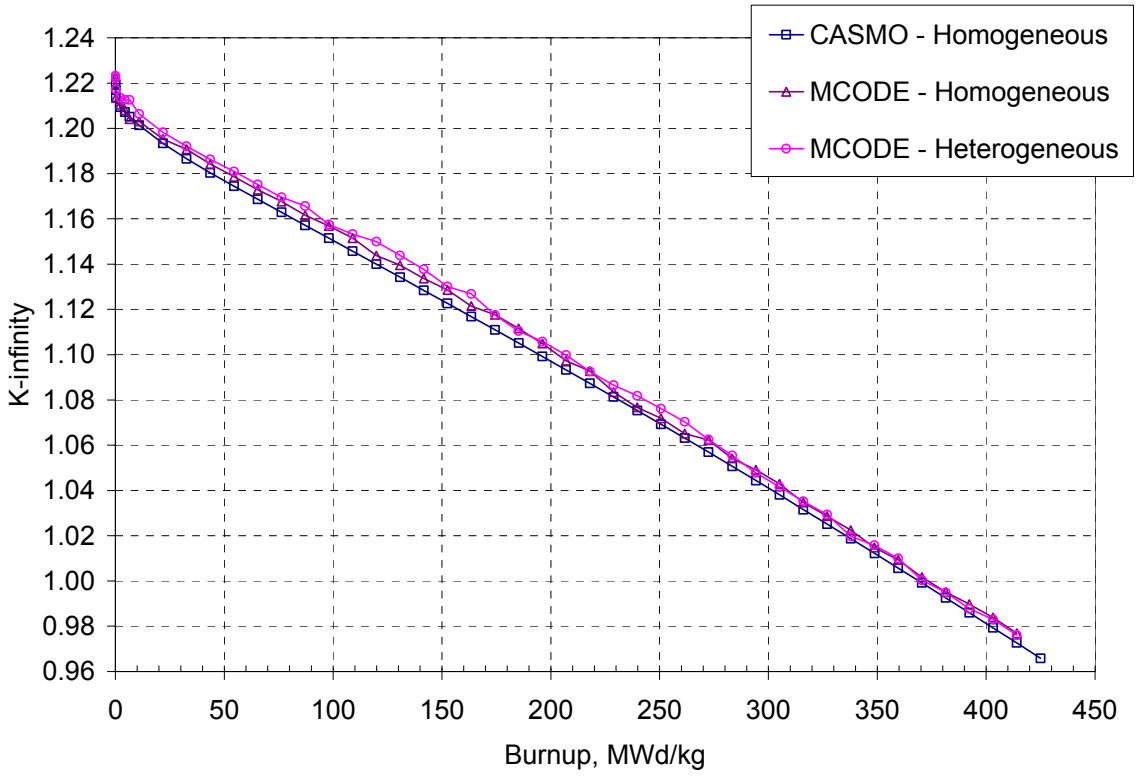

Figure 3.1.2 Criticality vs. Burnup for Homogeneous and Heterogeneous Geometries

In the homogeneous geometry, the difference between the values predicted by CASMO4 and those by MCODE ranges from zero to about 0.5%. At the beginning of irradiation k_∞ values agree very well, but the difference increases with burnup up to about 100 MWd/kg then becomes rather constant up to 400 MWd/kg. The larger k_∞ values predicted by MCODE can be mostly attributed to a discrepancy between the two codes in the prediction of Am242m evolution with burnup and due to a very large Am242m thermal fission cross-section (about 7000b). The Am242m number density as a function of burnup is shown in Figure 3.1.3. The Am242m number density calculated by CASMO4 is smaller than that calculated by MCODE by a factor of about 1.7 at 150 MWd/kg. The Am242m builds up primarily from neutron captures in Am241. Since the Am241 number density changes with burnup are very similar for both codes (Figure 3.1.4), a possible reason for the discrepancy in Am242m buildup can be the difference in the branching ratio between the metastable and ground state of Am242 in the codes or differences in cross-section libraries for Am242m as CASMO-4 uses the JEF2.2 cross section library while ENDF-VI was used in the MCODE calculation.

The predictions by the two codes of the number densities of all the Np, Pu and Cm isotopes are in reasonably good agreement. Minor discrepancies in the number densities prediction are most likely due to the differences in the cross-section data sets used. Selected results for the important actinides are summarized in Appendix A.

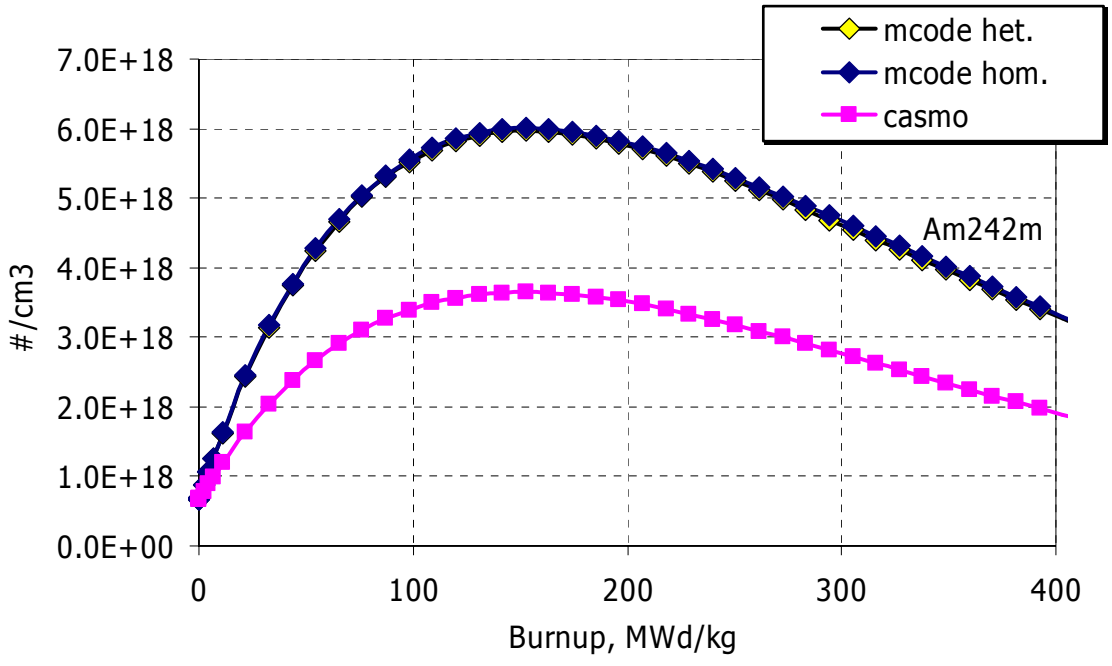

Figure 3.1.3 Evolution of Am242m Number Density with Burnup

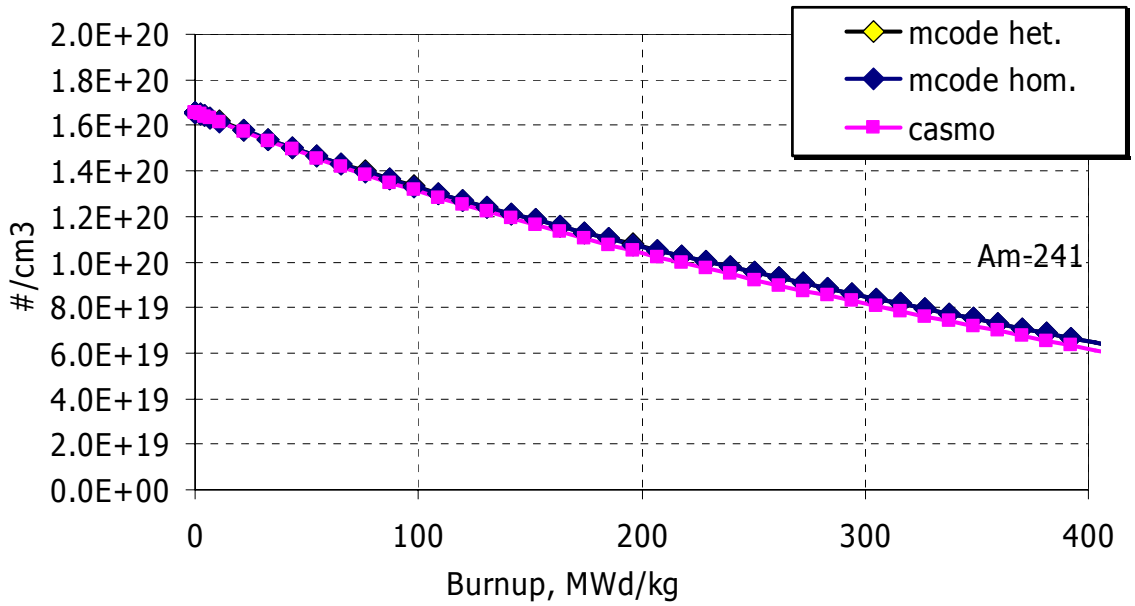

Figure 3.1.4 Evolution of Am241 Number Density with Burnup

In conclusion, the CASMO4 computer code can be used in scoping studies of the FFF designs with a reasonable degree of confidence. The treatment of Am242 branching ratio in CASMO4 and cross-section library differences, which probably lead to considerable discrepancies in predicted Am242m number densities, require additional investigation. Otherwise, the predictions of criticality and TRU nuclides number densities by CASMO4 and MCODE are in a fairly good agreement.

No effect due to the limited cross-section library energy group structure was observed. The effect of the fuel micro particles homogenization can be considered as minor and is neglected for the purposes of this study.

3.2. Choice of Inert Matrix Material

The requirements for the fuel matrix materials include:

- low neutron absorption
- chemical compatibility with the cladding and the coolant
- resistance to irradiation damage
- large heat capacity
- high melting temperature
- high thermal conductivity
- stable crystal structure in operating temperature range
- low thermal expansion
- good mechanical properties
- availability and low cost
- simple handling and fabrication
- simple reprocessing
- availability of industrial experience

Potential candidate matrix forms that can meet the acceptable neutronics requirements are metallic, silicides, nitrides, carbides and oxides, and among desired crystalline structures types are peroskovites, fluorites, yag, and rutile [Long Y. et al., 2003].

The use of metal, carbide and nitride fuels in LWRs is questionable because of their chemical interaction with water. An oxide is a preferred choice because of the vast experience in operation and manufacturing. The fluorite crystalline structure is also preferred for the same reason and because of its ability to incorporate actinides, rare earth elements and fission products.

The remaining candidate inert materials considered are zircon $ZrSiO_4$, stabilized zirconia $(Zr,Y)O_{2-x}$ and $(Zr,Ca)O_{2-x}$, Al_2O_3, MgO, spinel $MgAl_2O_4$, CeO_2, monazite $CePO_4$, SiC and some metals [Long Y. et al., 2003]..

Some of these candidates have significant disadvantages:

- zircon ($ZrSiO_4$) dissociates upon annealing to high temperatures and experiences extensive swelling under radiation
- Al_2O_3 experiences amorphization and large swelling

- MgO disintegrates in the event of cladding failure under PWR conditions
- monazite ($CePO_4$) has poor radiation stability and poor thermal conductivity.
- CeO_2 experiences polygonization and temperature dependent swelling.

However, the interest in some of these matrices still exists and their evaluation is in progress. For example, Mg and Ce oxide are being tested in France as potential candidates for Pu burning in LWRs.

Stabilized zirconia is a very robust fuel matrix with very good irradiation stability. Zirconia can be stabilized by either calcium or yttrium oxide (yttria). Y_2O_3 has small neutron induced swelling. Yttria stabilized zirconia (YSZ) is chemically stable, has a high melting temperature and good irradiation stability. It is a superior actinides host matrix. CaO is also a good candidate to stabilize zirconia. It has very good thermo-mechanical properties.

The major drawback of zirconia is its low thermal conductivity although addition of spinel can improve it. Spinel exhibits partial amorphization and polygonization and is unstable under fission product impact.

The hybrid fuel concept, however, can minimize the irradiation damage to the spinel matrix. In such concept, TRUs are homogeneously mixed with stabilized zirconia to form a fluorite phase as small sized particles (fissile phase) and then the particles are dispersed in a spinel matrix. In this way, fission fragments damage can be localized primarily to the fissile phase and YSZ. Specially, if a buffer zone around the particles can be created to accommodate the escaping fission products.

As a result, hybrid fuel types (CERCER or CERMET) are preferable to Solid Solution Pellet (SSP) fuel type because of the better potential to accommodate high fuel burnup.

The multi-phase CERCER and CERMET have several advantages. The use of two-phase materials prevents radiation damage by fission products to the inert matrix. Less radiation damage to the matrix helps to avoid degradation of its thermal conductivity, which in turn allows for higher burnup. Somewhat complicated manufacturing, possible hot spots, and absence of thermodynamic stabilization are among potential drawbacks of this concept.

In order to localize effectively the radiation damage to the fissile phase, restrictions on the fissile phase volume fraction and micro particle size may apply. The fission products have a finite range in the fuel (~ 8 – 10 μm). So that the volume of the region affected by fission products can be minimized provided that the fuel particles are large enough. However, the thermal gradient between the matrix and the particles increases with increasing particle size. This may result in degradation of the effective thermal conductivity of the fuel and increase fission gas release rate. It was shown that preferable particles size should be in a range between 150 and 200 μm. [Y. Yuan et al. 2001]

The CERCER fuel concept is currently being widely studied. The most promising matrix material proposed is $MgAl_2O_4$ (spinel) and TRUs are to be incorporated either in CaO or YSZ. It was also suggested to use $Y_3Al_5O_{12}$ instead of spinel and cerium oxide for the fissile phase.

In summary, for LWR applications, it is found that ceramic oxides are more promising than other materials, although currently ongoing research efforts have not yielded a broad consensus regarding the best matrix material yet. Zirconia (stabilized by yttria or calcia) and cerium oxide are currently considered as the most promising hosts for the TRU oxides [Long Y. et al., 2003]. The TRU – stabilized zirconia fuels must be dispersed in another material such as spinel ($MgAl_2O_4$) to enhance effective thermal conductivity of the fuel. The sensitivity of spinel matrix to fission product damage requires the use of hybrid CERCER type fuel with fissile phase particles containing TRU mixed with stabilized zirconia dispersed in a spinel matrix. The size of the particles must be in a range between 150-200 μm in order to minimize fission products damage to the spinel matrix.

3.3. Neutronic Assessment of Fertile-Free Fuel

The basic calculation methods and assumptions regarding the reference fuel pin geometry and reactor operating conditions used in the evaluation of TRU-thoria fuel apply also to the results reported in this section. The TRU isotopic composition vector used is shown in Table 3.3.I.

Table 3.3.I. Reference TRU Isotopic Composition

(UO_2, 4.2 w/o U235, 50 MWd/kg Burnup, after 10 Years of Cooling)

Isotope	Weight %
U-234	0.0001
U-235	0.0023
U-236	0.0019
U-238	0.3247
Np-237	6.641
Pu-238	2.7490
Pu-239	48.6520
Pu-240	22.9800
Pu-241	6.9260
Pu-242	5.0330
Am-241	4.6540
Am-242m	0.0190
Am-243	1.4720
Cm-242	0.0000
Cm-243	0.0050
Cm-244	0.4960
Cm-245	0.0380
Cm-246	0.0060

The fertile free fuel was evaluated with respect to two primary performance parameters: TRU destruction rate and achievable fractional burnup of TRU.

In the following analysis, we compare two possible PWR core arrangements: homogeneous and heterogeneous. The homogeneous option refers to the reactor core with a single type of fuel assemblies. Each of the assemblies is composed of TRU fuel with the isotopic vector presented in Table 3.3.I in combination with the fertile-free matrix. The heterogeneous reactor core includes two types of fuel assemblies. The fuel in the assemblies of the first type is composed of Pu only, while the fuel in the second type of assemblies is primarily composed of MA with some addition of Pu to sustain reasonable criticality constant of the assembly. This heterogeneous arrangement allows additional flexibility in optimization of TRU destruction efficiency. The Pu and Pu-MA containing assemblies can be optimized separately to burn efficiently the Pu and MA. In addition, the heterogeneous core allows separate fuel management schemes for the different types of assemblies. For example, if deeper MA burnup was found beneficial, the in-core residence time of the MA containing assemblies can be extended.

Homogeneous Option

Similar to the assessment of the TRU-thoria option, a scoping study was performed to investigate the TRU destruction rate and fractional burnup sensitivity to the fuel lattice H/HM ratio and initial TRU loading.

The burnup calculations were performed for the pin cell geometry. The H/HM ratio was varied in a wide range of values by changing the coolant density for the fixed pin cell geometry. However, alternate ways to achieve different H/HM values are expected to yield similar results.

The calculations were performed for 3 different initial TRU loadings of 10, 15 and 20 volume percent relative to the fuel pellet volume, which corresponds to 33.3, 50.0 and 66.7 v/o of TRU in the fuel micro particle volume respectively. The remaining volume fraction of the fuel micro particle was occupied by YSZ. The spinel matrix occupied a fixed (70 v/o) fraction of the fuel pellet volume for all cases. The choice of these three compositions was due to the following considerations: (1) The 10 v/o of TRU composition represents a realistic reference case which results in approximately 18 months fuel cycle length in the reference PWR geometry. (2) The 20 v/o of TRU is likely to be the limit of TRU loading from a materials behavior perspective as discussed in the previous section.

The results of the calculations are reported in Figures 3.3.1 through 4.3.5. The variation of H/HM ratio towards larger values results in a modest (up to 18%) increase in the reactivity limited burnup (Figure 3.3.1). The higher achievable burnup in turn leads to a more efficient destruction of TRU as demonstrated in Figure 3.3.2. Fuels with different TRU loadings have about the same optimal discharge burnup value for over-moderated lattices. As a result, the minimal residual fraction of TRU is approximately the same (~40%) for the fuels with different initial loadings. In the reference geometry and 10v/o TRU loading, which provides discharge burnup corresponding to 18 month fuel cycle, about 53% of initial TRU can be destroyed per one fuel batch path through the reactor core.

The difference in the discharge burnup for different H/HM values has no effect on the destruction rate (Figure 3.3.3). For the FFF, the TRU destruction rate is determined solely by the core power. For a typical PWR core power density, the TRU destruction rate is about 1140 kg per GWe Year. The slight variation in the destruction rate can be attributed to a small difference in energy per fission for different isotopes as they have different contribution to total power with the shift of neutron energy spectrum.

Although wetter than reference fuel lattices seem to be more attractive from a burnup viewpoint, for a fixed core volume and total power, an increase of H/HM ratio will result in a reduction of fuel volume and increase of power density in the fuel. Therefore, only moderate modifications in the fuel assembly geometry may be possible because of the thermal-hydraulics constraints. Alternatively, if the total core power is not fixed, satisfactory thermal-hydraulic design may be feasible by lowering the specific power in the fuel. However, this will result in considerable reduction in TRU destruction rate. Figure 3.3.4 illustrates that fact. The data shown in Figure 3.3.4 was obtained assuming that H/HM was changed through variation of the fuel pin cell pitch for the fuel rods of a fixed diameter.

The results of the calculations described above indicate that even in the reference PWR pin cell geometry the efficiency of TRU destruction is very close to the optimal one. This is a significant advantage because by using the reference assembly configuration, a near optimal burning efficiency can be achieved without impairing the destruction rate or changing the thermal-hydraulic design of the core.

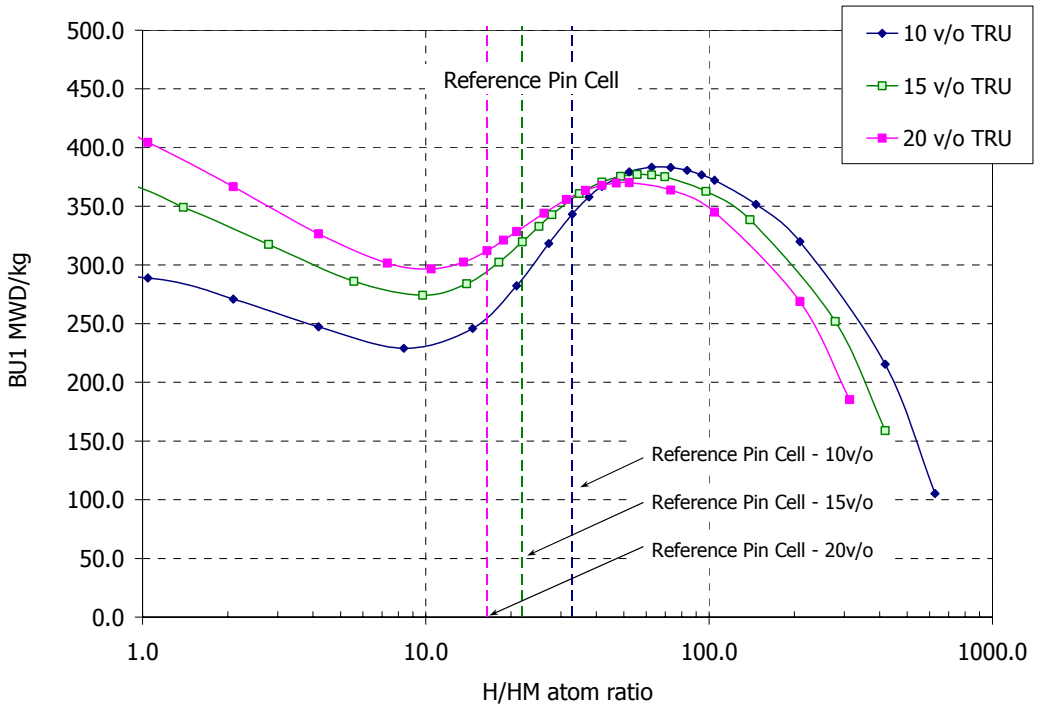

Figure 3.3.1. Single Batch Burnup vs. H/HM Ratio

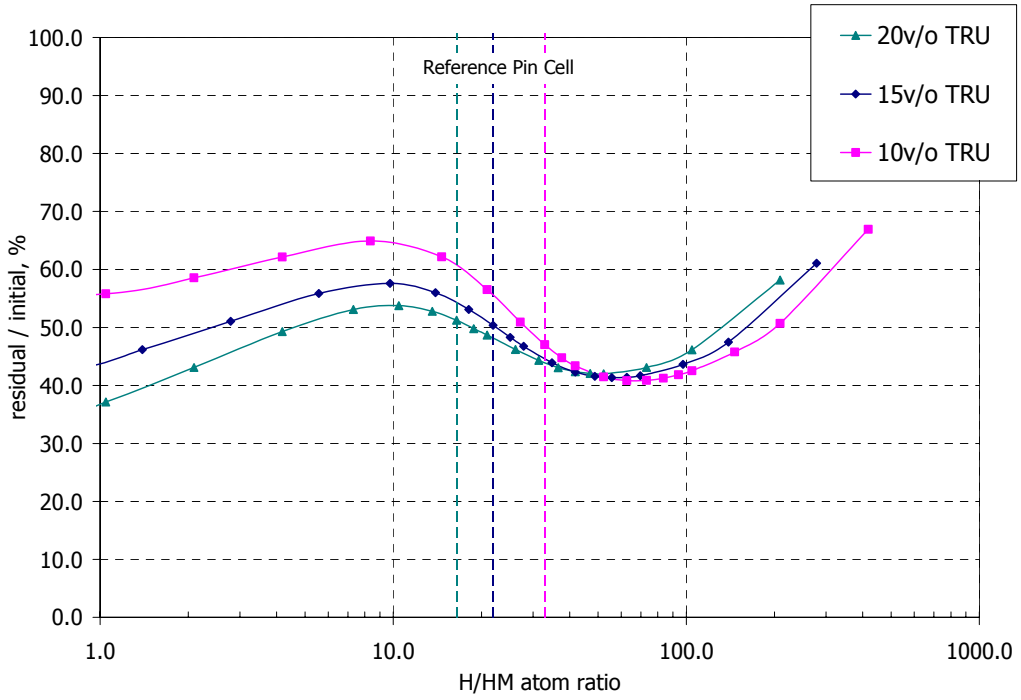

Figure 3.3.2. Residual Fractions of TRU in Discharged Fuel vs. H/HM Ratio

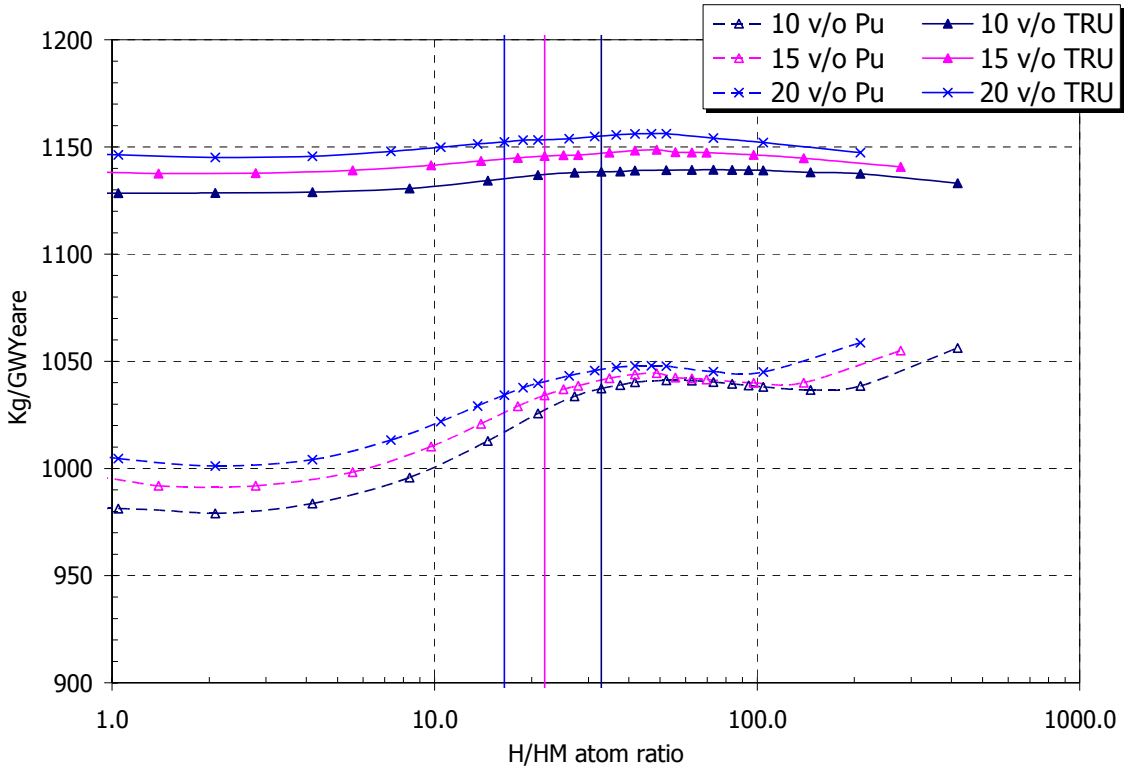

Figure 3.3.3 Energy Normalized Pu and TRU Destruction Rates vs. H/HM Ratio

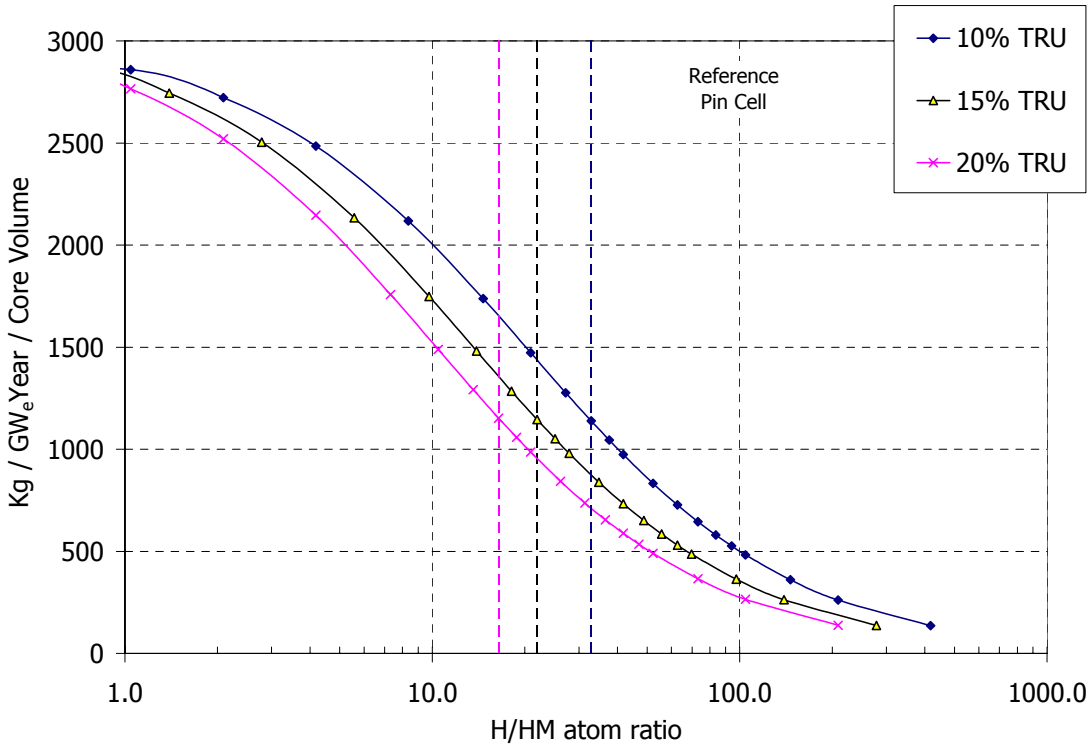

Figure 3.3.4. Pu and TRU Destruction Rates per Reference Core Volume

A reference PWR "assembly" burnup calculation with FFF containing 10 v/o of TRU was performed to assess the validity of the "pin cell" geometry calculations and to evaluate the possibility of an additional TRU recycling stage.

Burnable absorbers are likely to be used in a practical fuel design. Therefore, the burnable poison effect on the TRU destruction efficiency was also evaluated by calculation of a case with the addition of 1 v/o natural Er oxide (Er_2O_3) to the fuel. The main advantage of Er as a burnable absorber is the presence of a large absorption resonance in Er167 that overlaps with the fission resonance of Pu239. As a result, Er can potentially improve the fuel temperature reactivity feedback (Doppler Coefficient). The main disadvantage of Er is a reactivity penalty at the fuel discharge point due to the absorption in some of the residual Er isotopes.

Figure 3.3.5 shows an example of criticality curves for the assembly calculations with and without burnable poison for the single once-through case and for the case with an additional stage of TRU recycling. The composition of the once-recycled TRU fuel was chosen such that all the unburned TRUs from the first stage (after the fission products separation) are included and enough "fresh" TRU is added to be able to reach the first stage fuel cycle length.

Table 3.3.II summarizes the fractional TRU burnup for the poisoned and un-poisoned cases, with and without TRU recycling. The effect of BP addition is important since the BP considerably reduces TRU burning efficiency due to the residual reactivity penalty and loss of neutrons to BP that otherwise could be used for transmutation and fission TRU components.

Degradation of TRU isotopic vector after the 1st path makes TRU recycling unattractive because of considerably lower fractional burnup in the case where minimal reprocessing is the first priority. If multiple reprocessing is not of a great concern, an equilibrium fuel composition can be achieved after several recycles with the fractional TRU burnup converging to values between 25% and 30%. However, for such a relatively low fractional burnup, fuel material and positive void reactivity coefficient limitations on maximum TRU loading, and the requirement of at least 70% make up of "fresh" TRU to sustain a reasonably long fuel cycle length make 100% fertile free homogeneous core impractical if it is solely considered for multi-recycling burndown of the existing stockpile of TRU.

Table 3.3.II. TRU Destruction in Homogeneous FFF Core: Normalized Material Flow Summary

Case	1st path		2nd path	
	No BP	With BP	No BP	With BP
Discharge Burnup, MWD/kg	541	486	334	292
TRU Loaded, kg / GWeY	2037	2264	3295	3774
TRU Discharged, kg / GWeY	887	1112	2122	2594
Pu Loaded, kg / GWeY	1759	1954	2744	3137
Pu Discharged, kg / GWeY	671	850	1623	1996
% TRU Burned / path	56.5	50.9	35.6	31.3
% Pu Burned / path	61.8	56.5	40.8	36.4

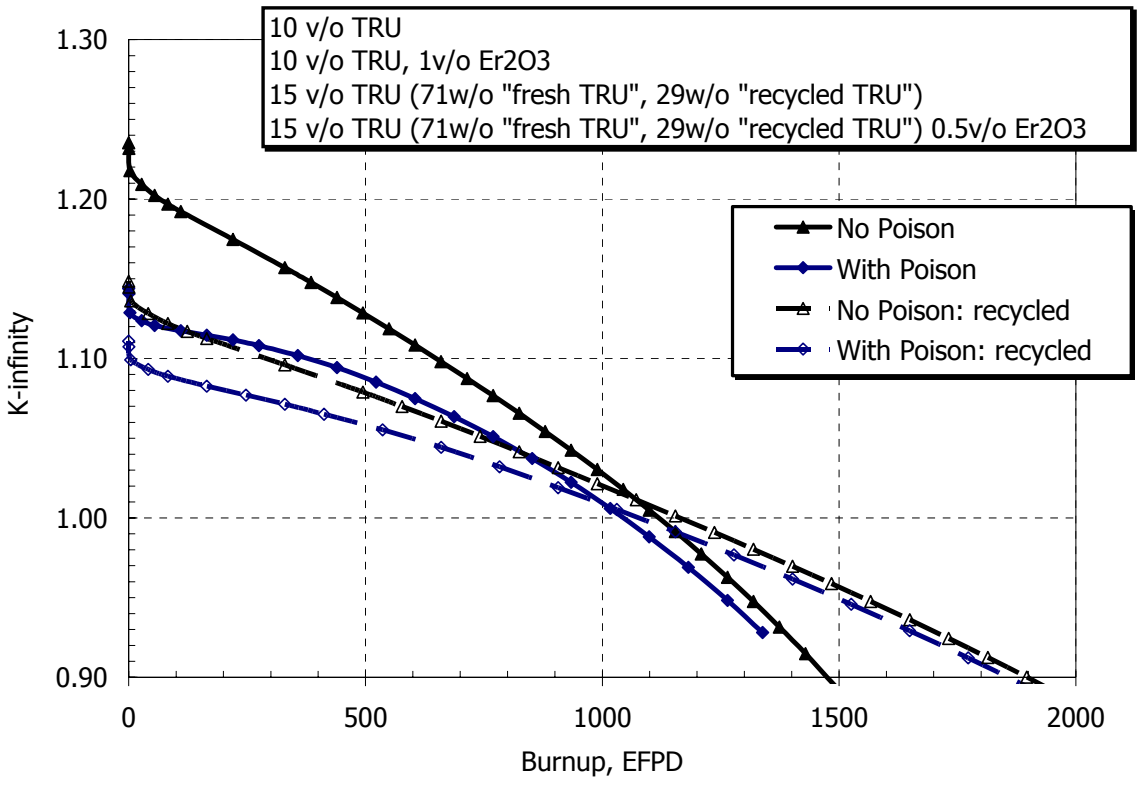

Figure 3.3.5 Criticality Curves for the FFF Assembly Cases

Macro-Heterogeneous Option

As mentioned earlier, heterogeneous core configurations allow additional flexibility in the optimization of TRU destruction efficiency.

This section examines the effect of variation of the relative amounts of Pu and MA in fuel assemblies as well as of the assembly lattice H/HM ratio on burning efficiency. Assuming that Pu and MA come in different streams from the chemical separation process, the relative amounts of Pu and MA can be changed so that most of the Pu is concentrated in one type of fuel assemblies, while all of the MA are concentrated in the second type of the assemblies.

The destruction rate of TRU in FFF is determined only by the specific power in the core. Therefore, the main objective was an increase in reactivity limited burnup, which leads to a higher degree of TRU destruction. An additional goal was the investigation of the possibility to accelerate MA destruction rate at the expense of Pu destruction rate.

The heterogeneous equilibrium core performance was modeled using the CASMO4 "colorset" option. This option allows 2D transport calculations with burnup for a 2x2 segment of different full size fuel assemblies (Figure 3.3.6).

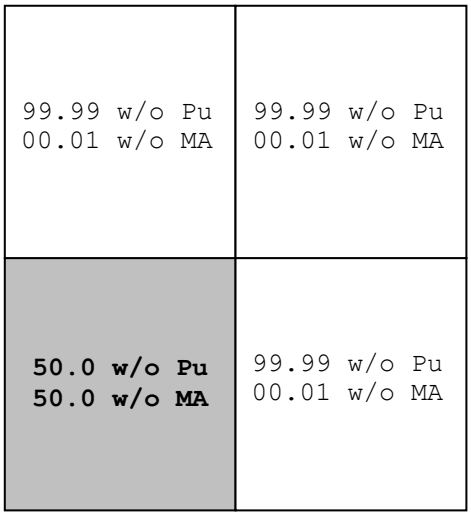

Figure 3.3.6 Example of CASMO Colorset Layout

A systematic analysis of different heterogeneous assembly configurations was performed by varying separately the composition and H/HM of the two assembly types. Several constraints were imposed on the optimization to ensure the feasibility of a realistic design:

- Colorset pin power peak ratio < 1.2.
- TRU volume fraction in the fuel particles < 70 v/o (< 20 v/o of the pellet volume).
- Variation in the fuel pin diameter < ± 20%.
- Colorset average Pu to MA ratio is conserved and equal to the one used in the homogeneous assembly evaluation (Table 3.3.I).

Representative macro heterogeneous cases analyzed are listed in Table 3.3.I. In Table 3.3.I, the heterogeneous case 2 denotes a colorset with the lattice geometry identical to the homogeneous assembly case. The Pu and MA containing assembly lattice H/HM ratio was varied in a range of ±20 % of the reference one. In the case 1, the Pu containing assembly has higher than reference H/HM by 20% and the Pu-MA assembly has lower than reference H/HM by 20%, while in the case 3, the Pu containing assembly has lower than reference H/HM by 20% and the Pu-MA assembly has higher than reference H/HM by 20%.

Table 3.3.I Representative macro heterogeneous cases

	H/HM MA assembly	H/HM Pu assembly
Case 1	Reference – 20%	Reference + 20%
Case 2	Reference	Reference
Case 3	Reference + 20%	Reference – 20%

Selected results comparing the homogeneous and heterogeneous options are reported in Table 3.3.II. The heterogeneous cases 1 and 3 (Table 3.3.I) are the best performing cases in terms of reactivity limited burnup and MA destruction rate respectively. The results show that no significant improvement in heterogeneous colorset burnup can be achieved in comparison with the homogeneously mixed Pu and MA assembly. Moreover, the rate of MA destruction in the heterogeneous configurations is always lower than in the homogeneous assembly under the imposed constraints. The lower MA destruction rate is a direct consequence of always lower than average colorset power in Pu-MA assembly.

Table 3.3.II Efficiency of TRU Destruction: Homogeneous vs. Heterogeneous Option

Case	Burned as % of Initial			Kg Burnt / GWeY		
	TRU	Pu	MA	TRU	Pu	MA
Homogeneous	56.3	61.6	23.0	1135	1072	63
Heterogeneous, (case1)	56.4	62.5	16.1	1134	1090	44
Heterogeneous, (case2)	55.4	61.5	16.4	1135	1089	46
Heterogeneous, (case3)	54.3	60.2	16.6	1135	1088	48

Although the heterogeneous option is not advantageous in terms of the TRU destruction efficiency in comparison with the homogeneous option, as mentioned earlier, the heterogeneous core configuration allows different fuel management schemes for different assembly types. An appropriate assessment of this option requires neutronic simulation of the whole core and was not performed in this study. In principle however, the degree of MA burnup can be improved by extending the MA assemblies residence time.

The MA burning assembly can be designed to have a very flat reactivity over the entire irradiation time. Figure 3.3.7 shows an example of criticality versus burnup curves for a number of possible compositions of the MA burning assembly. The flat reactivity would minimize the power peaking in heterogeneous Pu and Pu-MA assemblies core. However, the homogeneous option may be preferable because better transmutation efficiency can be achieved and because Pu and MA do not require separation during reprocessing.

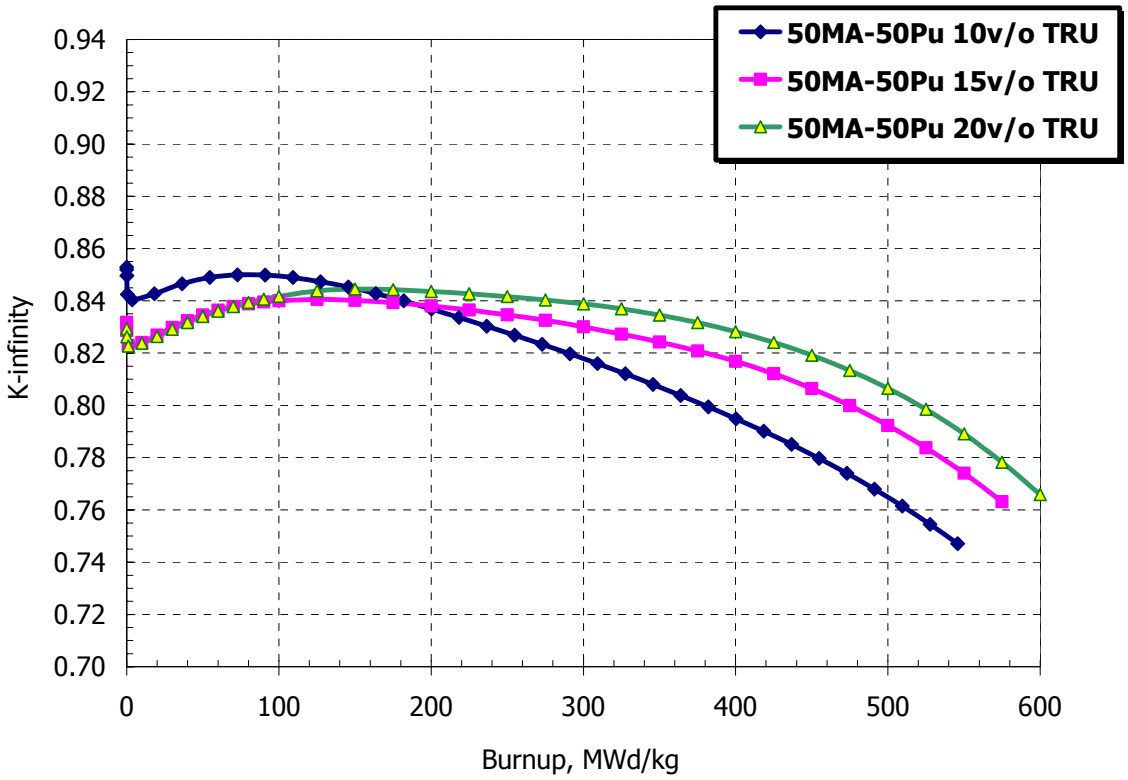

Figure 3.3.7 Criticality of MA Burning Assembly

3.4. Reactivity and Control Characteristics

The results of the reactivity coefficient as well as soluble boron worth calculations are summarized in Table 3.4.I. Only the homogeneous FFF option was evaluated since the heterogeneous core arrangement does not offer any significant advantages from the TRU destruction efficiency perspective.

The FFF assembly has a much lower value of DC than the conventional UO2 fuel case although its value is still negative. The presence of Er burnable poison does not improve DC notably. However, higher concentrations of Er enriched in Er167 isotope may have a significant impact on DC bringing it value close to that of the UO2 fueled core [Kasemeier U. et al., 1998]

The soluble boron worth (BW) is considerably lower for FFF in comparison with All-U fuel, however, it is comparable with MOX fuel. The lower BW for the FFF is due to the much harder

(than in conventional PWR) neutron spectrum as a consequence of a strong thermal neutrons absorption in Pu and MA isotopes.

The MTC and VC are also negative at BOL with the soluble boron concentration of 1000ppm. Realistic values for MTC and VC can be obtained only with a whole core simulation with reasonable burnable poison design and will be discussed in a following chapter.

Table 3.4.I. Reactivity Coefficients and Soluble Boron Worth

		FFF 1st path		MOX	All-U
		No Poison	with 2%Er		
DC	BOL	-0.63	-0.75	-2.73	-2.03
	MOL	-0.77	-0.77	-2.87	-2.65
	EOL	-1.04	-1.08	-3.03	-3.08
MTC	BOL	-21.88	-32.89	-42.48	-11.26
	MOL	-32.39	-41.27	-54.36	-39.54
	EOL	-51.75	-61.63	-73.98	-66.29
VC	BOL	-54.07	-80.94	-112.48	-34.76
	MOL	-92.02	-114.92	-148.78	-119.03
	EOL	-172.04	-197.64	-204.00	-205.98
BW	BOL	-2.34	-2.51	-2.70	-6.11
	MOL	-3.42	-3.46	-3.17	-7.09
	EOL	-8.02	-8.10	-3.91	-9.51

The results obtained do not indicate any significant FFF implementation problem related to reactivity feedback coefficients. Compared to a reference PWR, the much smaller soluble boron worth, which is common for Pu and MA containing fuels, is likely to impose additional requirements on the reactor reactivity control design features.

Another important fuel characteristic which directly affects the feasibility of reactor control is the effective delayed neutrons fraction (β_{eff}).

Figure 3.4.1 reports the effective delayed neutron fraction for an FFF assembly as a function of burnup for the 1st and 2nd TRU burn down path. The β_{eff} values for FFF at the beginning of irradiation are lower than 0.003 compared to about 0.007 for the UO_2 fueled PWR cores at BOL. β_{eff} increases monotonically with burnup due to an increasing contribution to the total power from Pu241 fissions and decreasing contribution of Pu239 fissions. Nevertheless, this relatively low initial value is likely to impose a major limitation on the feasibility of PWR core with 100% loading of TRU in FFF assemblies.

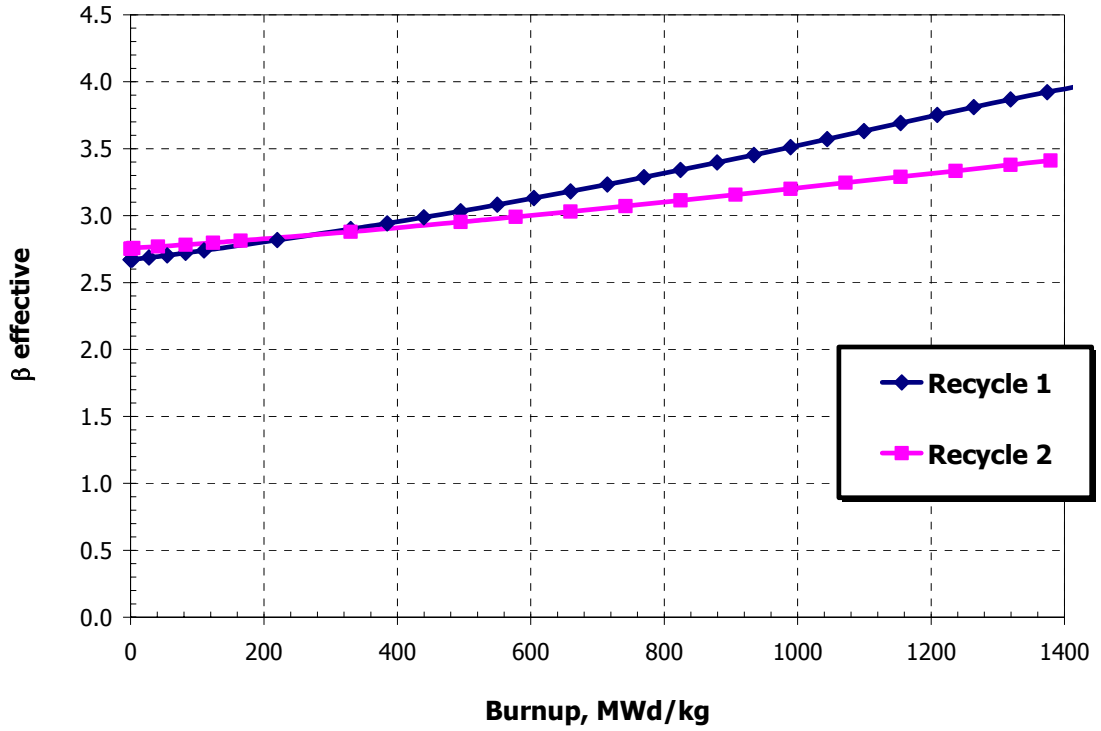

Figure 3.4.1 Effective Delayed Neutron Fraction × 10^3 vs. Burnup

3.5. Chapter Summary

In summary, FFF has the best potential for burning TRU in LWRs. For the standard PWR fuel lattice and about 10% volume fraction TRU loading the efficiency of TRU destruction is close to optimal and slightly exceeds 50% of TRU burned per one path through the reactor core. For higher TRU loadings, a fuel lattice with higher than reference H/HM is preferable and also results in close to 50% of atomic burnup of TRU per path.

Recycling of the once-through TRU burner is less attractive because of the degradation of Pu isotopics and, as a result, lower destruction efficiency (< 30 % atomic burnup at equilibrium), and the requirement for higher TRU loadings.

The heterogeneous core concept implying two different assembly types with different relative amounts of Pu and MA cannot improve the efficiency of TRU destruction beyond that of the homogeneous core with only one type of the assemblies.

Chapter 4. Comparison of Fuel Options

This chapter provides a comparison of the available fuel options with respect to their potential of burning TRU. Three types of fuel are considered: TRU-UO_2 mixed oxide, TRU-ThO_2 and fertile free fuel. The performance of each of these fuel types is evaluated in the following four categories:

- neutronic performance: potential TRU destruction rates and TRU destruction efficiencies
- feasibility of a practical design: safety and reactivity control, fuel performance at normal operation and during accidents
- potential for long term radiotoxicity reduction in a once-through burndown fuel cycle scenario
- proliferation resistance of the spent fuel

4.1. Comparison of TRU Destruction Characteristics

The comparison of neutronic performance is presented in Table 4.1.I. FFF-TRU-1 and FFF-TRU-2 are the single path and double path TRU burndown FFF options discussed in Chapter 3. The Th-Pu and Th-TRU mixed oxide fuel options assume the addition of appropriate amounts of natural uranium for the purpose of denaturing the generated U233 below the non-proliferation threshold [Forsberg C.W. et al., 1998]. All the results were obtained from the assembly level 2D burnup calculations performed with CASMO4 code. The 18 months fuel cycle length was conserved in all cases reported in this chapter.

Conventional UO_2 MOX fuel has the lowest potential due to the generation of TRU from U238. ThO_2 fuel has better performance because it is practically U238-free. However, the TRU destruction rate is about half that of the fertile free fuel because some of the energy is generated from bred U233. As a result, the efficiency of TRU destruction is lower than that of the FFF for the same atomic burnup. In the Th-Pu case, TRU are destroyed at lower rate than in Th-TRU case because the breeding of U233 in the latter case is less efficient. Th-TRU fuel requires higher TRU loading to achieve the same fuel cycle length which results in a harder spectrum which prevents efficient U233 breeding and efficient Pu239 destruction. The FFF, as expected, has the best neutronic performance with respect to TRU destruction capabilities.

Nevertheless, all fuel types are capable of burning TRU to some extent. Therefore, if repeated recycling of TRU is considered, these fuels, in principle, can be part of a combined cycle in which generation of TRU in UO_2 fuel can be offset by TRU destruction. The sustainable, zero TRU generating fuel cycle based on the TRU-UO_2 MOX fuel (CORAIL assembly concept [T. A. Taiwo et al. 2002]) and TRU-ThO_2 fuel [M. Todosow et al. 2002] were shown to be feasible. The relation between the amount of TRU fuel and UO_2 fuel in a sustainable fuel cycle is defined by the relative TRU destruction and generation rates. The higher the destruction rate the less TRU fuel is required to achieve sustainability. Thus, deviation of the reactor core characteristics from the reference UO_2 core will be minimal if the amount of TRU containing fuel in the core is minimal. In addition, a smaller amount of TRU recycling is required if more efficient TRU burning can be achieved, minimizing the fuel reprocessing cost.

In a once-through burndown fuel cycle scenario, more efficient and faster TRU destruction are also clearly advantageous.

Table 4.1.I. Burndown Scenario: Fuel options comparison.

	AllU	MOX-Pu	MOX-TRU	Th-Pu	Th-TRU	FFF-TRU-1	FFF-TRU-2
Discharge Burnup, MWd/kg	51	46	52	54	55	541	335
TRU generation rate, kg/GWe-Y	+260	-310	-480	-686	-793	-1150	-1150
Initial HM, kg/assembly	450	464	459	428	440	48.4	72.5
Initial TRU, kg/assembly	0.0	32.5	74.8	42.8	100.5	48.4	72.5
Discharged TRU, kg/assembly	5.5	25.3	63.6	26.8	82.0	21.4	46.7
Fractional burnup: TRU	-	0.22	0.15	0.37	0.18	0.56	0.36
Fractional burnup: TRU+U233	-	0.22	0.15	0.25	0.14	0.56	0.36
Discharged Pu , kg/assembly	5.0	23.8	55.2	24.5	70.4	17.1	35.7
Discharged Pu, kg/GWe-Y	237	152	179	122	173	82	84

4.2. Comparison of Proliferation Resistance Characteristics

The proliferation potential of the spent fuel for each fuel cycle scenario is also a concern. The isotopic composition of Pu in the spent fuel for the different options considered is presented in Table 4.2.I. The proliferation potential of Pu is related to: (1) the fraction of Pu238 in it due to the significant Pu238 heat generation which complicates weapons assembly and maintenance, (2) fraction of even Pu isotopes (Pu238, Pu240 and Pu242) due to high spontaneous fission source which complicates weapons design and may cause a weapon to fizzle, and (3) to some extent, the fraction of Pu240 due to a very large resonance integral which slightly increases the critical mass. The most desirable weapon material is Pu239 with very low heat generation, low neutron source and the highest fission to capture cross-section ratio in the fast spectrum region among all Pu isotopes.

As can be observed from the data in Table 4.2.I, spent fuel from any recycled Pu has improved proliferation resistance characteristics than initial UO_2 spent fuel. MOX UO_2 and ThO_2 fuel have similar characteristics while FFF has superior non-proliferation features. It has the highest Pu238 fraction among all other options. This is a consequence of two effects. Firstly, Pu238 builds up at higher rate through Np237 and Am241-Cm242 chains than in all other cases. Secondly, Pu239 burns out faster due to the absence of fertile nuclides which produce more Pu239 from U238 (MOX cases) or generate U233 which competes with Pu239 for neutron absorption (Th cases). Figure 4.2.1 shows the density change of Pu238 and Pu239 for the FFF-TRU-1 and Th-TRU cases illustrating the above observations.

Table 4.2.I. Discharge Pu Isotopic Composition.[1]

	All U	MOX-Pu	MOX-TRU	Th-Pu	Th-TRU	FFF-TRU-1	FFF-TRU-2
Pu-238	2.8	3.3	8.0	4.2	7.9	17.2	15.7
Pu-239	50.4	38.2	42.8	30.6	41.7	9.8	19.0
Pu-240	23.8	30.5	28.9	30.3	30.9	31.4	35.4
Pu-241	15.1	17.7	13.1	20.8	12.2	19.5	11.3
Pu-242	8.0	10.3	7.1	14.1	7.3	22.1	18.5

[1] The burnup is given in Table 4.1.I

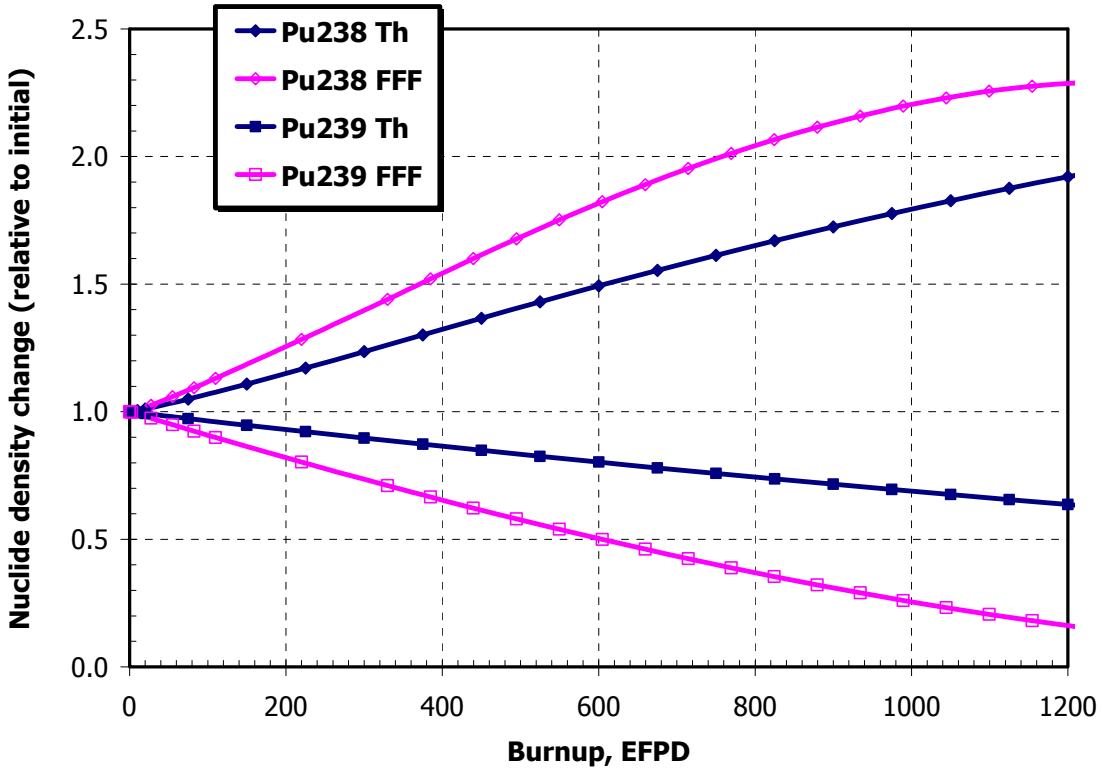

Figure 4.2.1. Pu238 and Pu239 density change with burnup

4.3. Comparison of Control and Safety Coefficients

Table 4.3.I compares reactivity feedback coefficients, control materials reactivity worth and effective delayed neutron fraction for the considered fuel types.

The Doppler coefficient is negative for all fuel types. FFF has the smallest magnitude of DC which can be a potential problem in rapid reactivity initiated accidents. This issue is addressed in Chapter 7 of this thesis. Pu-ThO_2 fuel, on the other hand, has a highly negative Doppler coefficient which can impose problems in cooling down accidents and will require increased shutdown margin. All other fuel options are comparable to UO_2 fuel.

The MTC is a limiting factor only for the TRU-MOX fuel due to the higher loading required to achieve the same cycle length as with Pu-MOX and therefore more epithermal spectrum.

The reactivity worth of the control materials is reduced for all TRU containing fuels compared with UO_2 fuel. The soluble boron worth is smaller by about a factor of two for all fuel types as compared with UO_2.

A small β_{eff} is another common problem of TRU containing fuels. This fact in combination with a small Doppler coefficient raises particular concern about the fuel response to RIAs.

Table 4.3.I. Safety and Reactivity Control Characteristics (2D assembly based depletion calculations).

	DC, pcm/K		MTC, pcm/K		BW, pcm/ppm		$\beta_{eff} \times 10^3$	
	BOL	EOL*	BOL	EOL*	BOL	EOL*	BOL	EOL*
All – U	-2.20	-3.33	-22.2	-78.8	-4.80	-6.23	7.2	4.8
Pu – MOX	-2.92	-3.20	-40.6	-73.8	-1.96	-2.76	4.0	4.2
TRU – MOX	-2.19	-2.32	-0.86	+0.40	-1.64	-1.96	3.4	3.7
Pu – Th	-4.32	-5.04	-49.1	-73.5	-1.95	-3.02	3.1	2.8
TRU – Th	-2.98	-3.15	-18.5	-23.4	-1.05	-1.24	2.6	2.5
FFF - TRU - 1	-0.63	-1.04	-21.9	-51.8	-2.34	-8.02	2.7	3.9
FFF - TRU - 2	-0.64	-0.93	-15.6	-42.3	-2.00	-3.38	2.8	3.3

* EOL – end of life (or end of fuel irradiation, $B_{discharge} = 1.5 \times B_1$)

4.4. Comparison of Spent Fuel Characteristics

Finally, the fuel options considered were evaluated in terms of their repository performance characteristics in case of a once-through burndown scenario. The decay heat and radiotoxicity of the spent fuel were calculated for a period of time between 0 and 10^6 years after discharge from the reactor. The resulting values were normalized per total energy generated by this TRU-burning fuel including the energy from the recycled UO_2 fuel that generated these TRU. ORIGEN2.2 computer code [RSICC, 2002] was used for these calculations. In addition, the ORIGEN2.2 library was updated with radiotoxicity coefficient in units Sv/Bq [ICRP, 1995].

The results of these calculations are presented in Figures 4.4.1 and 4.4.2. The results indicate that the once-through burndown option has no significant impact on waste characteristics in the

short or in the long term regardless of the TRU burning fuel type. As a result, multi-recycling of TRU is essential for appreciable improvement in the waste characteristics.

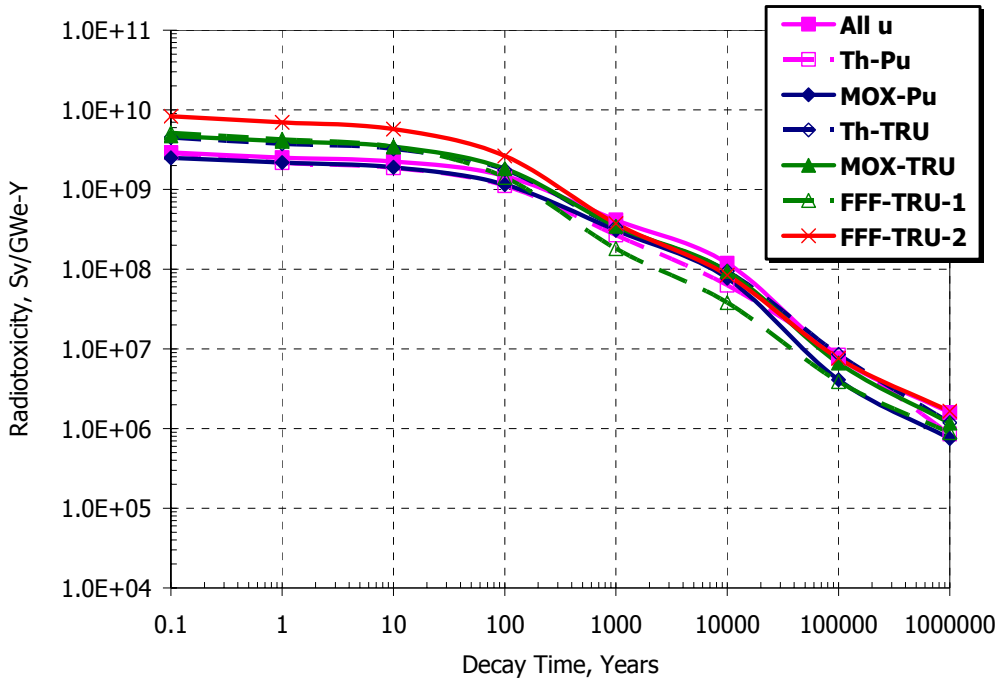

Figure 4.4.1. Normalized Ingestion Radiotoxicity

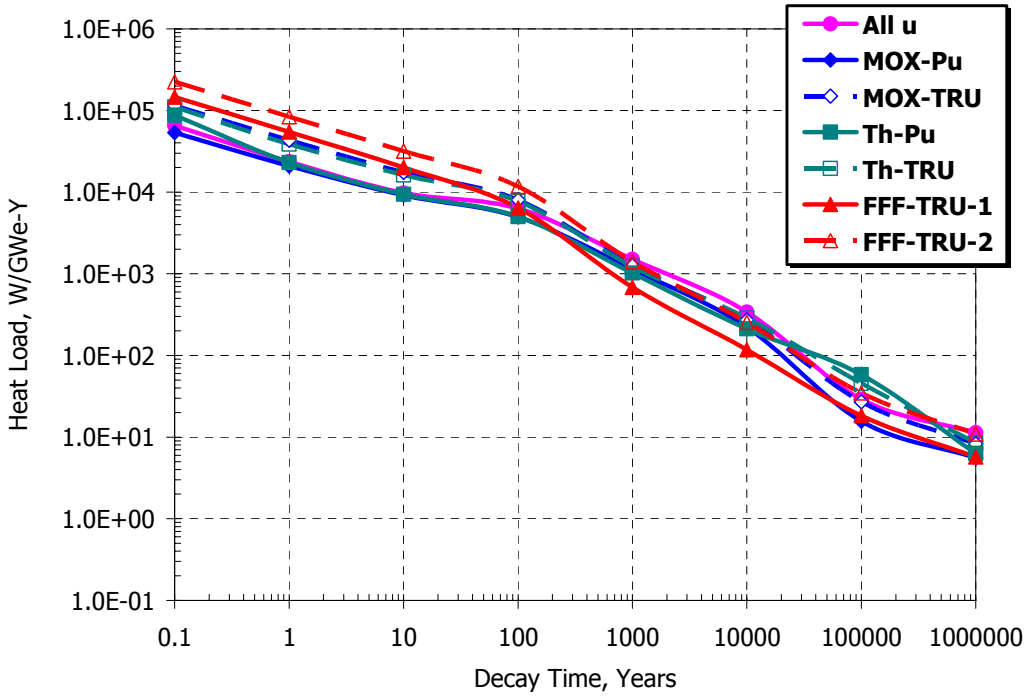

Figure 4.4.2. Normalized Decay Heat Generation

4.5. Summary

In summary, the main advantage of MOX-TRU fuel option is the available industrial scale experience. It is an existing and in many aspects perfected technology although its TRU burning potential is limited.

ThO_2-TRU fuel has better neutronic performance and it is a very robust fuel and waste form which can make it the most attractive option for the once-through burndown cycle. However, the small β_{eff} is a negative feature which must be evaluated in a comprehensive accident analysis.

The FFF fuel has superior TRU destruction capabilities with acceptable fuel performance and core design features which potentially make it the best choice for the transmutation of TRU in LWRs provided sufficient research and development effort is undertaken in the fuel design area.

Finally, comparison of the burndown cycle scenario waste characteristics has shown that none of the considered fuel options is capable of reducing the long term radiotoxicity and decay heat of the spent fuel to a considerable extent. Therefore, it is concluded that the only way to reduce substantially the impact of the nuclear fuel cycle on the environment is to keep all the long lived radioactive isotopes within the cycle and only allow the disposal of short lived fission products. The feasibility of such a fuel cycle is the main subject of subsequent chapters.

Chapter 5. A Sustainable PWR fuel cycle

5.1. The CONFU Assembly Concept

In this chapter, an innovative fuel assembly concept that would allow complete recycling of the TRU of a PWR fuel cycle is evaluated. This fuel assembly concept suggests displacing some of the UO_2 fuel pins in conventional PWR assembly with Fertile Free Fuel (FFF) pins (Figure 5.1.1). This concept is denoted as the Combined Non-fertile and Uranium (CONFU) assembly. Each time such a CONFU assembly is discharged from the core, the residual TRU from FFF pins and the TRU generated in UO_2 pins are separated and recycled together into a new CONFU assembly with "fresh" 4.2% enriched uranium pins and FFF pins that include the TRU from the previous cycle.

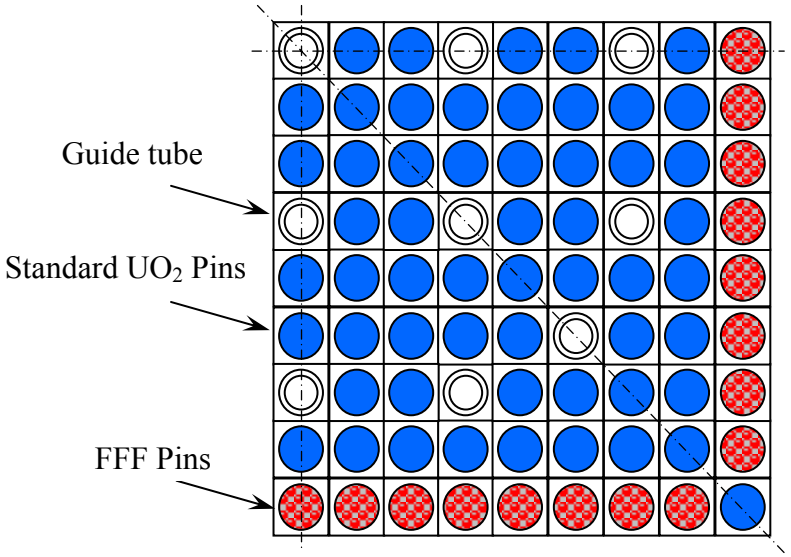

Figure 5.1.1. CONFU Assembly Configuration

The focus of this chapter is on evaluation of the CONFU assembly concept with respect to its ability to achieve an equilibrium state with zero net generation of TRU and a constant fuel cycle length. The effect of multi-recycling on fuel cycle length, TRU isotopic composition, and reactivity coefficients is evaluated. Finally, some waste stream characteristics of the CONFU assembly based fuel cycle are presented and compared with those of the conventional UO_2 once-through fuel cycle.

The major design constraints applied in this investigation can be summarized as follows.

- TRU volume fraction in the fuel is maintained below 20 v/o
- the local moderator to fuel volume ratio is varied within ± 40% of the reference UO_2 fuel value
- assembly pin power peaking is maintained below 1.25 throughout the fuel irradiation

5.2. Preliminary Evaluation

The number of FFF pins, initial loading of TRU and locations of FFF pins in the assembly have been adjusted in order to achieve an equilibrium state with balanced TRU generation and destruction. The TRU isotopic composition from the reprocessed UO_2 spent fuel used in this analysis was identical to that used for the evaluation of the burndown scenario (Table 3.3.I, Chapter 3). The results of the preliminary evaluation show that between 48 and 60 FFF pins per reference 17×17 PWR fuel assembly is sufficient to attain an equilibrium TRU balance when keeping the TRU volume fraction in the fuel micro particles between 33 and 66 v/o (or between 10 and 20 v/o of the total fuel pellet volume).

The location of the FFF pins has a significant effect on power in the FFF pins and, therefore, affects TRU destruction efficiency. The FFF pins generally have higher power when surrounded by UO_2 pins or have extra coolant (guide tube) in their vicinity. For such configurations, the power in the FFF pins is too high to satisfy the thermal-hydraulic limits.

Figure 5.2.1 shows several examples of the BOL pin-power maps for candidate CONFU assembly configurations and illustrates the effect of FFF pins location on their power. Grouping the FFF pins together and adding burnable poison (natural Er_2O_3) were explored as possible strategies to reduce pin peak power to acceptable values. The power map shown in Figure 5.2.1 at the right bottom corner (Case4) represents a possible CONFU assembly configuration with a reasonable power peaking factor of 1.25. In this particular case, 2 v/o of Er_2O_3 was added to the FFF pins. The power map at the left bottom corner in Figure 5.2.1 (Case 3) represents another possible CONFU assembly configuration without employing any burnable poison.

DNBR calculations were performed to ensure the feasibility of CONFU assembly thermal-hydraulic design. Detailed single assembly modeling was done using the VIPRE-01 [Cuta et al.,

1985] sub-channel analysis code which is widely used for evaluation of PWR thermal-hydraulics performance (Appendix A). The following assumptions were made to ensure conservative results: 18% core overpower, 294.7 ºC inlet coolant temperature (i.e. 2ºC above nominal values), 1.56 assembly to core average power peak, "chopped" cosine axial power profile with peak to average ratio of 1.55.

The MDNBR value obtained for the un-poisoned CONFU assembly configuration (Case 3 in Figure 5.2.1) using W-3L correlation with l-grids is 1.721 which indicates that the concept can potentially have a sufficient thermal margin.

Consequently, Case 3 and Case 4 shown in Figure 5.2.1 were chosen for further analysis as representative candidate configurations of un-poisoned and poisoned CONFU assemblies with acceptable thermal-hydraulic performance. More detailed discussion of thermal hydraulic performance is presented in Chapter 6.

Up to 20 subsequent cycles were modeled to assess the possibility of a sustainable scenario from the net TRU balance viewpoint. 7, 10 and 20 years of decay time intervals were assumed between the fuel discharge and its next loading to the reactor core to assess the effect of short lived isotopes decay on the neutronic performance and on fuel reprocessing and handling between recycles. The number of FFF pins per assembly and the amount of TRU loaded each cycle was conserved. In this case, the convergence of fuel cycle length to some constant value and stabilization of TRU composition would be the primary indicators of approaching an equilibrium state.

The presence of burnable poison in the FFF pins significantly impairs the efficiency of TRU destruction (Table 5.2.I) due to the lower power in FFF pins and competition for neutron absorption between TRU nuclides and the burnable poison. Therefore, a higher initial TRU loading would be required for the CONFU assembly with burnable poison to achieve equilibrium. Tables 5.2.II and 5.2.III summarize the cycle-by-cycle fuel materials flows for the un-poisoned and poisoned CONFU assemblies respectively with 7 years of decay between reloadings.

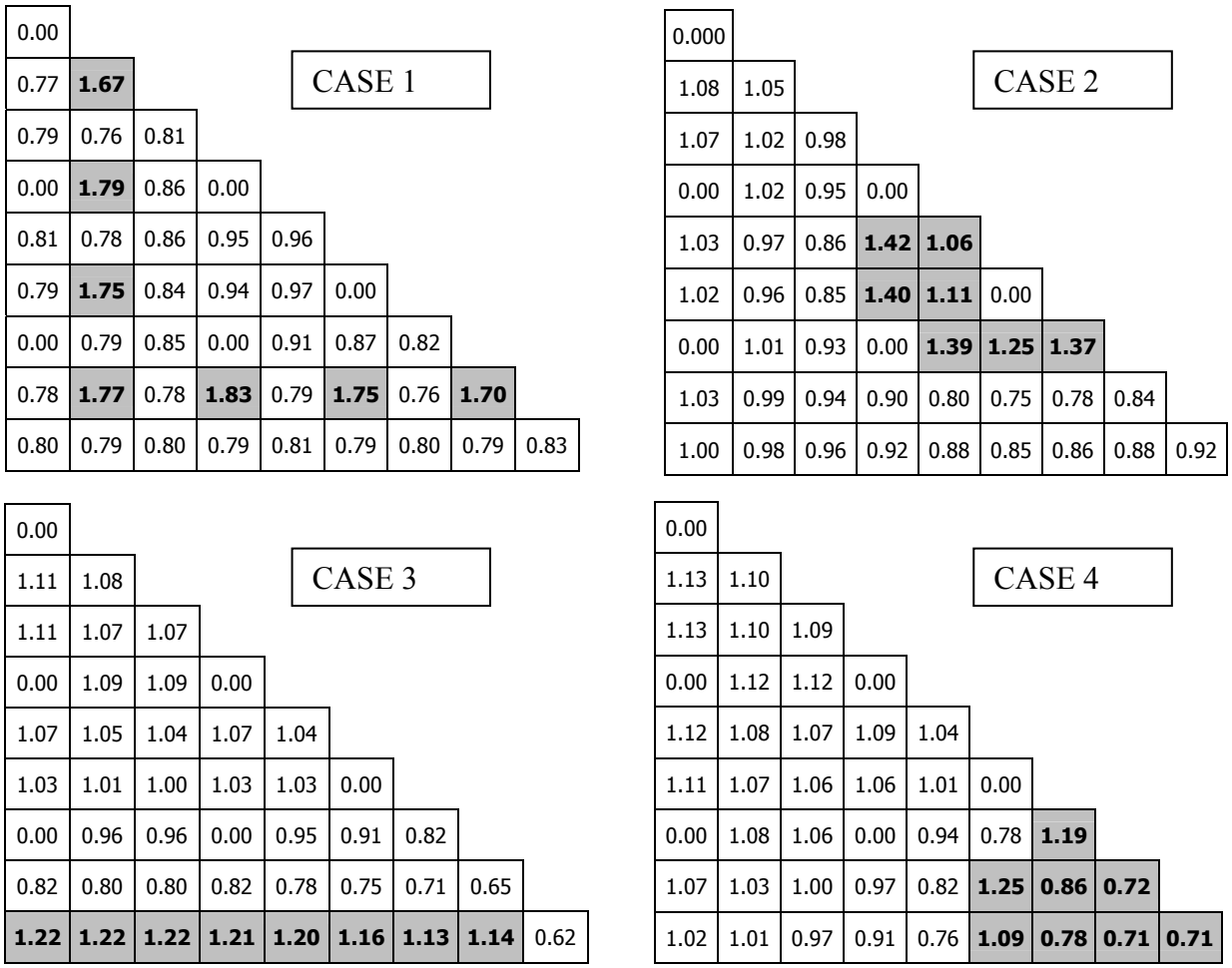

Figure 5.2.1. CONFU Assembly BOL Pin Power Distribution: Selected Design Options and Results

Table 5.2.I. TRU Destruction Efficiency for FFF Pins in CONFU Assembly (%)

Recycle Stage	1	2	3	4	5
TRU Burnup without BP	50.78	40.13	37.32	36.21	34.63
TRU Burnup with BP	32.62	30.60	27.94	26.96	26.60

The results of the calculations presented above prove that a sustainable fuel cycle design is feasible. Table 5.2.II and Table 5.2.III show clearly that the TRU generation balance and the fuel cycle length are converging to constant values for both poisoned and un-poisoned CONFU assemblies.

The effect of different inter-recycling (or cooling) times is illustrated in Figure 5.2.2. A decay period of 20 years noticeably (up to 10%) shortens the equilibrium fuel cycle length because of the decay of the important fissile Pu241 isotope to Am241 with a 14.4 year half-life. Am241 is difficult to transmute because following the neutron capture the daughter nuclide Am242 rapidly decays with high probability to Cm242 and then to Pu238. The α-decay of Cm242 results in He accumulation in the fuel and may aggravate fuel pin pressurization problem due to release of the helium gas. However, long cooling times before fuel reprocessing were found to be beneficial for handling the fuel because of the partial decay of Cf252 and Cm244 isotopes and therefore a substantial reduction in the spontaneous fission neutron dose during fuel reprocessing and fabrication. The cooling time has a limited impact on the TRU net generation as shown in Figure 5.2.3.

Figures 5.2.4 through 5.2.7 present the evolution of TRU isotopes with the number of TRU recycle stages. Each of the isotope concentrations shown in the Figures 5.2.4 through 5.2.7 is normalized per maximum value of its concentration between 1^{st} and 20^{th} recycle. The TRU isotopic vector composition saturates completely after about 20 recycles as far as most neutronically important isotopes are concerned. However, the buildup of some Cm (246,247,248) and Cf (249,250,251,252) isotopes require significantly greater number of recycles to saturate completely. As mentioned earlier, the importance of these isotopes buildup lays in the fact that even their minute amounts can significantly complicate the fuel handling and reprocessing due to very high spontaneous fission (SF) neutron source. The buildup of Np236 isotope was observed due to an increasing fraction of U236 in the recycled uranium traces. 99.995% separation efficiency was assumed for the separation of TRU from UO_2 fuel. No U-TRU separation was assumed for the reprocessed fertile free fuel.

Table 5.2.II. Un-Poisoned CONFU Assembly (Case 3): Materials Flow Summary (per 1 GWeY)

	Recycle Stage					
	1	2	3	4	5	6
Total HM Loaded, kg	16,149	18,698	19,330	19,470	19,538	19,582
Uranium Loaded, kg	15,578	18,037	18,647	18,781	18,847	18,889
TRU Loaded to FFF pins, kg	580	671	694	699	701	703
TRU Discharged from UO_2 pins, kg	209	227	231	231	228	230
TRU Discharged from FFF pins, kg	285	402	435	454	458	457
TRU Discharged Total, kg	495	629	665	684	685	687
Net TRU generation, kg	-85.1	-42.4	-28.7	-14.5	-15.8	-16.0
Discharge Burnup, MWd/kg	68.3	59.0	57.1	56.7	56.5	56.3
Discharge Burnup, EFPD	1428	1233	1193	1184	1180	1177

Table 5.2.III. Poisoned CONFU Assembly (Case 3): Materials Flow Summary (per 1 GWeY)

	Recycle Stage				
	1	2	3	4	5
Total HM Loaded, kg	17,996	19,486	20,539	20,916	21,019
Uranium Loaded, kg	17,334	18,770	19,784	20,147	20,247
TRU Loaded to FFF pins, kg	671	727	766	780	784
TRU Discharged from UO_2 pins, kg	218	232	239	241	242
TRU Discharged from FFF pins, kg	453	505	552	570	576
TRU Discharged Total, kg	671	737	791	811	817
Net TRU generation, kg	-0.8	9.7	24.8	30.8	33.0
Discharge Burnup, MWD/kg	61.3	56.6	53.7	52.7	52.5
Discharge Burnup, EFPD	1279	1231	1168	1147	1142

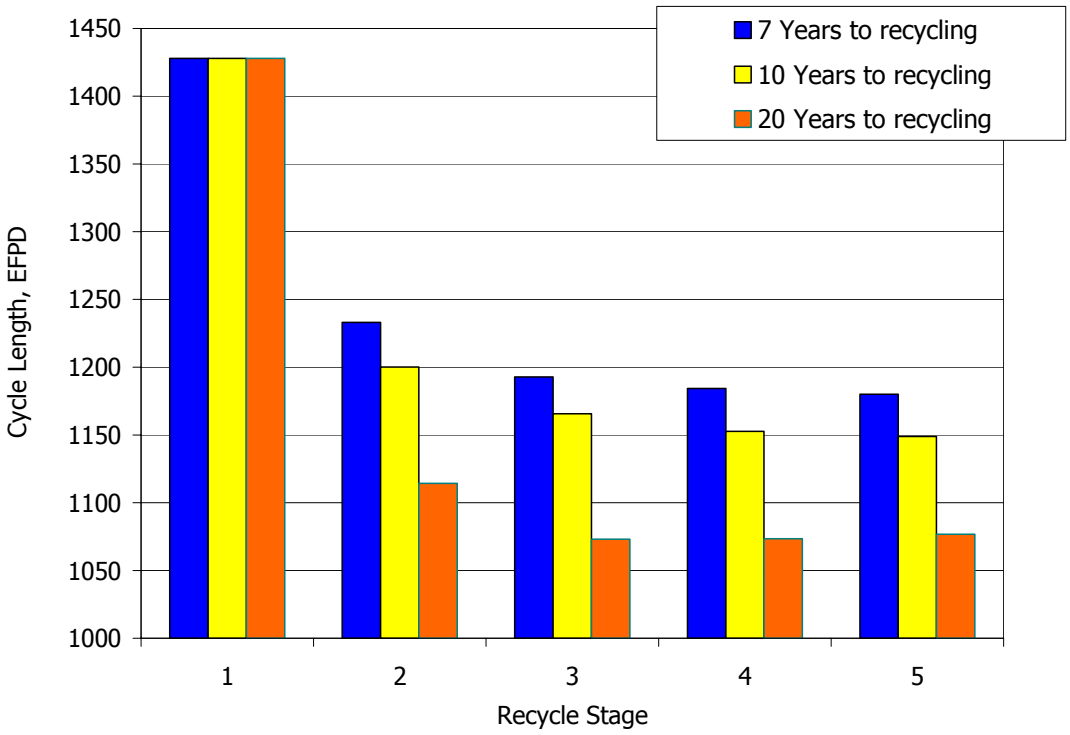

Figure 5.2.2. Fuel cycle length

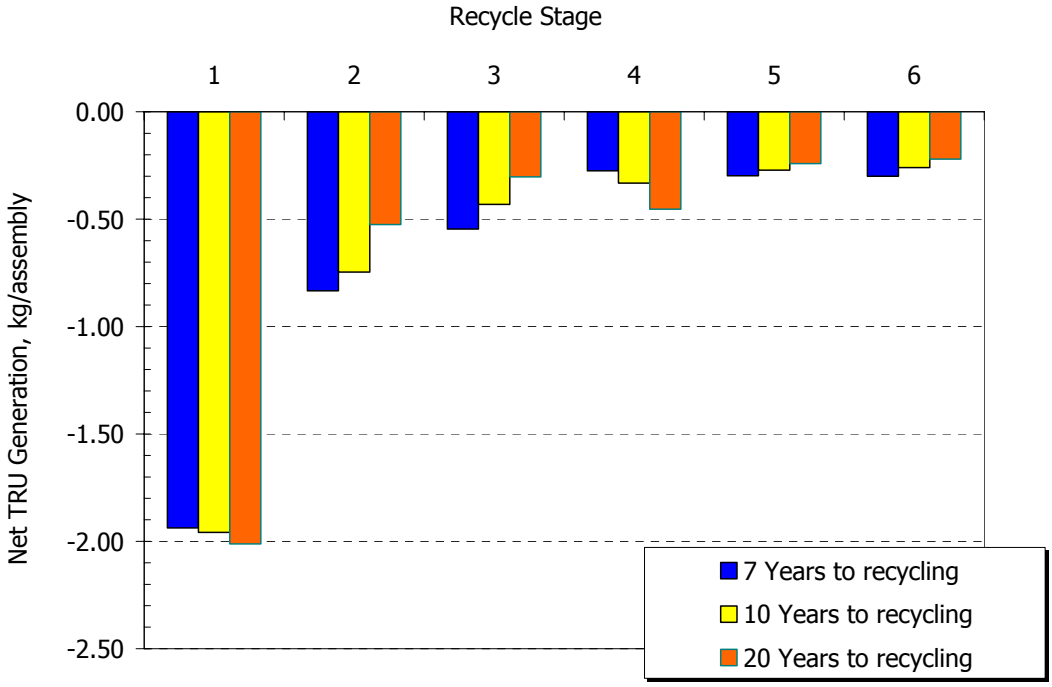

Figure 5.2.3. Net TRU generation

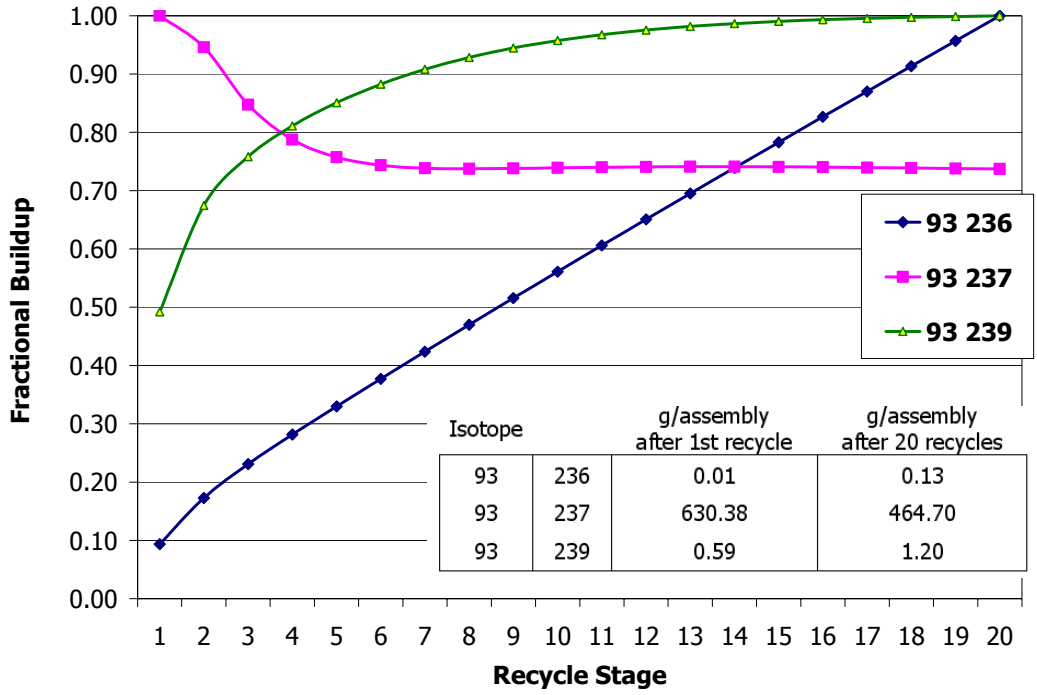

Figure 5.2.4. Np isotopes evolution with the number of TRU recycles

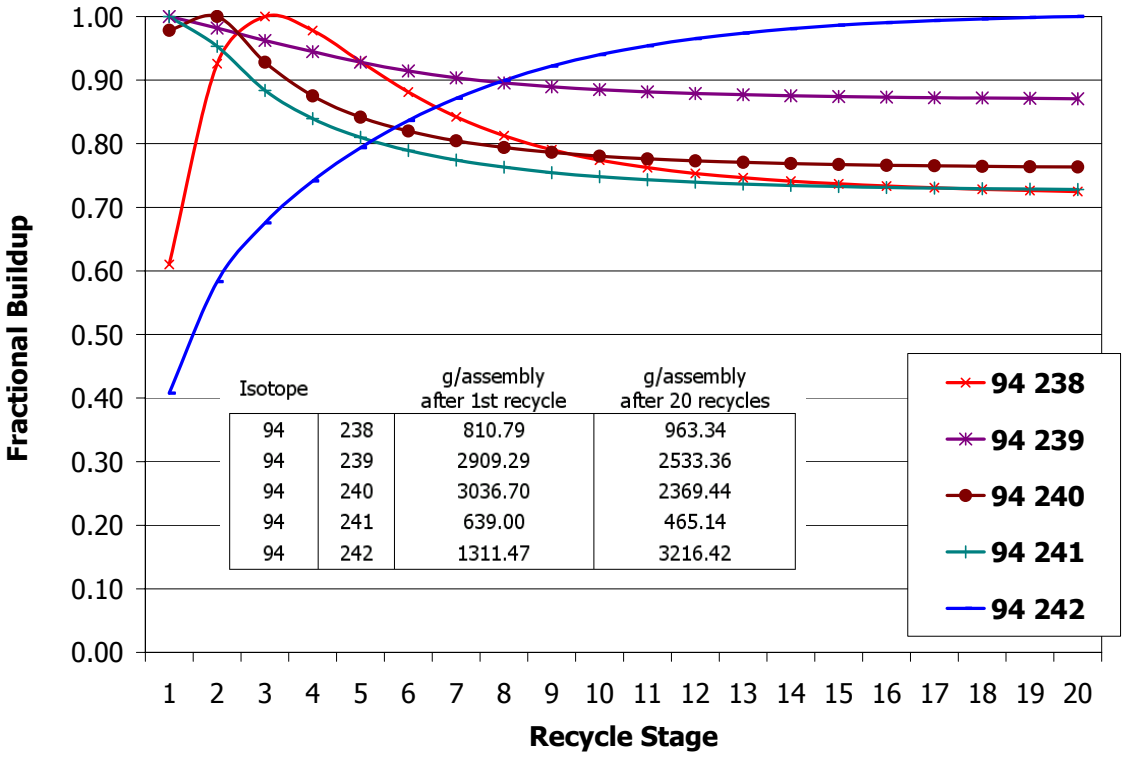

Figure 5.2.5. Pu isotopes evolution with the number of TRU recycles

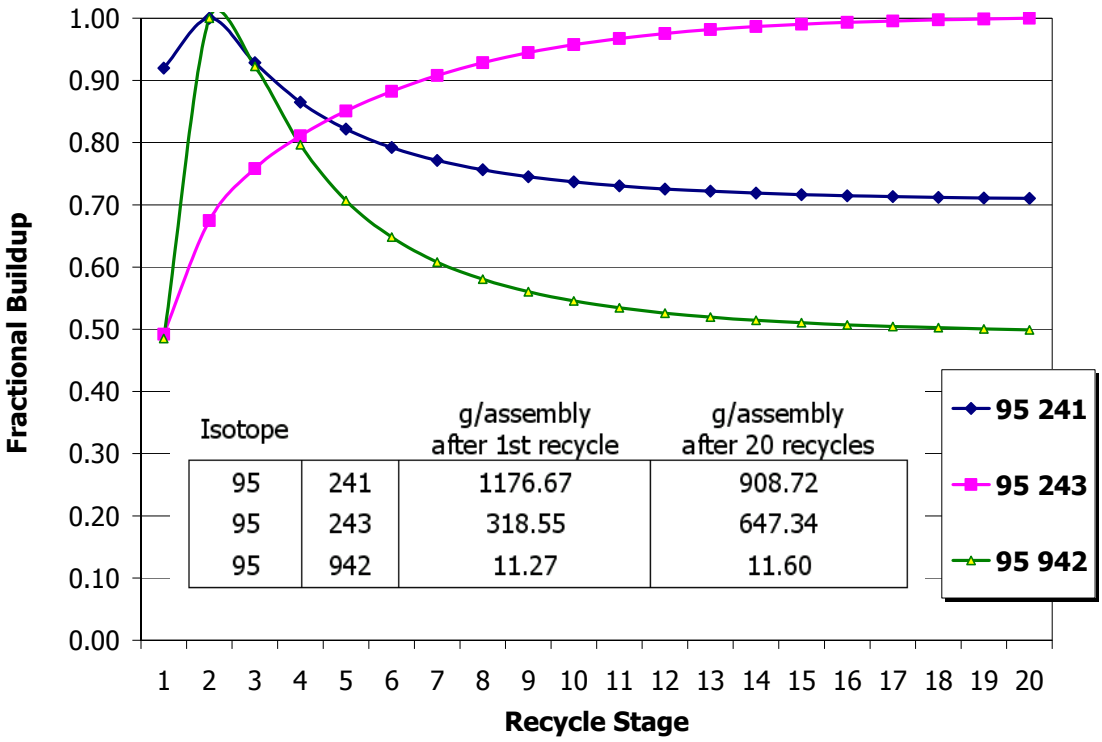

Isotope		g/assembly after 1st recycle	g/assembly after 20 recycles
95	241	1176.67	908.72
95	243	318.55	647.34
95	942	11.27	11.60

Figure 5.2.6. Am isotopes evolution with the number of TRU recycles

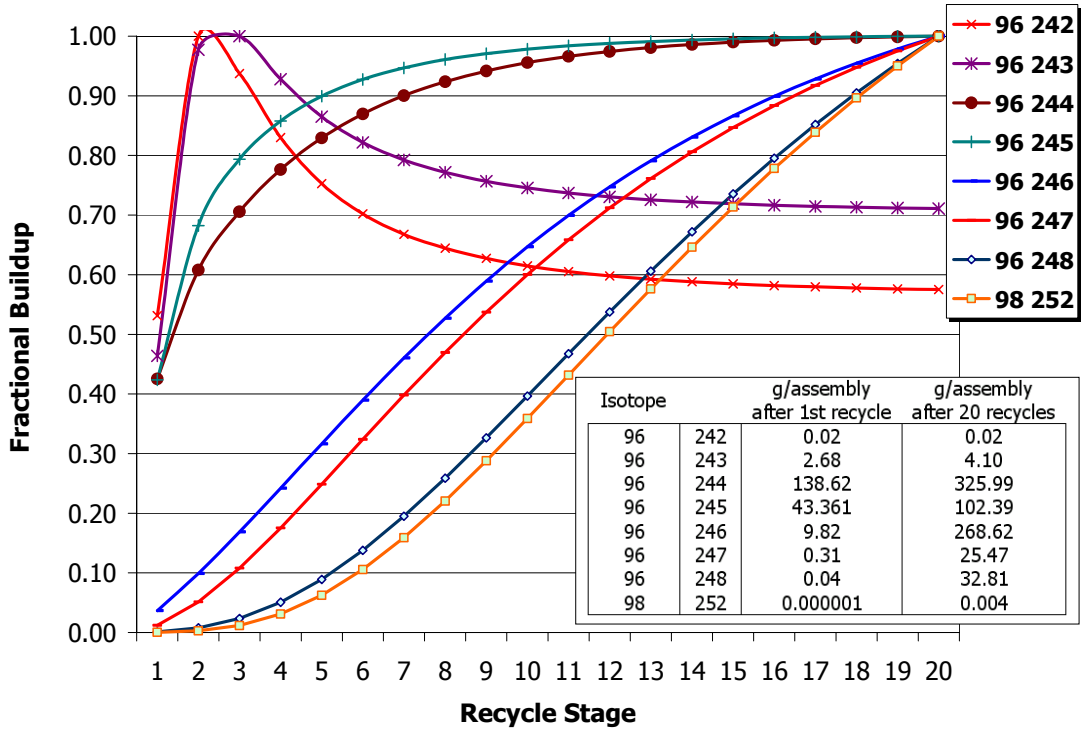

Isotope		g/assembly after 1st recycle	g/assembly after 20 recycles
96	242	0.02	0.02
96	243	2.68	4.10
96	244	138.62	325.99
96	245	43.361	102.39
96	246	9.82	268.62
96	247	0.31	25.47
96	248	0.04	32.81
98	252	0.000001	0.004

Figure 5.2.7. Cm and Cf isotopes evolution with the number of TRU recycles

It should also be noted that the equilibrium fuel cycle length is shorter than that of the reference 4.2% enriched UO_2 fuel by up to 20% for all the cases with different cooling down periods. As a result, higher enrichments will be required for the UO_2 pins in the CONFU assembly with equilibrium TRU isotopic vector in order to match the cycle length of the reference UO_2 fuel. Degradation of the TRU isotopic composition results not only in a shorter fuel cycle length but also lower power in the fertile free pins throughout the cycle and therefore lower TRU destruction efficiency. In a standard PWR fuel lattice, an FFF pin with equilibrium TRU isotopic mixture is subcritical even at the beginning of irradiation as can be observed from Figure 5.2.8.

The reactivity of FFF pins can be increased by

- increasing TRU loading in FFF pins and reducing their number. This will increase the number of UO_2 pins per assembly and therefore increase the fraction of the more reactive TRU from UO_2 pins in the TRU mixture to be loaded into FFF pins in the subsequent cycle
- improving neutron moderation (higher V_m/V_f)
- increasing the interface area between FFF and UO_2 pins since the thermal neutron flux is much higher in the UO_2 region and can be shared more effectively with FFF pins.

All three mentioned strategies have been explored. The TRU loading has a practical limit of 20v/o defined by the fuel material performance under irradiation [Long Y. et al., 2003]. Therefore, significant reduction in the number of FFF pins per assembly cannot be realized. If the number of FFF pins is too small, the TRU destruction will be too small to match TRU generation, and a balance cannot be maintained. In addition, reduction of the number of FFF pins leads to a greater power imbalance between UO_2 and FFF pins.

Changing the lattice parameters is also undesirable because increasing the coolant volume while conserving the core volume and total power will increase the specific power density and decrease the fuel to coolant heat transfer area, unless unconventional fuel geometries are adopted. Additionally, the equilibrium TRU mixture remains subcritical for most of its core residence time even if V_m/V_f is increased from 1.67 to 7.8. Figure 5.2.9 shows the results of a single FFF pin cell burnup calculations with different TRU loading. The fuel pin with the first time recycled TRU in FFF pin with only 10 v/o loading has k-inf greater than one almost throughout the entire in-core residence time. The FFF pins with equilibrium TRU vector, however, runs out of reactivity in a fraction of the first cycle.

The strategy of increasing the FFF-UO_2 pins interface area has been found to be more effective. Some optimization in the location of FFF pins within the CONFU assembly to obtain acceptable power peaking and satisfy thermal hydraulic design requirements resulted in the configuration presented in Figure 5.2.10. These improvements in the equilibrium CONFU assembly design do not result in an increase in the fuel cycle length sufficient enough to match the reference UO_2 fuel cycle length. The enrichment of UO2 pins in the equilibrium CONFU assembly has to be increased to 5% to achieve discharge burnup corresponding to that of the reference UO_2 fuel (1350 EFPD). The major characteristics of the equilibrium CONFU assembly are summarized in Table 5.2.IV. The fuel cycle length, net TRU generation, and TRU composition (with the exception of the above mentioned isotopes of Cm and Cf) remain constant from recycle to recycle. Thus, this assembly design was adopted for 3D core calculations, and for evaluation of the thermal hydraulic margins and economic analysis. The results of these analyses are presented in subsequent chapters of this thesis.

Table 5.2.IV Equilibrium CONFU Assembly Data

Total HM per assembly, kg	393
Uranium per assembly, kg	375
Uranium Enrichment, %	5.0
TRU Loaded to FFF pins, kg	17.54
TRU volume fraction in FFF pins, v/o	20.0
TRU Discharged from UO2 pins, kg	5.20
TRU Discharged from FFF pins, kg	12.23
TRU Discharged Total, kg	17.42
TRU Burned in FFF pins, %	30.30
Net TRU generation, kg	-0.12
BU3, MWD/kg	60.65
BU3, EFPD	1348

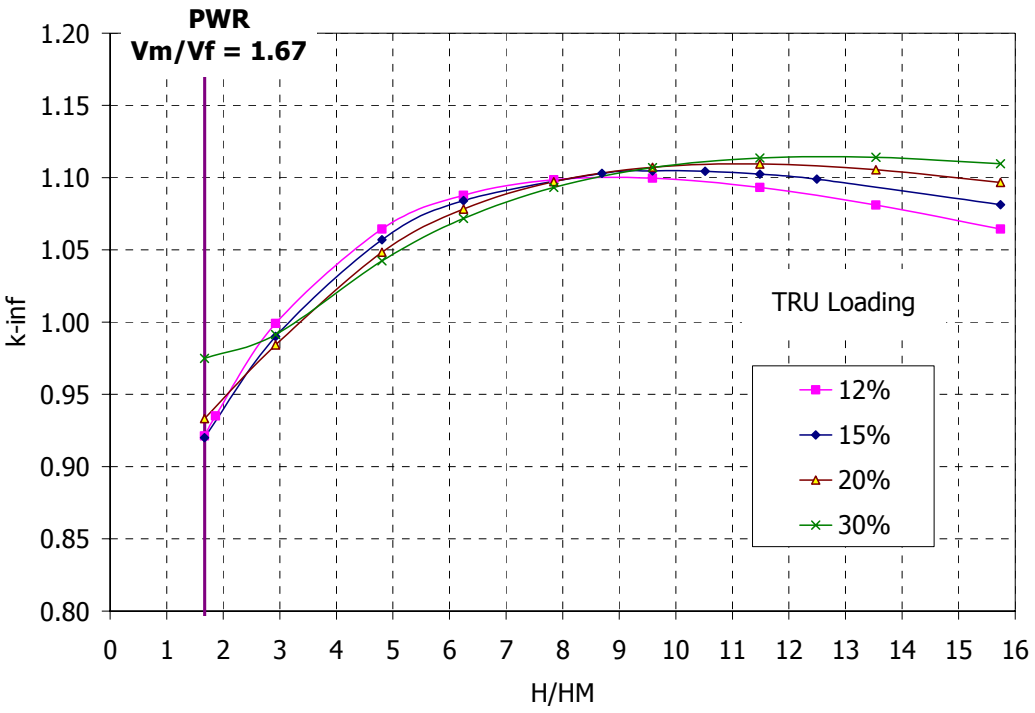

Figure 5.2.8. Moderation effect on criticality of FFF unit cell at BOL with equilibrium TRU mixture

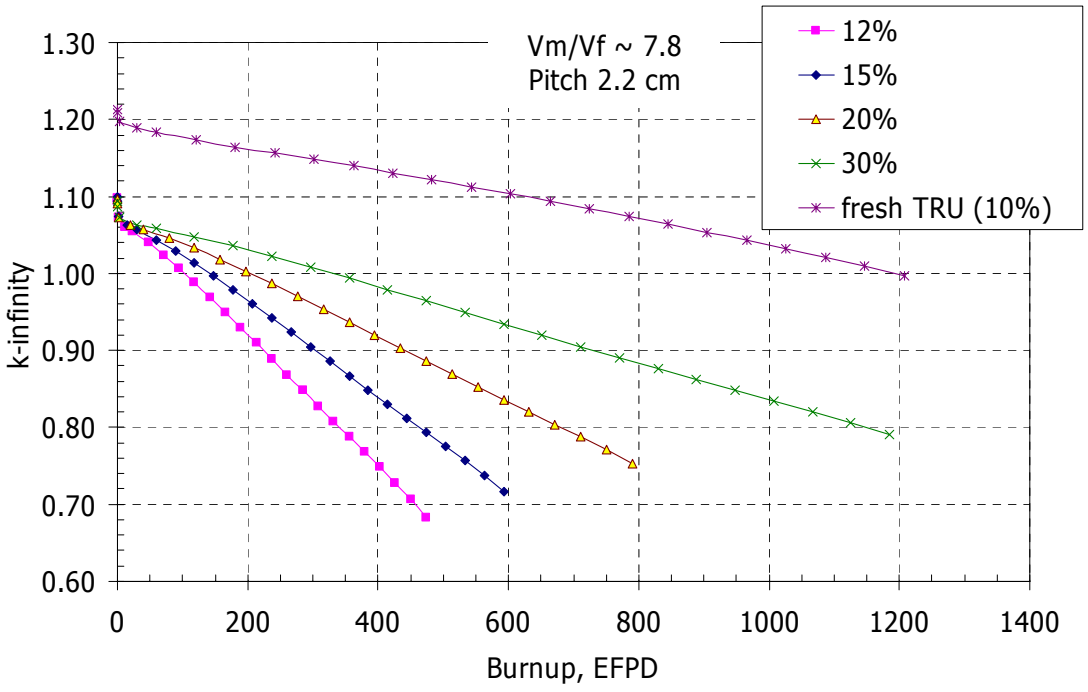

Figure 5.2.9. Burnup potential of well moderated FFF unit cell with equilibrium TRU mixture

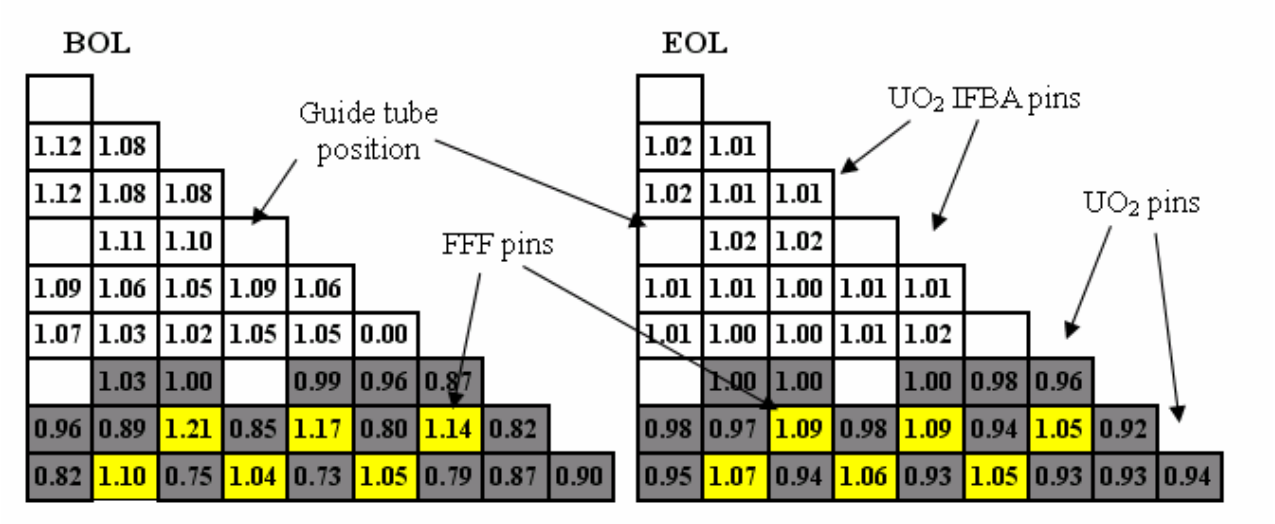

Figure 5.2.10. BOL and EOL pin power distribution for COFNFU assembly containing equilibrium TRU mixture

5.3. Waste Characteristics of the Sustainable Fuel Cycle

The processes of TRU chemical separation and fuel fabrication are not perfect and have some limited efficiency. Therefore, complete TRU recycling is impossible because some TRU will inevitably have to be discharged to the environment in the waste stream of separation and fabrication processes. Additional calculations were performed to quantify the effect of TRU losses on repository load and compare it with conventional UO_2 spent fuel characteristics. The total TRU losses during each recycle stage were assumed to be 0.1%. For conservatism, it was assumed that all the losses occur at one time point of 5 years after discharge. The waste stream characteristics were analyzed for the time interval between 0 and 1M years after separation.

The results are reported in Figures 5.3.1 through 5.3.4. All the data summarized in Figures 5.3.1 - 5.3.4 are normalized per cycle energy in GWe-Years. The results indicate that the activity, decay heat load and radiotoxicity due to TRU of the waste streams from the CONFU type fuel are up to 3 orders of magnitude lower than the same characteristics of the conventional once through UO_2 fuel cycle for the entire time interval considered. The magnitude of this reduction is a direct consequence of the efficiency of TRU separation. Although 0.1% of reprocessing losses may be

an ambitious assumption for the existing practice, the efficiency of separation is expected to improve with accumulation of industrial experience and extensive R&D effort provided that the closed fuel cycle option is actively pursued. The efficiency of separation on the order of 0.1% is considered to be achievable by reprocessing experts using technologies developed under the Advanced Fuel Cycle Initiative (AFCI) program [DOE/NE, 2003].

Figure 5.3.5 compares the UO_2 and CONFU fuel cycles' radiotoxicity relative to that of the equivalent amount of natural uranium ore. The CONFU cycle radiotoxicity decreases to the level of original uranium ore in about 1000 years period, which complies with the transmutation goals [Van Tuyle G.J., 2001].

It must also be noted that the data for environmental hazard characteristics reported here was obtained without any additional assumptions regarding the transport of radioactive nuclides. Namely, it was assumed that all the radioactive nuclides in the repository are immediately exposed to the environment and all engineering and geological barriers are ignored. In practice, some of the nuclides represent greater radiological concern in the long term not just because of the higher radiotoxicity but mainly due to their enhanced solubility in water and therefore greater mobility in the environment. Long lived fission product, in particular, Tc99 and I129 represent from 0.04% to 0.1% of total spent fuel radiotoxicity during the period between 10 thousand and 1 million years. However, these nuclides are major contributors to the collective dose from the repository in the same period due to their high mobility in the environment. Therefore, they must be also recycled in order to meet the collective dose reduction goal [Van Tuyle G.J. 2001]. The feasibility of Tc99 and I129 transmutation in various reactor types and the fuel cycle implications of Tc and I recycling are discussed in details in [Brusselaers P. et al., 1996].

Figure 5.3.6 compares the contribution of fission products to the waste stream decay heat load of the once through UO_2 cycle and closed CONFU cycle. The short term heat generation is dominated by the short lived fission products (SLFP). However, the total heat load decreases faster for the CONFU case because of the smaller contribution of the actinides. Figure 5.3.7 shows the difference in percent between fission products heat generation for the UO_2 and CONFU cases. The heat load level is up to 20% higher for the CONFU fuel case during the on-site cooling down period between 0 and about 5 years after discharge. However, the decay heat per energy produced in the CONFU cycle is somewhat lower during the period when the reprocessing is likely to take place. The decay heat per fuel assembly is always lower for the CONFU fuel because of the shorter equilibrium cycle as a result of TRU isotopics degradation.

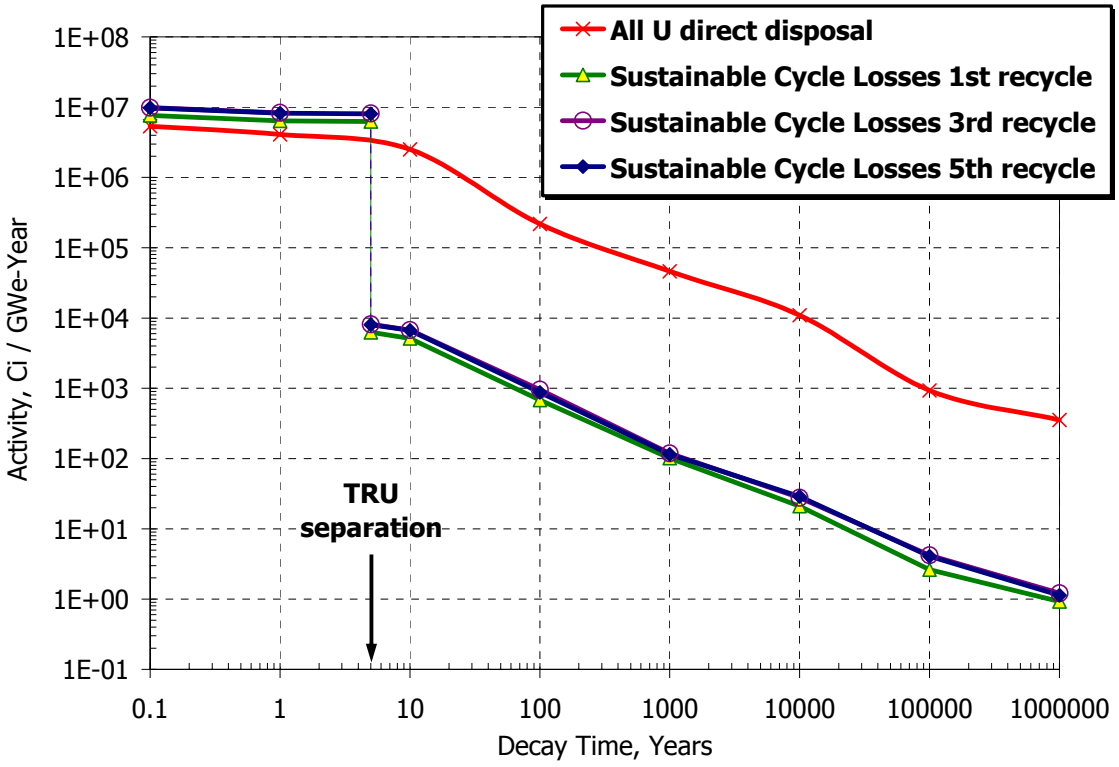

Figure 5.3.1. TRU losses from CONFU assembly recycling process: Activity

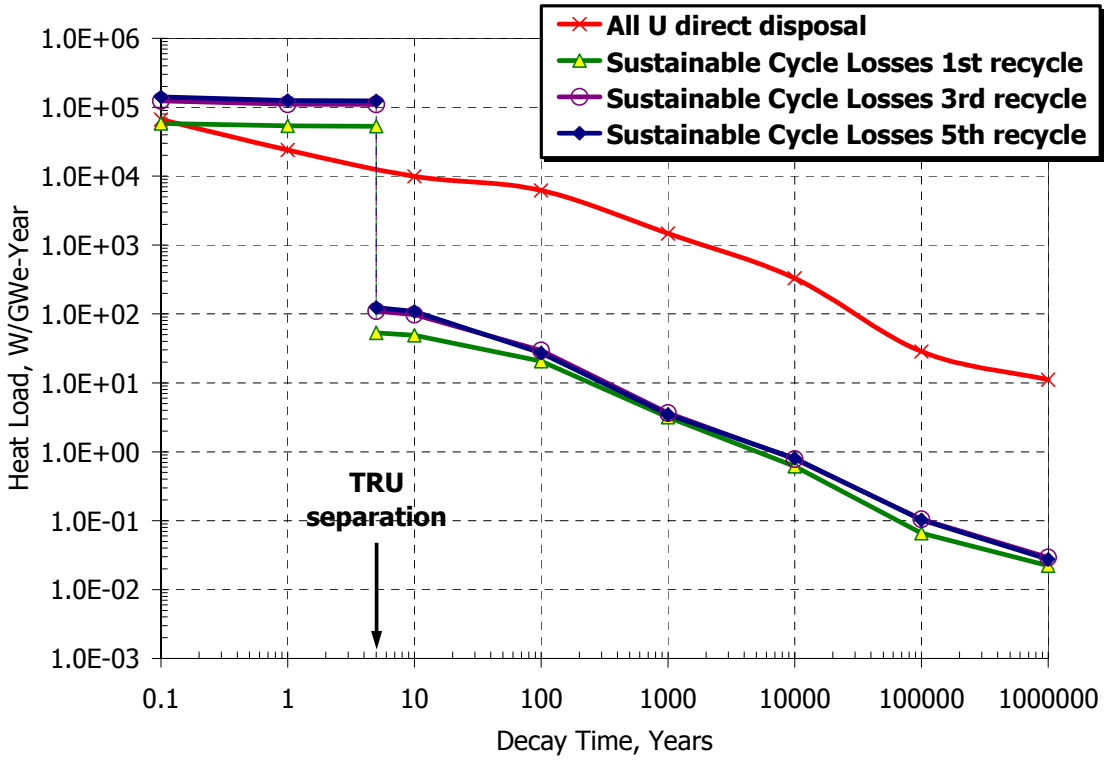

Figure 5.3.2. TRU losses from CONFU assembly recycling process: Heat load

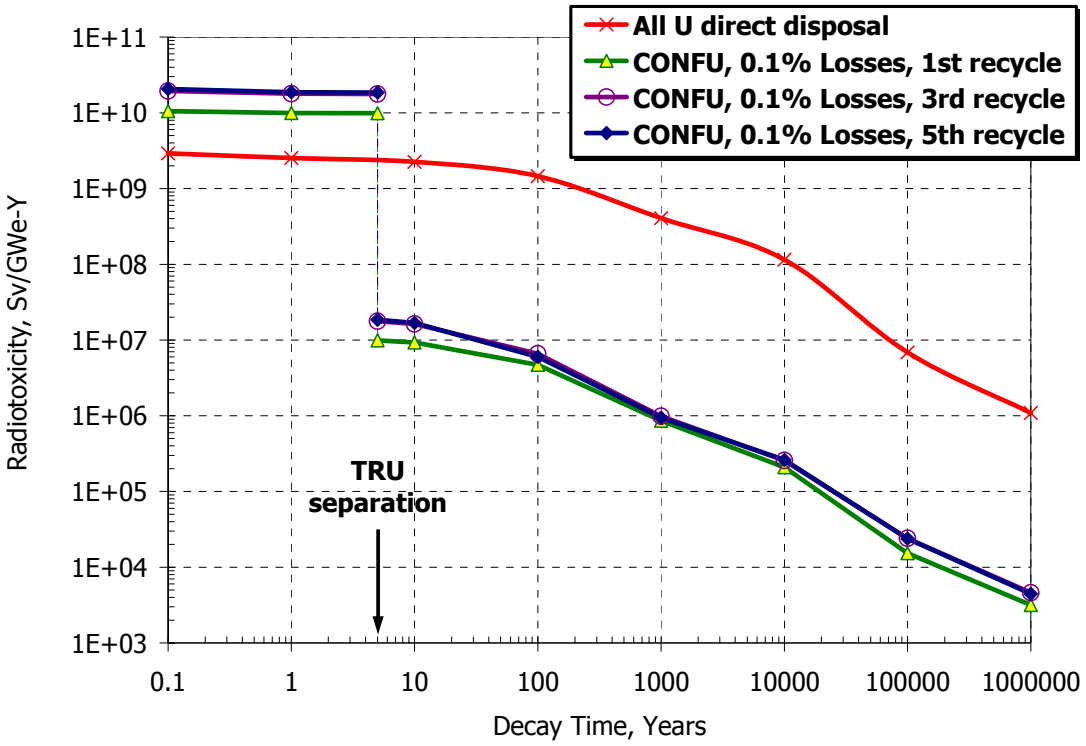

Figure 5.3.3. TRU losses from CONFU assembly recycling process: Ingestion radiotoxicity

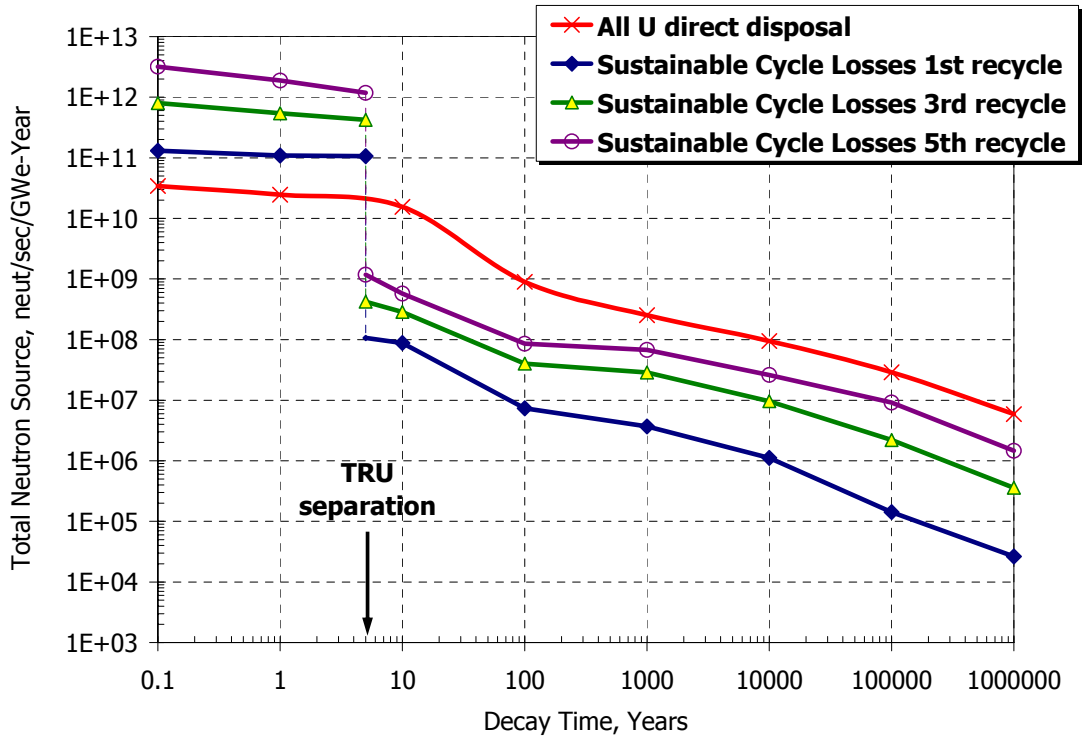

Figure 5.3.4. TRU losses from CONFU assembly recycling process: Total SF and (α,n) neutron source

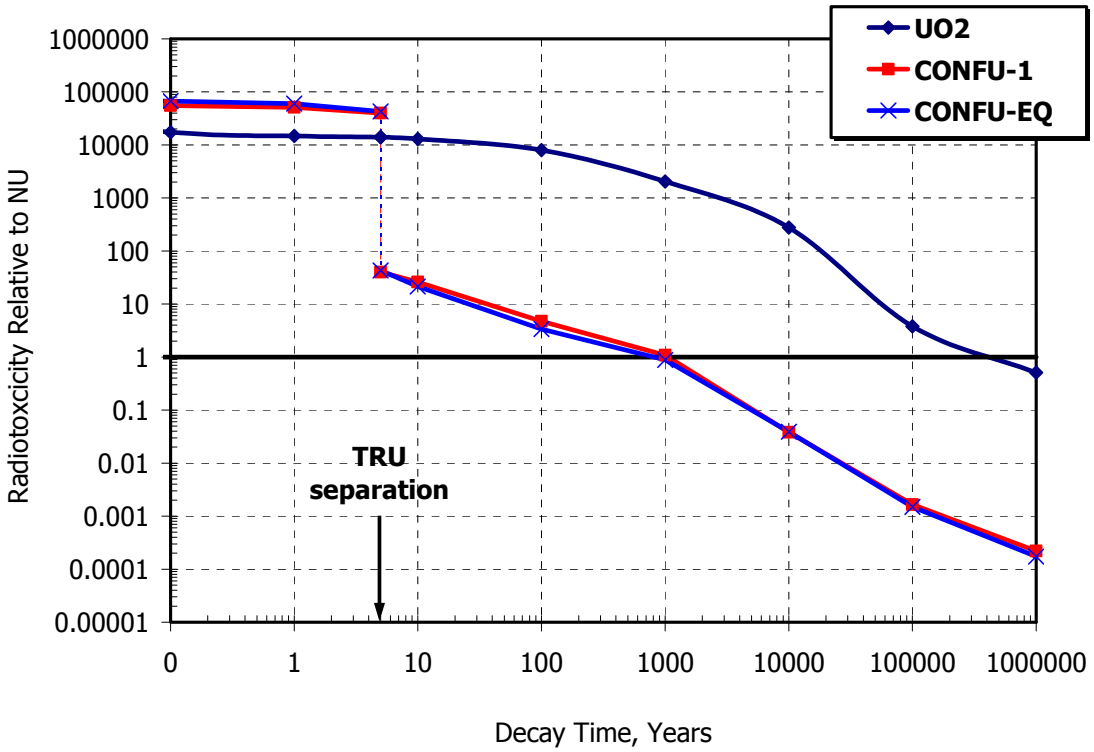

Figure 5.3.5. CONFU fuel cycle radiotoxicity relative to natural uranium ore

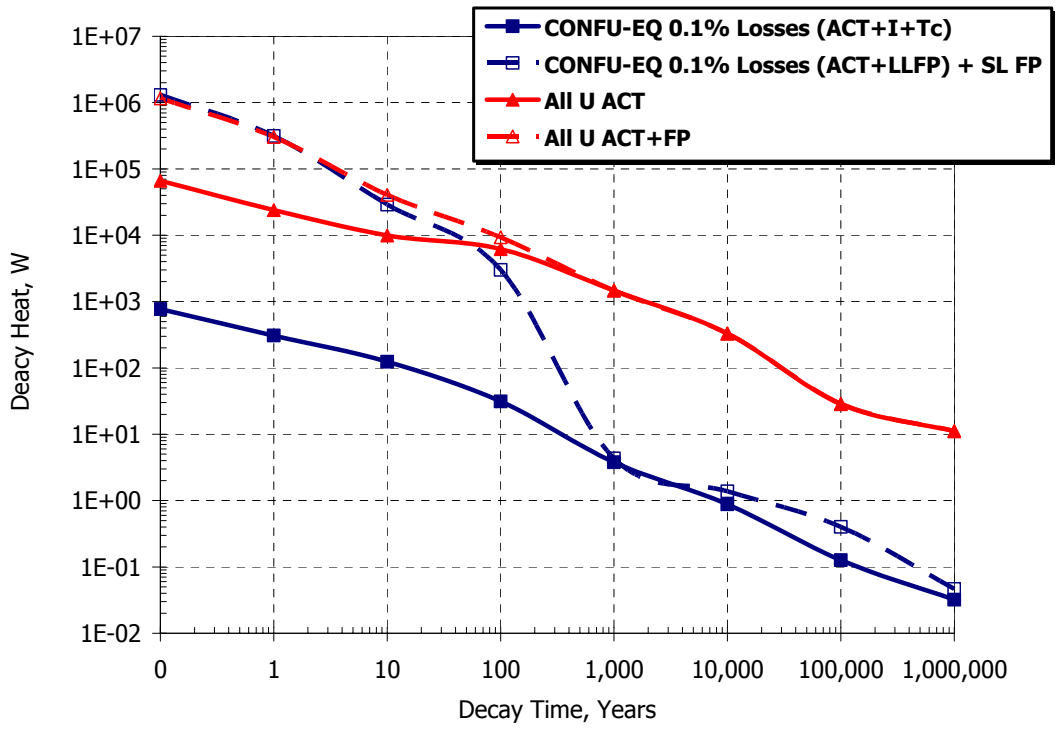

Figure 5.3.6. Fission products contribution to decay heat generation

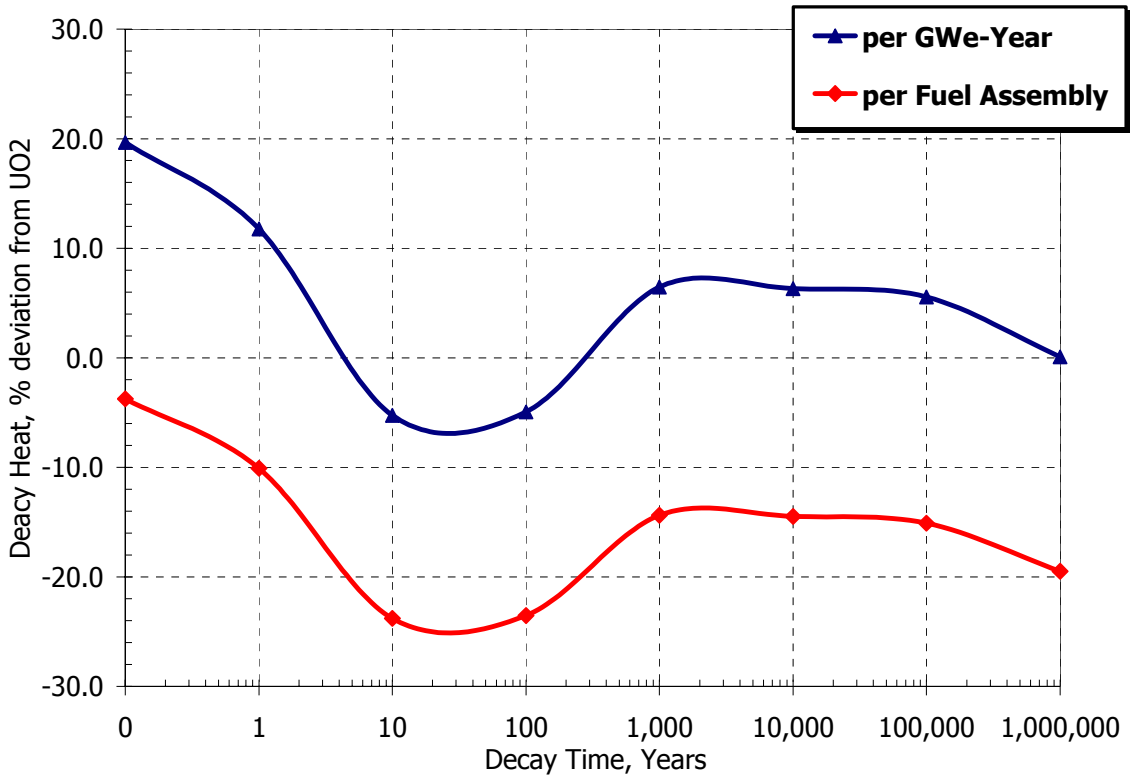

Figure 5.3.7. CONFU fuel cycle fission products decay heat relative to UO_2 cycle,

$100\% \times (P_{CONFU} - P_{UO2}) / P_{UO2}$

5.4. Reactivity and Control Characteristics

The CONFU assembly neutronic reactivity feedback coefficients should be close to the all UO_2 assembly. However, both the UO_2 enrichment and the addition of FFF pins may lead to a reduction in the presence of U238, thereby reducing the total resonance absorption in fertile nuclides. Therefore, the feedback coefficients need to be evaluated in order to assess the feasibility of retrofitting this concept into the current generation of PWRs. As in the previous sections of this thesis, the reactivity coefficients were calculated on an assembly basis at three time points – BOL, MOL and EOL with soluble boron concentrations of 1000ppm, 500ppm and 0ppm at BOL, MOL and EOL respectively. The MOX and reference all-U assembly reactivity coefficients were also calculated on the same basis for comparison purposes.

Selected results of the CONFU assembly reactivity coefficients and soluble boron worth (BW) calculations are reported in Table 5.4.I. The results show that all the coefficients as well as

BW fluctuate very slightly for different recycle stages. The DC tends to be more negative with increasing number of TRU recycles. Here, natural Er oxide was considered as a burnable poison to assess its effect on DC. The use of Er somewhat improves the DC of the CONFU fuel but the magnitude of this effect is small. Admixture of 2v/o of Er_2O_3 to FFF pins increases the absolute value of DC by up to 6%. In general, all of the CONFU assembly reactivity coefficients and soluble BW differ only slightly from the reference all-U fuel, which indicates a good potential compatibility of the CONFU fuel concept with conventional PWR systems.

Table 5.4.I. CONFU Assembly Reactivity Coefficients Summary

				No Poison, Recycle Stages			With Poison, Recycle Stages		
		MOX	All-U	1	3	5	1	3	5
DC	BOL	-2.73	-2.03	-1.77	-1.90	-1.90	-1.88	-1.95	-1.98
	MOL	-2.87	-2.65	-2.01	-2.17	-2.19	-2.11	-2.19	-2.23
	EOL	-3.03	-3.08	-2.30	-2.41	-2.45	-2.33	-2.41	-2.44
MTC	BOL	-42.48	-11.26	-13.33	-15.26	-15.64	-17.01	-17.62	-18.06
	MOL	-54.36	-39.54	-32.96	-36.03	-36.80	-37.20	-38.46	-38.79
	EOL	-73.98	-66.29	-55.08	-57.40	-58.25	-58.46	-59.02	-59.66
VC	BOL	-112.4	-34.76	-38.59	-44.37	-45.34	-47.95	-49.92	-50.88
	MOL	-148.8	-119.0	-96.35	-106.0	-107.9	-107.4	-111.5	-113.3
	EOL	-204.0	-205.9	-161.2	-172.9	-175.5	-172.1	-176.9	-178.9
BW	BOL	-2.70	-6.11	-5.16	-5.51	-5.54	-5.41	-5.64	-5.70
	MOL	-3.17	-7.09	-5.61	-6.02	-6.07	-5.81	-6.08	-6.13
	EOL	-3.91	-9.51	-6.98	-7.45	-7.57	-7.10	-7.43	-7.53

The harder than UO_2 neutron spectrum and considerably lower BW in the Pu-MOX case are likely to result in higher soluble boron concentration requirements than assumed in this analysis. Consequently, MTC and VC in the MOX case may have less negative values than the current estimation.

An evaluation of the effective delayed neutron fraction was performed in order to assess the effect of buildup of Cm isotopes with particularly small βeff with the number of recycle stages. The results are shown in Figure 5.4.1. The CONFU assembly βeff values at the beginning of fuel irradiation are moderately lower than corresponding values for the reference UO2 assembly because of Pu239 fissions in the fertile free pins. This difference disappears with burnup.

The effect of the small βeff for Cm isotopes was not observed due to the very small amounts of Cm in the fuel and thus, negligible contribution to total assembly power.

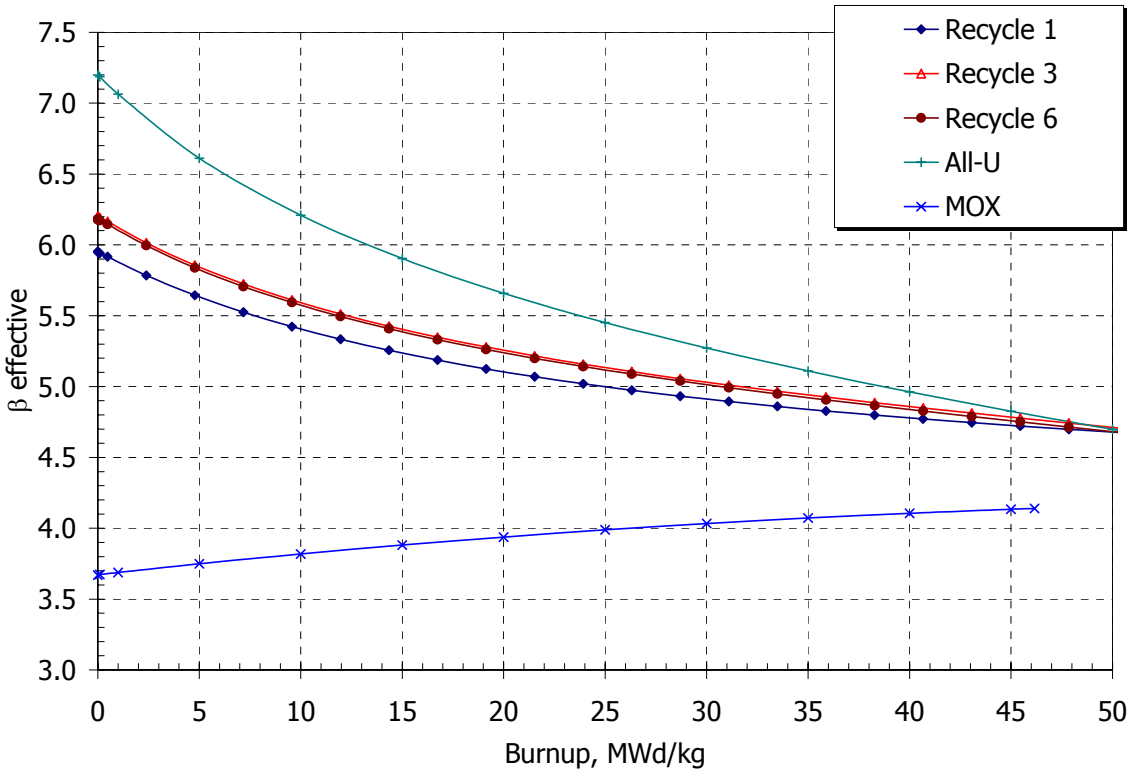

Figure 5.4.1. Effective Delayed Neutron Fraction × 10^3 vs. Burnup for CONFU Assembly

5.5. Chapter Summary

In this chapter, the potential of fertile free fuel concepts to design a sustainable fuel cycle for conventional PWRs with complete TRU recycling was evaluated through 2D assembly level depletion calculations. Evaluation of the sustainable cycle with zero net generation of TRU was based on the Combined Non-Fertile and Uranium (CONFU) assembly concept where some of the uranium fuel pins are replaced with FFF pins destined for destruction of TRU generated in the previous cycle. The results indicate that the CONFU type assembly can be designed to achieve an equilibrium state in terms of net generation of TRU and at the same time have acceptable reactivity control characteristics. Acceptable thermal-hydraulic performance of the CONFU core is expected based on evaluation of local pin power peaking.

Degradation of TRU isotopic vector with the number of recycles reduces the fuel cycle length of CONFU with equilibrium TRU mixture by up to 20% in comparison with the reference 4.2% enriched UO_2 fuel cycle length. The enrichment of UO_2 pins in the equilibrium CONFU assembly must be increased to about 5% in order to match the fuel cycle length of the reference 4.2% enriched UO_2 fuel. The fact that the mass of U235 in the equilibrium CONFU assembly with 5% enriched UO_2 pins is still lower than the mass of U235 in 4.2% enriched all UO_2 assembly may partially offset the increased cost of enrichment required for the CONFU fuel cycle. This effect is evaluated in the economics discussion of Chapter 9.

The impact on the environment of the CONFU based fuel cycle with complete recycling of TRU is limited by the materials losses during reprocessing. The CONFU based fuel cycle waste stream may have up to 3 orders of magnitude lower TRU values than the once-through All-U fuel cycle. Radiotoxicity of the sustainable fuel cycle waste stream becomes comparable to radiotoxicity of the original equivalent amount of natural uranium ore at about 1000 years – well within the lifetime of current waste disposal containers.

The buildup of some Cm and Cf isotopes that require a large number of recycles to saturate in LWR neutron spectra imposes potential limits on the number of TRU recycling stages due to a large spontaneous fission neutron source which can significantly complicate spent fuel handling, separation and fabrication procedures. Longer cooling time between recycles may be beneficial for reducing the SF neutron source. However, decay of valuable fissile isotope Pu241 shortens the

fuel cycle length. Therefore, higher make up UO_2 enrichment will be required if longer cooling times are employed.

The effect of Cm buildup on the effective delayed neutron fraction is negligible. The β_{eff} values for the CONFU assembly are comparable with the reference PWR UO_2 fuel.

Chapter 6. A Sustainable Fuel Cycle: Core Design Feasibility

6.1. 3-Dimentional Core Neutronic Analysis

The results of the analysis presented in the Chapter 5 were obtained from 2D fuel assembly level neutronic calculations. In practice, the neutronic characteristics of the whole core may differ significantly from the 2D assembly based results. It is difficult or practically impossible to extrapolate certain neutronic values obtained from the 2D calculations to the behavior of the whole core. The presence of fuel assemblies of different types or with different burnup levels, the presence of the soluble boron in the coolant (with constantly changing concentration with burnup) and the neutron leakage from the finite core dimensions are difficult to reflect accurately in the assembly based simulations.

In the proposed fuel cycle concept, significant amounts of TRU in the fertile free fuel matrix are assumed to be loaded into the core together with conventional UO_2 fuel. This addition results in significant changes in reactivity feedback coefficients, reactivity worth of control materials, reactor kinetics parameters, and power peaking factors. Therefore, 3-dimensional whole core simulation is required to demonstrate the feasibility of TRU recycling in PWRs. At the same time however, a detailed core design and evaluation at a level needed for licensing is beyond the scope of this thesis. Therefore, certain simplifying assumptions are made in the present designs so that the core performance parameters and characteristics are not to be judged on an absolute scale. The magnitude of the core design characteristics presented in this section relative to each other and to the reference UO_2 core should serve as the primary indicators of feasibility or measures of particular advantages of the suggested designs.

The following cases were chosen for 3D core analysis to cover a wide range of possible options:

- The reference 4.2% enriched UO_2 fueled core.
- A PWR core fully loaded with fertile free fuel containing TRU from reprocessed LWR fuel.
- A PWR core loaded with CONFU assemblies with first time recycled TRU from spent LWR fuel.
- A PWR core loaded with CONFU assemblies with equilibrium composition of TRU.

In addition, heterogeneous cores having a full scale UO_2-fueled assemblies and fertile free fueled assemblies (macro-heterogeneous core) are explored as an alternative option for the CONFU (micro-heterogeneous) assembly core. The separation of fertile free fuel pins from the UO_2 pin into different assemblies allows additional flexibility for the core design by choosing different fuel management scheme for the two assembly types. Longer than three cycles residence time for the fertile free fuel assemblies can allow deeper TRU burnup although it may challenge the fuel and cladding materials limits under irradiation.

The macro heterogeneous cases considered are:

- A PWR core loaded with UO_2 and fertile free fuel assemblies with first time recycled TRU from spent LWR fuel (case 5)
- A PWR core loaded with UO_2 and fertile free fuel assemblies with equilibrium TRU composition (case 6)
- A macro heterogeneous equilibrium TRU loaded core where FFF assemblies are managed in 4 and 5 batches while UO_2 assemblies are reloaded in 3 batches (cases 7 and 8 respectively)

Table 6.1.I presents nomenclature and brief description of the calculated cases mentioned above.

Table 6.1.I List of calculated 3D core simulation cases

	Designation in the text	Case description
Case 1	UO_2	Reference UO_2 core
Case 2	FFF	Fully FFF loaded core with 1st time recycled TRU
Case 3	CONFU-1	CONFU assembly core with 1st time recycled TRU
Case 4	CONFU-E	CONFU assembly core with equilibrium TRU composition
Case 5	M-CONFU-1	Macro-heterogeneous CONFU core with 1st time recycled TRU
Case 6	M-CONFU-E	Macro-heterogeneous CONFU core with equilibrium TRU
Case 7	M-CONFU-E4	Macro-het. CONFU core with eq. TRU – 4batch management for FFF
Case 8	M-CONFU-E5	Macro-het. CONFU core with eq. TRU – 5batch management for FFF

A number of design constraints were set to ensure that innovative fuel can be retrofit into existing PWRs without any major changes in the reactor technology, equipment or operating practices.

- The 18 months fuel cycle length corresponding to 450 EFPD per cycle was maintained the same for all calculated cases.

- Core power density (104.5 W/cm^3) is identical to UO_2 reference core
- 3 batch fuel management (except for the last two macro heterogeneous cases mentioned above)
- Overall nuclear peaking factors are comparable to UO_2 case
- Negative reactivity coefficients at HFP condition throughout the core lifetime
- Critical boron concentration should not exceed 2000 ppm at any time during the cycle
- TRU loading in FFF is limited to 20 v/o due to the fuel performance constraints

The main objectives of the 3D whole core simulation are

- to ensure that the FFF component of the core can achieve a burnup level sufficient to maintain zero net TRU generation balance as predicted by the 2D analysis
- to obtain 3-dimensional core power distribution with acceptable peaking factors to be used in thermal hydraulic analysis
- to obtain dynamic core parameters, reactivity coefficients and control rod worths to be used in reactivity initiated accident analysis

6.2. Local Pin Power Distribution Prediction Benchmark

The local power peaking factors have a direct impact on thermal hydraulic design and can be obtained through 3D core simulation. The CASMO-SIMULATE code package is widely used by the nuclear industry for analysis of conventional UO_2 cores and to some extent for MOX fueled cores. SIMULATE3, a 3D nodal diffusion code, includes a pin-power reconstruction module that can predict 3-dimensional pin power distribution in the UO_2 core with exceptional accuracy (of less than 1%) that can be used in thermal hydraulic and licensing calculations [K.R.Rempe, et al. 1989]. In the case of MOX fuel or FFF with the large loading of Pu or TRU, high thermal flux gradients may exist near the boundary between assemblies of different types so that the accuracy of pin power reconstruction accuracy may not be sufficient.

A set of simple benchmark cases were carried out in order to evaluate the capabilities of the available academic version of SIMULATE3 to reconstruct pin power distribution in the CONFU assembly and in the full FFF assembly.

First, the single CONFU assembly pin power distribution predicted by CASMO4 was compared to the Monte Carlo – ORIGEN2.2 (MCODE) results for fresh and depleted CONFU assemblies. In the MCODE calculation, each fuel pin was modeled individually to obtain correct EOL pin power distribution within an assembly. In the next stage, a 2-dimensional colorset of 4 CONFU fuel assemblies with different burnup as presented in Figure 6.2.1 (case B-2) was calculated with CASMO4 and the results were compared to those obtained with SIMULATE3. Additionally, a third set of calculations was performed for the 2x2 colorset of whole assemblies of UO2 and FFF pins. The setup of three benchmark cases is schematically presented in Figure 6.2.1.

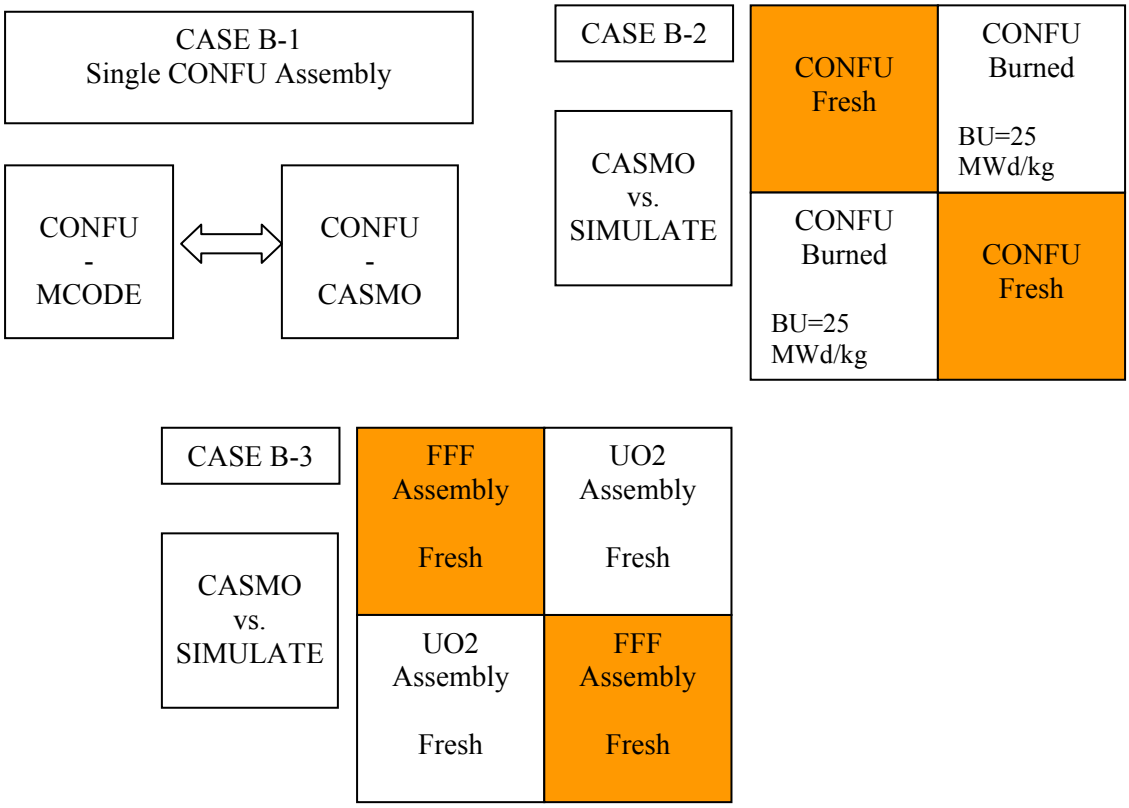

Figure 6.2.1. Schematic views of pin power distribution benchmark cases

The results of the three benchmark cases are presented in Figures 6.2.2 through 6.2.4. The data presented in Figure 6.2.2 is a direct fission heating (without γ-smearing) pin power distribution. γ-smearing was not considered because of the limited availability of MNCP photon interaction cross-section libraries for actinides with Z higher than 94. The agreement between pin

power distribution prediction of CASMO4 and MCODE is within 3% difference, which is sufficient for the purposes of this study.

The SIMULATE3 pin power reconstruction option also produces reasonable accuracy for the CONFU assembly core (Figure 6.2.3). For the heterogeneous FFF and UO_2 core (Figure 6.2.4), however, the discrepancy between CASMO4 and SIMULATE3 pin power distribution prediction is greater due to the large local flux gradient between assemblies of different types. In addition, in 3D calculations performed for cores fully or partially loaded with FFF assemblies, the use of pin power reconstruction option caused severe convergence problems in the SIMULATE3 routines. Therefore, it was concluded that for the thermal hydraulic analysis of FFF assemblies loaded core, the radial and axial nodal power distribution obtained from the SIMULATE will be used in combination with CASMO4 pin power distribution with corresponding assembly burnup and additional 10% power increase to account for the introduced uncertainty due to the limitation of the calculations.

The burnup dependant cross-section libraries are generated by CASMO and then used by SIMULATE for solving 3D nodal diffusion problem. The cross-sections are generated on a single assembly basis for each fuel type without accounting for the influence of different neutron spectra in the neighboring assemblies. Typically, the magnitude of this effect is small because of the relatively large size of the fuel assemblies – much larger than the neutron migration length. If, however, the differences in spectrum are substantial and the migration length is larger than for the typical UO_2 lattices due to the harder spectrum, the effect can be more pronounced. Therefore, a depletion calculation of 2-dinensional colorset used for the benchmark case B-3 (Figure 6.2.1) was performed in order to estimate the magnitude of this effect. The k-infinity and relative power fraction for each type of the assemblies in the colorset were calculated as a function of burnup with SIMULATE and compared with CASMO values. The results are presented in Figures 6.2.5 and 6.2.6. The agreement obtained was very good – within 0.5% for both k-infinity and power share prediction. Therefore, it was concluded that SIMULATE can perform 3D macro-heterogeneous core calculations with an accuracy sufficient for the purposes of current analysis.

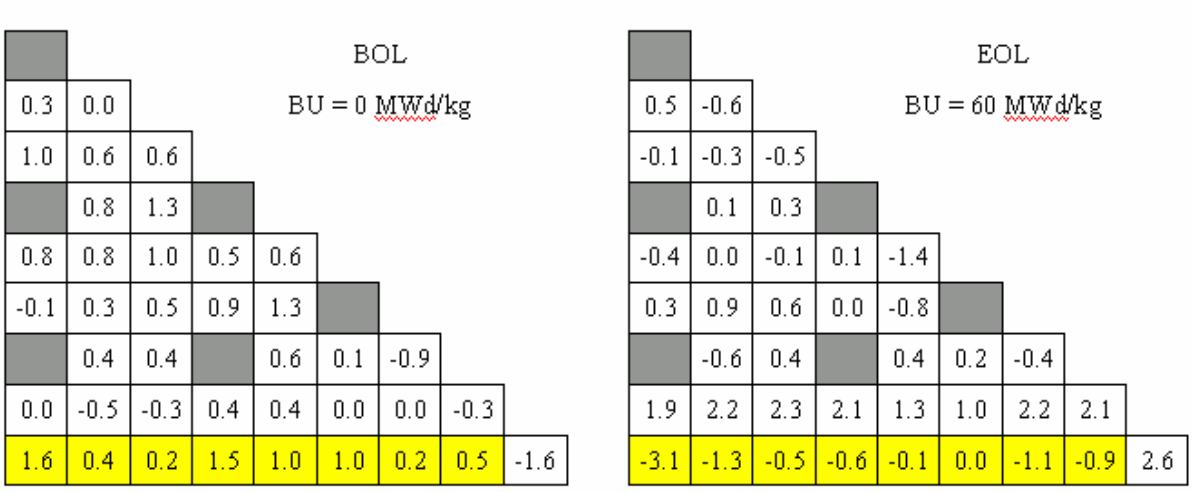

Figure 6.2.2. Difference (%) in pin power prediction (CASMO-MCODE)/CASMO:

Case B-1

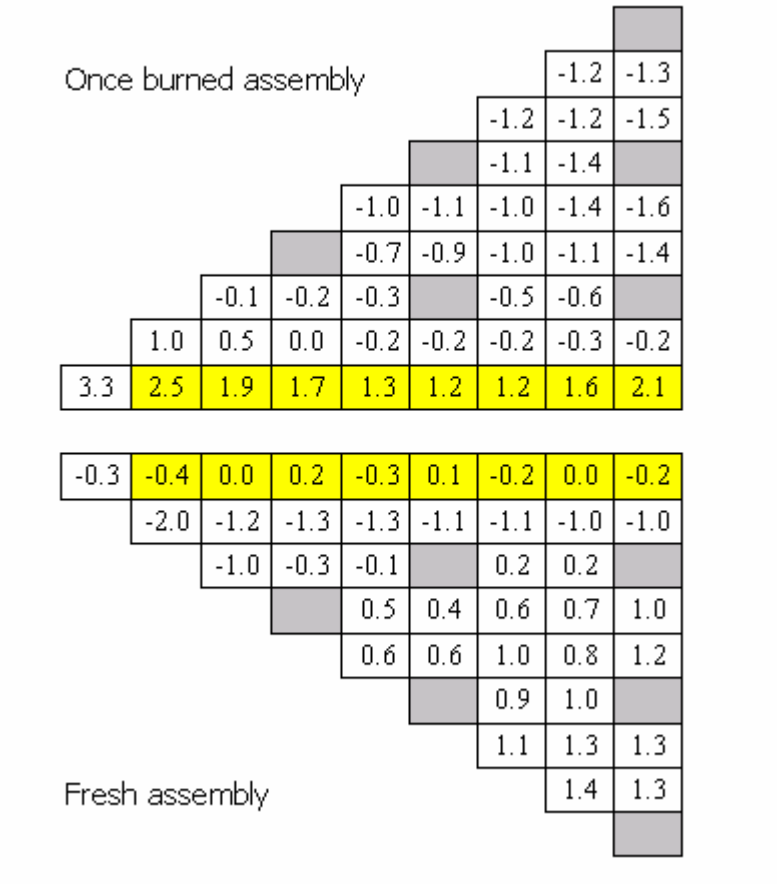

Figure 6.2.3. Difference (%) in pin power prediction (CASMO-SIMULATE)/CASMO:

Case B-2.

-	3.2	3.8	-	4.5	4.8	-	3.7	2.9
	1.5	0.7	1.4	0.2	0.8	1.9	0.8	1.6
		-0.7	0.1	-0.8	-0.7	0.7	-0.1	1.0
			-	-0.6	0.1	-	-0.1	1.0
				-1.8	-1.1	-1.1	-0.9	0.1
					-	-0.3	0.1	0.1
						-1.4	-0.6	-1.4
							-1.1	-3.8
								-9.6

FFF Assembly

-0.1	-0.8	-	0.3	1.1	-	1.5	2.0	-
-0.2	-1.0	-0.2	0.6	1.4	1.6	1.9	2.1	
-0.4	-0.9	0.0	0.9	1.4	1.6	1.8		
-0.8	-0.6	-	0.8	1.4	-			
-0.6	-0.9	-0.1	1.0	1.2				
-1.4	-1.3	-0.4	-					
-2.9	-2.0	-1.3						
-5.3	-3.0							
-9.7								

UO2 Assembly

Figure 6.2.4. Difference (%) in pin power prediction (CASMO-SIMLATE)/CASMO: Case B-3.

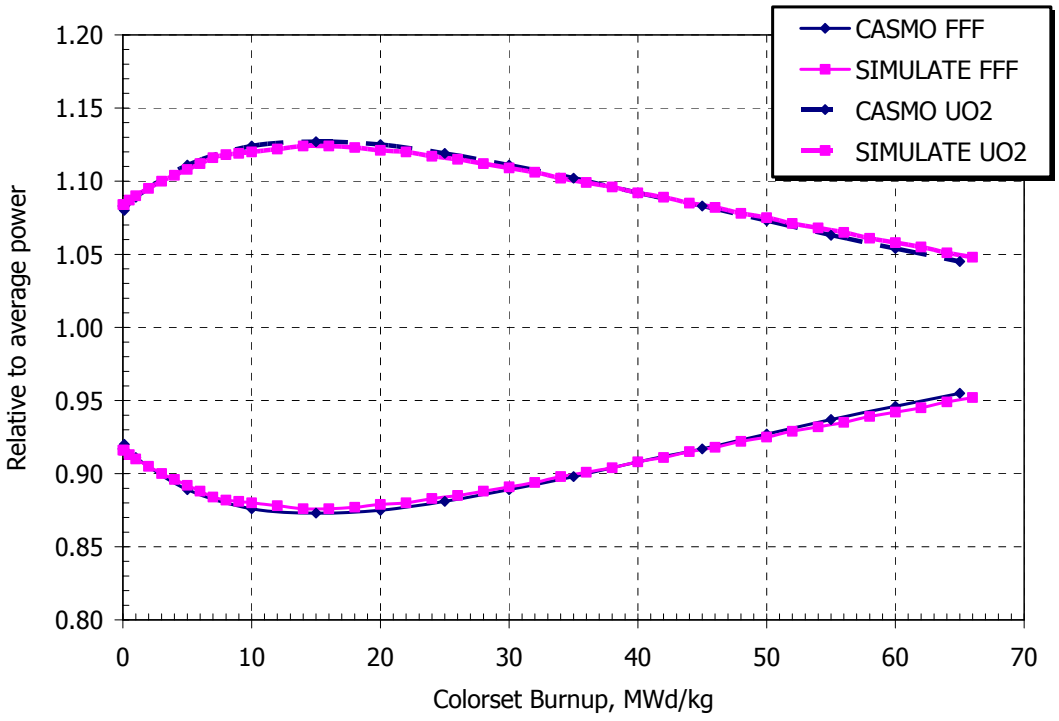

Figure 6.2.5. Relative power fraction for UO_2 and FFF assembly in colorset Case B-3.

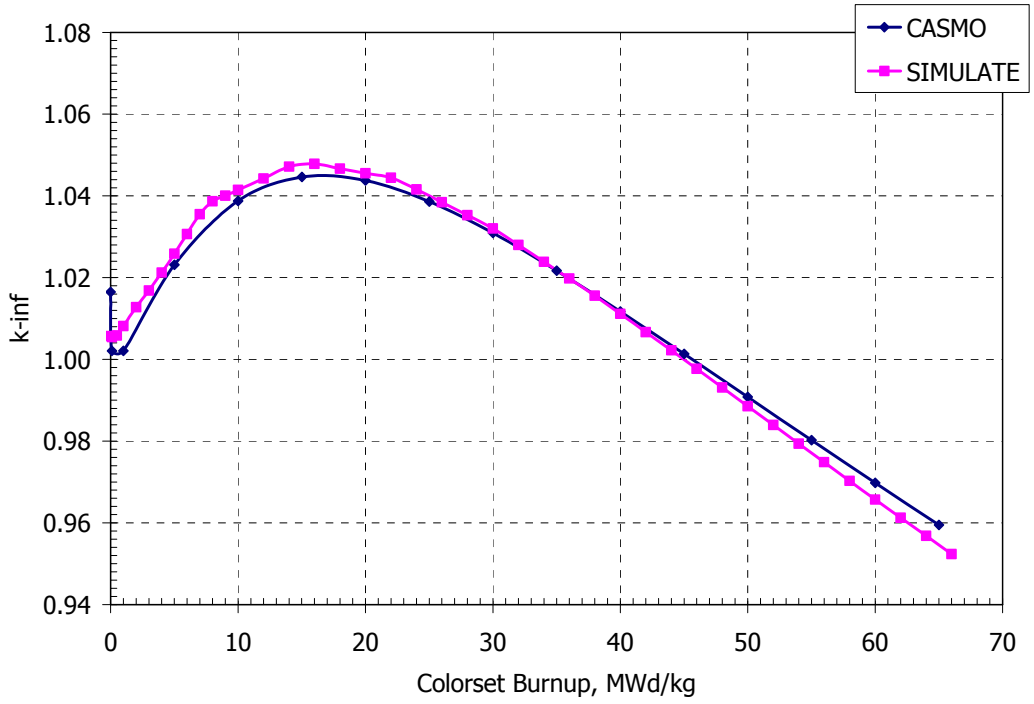

Figure 6.2.6. UO_2 and FFF assembly colorset criticality vs. burnup: Case B-3.

6.3. Analysis Assumptions

A standard Westinghouse 4 loop PWR core design was used as a reference for all 3D whole core simulations because it is one of the most common PWR plant designs throughout the world and in the United States. The major parameters of the reference core used for the calculations in this thesis are presented in Table 6.3.I.

Core loading

Table 6.3.II summarizes the equilibrium core fuel management data for each case. For cases 1 through 6, an equilibrium core configuration was obtained by 3 subsequent core cycles with reloading of 1/3 of the startup core after each cycle. The startup core was loaded with 3 batches of fuel at 3 different exposure levels corresponding to 0, 1/2 of BU1, and BU1, where BU1 is a single batch reactivity limited burnup obtained from the 2D CASMO4 assembly burnup calculations.

For case 7, the equilibrium core was simulated in a similar manner except for the fact that 4 reloading cycles were used to approximate the equilibrium core conditions. 52 fresh UO2 fuel assemblies were loaded in each cycle which is slightly more than 1/3 of the UO_2 assemblies in order to accommodate the larger fraction of FFF assemblies in the core (Table 6.3.II) while maintaining the same fuel cycle length. 1/4 of the FFF assemblies were reloaded after each cycle. The startup core FFF assemblies' average batch burnups were adopted from case 6 for once and twice burned assemblies. The initial burnup of the three-times burned FFF batch was assumed to be equal to the discharge burnup of the twice burned FFF batch from case 6.

For case 8, correspondingly, 5 cycles were modeled to achieve the equilibrium core conditions. 1/3-rd of UO_2 assemblies and 1/5-th of the FFF assemblies were reloaded with fresh ones each cycle. The initial average batch burnup in the startup core for the four-times burned FFF assemblies was assumed to be equal to the discharge burnup of the three-times burned FFF batch from the equilibrium core in case 7.

Figures C.1 through C.5 in Appendix C show fuel loading maps for all calculated cases. For homogeneous cores (cases 1, 3 and 4) an identical fuel loading map was used to ensure consistent comparison of the results. In cases 2 and 5 through 7, different loading patterns were adopted because of the greater number of fuel types in the core (cases 5 - 8) or unacceptably high power peaking (case 2).

In a realistic core design, the fuel loading pattern is optimized to maintain minimal power peaking throughout the cycle, to level out the control rod banks reactivity worth and to minimize the core leakage. In this study, optimization of loading pattern was not a major objective. However, a number of optimal core loading map features were maintained. A low leakage core loading strategy was adopted for all cases as can be observed from Figures C.1 through C.5 keeping the fresh fuel assemblies away from the core periphery. Radial assembly power peaking of less than 1.5 was assumed to be acceptable because this value lies between the practically achievable and the maximum allowed peaking factor values. The radial assembly power peaking factor of 1.587 is normally used for the licensing thermal hydraulic calculations while radial peaking factors between 1.3 and 1.4 are typical for the currently operating PWR reactors.

Table 6.3.I. Reference core design parameters

Plant description	
Number of primary loops	4
Core thermal power, MW_{th}	3411
Plant thermal efficiency, %	33.71
Plant electric power output, MW_e	1150
Core description	
Power density, W/cm^3	104.5
Average linear heat generation rate, W/cm	182.91
Primary system pressure, MPa	15.5
Total core flow rate, Mg/sec	18.63
Core coolant mass flux, kg/m^2-sec	2087.6
Core inlet temperature, °C	292.7
Fuel Rod	
Total number of fuel rod locations	50,952
UO_2 Fuel density, % of theoretical	94
Pellet diameter, mm	8.192
Pellet height, mm	13.4
Gap thickness, mm	0.082
Cladding material	Zircaloy-4
Cladding thickness, mm	0.572
Cladding outer diameter, mm	9.5
Active fuel height, m	3.66
Fuel Assembly	
Total number of fuel assemblies	193
Lattice type	Square
Assembly lattice geometry	17 × 17
Number of fuel rods locations per assembly	264
Number of grids per assembly	7
Fuel rod pitch, cm	1.26
Assembly pitch, cm	21.5 × 21.5
Control Rod Cluster	
Neutron absorbing material	Ag-In-Cd
Cladding material	304 SS
Cladding thickness, mm	0.46
Number of clusters	53
Number of absorber rods per cluster	24

Table 6.3.II. Core loading description for calculated cases

		UO_2 enrich-ment	% of FFF pins in the core	FFF pins TRU loading, v/o	UO_2 assemblies loaded per cycle	FFF assemblies loaded per cycle	Fuel Management, batches	
							UO_2 assemblies	FFF assemblies
Case 1	UO_2	4.20	0.00	-	64.3	0.0	3.0	-
Case 2	FFF-1	-	100.00	10.0	0.0	64.3	-	3.0
Case 3	CONFU-1	4.20	22.73	10.0	49.7	14.6	3.0	
Case 4	CONFU-E	5.00	18.18	20.0	52.6	11.7	3.0	
Case 5	M-CONFU-1	4.20	18.65	10.0	52.3	12.0	3.0	3.0
Case 6	M-CONFU-E	5.00	18.65	20.0	52.3	12.0	3.0	3.0
Case 7	M-CONFU-E4	5.00	24.87	20.0	52.3	12.0	2.7	4.0
Case 8	M-CONFU-E5	5.00	20.73	20.0	51.0	8.0	3.0	5.0

The reactivity worth of individual control rods as well as the worth of all control rods are important nuclear design parameters. Collectively, the worth of control rod banks should be high enough to satisfy the shutdown margin requirements for a particular reactor design. On the other hand, the reactivity worth of an individual control rod should not be too high to avoid high energy deposition in the fuel in case of a control rod ejection accident. Optimization of the loading pattern to balance the control rods worth and design of the control rod assembly were not the focus of our analysis and therefore were omitted. As a result, only average control rod worth values were used for the RIA analysis discussed in the following chapter.

Burnable poison design

The main objectives of the fuel assembly burnable poison design are

- to control the excess reactivity during the cycle
- to minimize the local pin power peaking
- to minimize soluble boron requirements for the core excess reactivity control
- to minimize global core power peaking through reduction of the fuel reactivity swing during irradiation.

The general requirements for any burnable poison are: constant and gradual depletion rate, no residual reactivity penalty and minimal impact on fuel performance characteristics.

Limited effort was made to address the above issues in the burnable poison design for the fuel types used in the present analysis. The primary goals of the design were to minimize local power peaking within the CONFU assembly and to maintain the whole core soluble boron concentration below 2000ppm. The burnable poison materials considered were: natural boron in the form of ZrB_2 fuel pellet coating (IFBA) and natural erbium oxide (erbia) or natural gadolinium oxide homogeneously mixed with the fuel.

Er167 is a strong resonance absorber with a large resonance overlap with fission resonances of Pu239 which is the major fissile isotope in TRU loaded fuel. Therefore, use of erbia as a burnable poison can potentially enhance the fuel Doppler coefficient. Additionally, Er167 tends to burn out gradually due to its large Resonance Integral (IR) and relatively small thermal cross-section allowing the design of fuel with a very flat reactivity over its lifetime. However, the option of using erbia was discarded because of its typically large residual reactivity penalty (because of the presence of other isotopes in natural Er), significant impact on the efficiency TRU destruction, and limited effect on the Doppler coefficient.

A large resonance integral makes Gd also an attractive candidate for the improvement of the fuel Doppler coefficient. However, much larger than Er167 thermal absorption cross-section of Gd155 and Gd157 may harden the neutron spectrum to such an extent that the addition of Gd will, in fact, result in less negative DC. Natural Gd oxide has negligible residual reactivity penalty but very large thermal absorption cross-section and therefore tends to burnout relatively quickly, potentially resulting in a high core power peaking. Nevertheless, the burnout rate can be slowed down if Gd is lumped into a few BP pins taking advantage of the self-shielding effect in Gd155 and Gd157 with relatively large IR. In this manner, the effect of BP can be extended by higher Gd loading while the magnitude of reactivity reduction can be controlled by the number of BP pins in the assembly. Although the lumping of Gd into a few BP pins improves the fuel assembly reactivity vs. burnup behavior and global core power peaking, it typically results in a high assembly local pin power peaking due to the strong power depreciation in Gd loaded pins. Additionally, if mixed with the fuel, Gd oxide degrades the fuel/matrix material properties such as thermal conductivity and melting point.

B10 constitutes about 20a/o of natural boron and it is an almost pure 1/v type absorber. It tends to burnout gradually and does not have any reactivity penalty. The distribution of boron within the assembly has small effect on its depletion rate or on initial reactivity depreciation. The major disadvantage of boron is the He gas production via the (n,α) reaction in B10 which results in pressurization of the fuel pin and limits the maximum BP loading.

Gd oxide was used as a burnable poison for FFF assemblies in cases 2 and 5 because it results in minimal residual reactivity penalty and provides greater flexibility in adjusting the burnout rate and initial reactivity reduction. In the CONFU assembly cases, the use of Gd in FFF pins alone or in combination with natural boron (as ZrB_2 IFBA) in UO_2 pin was found to exhibit inferior performance due to a large power imbalance between the UO_2 and FFF pins and relatively fast Gd depletion. Instead, ZrB_2 IFBA design was adopted for both UO_2 and FFF types of pins with different boron loadings to improve the CONFU assembly pin power peaking. Major parameters of BP designs used in all calculated cases are summarized in Table 6.3.III.

Table 6.3.III. Burnable poison design summary

			BP material	Type	BP pins per assembly	BP loading
Case 1	UO_2		ZrB_2	IFBA	264	0.052 mg/cm
Case 2	FFF-1		Nat. Gd	mixed with fuel	52	2.5 v/o
Case 3	CONFU-1	UO_2 pins	ZrB_2	IFBA	144	0.047 mg/cm
		FFF pins	ZrB_2	IFBA	60	0.094 mg/cm
Case 4	CONFU-E	UO_2 pins	ZrB_2	IFBA	112	0.035 mg/cm
		FFF pins	ZrB_2	IFBA	48	0.082 mg/cm
Case 5	M-CONFU-1	UO_2 pins	ZrB_2	IFBA	264	0.052 mg/cm
		FFF pins	Nat. Gd	mixed with fuel	52	2.5 v/o
Case 6	M-CONFU-E	UO_2 pins	ZrB_2	IFBA	264	0.061 mg/cm
		FFF pins	no BP	-	-	-
Case 7	M-CONFU-E4	UO_2 pins	ZrB_2	IFBA	264	0.061 mg/cm
		FFF pins	no BP	-	-	-
Case 8	M-CONFU-E5	UO_2 pins	ZrB_2	IFBA	264	0.061 mg/cm
		FFF pins	no BP	-	-	-

Fuel temperature reactivity feedback

The Doppler reactivity coefficient has a significant effect on the reactivity of the whole core. Hence, SIMULATE3 has a model for calculating the fuel temperature in order to obtain the Doppler reactivity feedback in each node. The generalized form of the model equation is:

$$T_{fuel} = T_{coolant} + A \times P + B \times P^2$$

where T fuel is the average fuel temperature in the node, P is the fraction of rated node averaged power, T coolant is the coolant temperature in the node. The coefficients A and B must be specified by the user. In addition, coefficient A can be a function of any two state variables (e.g. node exposure, void fraction, boron concentration etc.). Each fuel type in the core can have a different set of coefficients A and B and different dependence of A on the state variables.

The FFF matrix has superior thermal conductivity to UO_2 fuel and therefore for the same linear power generation rate will have lower fuel temperature. The separate sets of coefficients A and B to be used in the SIMULATE core analysis were calculated by solving numerically the one dimensional steady state heat conduction equation for cylindrical fuel pin with 14 equi-volumetric zones in the fuel pellet and temperature dependent thermal conductivity of the fuel. An approach for modeling the effective thermal conductivity of the dispersed fuel particles fuel is described in the following chapter. The resulting average fuel temperature as a function of relative power is plotted in Figure 6.2.1. The data presented in the Figure 6.3.1 was fitted to a second order polynomial for the local to nominal power ratios in the range between 0 and 2.5. The upper and lower bounds of this range correspond to maximum licensing power peak in a node and to hot zero power (HZP) conditions respectively. The obtained coefficients, used for the SIMULATE fuel temperature calculation input card, are as follows:

FFF: A = 289.5 B = 27.0

UO_2: A = 308.4 B = 81.1

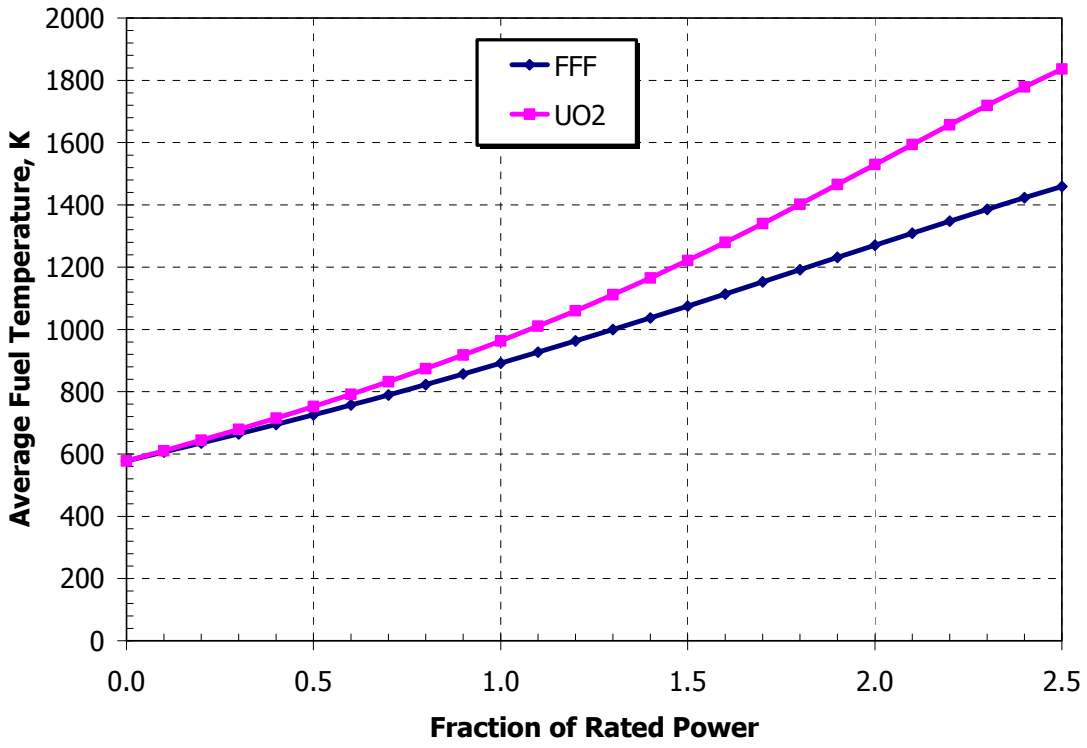

Figure 6.3.1 Average fuel temperature as a function of relative to nominal node power

6.4. 3D Core Neutronics Results

The confirmation of the possibility of maintaining zero net balance for TRU generation and destruction in the fuel cycle is one of the major goals of the 3D whole core analysis. Table 6.4.I shows the TRU destruction efficiency and the TRU mass balance for all calculated cases. Both macro (Case 6) and micro (Case4) equilibrium TRU options can maintain zero net production of TRU. The micro heterogeneous CONFU assembly option is slightly superior to the macro option. This is due to the fact that the TRU in FFF pins generally have higher reaction rates when surrounded by UO_2 pins and therefore affected by the UO_2 neutron spectrum. In the macro heterogeneous case, the influence of UO_2 spectra on FFF pins is small because of the large assembly size compared with the neutron migration length. In fact, the effect of spectrum overlap is not reflected at all in the 3D SIMULATE calculation as discussed earlier.

Case 7, where the TRU equilibrium FFF assemblies are managed in 4 batches, seems to have a superior TRU destruction efficiency. However, this is mainly due to the fact that FFF pins comprise considerably larger fraction of the fuel in the core (Table 6.3.II): about 25% versus about 19% for Case 6. The TRU burnup performance achieved in Case 7 is fairly close to the limit because any increase in TRU core loadings would require further increase in UO_2 enrichment (or more frequent reloading of the UO_2 assemblies) to maintain comparable fuel cycle length. In Case 8, for example, FFF pins account for about 20% of the fuel pins in the core and allow maintenance of comparable fuel cycle length without increasing the UO_2 enrichment. At the same time, although higher fractional TRU burnup can be achieved by the longer irradiation time, the TRU destruction rate is not sufficient to maintain zero net balance of TRU. The tradeoff, in this case, is precisely as before: increasing the number of FFF assemblies at the expense of higher UO_2 enrichment. Similar logic applies to all equilibrium TRU cases.

Table 6.4.I. Burnup and TRU mass balance summary

		Discharge BU UO_2 pins, MWd/kg	Discharge BU FFF pins, MWd/kg	TRU fractional BU	TRU production, kg/GWe Y	TRU destruction, kg/GWe Y	Net TRU production, kg/GWe Y
Case 1	UO_2	50.9	-	-	300	-	300
Case 2	FFF-1	-	470	0.50	-	1160	-
Case 3	CONFU-1	53.1	527	0.56	232	299	-67.0
Case 4	CONFU-E	52.6	275	0.29	245	252	-6.8
Case 5	M-CONFU-1	51.0	504	0.53	244	252	-8.5
Case 6	M-CONFU-E	49.9	273	0.29	241	245	-3.8
Case 7	M-CONFU-E4	46.3	318	0.34	270	310	-40.2
Case 8	M-CONFU-E5	48.9	369	0.39	238	231	6.3

An additional objective of the 3D core analysis is to demonstrate the feasibility of practical core design by comparison of the TRU containing core neutronic characteristics to those of the reference conventional UO_2 core. Namely, the analysis addressed the following core characteristics:

- Maximum critical soluble boron concentration
- Soluble boron reactivity worth (SBW)
- Power peaking factors
- Reactivity coefficients at hot full power (HFP) and hot zero power (HZP) conditions

Furthermore, core kinetics parameters (namely, the 6 group delayed neutrons data and prompt neutrons lifetime) and individual control rod cluster worths were calculated to be used in reactivity initiated accident analysis as discussed in the following chapter.

The critical soluble boron concentrations for Cases 1 through 6 are presented in Figure 6.4.1. The upper limit on the critical boron concentration emanates from two factors. Water chemistry considerations allow reactor operation with up to 2000 ppm of boron in the coolant. Positive moderator temperature coefficient at HFP is another factor that limits the maximum allowable boron concentration in the coolant.

A critical boron concentration below 2000 ppm is practically feasible for all cases considered. The fully FFF loaded core (Case 2) is the most challenging to control. It has the lowest excess reactivity at BOL and yet the critical boron concentration required is the highest of all cases. As discussed earlier, the observed effect is a result of a harder neutron spectrum in the FFF core and, subsequently, lower boron reactivity worth. All other cases have comparable boron concentration requirements. Furthermore, even closer match between boron concentration values for Cases 1 and 3 through 6 can be obtained with some minor adjustments in the burnable poison loading.

Figures 6.4.2 and 6.4.3 show maximum 3-D nodal power peaking factor and maximum 2-D radial assembly power peaking factor respectively as a function of burnup for the Cases 1 through 6. The initial goal to design a core loading pattern that provides radial core power peaking factor lower than 1.5 was met for all cases. The results demonstrate that all considered TRU containing core options can be designed to have comparable peaking to the reference UO_2 core and therefore comparable thermal margin. The comparable thermal margin for UO_2 and micro heterogeneous CONFU cases is also expected due to the fact that high power FFF pins in a CONFU assembly are always surrounded by much “cooler” UO_2 pins having below average power peaking. The effects of intra-assembly pin power peaking and detailed evaluation of thermal hydraulic margin for the cases considered are described in the following section.

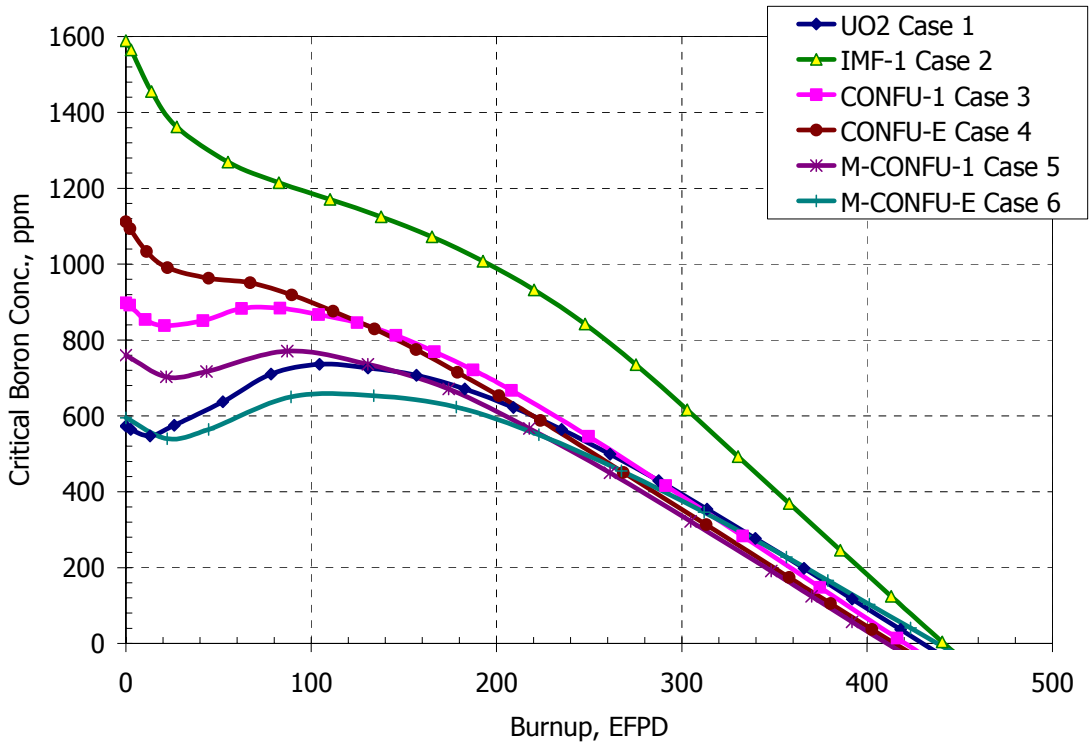

Figure 6.4.1. Critical boron concentration: Cases 1- 6

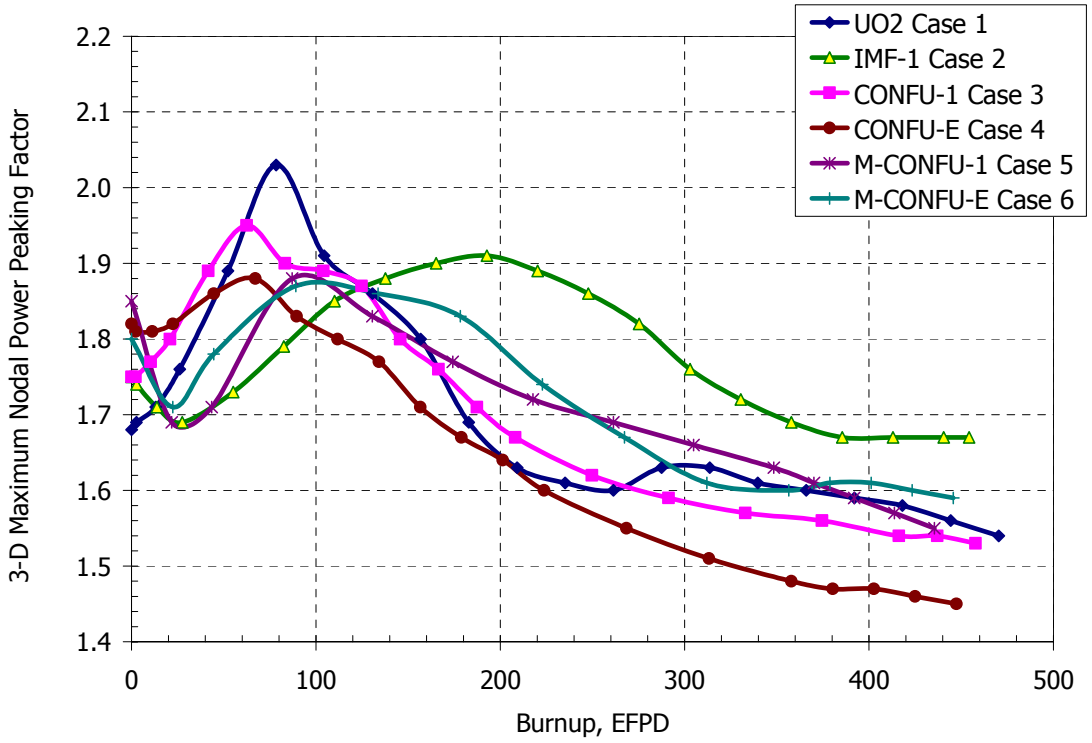

Figure 6.4.2. Maximum 3-D nodal power peaking factor: Cases 1- 6

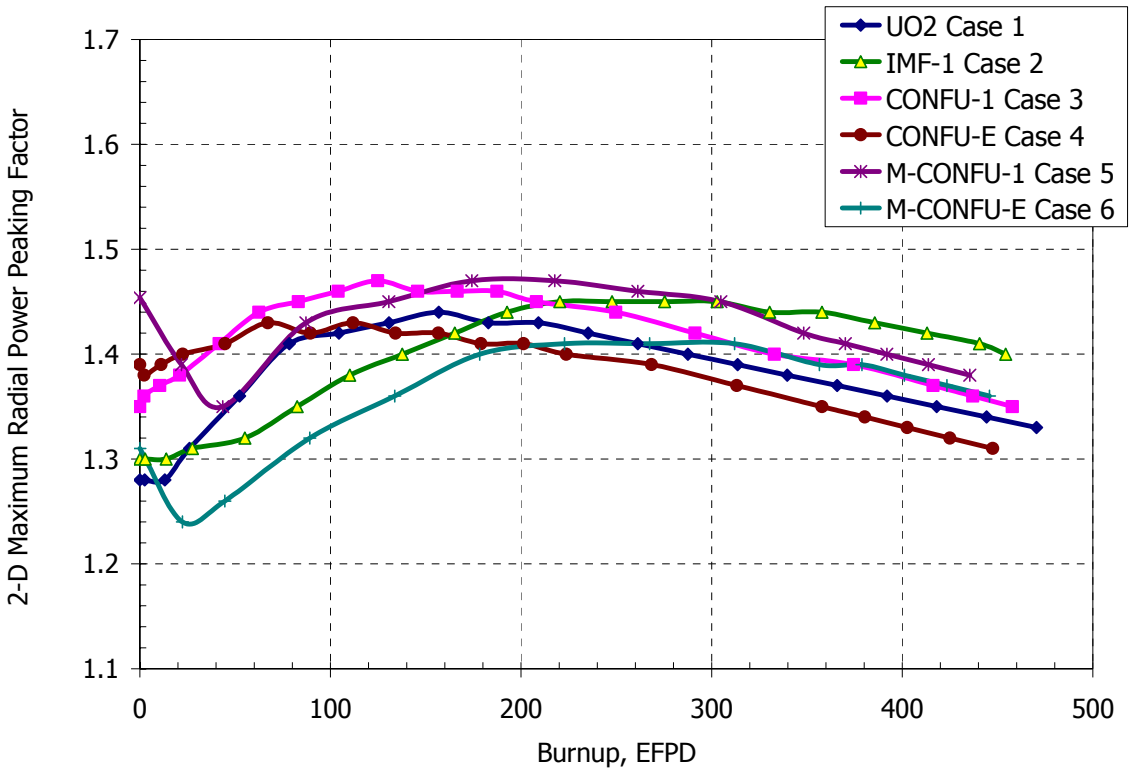

Figure 6.4.3. Maximum 2-D core radial power peaking factor: Cases 1- 6

The moderator temperature coefficient (MTC) and distributed Doppler coefficient (DDC) were calculated at HFP and at HZP conditions. The distributed Doppler coefficient is defined as the reactivity change associated with a change in fuel temperature having the same spatial distribution as the power divided by the change in the averaged fuel temperature. The results of the DDC and MTC calculations at HFP conditions during core lifetime are presented in Figures 6.4.4 and 6.4.5 respectively.

The reactivity coefficients have negative values for the whole period of irradiation for all calculated cases. The magnitude of the DDC for the fully FFF loaded core (Case 2) is smaller than that of the UO_2 core by almost a factor of four. Macro and micro heterogeneous (CONFU) core options have slightly less negative DDC (by up to 30%). Less negative temperature feedback than for the UO_2 fuel case implies inferior core behavior in rapid reactivity excursions.

The MTC was also found to be negative in all calculated cases (Figure 6.4.4). The MTC value is determined by the neutron spectrum and by the boron concentration in the coolant. As a

result, the MTC for Case 2 is less negative than MTC for all other cases primarily due to the substantially higher soluble boron concentration. The MTC values for Cases 3 through 6 are close to the reference UO_2 fuel values.

Figure 6.4.6 shows soluble boron reactivity worth (SBW) as a function of burnup for Cases 1 through 6. The difference in reactivity worth of soluble boron is a direct consequence of neutron spectrum hardening due to the presence of large amounts of TRU with particularly high thermal absorption cross-sections. As a result, SBW is directly related to the amount of TRU in the core. The highest and lowest SBW values correspond to Case 1 and Case 2 respectively. For the combined, partially TRU loaded cores, the SBW decreases (Figure 6.4.6) with increasing TRU core loading (Table 6.3.II). All cases exhibit a general trend of increased SBW towards the end of the core life due to actinides depletion and resulting softening of the spectrum.

The choice of a macro vs micro heterogeneous core structure has a minor effect on the SBW for cases with comparable TRU loading (Cases 4 and 6). The difference in SBW between micro (Case 4) and macro (Case 6) cores can be a result of FFF assembly locations. In Case 6, the fresh FFF assemblies with particularly hard neutron spectrum are positioned at the core periphery which mitigates the core average spectrum hardening effect due to preferential leakage of fast neutrons. As a result, SBW is slightly higher for the macro heterogeneous (Case 6) than for the micro heterogeneous (Case 4), despite a higher TRU loading in Case 6.

The soluble boron worth, reactivity feedback coefficients and power peaking factors for Cases 7 and 8 (not shown in the Figures 6.4.1 – 6.4.6) are similar to those of Case 6.

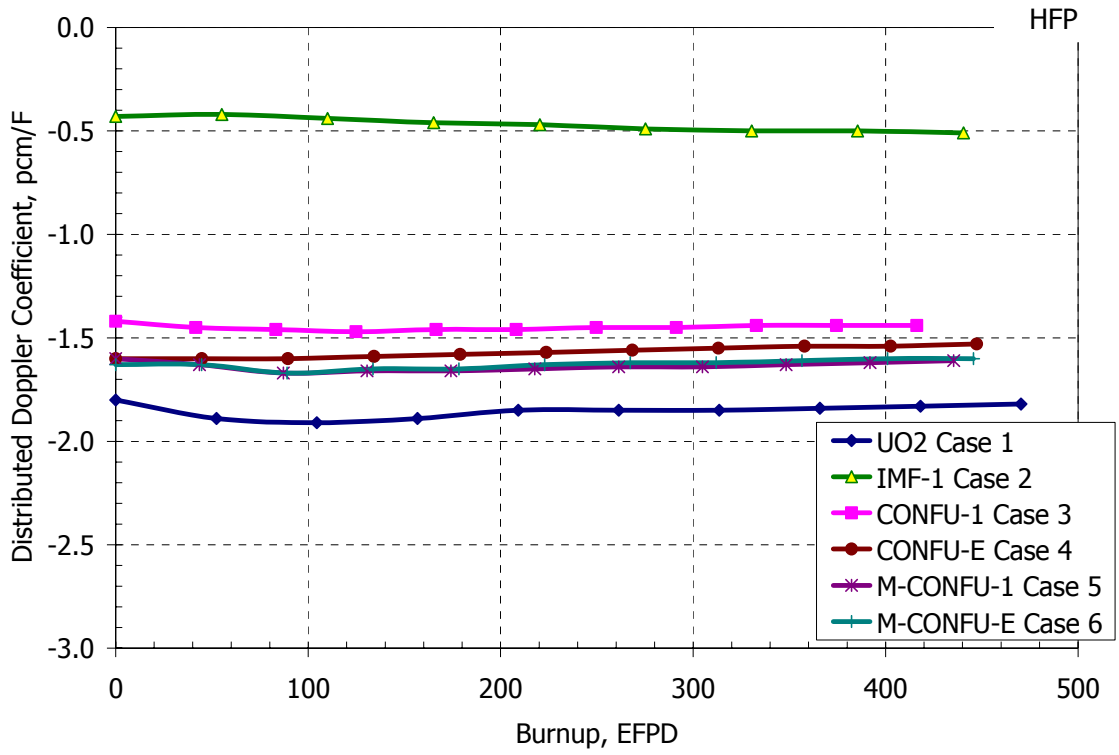

Figure 6.4.4. Distributed Doppler coefficient: Cases 1- 6

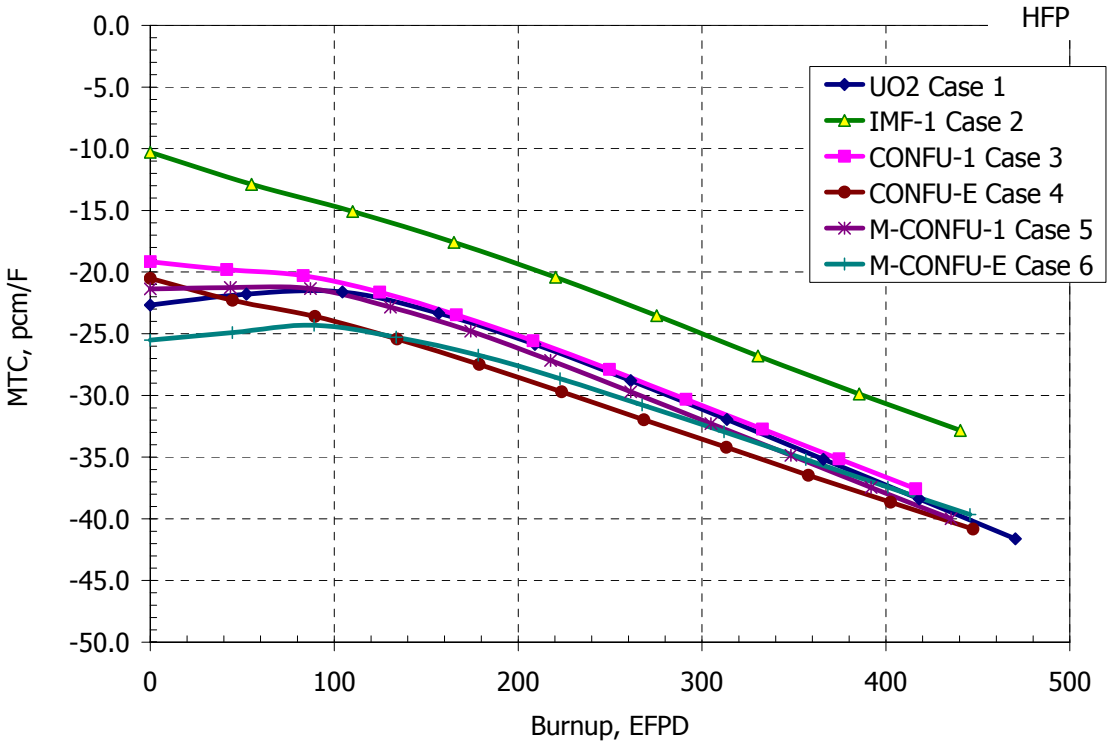

Figure 6.4.5. Moderator temperature coefficient: Cases 1- 6

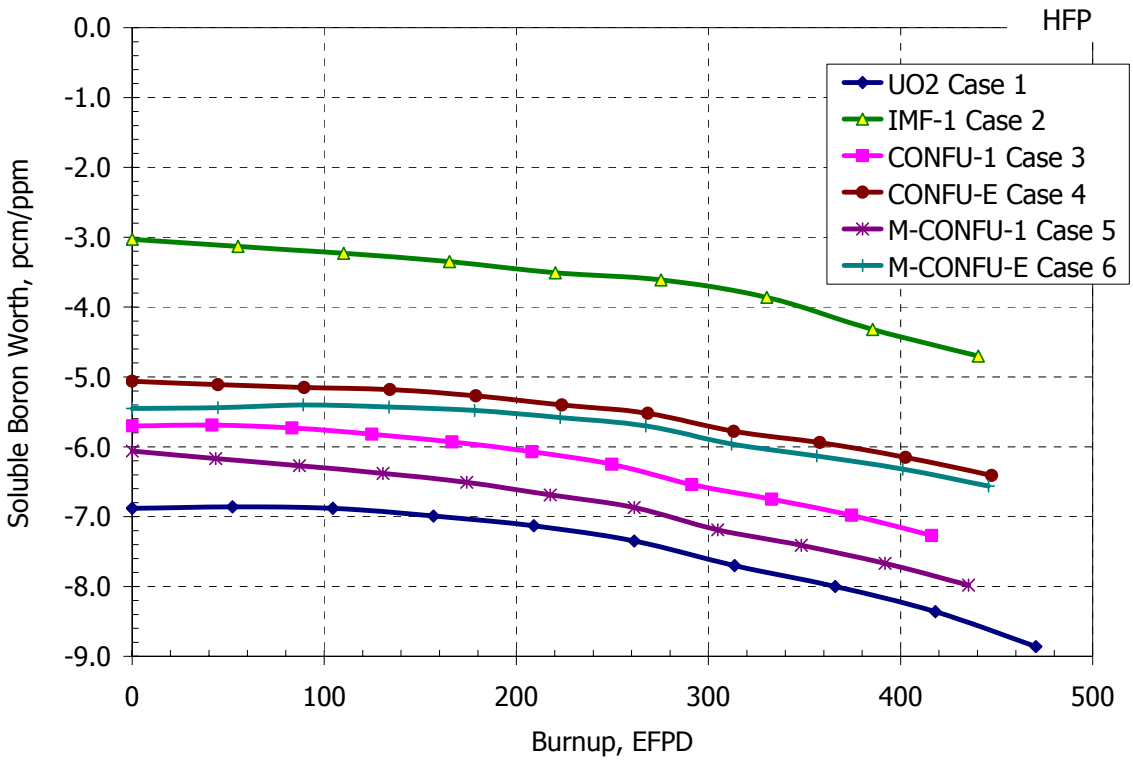

Figure 6.4.6. Soluble boron reactivity worth: Cases 1- 6

6.5. Thermal Hydraulic Analysis

Thermal hydraulic analysis was performed to examine feasibility of TRU loaded PWR cores by comparing their characteristics with the reference UO_2 core. FFF pins generally have higher power rating when subjected to particularly high thermal neutron flux from the neighboring UO_2 pins or when in the vicinity of guide tubes with extra water that provides improved neutron moderation. Therefore, the fertile free TRU loaded fuel in a PWR core may have a moderately higher power peaking than in typical PWR. As a result, there is a need to study the effect of higher than typical power peaking on the reduction of MDNBR margin.

The cases considered for analysis are UO_2, FFF-1, CONFU-1, CONFU-E, M-CONFU-1, and M-CONFU-E as described in Table 6.1.I in Section 6.1. As a first step, single assembly calculations were performed for each case assuming conservative power peaking profiles for each

case. Then, the most limiting case was identified and the whole core simulation was performed for that case and for the reference UO_2 PWR core.

The VIPRE-01 sub-channel analysis computer code was used for the calculations of MDNBR. It is widely used by the nuclear industry for LWR analysis and it is approved by NRC for licensing applications.

The reference typical Westinghouse design 4-loop PWR core parameters were used for all calculated cases (Table 6.3.I). All calculations were performed assuming 118% core average power to account for Condition I and II events. The inlet coolant temperature used was 294.7 °C (2 °C greater than nominal) and the total coolant flow rate was reduced by 5% to account for bypass flow and uncertainty associated with the core wide flow distribution. Additional assumptions used in the VIPRE model are presented in Table 6.5.I.

L-type grids spread apart by 50.8 cm interval with mixing vanes were used. For turbulent mixing, a conservative value of $\beta = 0.038$ for the mixing coefficient of the grids with mixing vanes was assumed.

Figure 6.5.1 schematically presents the modeled 1/8 of the hot assembly configuration with sub-channel and fuel rod numbering. The assembly relative pin power distribution was obtained from the 2D CASMO results at the burnup point with maximum peaking factor for each calculated case. The pin power distributions used for each case considered are presented in Figure 6.5.2. A chopped cosine with peak to average ratio of 1.55 was used for the axial core power profile. This power shape normally provides conservative results.

Two sets of calculations were performed. First, a radial assembly power peak of 1.587 typically used for licensing calculations was assumed in all calculated cases. In the second set of calculations, the reference UO_2 case radial assembly power peak remained the same (1.587) while the values for other cases were obtained as follows. The maximum over the lifetime 3D nodal power peaking factors for each case were obtained from the SIMULATE results. Relative to the UO_2 case 3D nodal peaking factors were calculated and the radial 1.587 peak value was scaled accordingly for each case. In this approach, the licensing peaking factor is adjusted for each case to maintain the same margin between calculated and licensing power peaking values. Scaling the radial assembly licensing peaking factor with 3D nodal power peaking values was assumed to

reflect the effect of the differences in axial power shape profiles for different cases. The extra 10% power increase was applied to macro heterogeneous cases to accommodate the uncertainty associated with pin power distribution at the interface between UO_2 and FFF assemblies.

Table 6.5.I. VIPRE-01 Model Assumptions

Parameter	**Specification**
Axial power profile	Chopped cosine, peak-to-average ratio =1.55
Reactor power	Overpower at 118% (4025MWth)
Power deposited directly in coolant	2.6%
Core mass flux	Reduced by 5% (3542kg/s-m^2)
Core inlet temperature	Increased by 2°C (294.7°C)
Cross flow resistance coefficient	$K_G = 3.15\ Re^{-0.2}$
Turbulent mixing model	$w' = \beta s \overline{G}$; β=0.038
Turbulent momentum factor	FTM=0
Axial friction coefficient for turbulent flow	$f_{ax} = 0.184\ Re^{-0.2}$
Form loss coefficient for mixing vane grids	0.8
CHF correlation	W-3L, mixing factor 0.043, grid spacing factor 0.066
Void correlations	Levy for subcooled void, HEM for bulk boiling and two-phase friction multiplier
Heat transfer correlations	Dittus-Boelter for single-phase flow, Thom correlation plus single-phase correlation for subcooled and saturated nucleate boiling

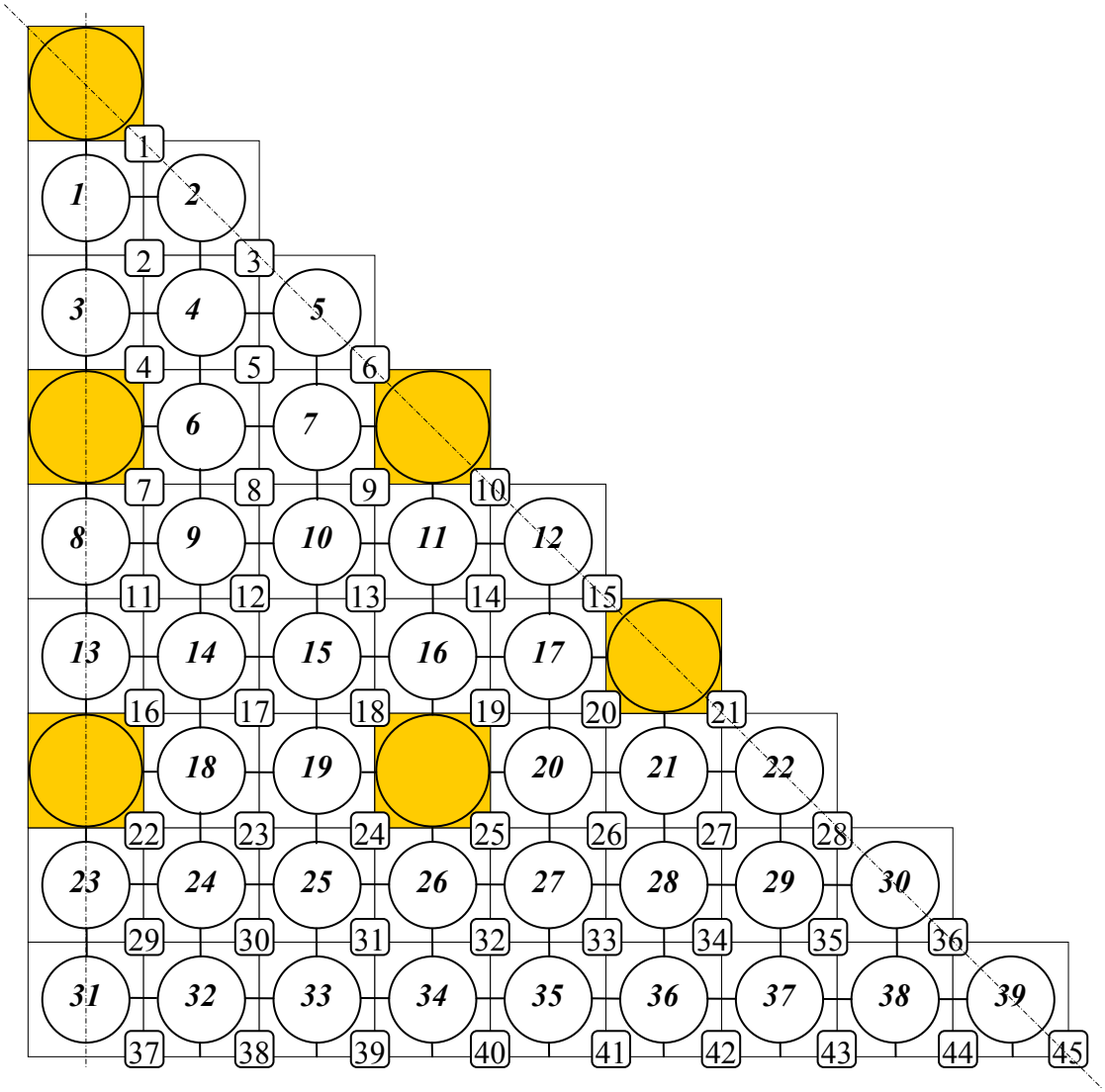

Figure 6.5.1. 1/8 of the hot assembly model: channels and rods numbering

UO2 e = 4.2%

1.03	1.00							
1.03	1.00	1.00						
	1.03	1.04						
1.03	1.00	1.00	1.04	1.03				
1.03	1.00	1.00	1.04	1.06				
	1.03	1.03		1.04	1.02	0.97		
1.02	0.99	0.99	1.02	0.98	0.96	0.95	0.94	
0.98	0.98	0.98	0.98	0.97	0.96	0.96	0.96	0.97

UO2 e = 5%

1.03	1.00							
1.03	1.00	1.00						
	1.03	1.04						
1.03	1.00	1.00	1.04	1.03				
1.03	1.00	1.00	1.05	1.06				
	1.03	1.03		1.05	1.02	0.97		
1.02	0.99	0.99	1.02	0.98	0.96	0.94	0.94	
0.98	0.98	0.98	0.98	0.97	0.96	0.95	0.96	0.97

CONFU-1

1.05	1.01							
1.05	1.01	1.01						
	1.04	1.04						
1.03	1.00	1.00	1.04	1.01				
1.01	0.98	0.98	1.02	1.02				
	0.96	0.96		0.97	0.94	0.87		
0.89	0.87	0.87	0.89	0.86	0.83	0.79	0.74	
1.19	**1.19**	**1.19**	**1.19**	**1.18**	**1.15**	**1.13**	**1.15**	0.72

CONFU-E

1.12	1.08							
1.12	1.08	1.08						
	1.11	1.10						
1.09	1.06	1.05	1.09	1.06				
1.07	1.03	1.02	1.05	1.05				
	1.03	1.00		0.99	0.96	0.87		
0.96	0.89	**1.21**	0.85	**1.17**	0.80	**1.14**	0.82	
0.82	**1.10**	0.75	**1.04**	0.73	**1.05**	0.79	0.87	0.90

FFF-1

1.11	1.05							
0.80	1.04	0.77						
	1.11	1.10						
1.11	1.05	0.77	1.12	1.09				
0.80	1.04	1.04	1.12	0.82				
	1.09	0.79		1.14	1.10	0.76		
0.79	1.04	1.04	1.10	0.76	0.99	0.98	0.98	
1.00	1.02	1.03	1.02	1.01	1.00	1.01	1.01	1.04

FFF-E

1.05	1.00							
1.05	1.00	1.00						
	1.05	1.05						
1.05	1.01	1.01	1.07	1.06				
1.05	1.00	1.01	1.07	1.10				
	1.04	1.05		1.09	1.04	0.97		
1.03	0.98	0.98	1.03	0.98	0.94	0.92	0.90	
0.95	0.95	0.95	0.95	0.95	0.93	0.92	0.92	0.94

Figure 6.5.2. Pin power distributions used in the cases considered

The results of the single assembly VIPRE-01 calculations are presented in Table 6.5.II. The reference UO_2 case has the largest MDNBR margin. The CONFU-1 and the UO_2 assembly in the macro heterogeneous option M-CONFU-1 exhibit the most limiting DNBR performance. For these cases the margin is reduced by about 10% remaining however well above the postulated minimum value of 1.3 established for W3-L correlation.

The macro heterogeneous cases do not represent a significant concern from the MDNBR performance perspective because the most reactive FFF assemblies can be positioned on the core periphery and therefore will exhibit lower than average power peaking. As a result, the MDNBR values for the FFF assemblies in the macro heterogeneous CONFU cases are greater than for the UO_2 case even with extra power increase to account for the pin power peaking uncertainty.

Table 6.5.II. Results of the single assembly analysis.

Case	Radial power peak	MDNBR	Hot rod	Hot channel	Radial power peak	MDNBR	Hot rod	Hot channel
UO_2	1.587	1.73	17	14	1.587	1.73	17	14
FFF-1	1.587	1.61	17	14	1.49	1.64	17	14
CONFU-1	1.587	1.48	33	38	1.52	1.56	33	38
CONFU-E	1.587	1.52	25	23	1.47	1.67	25	23
M-CONFU-1 (UO_2)	1.587	1.73	17	14	1.62	1.56	17	14
M-CONFU-E (UO_2)	1.587	1.73	17	14	1.61	1.70	17	14
M-CONFU-1 (FFF)	-	-	-	-	1.38	1.93	17	14
M-CONFU-E (FFF)	-	-	-	-	1.04	1.91	17	14

Whole core simulation

The micro heterogeneous CONFU assembly with the first time recycled TRU showed the largest reduction in MDNBR margin in the single assembly calculations. Thus, this case was chosen for the full core VIPRE-01 simulation to estimate more realistic MDNBR for this case and compare it with the reference UO_2 core value. The CONFU-EQ case was also analyzed for comparison.

The full core was modeled by positioning the hot fuel assembly in the center and explicitly modeling the candidate limiting DNBR channels in this hot assembly. The channels were gradually lumped to increasingly larger regions towards the core periphery. An identical approach for the sub-channel lumping was employed for the UO_2 and CONFU-EQ cases. Figures 6.5.3 and 6.5.4 show the channel and rod numbering for the UO_2 and CONFU-EQ cases in the hot assembly and in the whole core respectively. In the CONFU-1 case however, the suspected limiting DNBR sub-channel was expected to be between the neighboring assemblies. Therefore, a slightly different channel lumping scheme was used (Figure 6.5.5). The power peaking factors in the assemblies surrounding the hot assembly were artificially increased to match the hot assembly power to assure conservative results. Additionally, all the correlations, axial nodes division, grid parameters, and the boundary conditions were identical for both cases to ensure consistent comparison.

The core wide radial assembly power distribution was obtained from the SIMULATE calculations at the burnup step with the highest peaking factor for all cases. The hot assembly pin power distribution was also obtained from the SIMULATE pin power reconstruction module which was shown to yield a sufficient accuracy for the pin power peaking prediction in the UO_2 and the CONFU-1 cases (see Section 6.2).

The results of the full core VIPRE-01 calculations are consistent with single assembly simulation results. However, in contrast to single assembly case, channel 1 (Figure 6.5.3) appears to be the limiting MDNBR location in CONFU-EQ case despite the fact that the hot FFF pins are located on the periphery of the assembly. This is due to beneficial effect of mixing from cooler channels in neighboring fuel assemblies. The single assembly model did not account for the mixing effect. In addition, the channel 1 has higher total power input than any of the channels in the neighborhood of FFF pins.

Similarly to the single assembly calculation results, the MDNBR margin for the CONFU-1 case is reduced by about 20% in comparison with the reference UO_2 case. The DNBR as a function of relative active core height for the limiting MDNBR locations for the UO_2, CONFU-EQ, and CONFU-1 cases is depicted in Figure 6.5.6. The MDNBR value for the UO_2 case is 1.71 while the minimum DNBR value for the CONFU-1 case is 1.43. The CONFU-EQ case exhibit intermediate performance with MDNBR of 1.51. As before, all MDNBR values are greater than the established W3-L correlation limit of 1.3.

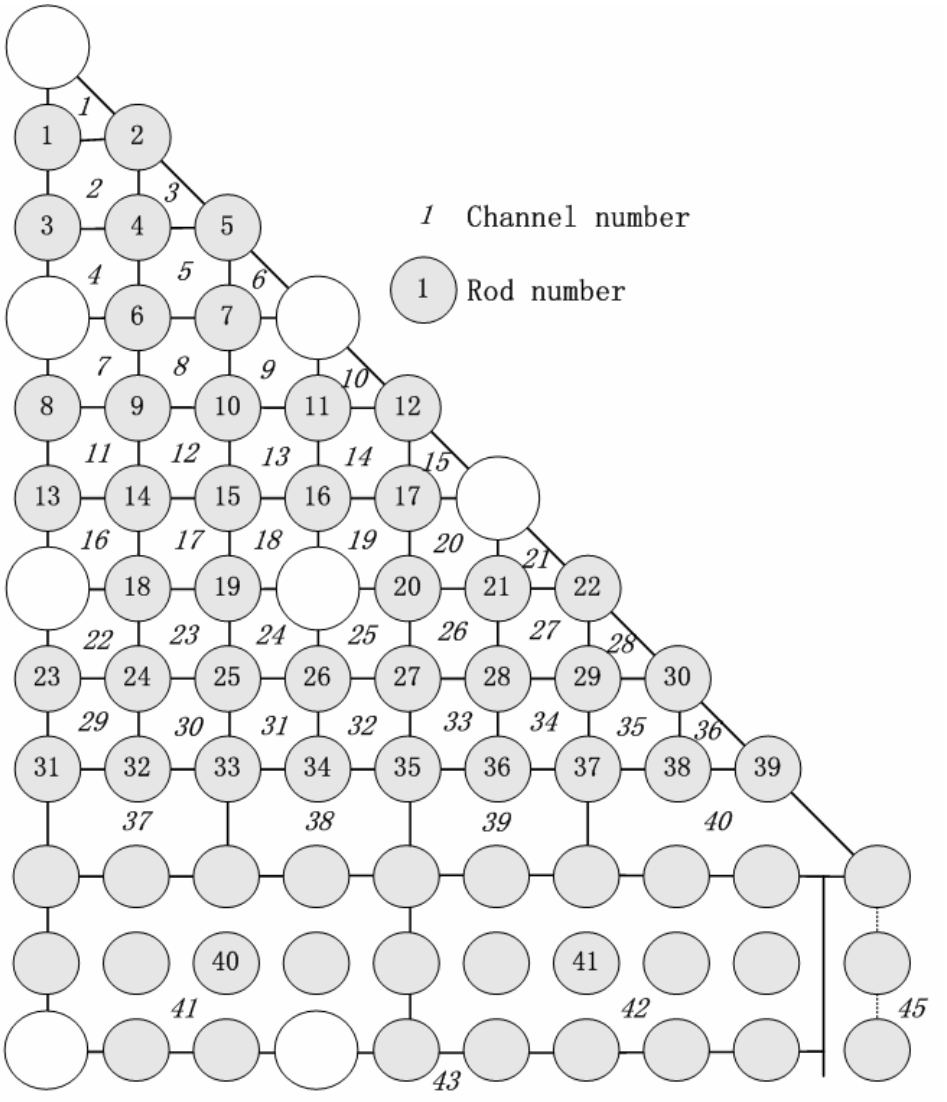

Figure 6.5.3. Rod and channel numbering scheme for the hot UO_2 and CONFU-EQ assemblies

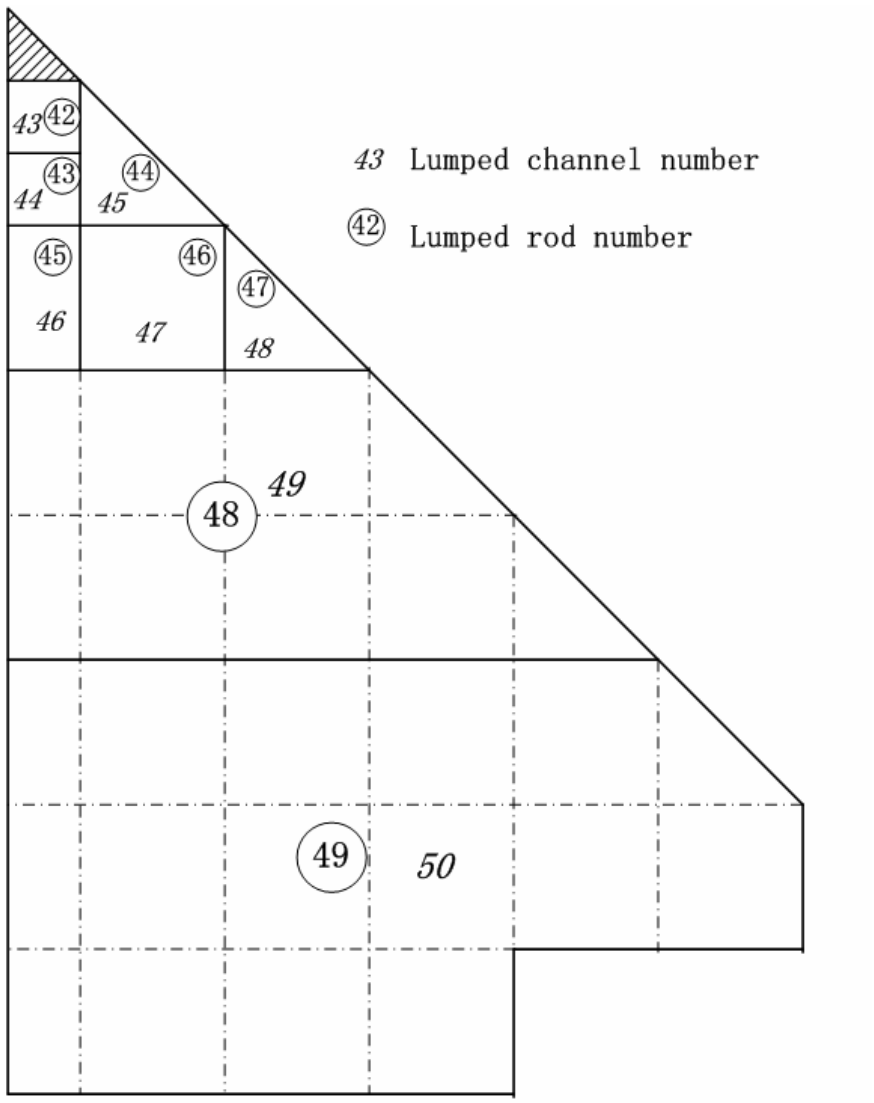

Figure 6.5.4. Rod and channel numbering scheme for the UO_2 and CONFU-EQ core

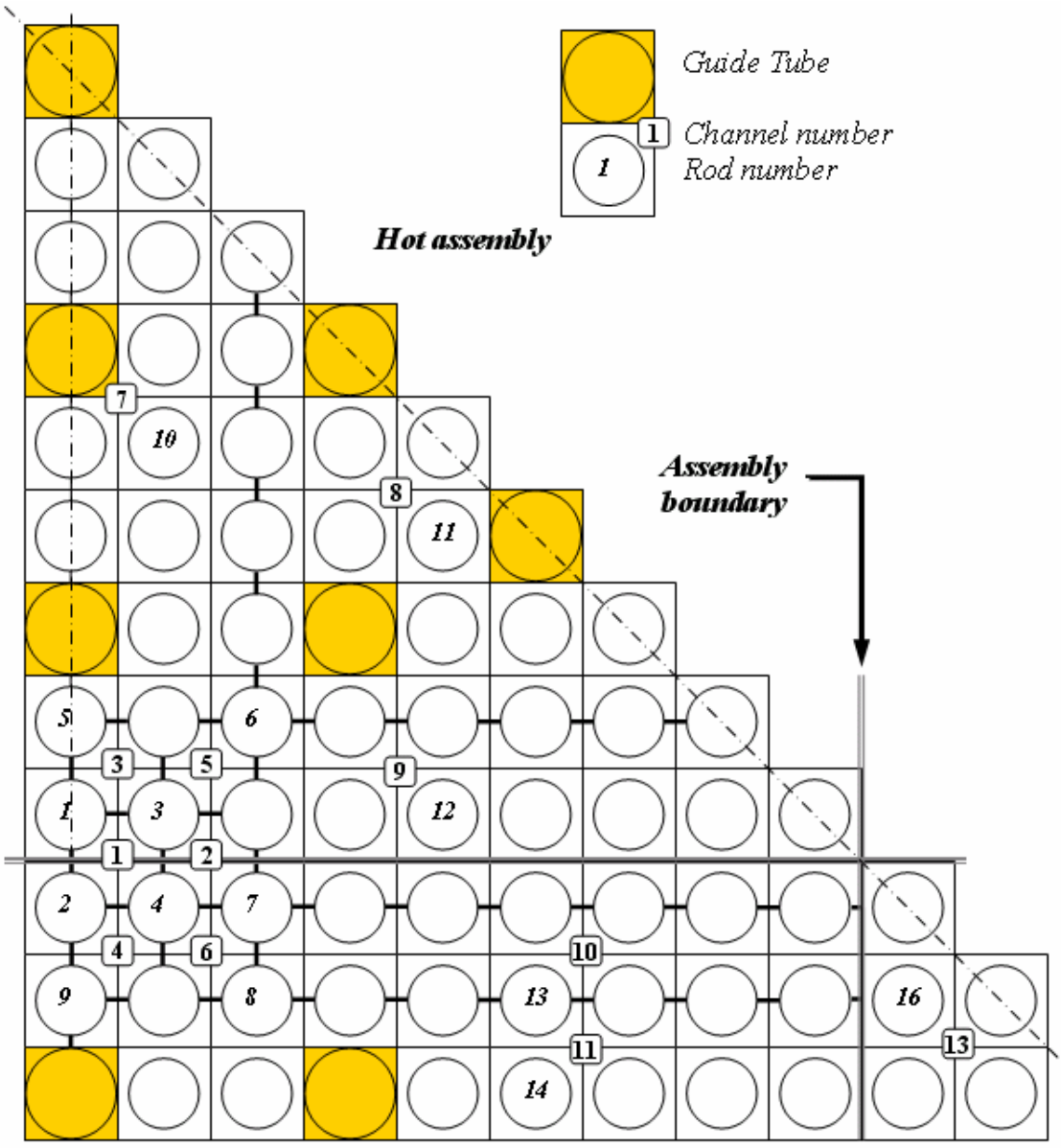

Figure 6.5.5. Rod and channel numbering scheme for the hot CONFU-1 assembly

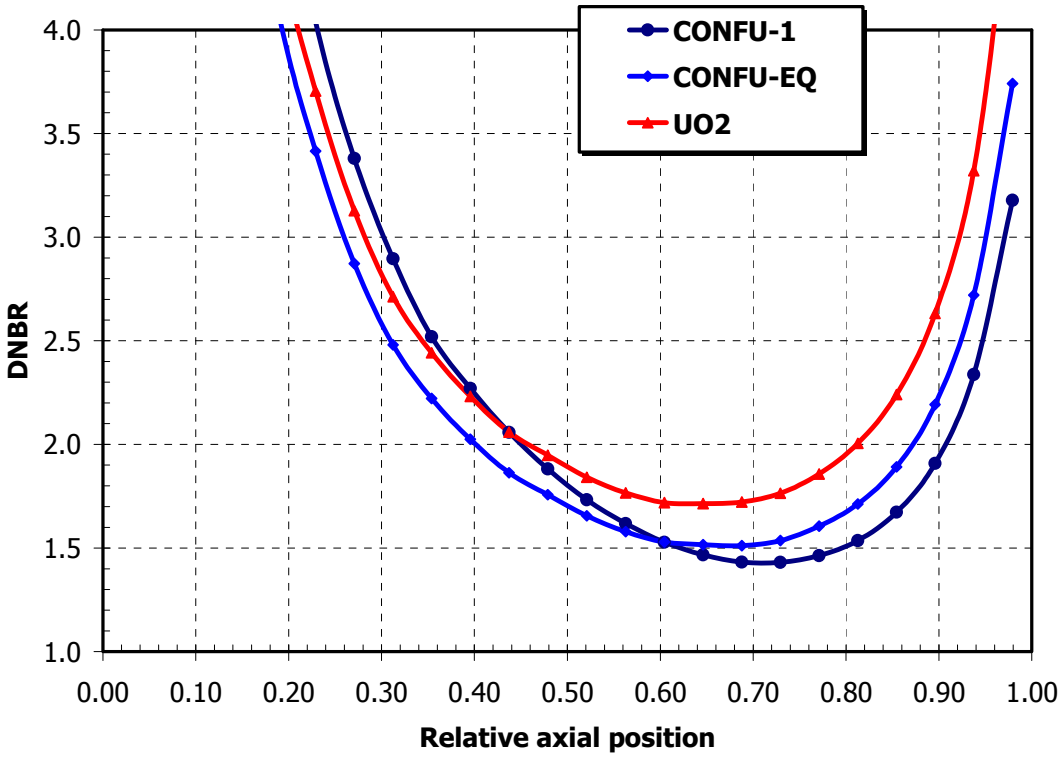

Figure 6.5.6. DNBR as a function of fuel height

6.6. Chapter Summary

This chapter has presented the results of 3-dimensional simulation of cores partially or fully loaded with TRU. In a previous chapter, the results of 2D fuel assembly level neutronic analysis suggested the possibility of attaining zero net generation of TRU in a closed PWR fuel cycle while maintaining the core neutronic characteristics comparable to a conventional UO_2 core. The main objective of this chapter was to confirm the feasibility of a sustainable PWR fuel cycle by performing a detailed 3D whole core neutronic simulation and thermal hydraulic analysis for a number of representative core configurations.

The calculated cases in the neutronic 3D core analysis included micro (CONFU) and macro (whole FFF and UO_2 assemblies) fuel options. For each configuration, the first time recycled and equilibrium TRU compositions were studied. For the macro heterogeneous option, cases with FFF assemblies being managed in 3, 4 or 5 batches were evaluated. Additionally, two limiting

cases for the core fully loaded either only with FFF or only with UO_2 assemblies were simulated for comparison.

A series of computational benchmarking studies were performed to assure accuracy of the obtained results. In general, the benchmark results revealed good agreement between the code predictions with the exception of the limited credibility of pin power reconstruction from the SIMULATE code for macro heterogeneous configurations.

The ZrB_2 IFBA design was used as a burnable poison for UO_2 and micro heterogeneous (CONFU) cases. Natural Gd oxide BP pins were used in macro heterogeneous FFF assemblies.

Results of the analyses confirmed the feasibility of partially TRU loaded PWR core designs. The exposure levels achieved by the UO_2 and FFF parts of the core proved the possibility of sustaining zero TRU generation within the PWR cycle, with both micro and macro heterogeneous options.

The micro-heterogeneous CONFU option is slightly superior to the macro-heterogeneous one in terms of TRU destruction efficiency due to a more thermalized spectrum in FFF pin regions as they are surrounded by UO_2 pins. In the whole FFF assembly in macro-heterogeneous cases, the spectrum "overlap" with UO_2 pin regions is smaller resulting in slightly lower TRU burnup. For the same reason, the local pin power peaking is higher in the micro-heterogeneous CONFU case. The main advantage of the macro-heterogeneous option is a flexibility of fuel management and handling. Fresh FFF assemblies can be placed in the core periphery to ensure acceptable power peaking. Irradiation time can be varied separately for UO_2 and FFF assemblies. Finally, less fuel handling would be required in the fuel cycle scheme where UO_2 and FFF pins are to be reprocessed by different methods or in different locations.

All neutronic characteristics of partially TRU loaded cores are comparable to those of a conventional UO_2 core. The differences in core parameters relate to the neutron spectrum hardening as the loading of TRU in the core increases. The major consequence of this effect is to lower the control materials reactivity worth and therefore potentially require higher soluble boron concentration which can in turn result in a less negative moderator temperature coefficient.

Another consequence of the addition of TRU into the PWR core is a reduced Doppler coefficient because of the higher relative fissile to fertile actinide amounts. In other words, U238, the major contributor to the negative Doppler coefficient in conventional UO_2 core is displaced with neutronically inert FFF matrix material. The main concern regarding the reduced Doppler coefficient is that, in combination with smaller effective delayed neutron fraction, it may imply inferior core response to rapid reactivity initiated accidents. The TRU loaded PWR core behavior in such accidents is discussed in the Chapter 7.

Thermal hydraulic calculations were carried out to study the MDNBR performance of the several suggested TRU loaded PWR core options. The single assembly simulations with conservative power peaking assumptions revealed that the TRU loaded cores have slightly inferior to the reference UO_2 core MDNBR performance reducing the MDNBR margin by 10% to 20% for the most limiting (CONFU-1) case. The whole core analysis was performed for the CONFU-1 case with detailed power distribution data obtained from 3D neutronics calculations to confirm the single assembly simulation findings. The results of the whole core and the single assembly calculations were found to be consistent. The MDNBR is reduced from the 1.71 for the UO_2 case to 1.43 for the CONFU-1 case. Both values, however, remain above the W3-L correlation MDNBR limit of 1.3.

Chapter 7. Accident Behavior Considerations

The presence of large amounts of TRU in a PWR core implies several major differences that can alter the dynamic behavior of the core under accident conditions.

As mentioned earlier, a harder neutron spectrum than typical for UO_2 fuel drives the impetus for re-assessment of the reactor control features. Generally higher concentrations of control materials would be required to compensate for their lower reactivity worth caused by the spectrum hardening. This effect is partially offset by the lower (than in all-UO_2 fuel case) initial core excess reactivity due to presence of fertile TRU isotopes with high cross-sections for neutron absorption. These isotopes act in a way as fertile poisons reducing the reactivity swing of the fuel over its irradiation time.

Another major implication of the large presence of TRU in a PWR core is reduced effective delayed neutron fraction (β_{eff}) as most of the fissile TRU isotopes typically have β_{eff} considerably lower than U235. This was also demonstrated in the previous chapter. The major consequence of the reduced β_{eff} is inferior core behavior in rapidly developing reactivity initiated accidents.

Introduction of the fertile free fuel matrix brings in an additional matter of concern. Displacement of U238 in a PWR core with a neutronically inert matrix leads to a significant reduction in the Doppler coefficient (DC). For a core fully loaded with FFF, the Doppler coefficient is reduced by about a factor of four relative to a typical UO_2 core as shown earlier.

One of the ways to improve DC of a FFF without impairing Pu or TRU consumption is by an addition of small amounts of Th232 into the fuel. [Lombardi, et al. 1999, Damen, et al. 1999, Akie et al. 1999] Thorium has about three times smaller resonance integral than U238 but much greater Doppler response to the fuel temperature changes.

A negative value of the DC is an obvious requirement for a stable reactor operation under normal conditions. However, the magnitude of the DC is especially important in accidents. In very rapid reactivity initiated accidents, the DC provides the most important immediate negative feedback that prevents prompt critical power excursions. Therefore, the height and duration of a power pulse initiated by fast reactivity insertion into the core and, consequently, the total energy

deposited in the fuel during the pulse are directly related to the magnitude of the Doppler coefficient.

According to the Nordheim-Fuchs model [Hetrick D.L., 1985] for a fast reactivity insertion accident, the total energy deposition in the fuel is given by the following expression:

$$E = \frac{2\,\rho_{fuel} C_p\,(\rho_0 - \beta)}{\alpha_{DC}} \qquad (7.1)$$

where $\rho_{fuel}\,C_p$ is the volumetric fuel heat capacity [J/cm^3-K], ρ_0 is the initial reactivity inserted, β is the effective delayed neutron fraction, and α_{DC} is the Doppler coefficient.

The model assumes a very short accident timescale and therefore neglects the delayed neutrons effect and heat transfer to the coolant. The total energy deposition in the fuel provides a measure of the fuel performance during the accident. The NRC specifies the value of 280 cal/g at any axial location in any fuel pin for UO_2 fuel as a threshold value above which fuel damage and release of FP into the coolant is expected. [US NRC, 1974] This value corresponds to about 12.19 kJ/cm^3 of UO_2 fuel. The fuel failure threshold expressed in units of energy per unit of fuel volume is a useful parameter for the comparison of UO_2 and FFF because the density of the latter is about two times lower. The 280 cal/g fuel damage threshold value is under review as being excessively high for the high burnup fuels [Diamond D. et al., 2002].

The relation 7.1 clearly shows that the energy deposition in the fuel depends on a combination of parameters which differ considerably for the conventional UO_2 and TRU containing cores. The smaller α_{DC} and β_{eff} for the FFF loaded core should make a negative contribution to the fuel performance in reactivity initiated accidents increasing the energy deposition in the fuel. However, lower ejected control rod reactivity worth (ρ_0) in combination with a larger thermal inertia ($\rho_{fuel} \times Cp$) of the FFF will compensate for the negative effects of the smaller α_{DC} and β_{eff} to some extent.

Here we attemp to compare the fuel performance of the FFF containing cores with conventional UO_2 core in reactivity initiated accidents (RIA) by constructing a physical model that will account for the differences in the neutronics as well as in fuel material properties of the two fuel types. A computer code was developed in Mathematica® programming environment

[Wolfram S., 1999] to solve a set of differential equations approximating the dynamic behavior of the reactor coupled with a one dimensional heat transfer model that provides the reactivity feedback to the neutronic part of the model.

Realistic core average values for the DC, MTC, delayed neutron data, and reactivity worth of the ejected control rod are obtained from 3D SIMULATE calculations and used as input data for the developed computer code model. Temperature dependent materials properties were used to obtain a closer approximation to realistic core conditions. It has to be noted however, that the current analysis assumes the FFF in the form of $(TRU)O_2$ – YSZ particles dispersed in $MgAl_2O_4$ (spinel) matrix. Although fertile free matrix composition is not likely to affect significantly the steady state neutronic characteristics of FFF, the dynamic behavior of the core under accident conditions may be different because of the differences in thermal properties of the fertile free matrix.

The developed code generates power, fuel, cladding, and coolant temperature profiles as a function of time after the control rod ejection accident (REA). The generated data is subsequently used for comparison of the considered cases to the reference UO_2 fuel case.

7.1. RIA Analysis Code Model Description

Reactor kinetics model

A point reactor kinetics model [Hetrick, 1985] was used to describe the reactor power evolution with time. The model assumes that the spatial power distribution in the reactor is completely time independent. That is, the whole reactor core behaves in time as a zero dimensional power source. The point reactor approximation yields reasonable results for systems where the core dimensions are smaller or of the same order as the average migration length of neutrons in that system. Research and test reactors (due to their small dimensions) or fast spectrum reactors (due to large migration length) are examples of such systems. However, a typical PWR core has many times larger dimensions than the neutron migration length. Therefore, in the control rod ejection accident, where the power distribution changes rapidly with time, the point kinetics model assumptions are no longer valid. More sophisticated computational tools

such as PARCS [Joo et al., 1998] employ a space-time dependent reactor kinetics model that reflects more accurately the dynamic behavior of large reactor systems such as PWRs.

Nevertheless, the main objective of this part of the thesis is to evaluate the feasibility of innovative fuel designs for a sustainable PWR fuel cycle by providing a consistent comparison between conventional UO_2 fuel and TRU containing FFF options rather than to obtain realistic accident analysis simulation results. Thus, it was concluded that the point reactor kinetics model is a sufficient approximation for purposes of the current study. A similar methodological approach was employed in [Damen and Kloosteramn 1999, 2000, 2001] for the neutronic analysis of surplus Pu disposition studies. Additionally, an elaborate PWR REA study performed with the PARCS computer code was reported in [Diamond et al., 2002]. The detailed 3D space-time kinetics analysis has shown that even the simplest point kinetics Nordheim-Fuchs model predicts the correct trends and sensitivities to various parameters.

According to the point reactor kinetics model, the change of the reactor power with time is governed by the system of differential equations 7.1.1:

$$\begin{aligned}
&\frac{dP(t)}{dt} = \frac{\rho(t) - \sum_{i=1}^{6}\beta_i}{\Lambda} P(t) + \sum_{i=1}^{6}\lambda_i C_i(t) \\
&\frac{dC_1(t)}{dt} = \frac{\beta_1}{\Lambda} P(t) - \lambda_1 C_1(t) \\
&\cdots\cdots\cdots \\
&\frac{dC_6(t)}{dt} = \frac{\beta_6}{\Lambda} P(t) - \lambda_6 C_6(t)
\end{aligned} \qquad (7.1.1)$$

Here, 6 groups of delayed neutrons were used. β_i and λ_i are the yield and the decay constant corresponding to each of the delayed neutron group. Λ is the prompt neutrons generation time. P is the reactor power and the C_i is the concentration of the delayed neutron precursor isotopes for the group *i*. $\rho(t)$ is the core reactivity which is equals to zero in steady state conditions.

Thermal feedback model

Thermal hydraulic feedback for the neutronic point kinetics model is provided by solving a heat balance equation in three zones (fuel, cladding, and coolant) for each time step. The calculated fuel and the coolant temperatures are then used to calculate the change in reactivity for the subsequent time step. Linear Doppler and MTC feedback were assumed. Namely, the reactivity for the time step *i* is calculated as

$$\rho_i = \rho_{i-1} + \alpha_{DC} \, (T_i^{fuel} - T_{i-1}^{fuel}) + \alpha_{MTC} \, (T_i^{coolant} - T_{i-1}^{coolant}) \qquad (7.1.2)$$

where α_{DC} and α_{MTC} are the Doppler and moderator temperature coefficients respectively and T_i^{fuel}, T_{i-1}^{fuel}, $T_i^{coolant}$, $T_{i-1}^{coolant}$ are the fuel and the coolant temperatures at the current and the previous time steps.

The heat balance equation was solved numerically for each time step. The fuel region in the fuel pin was subdivided into 14 equivolumetric zones to reflect the differences in thermal properties as well as in radial power density for different fuel types and operating conditions. The set of differential equations 7.1.3 describes the change in the fuel, cladding, and coolant temperatures with time.

$$\begin{aligned}
M_j^{fuel} \, Cp_j^{fuel} \frac{dT_j^{fuel}(t)}{dt} &= P_j(t) + h_{j-1,j}(\overline{T}_{j-1,j}^{fuel}) \times (T_{j-1}^{fuel} - T_j^{fuel}) - \\
&- h_{j,j+1}(\overline{T}_{j,j+1}^{fuel}) \times (T_j^{fuel} - T_{j+1}^{fuel}), \qquad j = 1,....,14 \\
M^{clad} \, Cp^{clad} \frac{dT^{clad}(t)}{dt} &= h_{14,clad}(T_{14}^{fuel}, T^{clad}) \times (T_{14}^{fuel} - T^{clad}) - \\
&- h_{clad,water}(T^{clad}) \times (T^{clad} - T^{water}), \qquad (7.1.3) \\
M^{water} \, Cp^{water} \frac{dT^{water}(t)}{dt} &= h_{clad,water}(T^{clad}) \times (T^{clad} - T^{water}) - \\
&- \frac{2 \times \dot{m} \times Cp^{water}}{H^{core}} \times (T^{water} - T^{inlet})
\end{aligned}$$

where:

M_j^{fuel} – mass per unit length of the fuel in the region *j* (g/cm),

M^{clad} – mass per unit length of the cladding (g/cm),

M^{water} – mass per unit length of the water based on average water density (g/cm),

Cp_j^{fuel} – temperature dependent specific heat of the region *j* (J/g-K),

Cp^{clad} – temperature dependent specific heat of the cladding (J/g-K),

Cp^{water} – specific heat of coolant (J/g-K),

T_j^{fuel} – fuel temperature in the region *j*, (K)

T^{clad} – average cladding temperature, (K)

T^{water} – average coolant temperature, (K)

P_j – power generated in the region *j* of the fuel (W/cm)

$h_{i,j}$ – reciprocal of thermal resistance between the regions *i* and *j*, (W/cm-K)

$\overline{T}_{i,j}^{fuel}$ – average fuel temperature between the regions *i* and *j*, (K)

$\dot{m}$ – coolant mass flow rate per one fuel channel, (g/sec)

H^{core} – active core height, (cm)

The thermal resistances between fuel regions were calculated as follows:

$$h_{i,j}(T_i^{fuel}, T_j^{fuel}) = \frac{2\pi \times k^{fuel}\left(\frac{T_i^{fuel} + T_j^{fuel}}{2}\right)}{Log\left(\frac{r_i^{fuel}}{r_j^{fuel}}\right)} \tag{7.1.4}$$

where r_i^{fuel} and r_j^{fuel} are the mean radii of the fuel regions *i* and *j* and k is the fuel thermal conductivity.

The thermal resistance between the outermost fuel region and the cladding was calculated as the sum of thermal resistances at the mean radius of the last fuel region, across the gap and the mean radius of the cladding region. Similarly, the resistance between the cladding and the coolant was obtained as a sum of resistances between the mean radius of the cladding region and the cladding outer surface plus the resistance associated with heat transfer from the cladding wall to the coolant bulk (Eq. 7.1.5).

$$\frac{1}{2\pi\ h^{clad\text{-}water}\ (r_{co} + r_{ci})/2} = \frac{Log\left(\frac{r_{co}}{(r_{co} + r_{ci})/2}\right)}{2\pi\ k^{clad}} + \frac{1}{2\pi\ r_{co}\ h^{water}} \tag{7.1.5}$$

The forced convection heat transfer coefficient from the cladding wall to coolant was calculated from the Dittus-Boelter single phase heat transfer correlation [Todreas N.E. and Kazimi M.S., 1990]. The gap conductance was obtained by solving the steady state heat balance equation under nominal operating conditions. The resulting value for the gap conductance of 0.6084 W/cm^2-K is typical for un-irradiated UO_2 fuel. The effect of the fuel pellet dimensional changes under irradiation was neglected because gap closure for irradiated fuel will increase the gap conductance and improve the heat transfer to the coolant. This is a beneficial feature for the RIA therefore assuming unirradiated fuel gap conductance for all cases is a conservative assumption.

The model assumes constant heat transfer coefficient to the coolant and linear moderator temperature coefficient feedback. Therefore, any changes in heat transfer or MTC due to boiling as a result of increased cladding temperature are neglected.

The dependence of UO_2 fuel thermal conductivity on temperature was obtained from [Fink J.K., 2000]. The recommended dependence has the following form

$$k_{UO_2}(T) = \frac{100}{7.5408 + 17.692 \times \frac{T}{1000} + 3.611 \times \left(\frac{T}{1000}\right)^2} + \frac{6400}{\left(\frac{T}{1000}\right)^{5/2}} \times e^{\left(-\frac{16350}{T}\right)} \text{ [W/m/K]} \tag{7.1.6}$$

where T is the fuel temperature in Kelvin

The thermal conductivity of the FFF was calculated according to the Maxwell-Eucken equation for dispersed particle type fuels [Tong and Weisman, 1996]

$$k_d = \frac{1 - \left(1 - \frac{a\, k_p}{k_m}\right) b}{1 + (a - 1)\, b} \tag{7.1.7}$$

where k_d is the effective thermal conductivity of dispersion fuel, k_p and k_m are the thermal conductivities of the particles and the matrix respectively, b is the particles volume fraction and a is given by

$$a = \frac{3\,k_m}{2\,k_m + k_p} \tag{7.1.8}$$

Equation 7.1.8 approximately holds up to the particle volume fraction of 0.5.

The conductivity of the fuel micro particles composed of homogeneously mixed $(TRU)O_2$ and yttria stabilized zirconia was calculated according to the Vegard's law [Berna et al. 1997].

$$k_p = k_{(TRU)O2} \times x_{(TRU)O2} + k_{YSZ} \times x_{YSZ} \tag{7.1.9}$$

where k_{TRUO2} and k_{YSZ} are the thermal conductivities of $(TRU)O_2$ and YSZ respectively and x_{TRUO2} and x_{YSZ} are their corresponding molar fractions.

The data for thermal conductivity of TRU oxides is not available. PuO_2 data was used instead as Pu comprises the major part of the TRU (>85w/o initially). The equation used for PuO_2 conductivity is recommended in [Carbajo J.J. et al. 2001]

$$k_{PuO_2}(T) = \frac{1}{4.4819\times10^{-2} + 4.418\times10^{-4}\ T} + \frac{5.516\times10^{9}}{T^2} \times e^{\left(-\frac{16347.8}{T}\right)} \quad [W/m/K] \tag{7.1.10}$$

where T is the fuel temperature in Kelvin.

The expressions used for the conductivity of spinel matrix, YSZ, [Yuan Y. et al. 2001] and Zircaloy-4 cladding [INSC] are presented in Equations 7.1.11 through 7.1.13.

$$k_{Spinel}(T) = \frac{1.2}{0.036 + 1.6\times10^{-4}\ T} + \frac{8\times10^{9}}{T^2} \times e^{\left(-\frac{13000}{T}\right)} \quad [W/m/K] \tag{7.1.11}$$

$$k_{YSZ}(T) = 2.0 + 4.72\times10^{-4} \times (T - 300) \qquad [W/m/K] \tag{7.1.12}$$

$$k_{Zr-4}(T) = 12.276 - 5.4348\times10^{-4} \times T + 8.9818\times10^{-6} \times T^2 \qquad [W/m/K] \tag{7.1.13}$$

where T is in Kelvin

The resulting effective thermal conductivity of the dispersed FFF is compared with that of UO_2 in Figure 7.1.1.

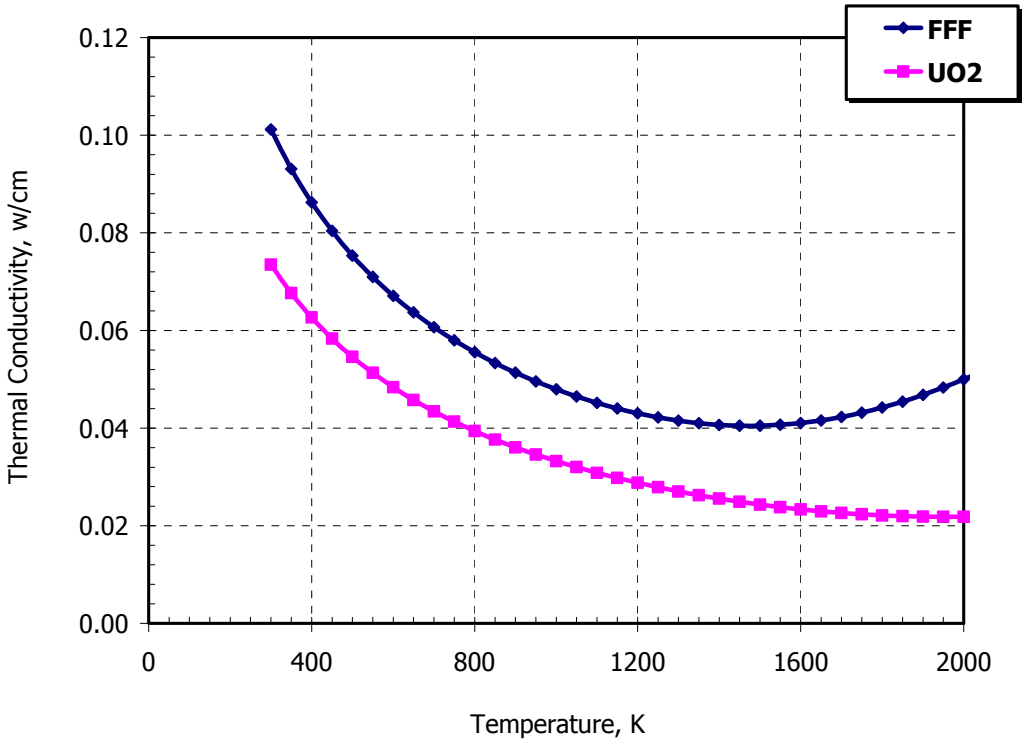

Figure 7.1.1. Thermal conductivity of UO_2 and dispersed type FFF

The UO_2 fuel specific heat temperature dependence was also adopted form [Fink J.K., 2000]. The expression for Cp of UO_2 fuel is given in Equation 7.1.14.

$$Cp_{UO2}(T) = \frac{302.27 \times 548.68^2 \times e^{\frac{548.68}{T}}}{T^2\left(e^{\frac{548.68}{T}} - 1\right)^2} + 2 \times 8.463 \times 10^{-3} \times T + \frac{8.471 \times 10^7 \times 18531.7 \times e^{-\frac{18531.7}{T}}}{T^2} \quad [J/kg/K] \tag{7.1.14}$$

where T is the temperature in Kelvin.

For the specific heat of the FFF, the Neumann-Kopp law was adopted to quantify the specific heat of complex materials [Seitz, 1940]

$$Cp = \sum x_i \times Cp_i \qquad (7.1.15)$$

where x_i is the molar fraction of the material *i* in the mixture and C_{pi} is the specific heat of the material *i*.

The specific heat of ZrO_2 exhibits a weak dependence on Y_2O_3 content and on the temperature in the range between 600 and 1500K [Degueldre et al., 2003]. Therefore, it was assumed to be independent of the temperature for the purposes of this analysis and to be equal to 0.45 J/g-K. The chosen value is conservative as it represents the lower bound of the available experimental data for the high temperature specific heat of zirconia [Hidaka, et al., 1997].

The specific heat data for Spinel was reported in [Matzke, et al., 1999]. The reported data was fit to a second order polynomial in the range between 800 and 1600K for the practical purposes of the numerical calculations.

The equation recommended in [Carbajo et al. 2001] for PuO_2 was used to approximate the specific heat of the $(TRU)O_2$ component of FFF.

$$Cp_{PuO2}(T) = \frac{322.49 \times 548.68^2 \times e^{\frac{548.68}{T}}}{T^2\left(e^{\frac{548.68}{T}} - 1\right)} + 2 \times 1.4679 \times 10^{-2} \times T \quad [J/kg/K] \qquad (7.1.16)$$

The resulting Cp of the FFF fuel exhibits a moderate variation with temperature. In the range of interest between 600K and 2000K, the Cp of the FFF varies between 1.0 and 1.15 J/g-K. Note that the Cp values of FFF are greater than those for UO_2 fuel by more than a factor of three while the density of FFF is only about a factor of two smaller than UO_2. This implies an overall larger thermal inertia for the FFF which is beneficial for the fuel performance in accidents.

Fuel Pin Radial Power Profiles

The radial power distribution within the fuel pin changes significantly with fuel burnup. The resonance self-shielding effect in U238 typically results in preferential buildup of Pu in the region near the fuel pellet surface (so-called “rim effect”). The power generated in the periphery of the

fuel pin increases substantially because of the high Pu concentration at the EOL. This power increase may cause undesirable fuel restructuring degradation of properties in the rim region and release of the fission gas. [Long Y. et al., 2000].

The radial power shape in the fuel pellet, however, also affects the fuel temperature distribution within the fuel. A larger power fraction generated in the fuel periphery would result in lower maximum fuel temperature because effectively larger amount of heat would have to overcome lower thermal resistance in order to be conducted to the coolant.

In the FFF pin, the concentration of fertile resonance actinides is lower than in the UO_2 fuel. Thus, the rim effect is expected to be less pronounced than in the UO_2 fuel. Detailed radial power distribution profiles were calculated for the FFF and UO_2 fuel pins to reflect appropriately the differences in the rim effect for the two fuel types. BOL and EOL distributions were obtained and then used in the thermal feedback module of the RIA analysis code for calculation of the temperature distribution in the fuel.

UO_2 and FFF unit cell burnup calculations were performed with the MCODE [Xu et al., 2002]. Operating conditions typical for PWR core and identical to those used for the neutronic evaluation of the FFF option and the reference UO_2 fuel were used. The MCNP model of the fuel region consisted of 14 burnup zones with the same dimensions as used for the thermal hydraulic feedback module. The schematic view of the MCNP fuel pellet model is presented in Figure 7.1.2. The calculations were performed up to equivalent 1350 EFPD of fuel burnup.

The resulting radial power profiles for the UO_2 and the FFF at BOL and EOL are presented in Figure 7.1.3. The UO_2 results are consistent with previously reported data [Long et al., 2000]. The BOL power distribution for the UO_2 fuel is relatively flat while at the EOL the power peaks significantly in the rim of the pellet. The FFF on the other hand, exhibits a completely opposite trend. The power is generated preferentially in the outer region of the pellet at BOL due to a moderate self-shielding of fissile Pu resonances. At EOL the power is shifted towards the inner part of the FFF pellet because of the depletion of fissile Pu on the periphery. Furthermore, the power distribution in general is relatively even for the FFF pellet throughout the fuel lifetime as a result of considerably reduced overall resonance self-shielding effect.

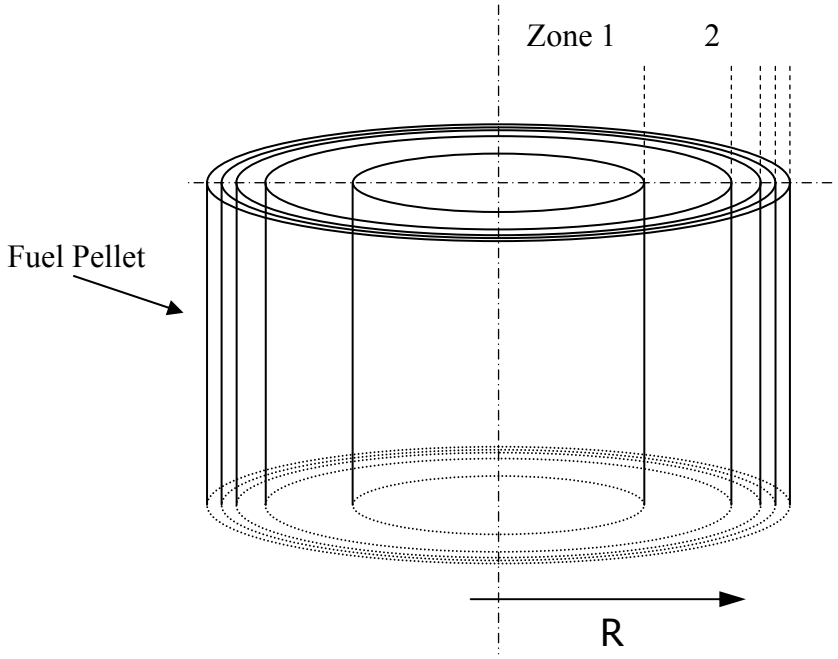

Figure 7.1.2. Schematic representation of fuel burnup regions

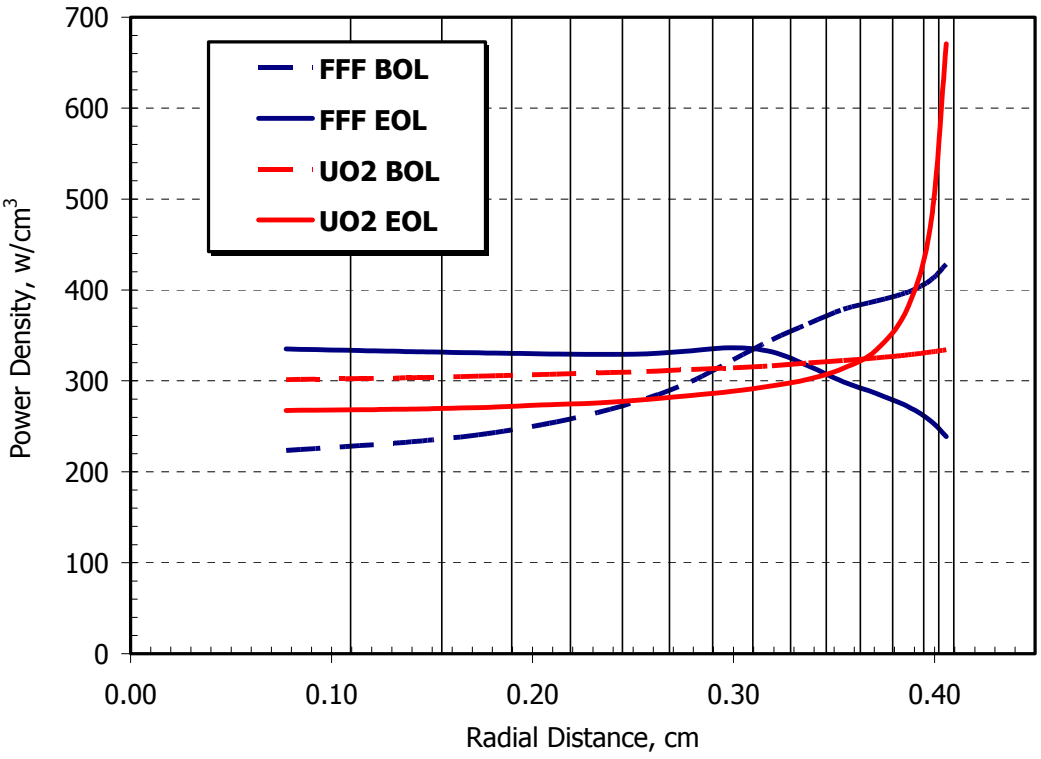

Figure 7.1.3. Radial power profile for UO_2 and FFF

7.2. RIA Analysis Results

The model developed for the RIA accident analysis has no built-in capabilities for representing heterogeneous fuel configurations such as the CONFU assembly. Therefore, the calculations were performed first for the UO_2 and full core FFF case as two representative limiting cases. Each case was analyzed at four potentially operating condition states: at HFP-BOL, HZP-BOL, HFP-EOL, and HZP-EOL. Then, the most limiting in terms of energy deposition and fuel temperature state was identified for each fuel type. Finally, the heterogeneous cases were analyzed at this most limiting state using the neutronics data for this heterogeneous option but performing the calculation twice: once using the FFF pins thermal properties then using the UO_2 fuel properties. The comparison of the results would show which part of the heterogeneous assembly exhibits the limiting behavior.

This strategy should provide a realistic approximation for the micro-heterogeneous CONFU option because of the small range of spatial separation of FFF and UO_2 pins. The applicability of this strategy to the macro-heterogeneous CONFU case, however, is only marginal because the UO_2 and FFF pins regions are large enough to be considered less neutronically coupled with each other especially on the very small timescales typical for RIA accidents.

Table 7.2.I lists all the cases considered for analysis and summarizes the major nuclear data obtained from SIMULATE 3D calculations that was applied. Two additional assumptions were made. Since the fuel loading pattern was not optimized, neither for the reduction of power peaking factors nor for the smaller scatter in control rod worths, the average control rod worth values were used for each case and the nominal power level was assumed in all calculated cases. The power level at HZP conditions used was 1% of the nominal. The ejection of the control rod was assumed to occur in 100 ms with the constant rate of reactivity insertion.

Table 7.2.II and 7.2.III show the results of the UO_2 and the FFF REA simulation. Table 7.2.II shows the maximum fuel pellet enthalpy increase during the power pulse following the REA. The enthalpy increase is reported in J/cm^3 and cal/g units. The simulations were performed for the average core power. Therefore, the obtained energy deposition values are not conservative and cannot be compared to the fuel failure criteria of 280 cal/g. The primary purpose of this analysis is relative comparison of FFF and CONFU with the reference UO_2 case. Nevertheless, the maximum fuel pellet enthalpy rise including a conservative 3D power peaking factor of 2.5 is

also included in Table 7.2.II. The UO_2 core fuel enthalpy rise with 2.5 power peak agrees well with the corresponding value reported in a detailed PWR REA study performed with the PARCS computer code [Diamond D. et al., 2002]. EOL-HFP conditions case is the most limiting one for both fuel options. At EOL-HFP, the fuel pellet enthalpy rise in FFF case is more than a factor of two larger than in UO_2 case.

Table 7.2.III reports asymptotic increase in the fuel central line, cladding and coolant temperatures. As expected, the incremental temperature raise for the fuel, cladding and coolant are considerably higher for FFF case at all considered operating conditions. The results are a direct consequence of reduced DC and β_{eff} for the fully FFF loaded core.

Figures 7.2.1 through 7.2.6 illustrate the dynamic behavior of the FFF and UO_2 fuels after the REA. The peak of the power pulse is almost a factor of four larger for FFF than for UO_2 fuel at EOL-HFP conditions, again, as a result of considerably smaller Doppler coefficient and β_{eff} (Figures 7.2.1 and 7.2.4). The EOL at HFP is associated with the highest peak power , but BOL at HFP has comparable total energy input.

Table 7.2.I. List of analyzed cases and their neutronic parameters

Case		Operating conditions	Irradiation time	DC, pcm/K	MTC, pcm/K	prompt life time, sec	β_{eff}	CRD worth, $
1	UO2	HFP	BOL	-3.24	-40.81	1.69E-05	6.03E-03	-0.97
2	UO2	HFP	EOL	-3.28	-74.92	2.00E-05	5.18E-03	-1.41
3	UO2	HZP	BOL	-4.52	-15.35	1.69E-05	6.03E-03	-0.99
4	UO2	HZP	EOL	-8.55	-37.76	2.00E-05	5.18E-03	-1.25
5	FFF	HFP	BOL	-0.77	-18.52	6.95E-06	3.02E-03	-1.07
6	FFF	HFP	EOL	-0.92	-59.09	1.02E-05	3.40E-03	-1.42
7	FFF	HZP	BOL	-0.92	-5.51	6.95E-06	3.02E-03	-1.02
8	FFF	HZP	EOL	-2.02	-33.91	1.02E-05	3.40E-03	-1.26
9	CONFU-1	HFP	BOL	-2.56	-34.47	1.37E-05	5.34E-03	-1.27
10	CONFU-1	HFP	EOL	-2.59	-67.63	1.70E-05	4.82E-03	-1.45
11	CONFU-1	HZP	BOL	-3.55	-11.07	1.37E-05	5.34E-03	-1.21
12	CONFU-1	HZP	EOL	-6.17	-33.86	1.70E-05	4.82E-03	-1.50
13	CONFU-E	HFP	BOL	-2.88	-36.92	1.20E-05	5.51E-03	-0.99
14	CONFU-E	HFP	EOL	-2.75	-73.48	1.41E-05	4.94E-03	-1.26
15	CONFU-E	HZP	BOL	-3.94	-12.15	1.20E-05	5.51E-03	-0.90
16	CONFU-E	HZP	EOL	-6.23	-38.93	1.41E-05	4.94E-03	-1.13

Table 7.2.II. UO_2 and FFF RIA results: energy deposition

	Case	Conditions		Core average power		2.5 power peak	
				Enthalpy rise, J/cm^3	Enthalpy rise, cal/g	Enthalpy rise, J/cm^3	Enthalpy rise, cal/g
UO2	1	HFP	BOL	573	13.2	1433	32.9
	2	HZP	BOL	91	2.1	228	5.2
	3	HFP	EOL	725	16.7	1813	41.6
	4	HZP	EOL	152	3.5	380	8.7
FFF	5	HFP	BOL	1276	61.5	3189	153.9
	6	HZP	BOL	761	36.7	1903	91.8
	7	HFP	EOL	1498	72.3	3744	180.7
	8	HZP	EOL	714	34.4	1784	86.1

Table 7.2.III. UO_2 and FFF RIA results: fuel, cladding, and coolant temperature rise

	Case	Conditions		ΔT_{fuel}, K	ΔT_{clad}, K	$\Delta T_{coolant}$, K
UO2	1	HFP	BOL	201.1	13.4	5.2
	2	HZP	BOL	161.2	17.3	6.2
	3	HFP	EOL	180.1	13.4	5.2
	4	HZP	EOL	84.5	10.1	3.4
FFF	5	HFP	BOL	306.8	32.4	12.1
	6	HZP	BOL	388.7	50.4	18.5
	7	HFP	EOL	192.4	17.7	6.4
	8	HZP	EOL	172.8	21.3	7.8

The cladding surface temperature as a function of time for the UO_2 and FFF are shown in Figures 7.2.2 and 7.2.5 respectively. The cladding peak temperature increase is about twice as large for the FFF than for UO_2 fuel under the most limiting EOL-HFP conditions. In the HFP FFF cases, the peak cladding surface temperature exceeds water saturation temperature by up to 15 °C implying incipient boiling at some stage of the accident while the UO2 HFP-EOL cladding temperature exceeds T_{sat} of the coolant by about 5°C for a fraction of a second. However, this is not a significant concern with regards to reaching a DNB. Coolant boiling would enhance the heat transfer to coolant and the voiding would provide a very strong negative reactivity feedback reducing the power. The boiling heat transfer and void reactivity feedback effects were both neglected in this study. Note, however, that the analysis also neglected power peaking factors and

potential of having a larger than average reactivity worth of the ejected control rod. Therefore, the DNB limit is more likely to be reached for FFF than for UO_2 fuel under the REA conditions should all the conservative values for the power peaking and CR worth apply. A recent review of LWR safety criteria during RIA concluded on the basis of accumulated experimental data that irradiated fuel failure is related to fuel pellet-cladding mechanical interaction (PCMI) and fission gas release effects rather than to critical heat flux [OECD/NEA, 2001].

The fuel meltdown, on the other hand, is one of the major concerns during the REA. Under nominal operating conditions, the FFF central line temperature is about 180K lower than that of the UO_2 fuel at BOL under the same conditions due to a better thermal conductivity of the FFF. At the EOL, however, the difference reduces to just about 70K as a result of the rim effect discussed earlier. At the same time, the melting temperature of the Spinel matrix is about 2200K as opposed to about 2800K for the UO_2. As a result, the FFF and UO_2 fuels have different margins to melting at the steady state conditions. A new performance index is suggested to compare the relative margin to fuel melting reduction during the accident for the fuels of different types[2]. The quantity *I*, fuel melting margin degradation index, is defined as follows:

$$I(t) = \frac{T(t) - T_{steady\ state}}{T_{melt} - T_{steady\ state}} \qquad (7.2.1)$$

The index *I* takes up values between zero and unity. At steady state, the fuel nominal index of degradation of margin to melting is zero. The margin vanishes completely ($I = 1$) when the maximum fuel temperature reaches its melting point.

The quantity *I* is plotted in Figures 7.2.3 and 7.2.6 for the UO_2 and FFF cases respectively. The peak fuel temperature values are highest at HFP-EOL for both cases immediately following the CRE. The asymptotic values, however, are higher at HFP-BOL for both cases due to the considerably lower moderator temperature feedback at BOL especially in the FFF case (Table 7.2.I). The evolution of the index *I* as a function of time after the CRE indicates that the peak margin reduction is about 30% for the FFF case while it stays just around 10% for the UO_2 case.

[2] Saha P. *Private communication*, 2003

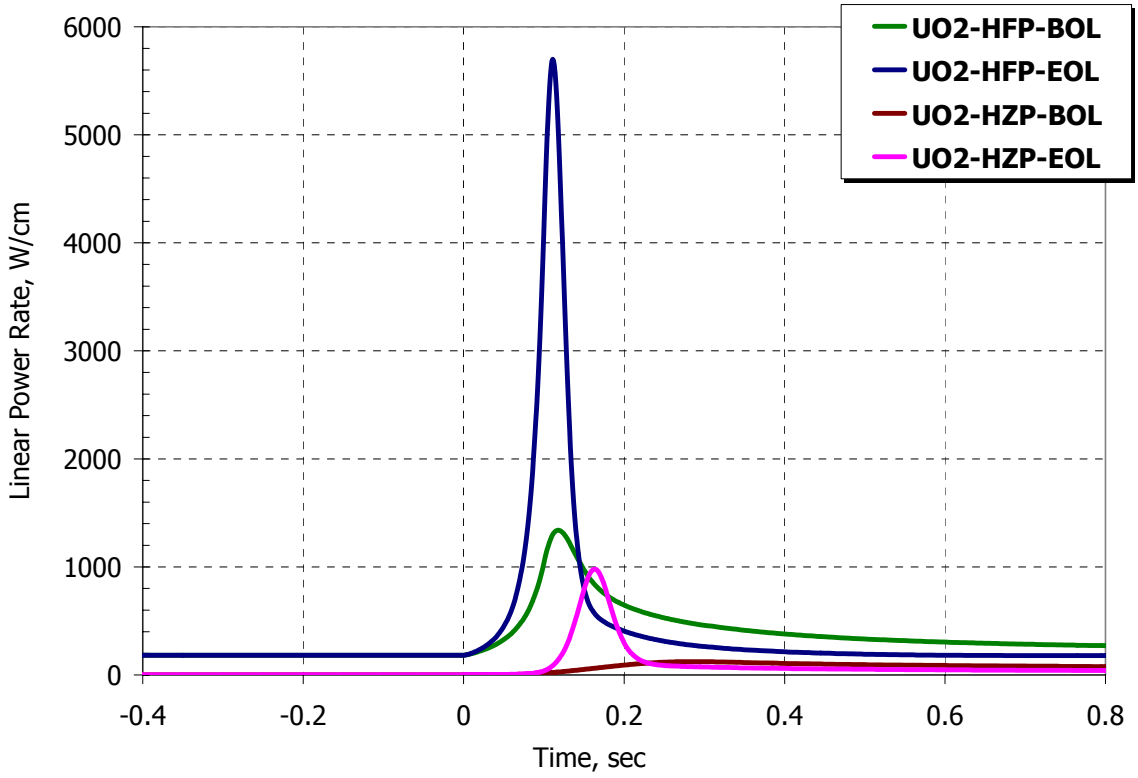

Figure 7.2.1. REA: Linear power vs. Time, UO_2 fuel

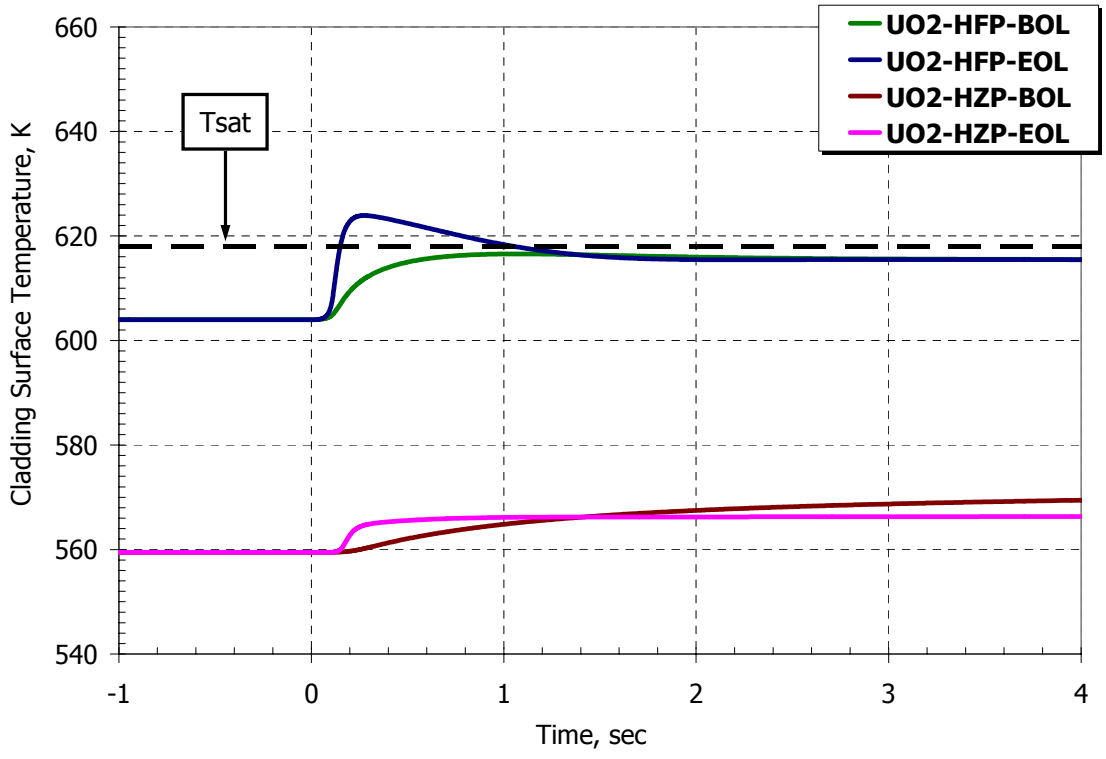

Figure 7.2.2. REA: Cladding surface temperature vs. Time, UO_2 fuel

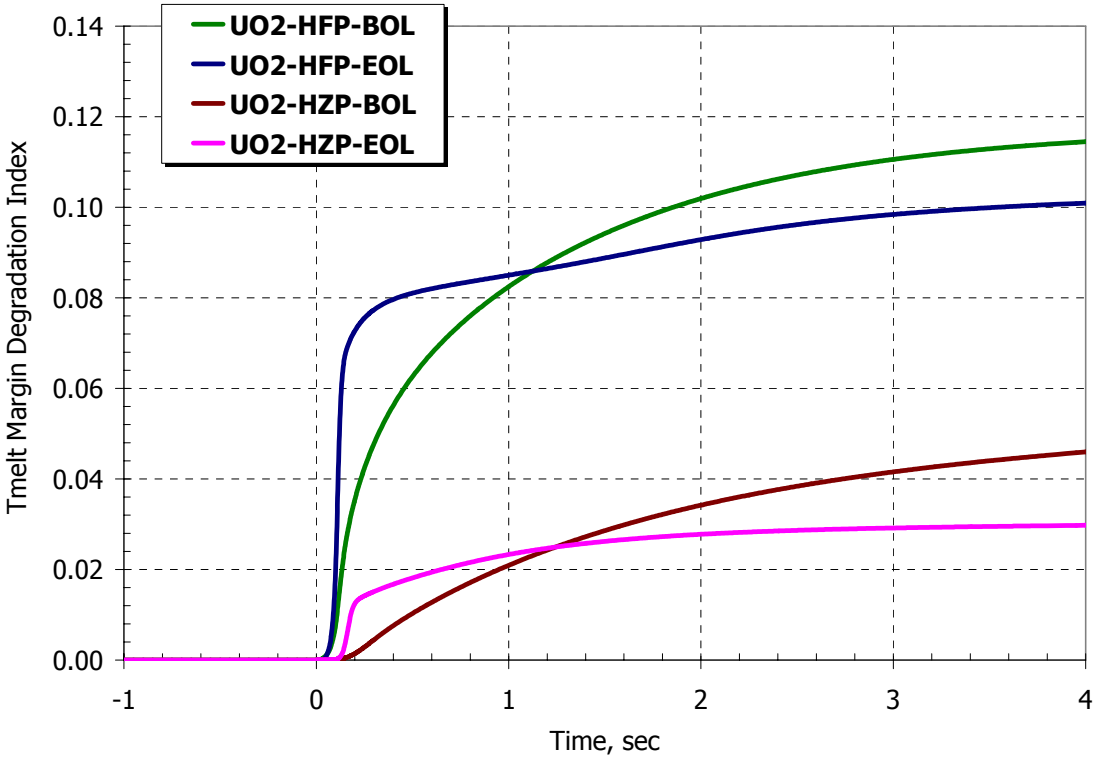

Figure 7.2.3. REA: Fuel melting margin degradation vs. Time, UO_2 fuel

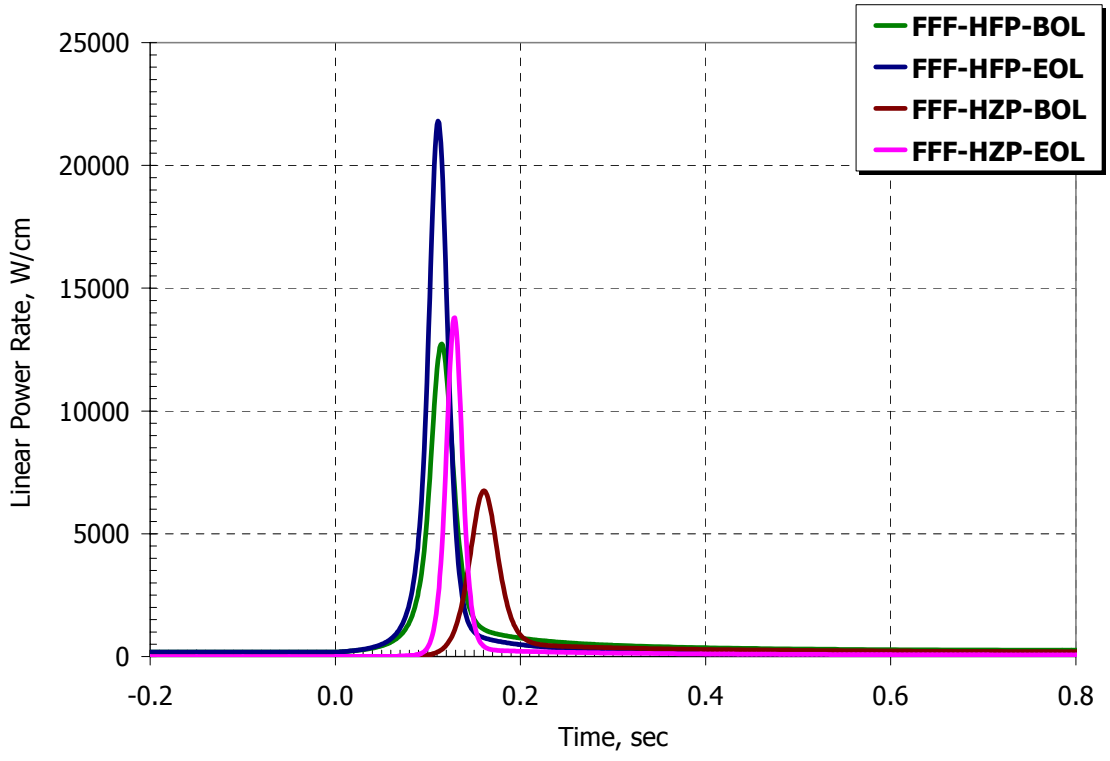

Figure 7.2.4. REA: Linear power vs. Time, FFF

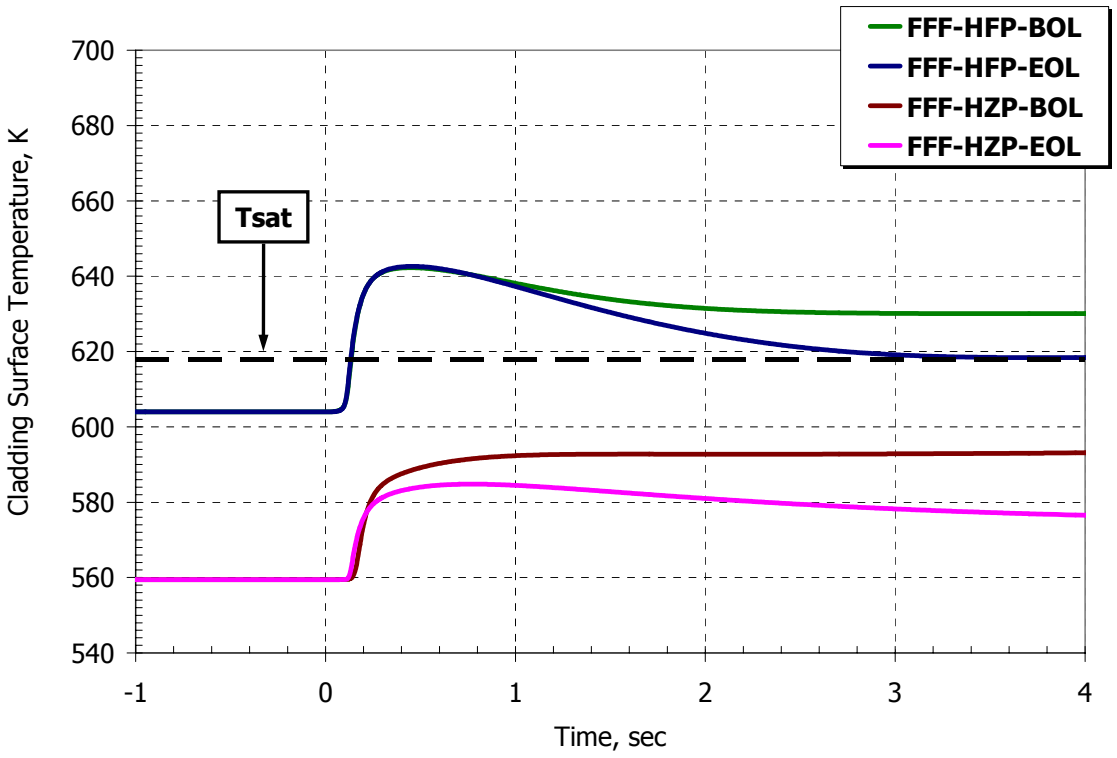

Figure 7.2.5. REA: Cladding surface temperature vs. Time, FFF

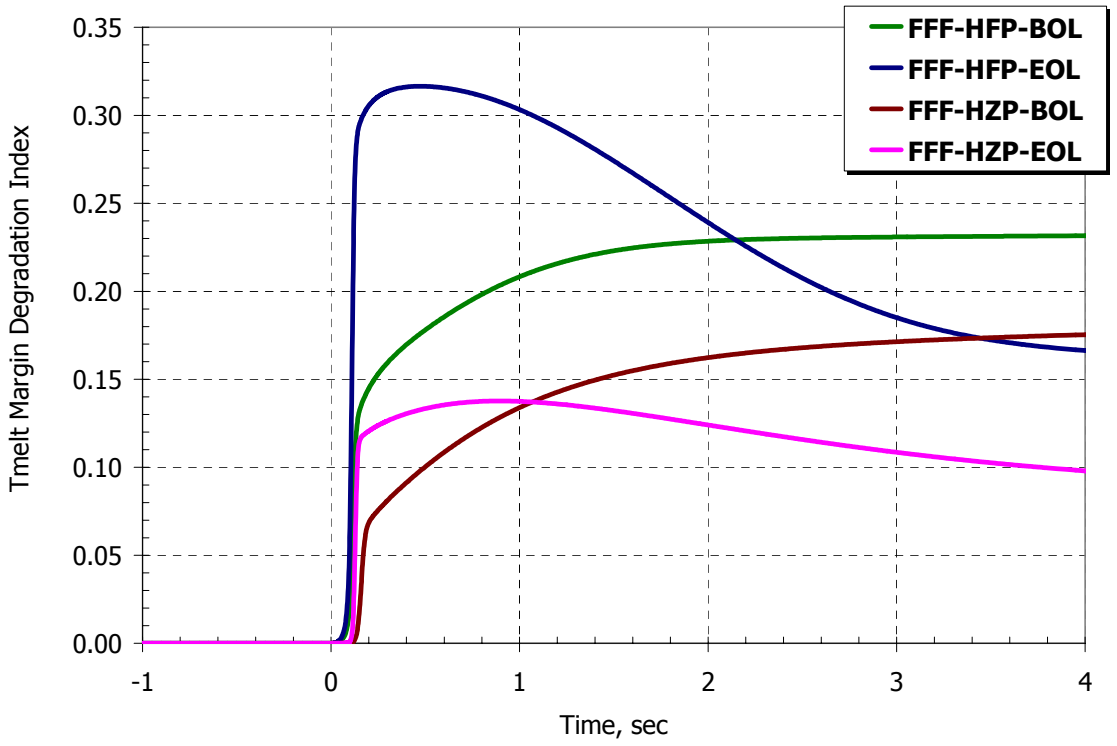

Figure 7.2.6. REA: Fuel melting margin degradation vs. Time, FFF

The HFP-EOL condition was identified as the most limiting, for both UO_2 and FFF cases, with regards to the total energy deposition and the maximum fuel temperature. Therefore, the calculations for the micro-heterogeneous CONFU cases were performed at this state separately for UO_2 and FFF pins with CONFU neutronic parameters to reveal the limiting fuel pin type.

Table 7.2.IV and 7.2.V compare the results of the simulation. Table 7.2.IV reports the enthalpy increase for the nominal power condition and with conservative local power peaking of 2.5 applied. Additional 15% of power increase was applied to FFF pins to reflect the power distribution within the CONFU assembly. Table 7.2.V reports the incremental fuel, cladding, and coolant temperature raise. As expected, the CONFU assembly performance is very close to the reference UO_2 case due to their close neutronic characteristics. Here again, the FFF pins in the CONFU cases exhibit the most limiting performance. The CONFU-1 case is somewhat worse than the CONFU-E case because of the larger contribution of TRU to the total assembly power and therefore larger effect on the assembly average neutronic characteristics.

The power evolution with time and the melting temperature margin degradation index (I) for the CONFU-1 and CONFU-E cases are compared with those of the UO_2 case in Figures 7.2.7 through 7.2.10. The power pulse peak height is the largest for the FFF pin in the CONFU-1 case while for the CONFU-E cases, the reference UO2 fuel exhibits larger power increase than both CONFU-E fuel types.

The FFF pins are still the most limiting as far as the fuel melting is concerned. The melting margin degradation is 1.2 to 2 times larger for the FFF than for the UO_2 pins in both the reference UO_2 and CONFU cases due to the lower melting point of FFF spinel matrix and despite its enhanced thermal conductivity.

Table 7.2.IV. CONFU REA simulation results: energy deposition

Case			Conditions		Core average power		2.5 power peak*	
					Enthalpy rise, J/cm^3	Enthalpy rise, cal/g	Enthalpy rise, J/cm^3	Enthalpy rise, cal/g
3	UO_2		HFP	EOL	725	16.7	1813	41.6
10a	CONFU-1	FFF	HFP	EOL	905	43.7	2603	125.6
10b		UO_2	HFP	EOL	797	18.3	1993	45.8
14a	CONFU-E	FFF	HFP	EOL	735	35.4	2112	101.9
14b		UO_2	HFP	EOL	653	15.0	1632	37.5

* power peaking factor of 2.875 is applied to FFF cases

Table 7.2.V. CONFU REA simulation results: fuel, cladding, and coolant temperature rise

Case			Conditions		ΔT_{fuel}, K	ΔT_{clad}, K	$\Delta T_{coolant}$, K
3	UO_2		HFP	EOL	180.1	13.4	5.2
10a	CONFU-1	FFF	HFP	EOL	188.3	15.3	5.8
10b		UO_2	HFP	EOL	186.7	15.9	5.8
14a	CONFU-E	FFF	HFP	EOL	146.9	13.4	5.2
14b		UO_2	HFP	EOL	169.1	12.8	4.6

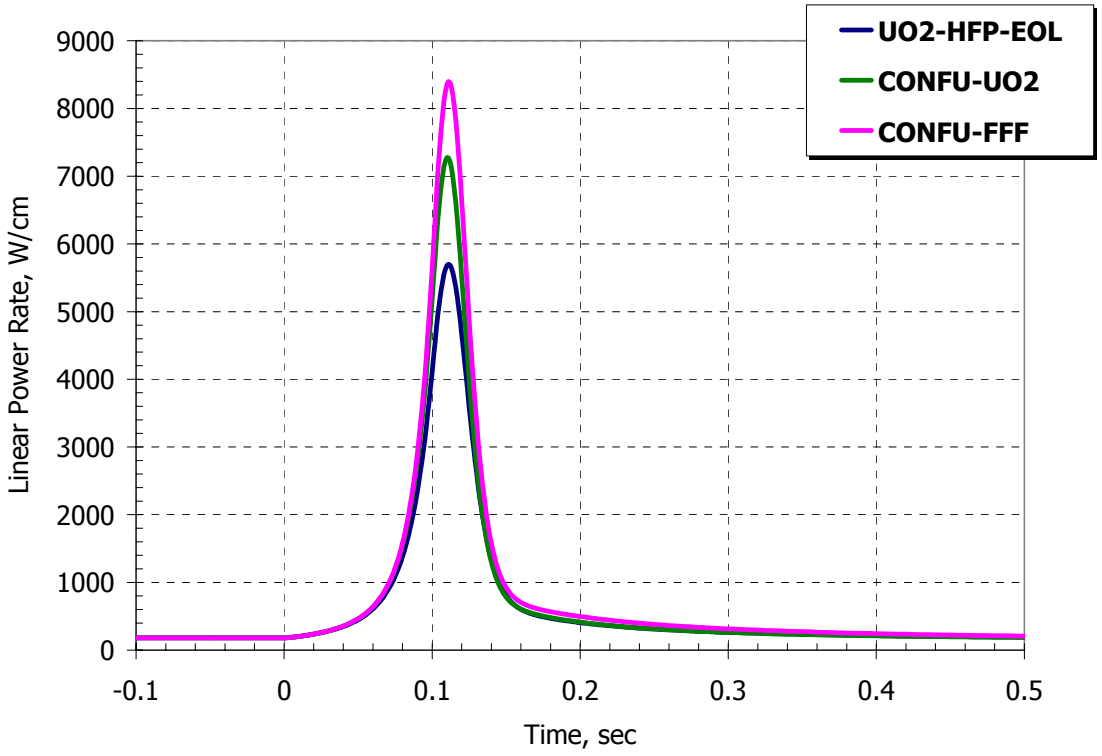

Figure 7.2.7. REA: Linear Power vs. Time, UO_2 – CONFU

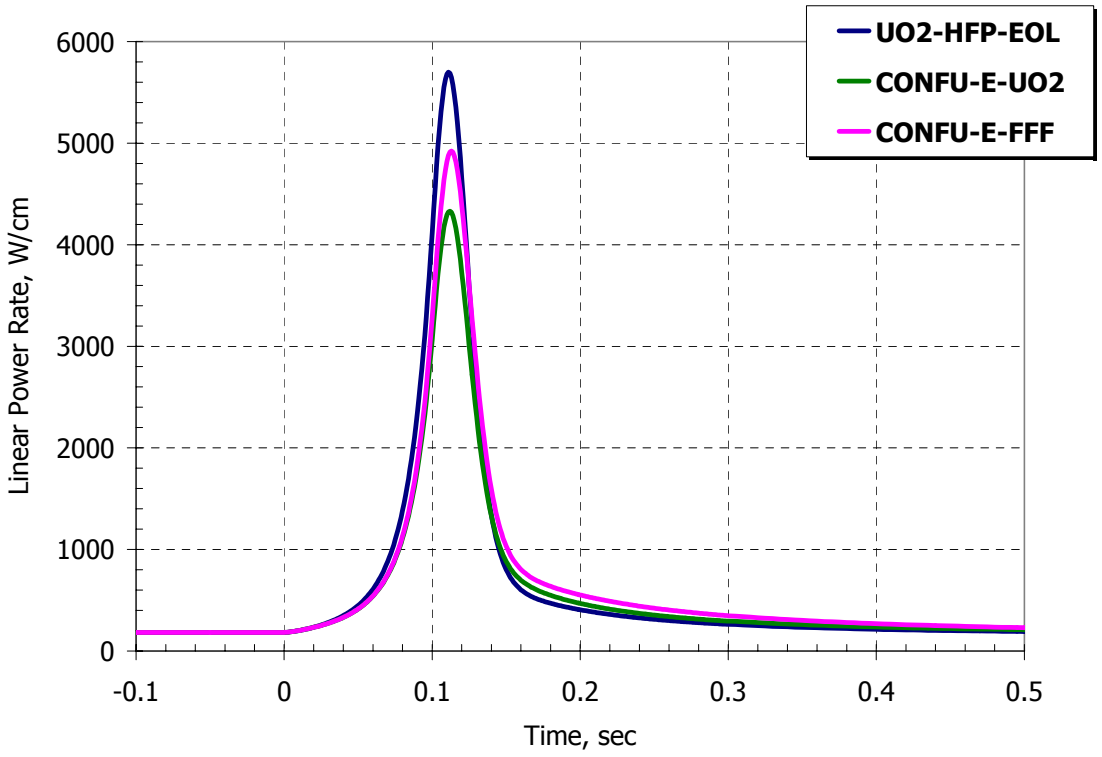

Figure 7.2.8. REA: Linear Power vs. Time, UO_2 – CONFU-E comparison

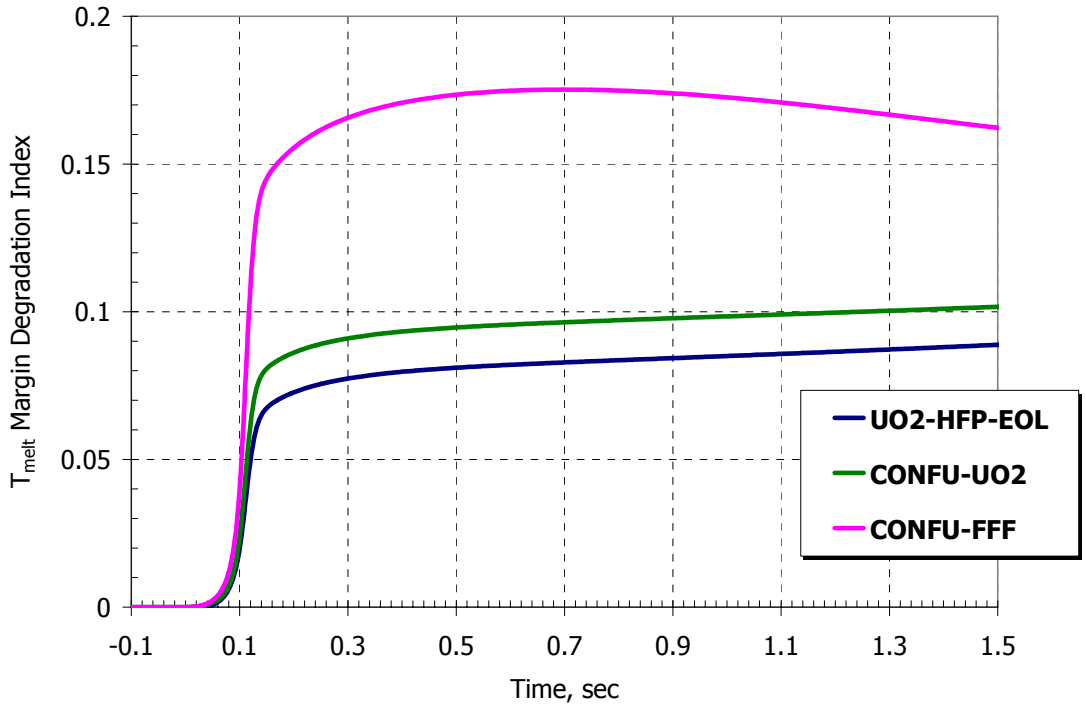

Figure 7.2.9. REA: Fuel melting margin degradation vs. Time, UO_2 – CONFU comparison

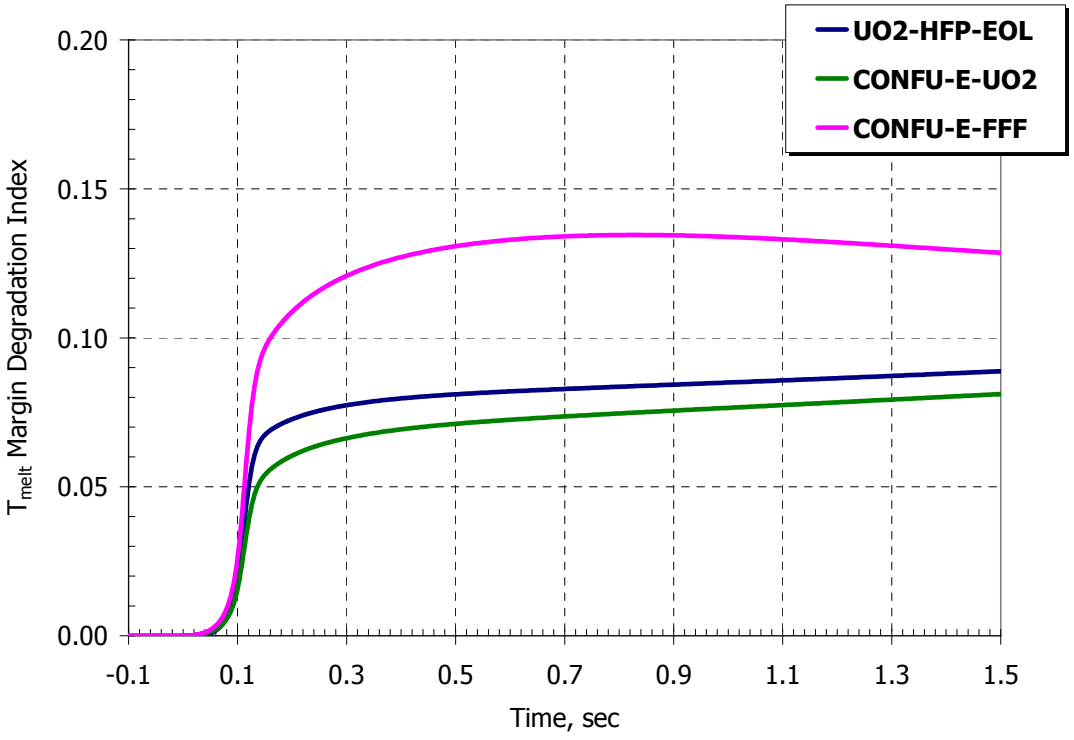

Figure 7.2.10. REA: Fuel melting margin degradation vs. Time, UO_2 – CONFU-E comparison

7.3. Loss of Coolant Accident Consideration

The major difference in the Loss of Coolant accident (LOCA) between UO_2 and FFF rises from the difference in the stored energy and specific heat for the two fuel types. In a typical PWR LOCA, the cladding temperature peaks twice: first, during the coolant blowdown phase of the accident and then during the reflood phase. Figure 7.3.1 depicts typical results of LOCA simulation [Iguchi T., 1998]. The blowdown peak cladding temperature is roughly proportional to the fuel stored energy, while the heat up peak is related to thermal inertia of the fuel.

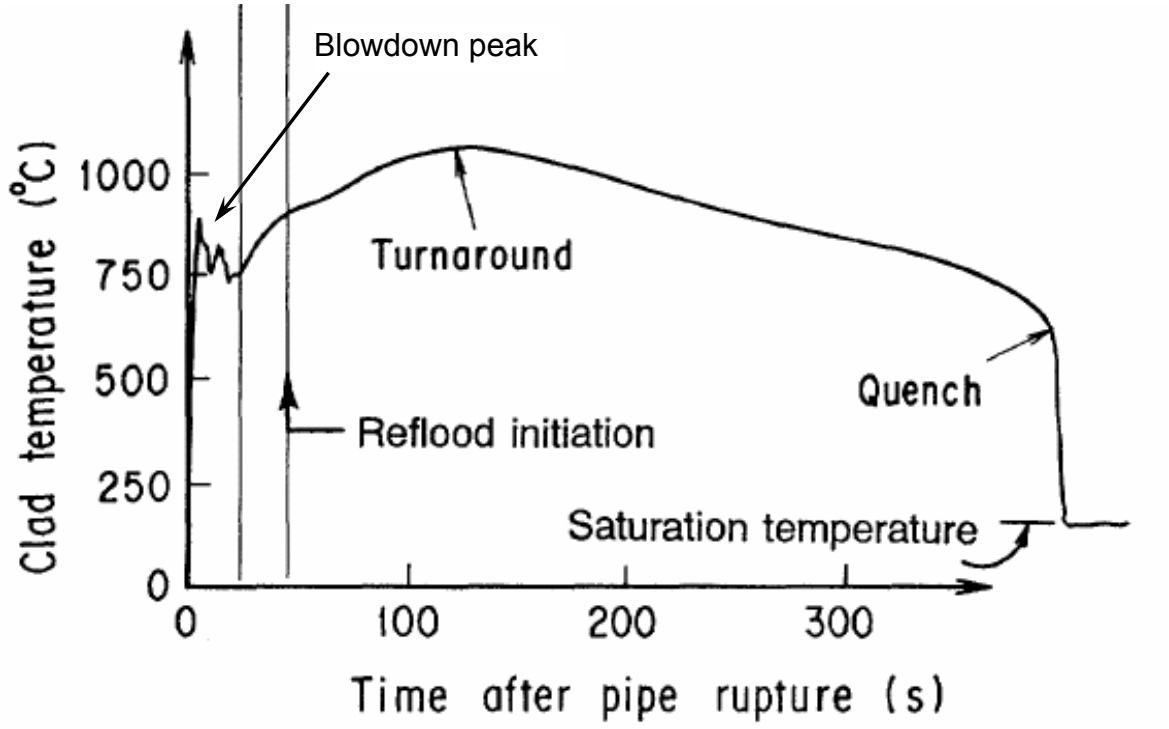

Figure 7.3.1. Example of cladding temperature vs. time during PWR LOCA (adopted from [Iguchi T., 1998])

Table 7.3.I compares the stored energy for FFF and UO_2 fuel at the same power density. The FFF stored energy is somewhat lower (by about 10%) than that of UO_2 fuel. However, the power peaking is typically higher in FFF pins than in UO_2 pins in all UO_2 core by about 5 to 15%. (1.2 in the CONFU assembly vs. about 1.06 in the all-UO_2 assembly) Therefore, the real difference in stored energy FFF pins would also be greater (by about 8% in the case of additional 1.15 power peaking, Table 7.3.I) implying that FFF pins are more limiting than UO_2 pins during blowdown phase in LOCA.

Table 7.3.I. Stored energy comparison

	UO_2	FFF nominal power	FFF 1.15 power peak
Density, g/cm^3	10.4	4.94	4.94
Specific heat, J/g-K	0.31	0.75	0.76
Fuel temperature, K	935	855	905
Stored energy [$\rho \times Cp \times (T_{fuel}-T_{coolant})$], J/cm^3	1122	1011	1209

Overall, the FFF fuel has a larger thermal inertia than UO_2 due to a substantially larger specific heat of the spinel matrix which dominated the Cp value of the dispersed fuel. As a result, the Cp of FFF is fairly sensitive to the volume fraction of the spinel matrix. The Cp value of FFF ranges from about 0.7 J/g-K for 50v/o of spinel to slightly above 1 J/g-K for 70v/o. Re-flood capabilities in the course of LOCA should be comparable for the two fuel types because the same fuel pin and assembly geometry is used for both fuel options. The heat flux to coolant, however, is higher in the CONFU case than in all-UO_2 case, despite identical fuel pin geometry, due to the higher power peaking in the FFF pins in CONFU assembly.

Figure 7.3.2 qualitatively compares the performance of FFF under LOCA conditions with UO_2. It shows the fuel temperature rise, starting from the reactor scram, under adiabatic conditions. Total core cooling capability loss was assumed implying that all the energy generated in the fuel is affecting its temperature increase. The curves presented in Figure 7.3.2 were obtained by integrating the energy conservation equation:

$$T^{fuel}(t) = T_0^{fuel} + \frac{1}{\rho Cp}\int_0^t P(t)dt \qquad (7.3.1)$$

where P(t) is the ANS standard decay power curve for infinite irradiation time [Todreas N.E. and Kazimi M.S., 1990]. A constant Cp was assumed for simplicity.

This simplistic analysis shows that the larger thermal inertia of the FFF results in a lower temperature rise rate and comparable or even favorable LOCA performance of FFF compared to that of the UO_2 despite the lower melting temperature of the FFF. However, as mentioned earlier,

the power peaking is typically higher in FFF pins by up to 15% which may result in higher decay power and therefore earlier fuel melting (Figure 7.3.2).

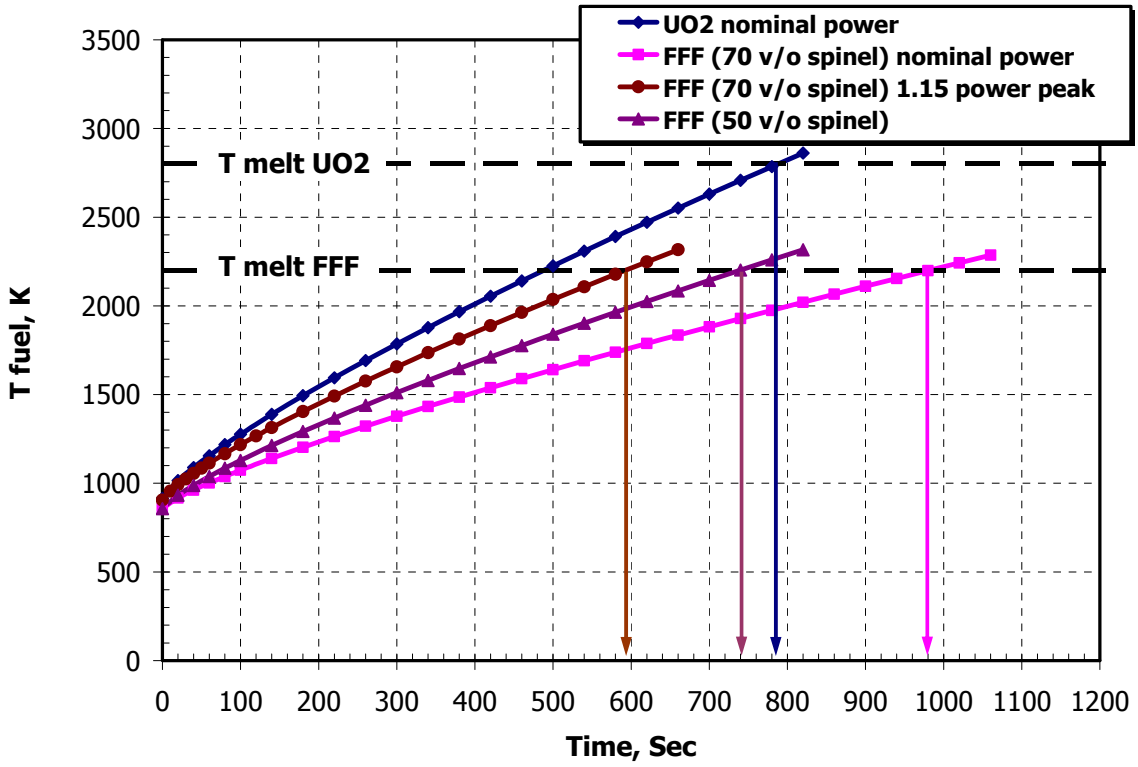

Figure 7.3.2. Fuel temperature raise during LOCA

An additional concern with regards to LOCA applies to the very unlikely event of LOCA without scram accident or very significant local voiding in isolated region of the core. Figure 7.3.3 shows the reactivity of different fuel assembly types in an infinite medium as a function of coolant void fraction. The loading of Pu or TRU was adjusted for each case to provide the fuel cycle length equivalent to 18 calendar months. It can readily be seen that FFF, Th-TRU, and MOX-TRU fuels exhibit positive reactivity feedback when the void fraction in the coolant reaches above 60%. Figure 7.3.3 shows that only the cases where Pu constitutes a considerable fraction of the fuel exhibit positive void reactivity feedback. This is due to two complimentary factors: high Pu loading and small U238 or Th232 fraction.

All Pu isotopes can be fissioned by fast neutrons. Unlike in the thermal spectrum, fast fission cross-sections of all Pu isotopes have about the same order of magnitude. The fission neutrons yield per neutron absorbed (η factor) also increases with increasing incident neutron energy for all

Pu isotopes. Typically, shifting the neutron spectrum to epithermal region will result in a decrease in fuel reactivity due to the resonance absorption. However, additional spectrum hardening for Pu containing fuel will eventually result in a reactivity increase and positive void reactivity feedback. Absorption in Pu240 and Pu242 resonances at about 1 eV region is particularly important because of the large magnitude of these resonances. Th232 and U238, however, have fast fission cross-section thresholds at relatively high energy. Also, the η factor of Th232 and U238 increase only moderately with incident neutron energy. As a result, assembly of finite critical dimensions is impossible if U238 or Th232 constitute a large enough fraction of the fuel. Therefore, the presence of these isotopes in the core mitigates the positive void reactivity effect caused by Pu cross-sections behavior in the fast spectrum.

For the Pu-MOX and Pu-Th cases much smaller fissile fractions are needed for reaching 18 months fuel cycle length than for the cases where MA are also part of the fuel. Higher TRU loading is required because of the additional thermal absorption by MA. In the fast spectrum however (e.g. in the case of significant voiding in the core), MA such as Np237 and Am241 have high fission cross-sections contributing to positive void reactivity feedback. On the other hand, smaller loading of Pu (no MA) implies higher fraction of Th232 or U238 in addition to softer neutron spectrum. Therefore, the positive void feedback effect is not observed in the Pu-MOX and Pu-Th cases.

Consideration of leakage in a finite system, which increases with increasing void fraction and spectrum hardening, does not substantially improve the picture. The leakage from a finite reactor core is roughly proportional to its surface to volume ratio (S/V) and to the average neutron migration length. Assuming a flat with "drooping ends" core power shape the leakage reactivity defect is given by [Driscoll et al., 1990]:

$$\rho_{leakage} = \frac{S}{V} \times \frac{M}{4} \qquad (7.3.2)$$

The reactivity of the fuel assembly for the same set of cases corrected for spectrum dependant leakage in a finite dimension system is shown in Figure 7.3.4.

The CONFU concept does not show a positive void coefficient trend for the range of void fractions up to 100% because of the minimal TRU loading in the core which is possible by utilization of fertile free fuel. The Th-TRU and MOX-TRU cases require much larger TRU

content in the core to compensate for large thermal and resonance absorption of U238 and Th232. Therefore, positive void coefficients are possible in these two cases.

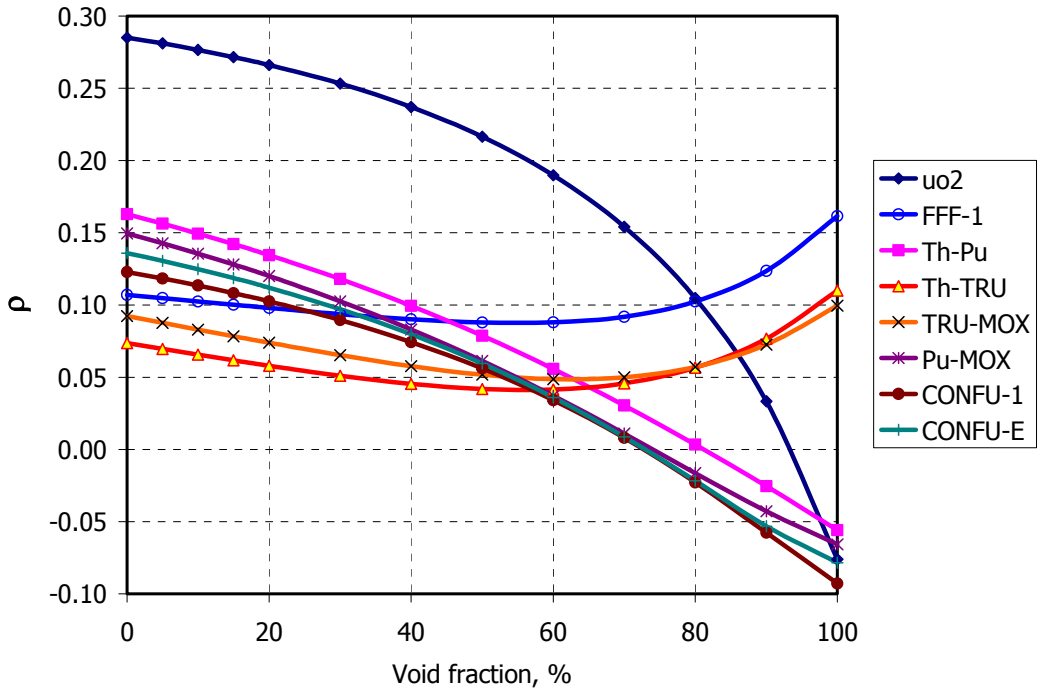

Figure 7.3.3. Unpoisoned fuel reactivity vs. coolant void fraction

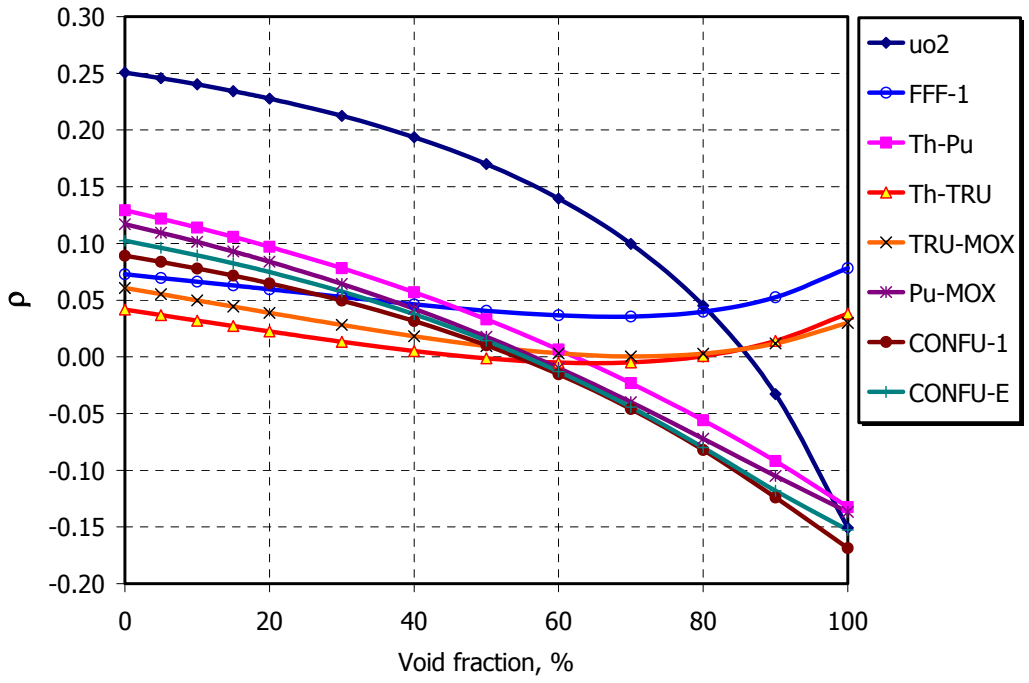

Figure 7.3.4. Unpoisoned fuel reactivity corrected for leakage vs. coolant void fraction

7.4. Chapter Summary

This chapter addressed the issues of inferior neutronic characteristics of TRU containing cores concerning reactivity initiated and loss of coolant accidents.

A computer model for simulation of the dynamic behavior of different fuel types was developed. The model accounts for the differences in the neutronic characteristics of the fuel as well as for its thermal properties. A numerical simulation of control rod ejection accident was performed for a number of cases of interest using this model.

It was concluded that in order to achieve sustainability with regards to TRU generation, the application of the CONFU assembly concept to the PWR fuel cycle results in only minor deviation of fuel performance characteristics in reactivity initiated accidents. This similarity in fuel behavior is a consequence of the fact that the UO_2 fuel dominates the neutronics characteristics of the core. The most efficient TRU destruction potential in FFF matrix in CONFU assembly allows minimization of the amount of TRU in the core and therefore mitigates the effect of TRU presence.

The effect of improved thermal conductivity and higher specific heat of FFF compared to that of UO_2 does not offset the effect of the lower melting temperature of the fertile free matrix. As a result, the FFF pins in the CONFU type fuel assembly exhibit more limiting performance than the reference UO_2 fuel by having greater fuel melting temperature margin degradation during the REA. Therefore, fuel melting is expected at somewhat earlier stages of the transient in the FFF as was experimentally demonstrated in [Nakamura T., et al., 2003].

The macro-heterogeneous CONFU cases were not analyzed because of the limited capabilities of the developed calculation procedure. However, it is expected that macro-heterogeneous CONFU options will exhibit intermediate performance between micro-heterogeneous CONFU cases and fully loaded FFF core under RIA conditions.

High thermal inertia of the FFF indicates comparable or slightly better performance in LOCA than UO_2 fuel with regards to the fuel melting, depending on the local peaking factor of the FFF.

In the case of LOCA without scram, full core FFF has a potential for positive void coefficient at high void fractions. The same effect is possible for Th and MOX based TRU containing fuels because of the higher fissile Pu loading requirement and displacement of fertile U238 and Th232. Similarly to UO_2 fuel, the CONFU-type core exhibit always decreasing reactivity trend with increasing void fraction due to minimal TRU loading.

Chapter 8. Feasibility of TRU Multi-recycling

It has been shown in previous chapters that existing PWR reactors can operate in a sustainable fuel cycle mode with zero net production of TRU, while maintaining the safety and control characteristics of the core comparable to those of the conventional UO_2 fueled PWRs. This chapter addresses several issues related to the out-of-core aspects of the sustainable PWR fuel cycle and discusses the feasibility of TRU multi-recycling from a fuel reprocessing and fabrication perspective.

The first concern relative to closed fuel cycles is associated with the availability of reprocessing technologies that can provide partitioning of TRU and fission products from the spent fuel efficiently to meet the environmental goals of sustainability and be economically viable. In addition, higher levels of radiation due to multi-recycling of TRU introduce an additional level of complexity into fuel reprocessing, handling and fabrication technologies, thus increasing overall costs of the fuel cycle.

In this chapter, a brief overview of the fuel reprocessing technique is presented. Then, the key spent fuel characteristics such as decay heat load as well as γ and spontaneous fission neutron dose rates at the fuel reprocessing and fabrication stages are reported and compared with those of conventional MOX fuel in order to evaluate the feasibility of TRU multi-recycling in PWRs.

8.1. Reprocessing Technologies Overview

Aqueous Reprocessing

Reprocessing of commercial LWR spent fuel is done routinely in many countries around the world on an industrial scale (France, UK, Russia) or ready to be implemented on an industrial scale (India, Japan) [National Research Council, 1996]. Extensive experience exists also in the United States although no commercial fuel reprocessing currently takes place. The reprocessing of spent LWR fuel is done for the purpose of Pu extraction and its subsequent use as MOX fuel in the commercial reactors. The current reprocessing practice also allows a substantial volume reduction of the waste by separation of non-radioactive uranium and conditioning of the remaining high level waste (HLW) into a chemically stable form for permanent geological disposal.

Aqueous and "dry" reprocessing are two conceptually different techniques that are currently being developed for the extraction and recycling of TRU in various transmutation reactor systems. Aqueous processes involve chemical dissolution of spent fuel in inorganic solvent and subsequent use of various extracting agents to selectively extract species of interest. Ion exchange is another technique that allows TRU recovery from the aqueous phase.

All of the suggested aqueous reprocessing methods are based on the PUREX process which is universally employed for the extraction of Pu from the spent fuel. It is a variation of solvent extraction techniques that uses tri-butyl phosphate (TBP) as an organic extracting agent which exhibits the property of extracting actinide cations in odd oxidation states. Pu (as Pu^{+4}) and U (as UO_2^{+2}) are recovered in the PUREX process with industrial yield over 99.9 %.

The standard PUREX process however is not capable of extracting Np, Am, Cm with sufficient yields. Therefore, numerous modifications and additional steps were proposed as an extension to the PUREX process. The most significant challenge in aqueous processes is the separation of Am and Cm from lanthanides (Ln) fission products. The difficulty arises from the fact that Am, Cm and Ln are present in the solution in the same oxidation state (+3) and they have very similar ionic size, therefore, their chemical properties are very similar. Additionally, Ln are present in typical spent LWR fuel in much larger amounts (by more than a factor of 20) than Am and Cm. The actinide/lanthanide (An/Ln) separation can be accomplished in two ways: An-Ln co-extraction (TALSPEAK, DIDPA, TRUEX, TRPO and DIAMEX) with subsequent selective stripping using complexants such as DTPA or by selective extraction of An using extracting agents with high selectivity such as TPTZ or CYANEX-310 [OECD/NEA, 1999].

Am and Cm can be separated by two types of processes. The SESAME process utilizes the fact that Am can exist in solution in oxidation states higher than +3 which is practically impossible for Cm in aqueous medium. The DAIMEX process takes advantage of the difference in partition coefficients of Am and Cm in the DIAMEX solvent which allows extraction of Am, and leaves Cm in the aqueous phase given a sufficient number of separation stages.

Np and long-lived fission products such as Tc99 and I129 can also be recovered by modified PUREX-type processes with yields sufficient enough to meet the sustainable fuel cycle environmental goals [OECD/NEA, 1999].

The vast operating experience and existing industrial capacities make PUREX based separation the most attractive option for TRU recycling in existing LWRs. The Advanced Fuel Cycle Initiative program (AFCI) in the US uses UREX+ as a reference process for actinide and fission products partitioning. UREX+ is also an extension of the conventional aqueous chemistry based PUREX process [DOE/NE, 2003]. The technological maturity status of various aqueous separation technologies is summarized in Table 8.1.I.

Table 8.1.I Maturity status of aqueous separation technologies [OECD/NEA, 1999]

		Feasibility in principle	Engineering feasibility	Industrial scale feasibility
U - Pu separation	PUREX	Achieved industrially		
Np separation	PUREX		☑ (>95% sep.)	☑ (~95% sep.)
	DIDPA		☑	
	HDEHP		☑	
	TRUEX		☑	
Am + Cm separation				
Based on An/Ln co-extractioin				
	TALSPEAK			☑
	DIDPA		☑	
	TRUEX		☑	
	TRPO		☑	
Based on An selective extraction				
	TPTZ	☑		
	Picolinamides	☑		
	CYANEX301	☑		
Based on percipitation				
	Ferricyanide	☑		
Am – Cm separation				
	SESAME		☑	
Tc separation	PUREX	☑ (insoluble Tc)		☑ (soluble Tc)
Tc – Platinum group metals separation				
Denitration precipitation			☑	
Active Carbon adsorption			☑	
I separation	PUREX			☑

The most significant disadvantage of aqueous reprocessing is the degradation of organic extracting agents in radiation fields. In the TRU multi-recycling scenario, the activity and decay heat load per unit volume of the spent fuel steadily increase for the initial recycle stages as will be demonstrated later in this chapter. Major modifications in the existing reprocessing plants will be required to partially overcome this complication. However, new plants are likely to be able to accommodate the design requirements. The required dilution of the actinide stream will lead to additional increases in volume of reactants and in waste volume per unit mass of the reprocessed spent fuel.

It should also be noted that current aqueous reprocessing is based on the element-by-element separation approach which greatly complicates the system. Moreover, separation of potentially weapons usable nuclides at different reprocessing stages raises nuclear proliferation concerns.

Pyrochemical Reprocessing

The most promising concept among non-aqueous separation techniques is pyrochemical reprocessing. [Boullis et al., 2000] The concept is based on the high-temperature separation of actinides reduced to a metal state in molten salt media (usually alkali metal chlorides or fluorides). Typically, the spent fuel elements are dissolved in a molten salt eutectic at temperatures in a range between 500 and 800 °C which is then followed by selective recovery of the elements of interest. The separation of spent fuel constituents can be accomplished by different methods: separation by extraction, electrodeposition, or precipitation. Various types of pyrochemical reprocessing techniques have been actively studied around the world. At the Argonne National Laboratory (ANL), extensive research was carried out as a part of the Integral Fast Reactor (IFR) Program [Chang Y.I., 1989]. RIAR (Russia) is currently developing the technology for reprocessing of fast reactor MOX fuel in conjunction with vibro-packing fuel fabrication techniques [Bychkov A.V. et al, 1997].

The well recognized advantages of the pyrochemical reprocessing are as follows.

- Simplicity and compact size of the reprocessing plant
- Reduced waste stream volumes in comparison with aqueous methods
- As a result, the process is expected to be more economically attractive

- High proliferation resistance because Pu is never separated from the rest of TRU during the process
- The process is completely insensitive to high radiation fields which allow reprocessing of the fuel after short cooling times as well as complete recovery and recycling of materials involved in the process
- The process can be equally applied to different fuel types although an extra reduction to the metallic state step is required for non-metallic fuel forms

Nevertheless, pyrocemical reprocessing is far from being ready for a large scale industrial deployment. Although comparable recovery yields for TRU have been reported for aqueous and pyrochemical methods [Koch, 2000], significant R&D effort must be carried out on pyro-reprocessing techniques for them to achieve an equivalent level of technological maturity as currently exists for the aqueous separation methods.

The two types of separation processes can also be combined to achieve better economic performance and high recovery yields. It was suggested, for example, that uranium be removed from the spent fuel with an aqueous UREX process while the separation of TRU from the FP be done by an electrometallurgical process [Laidler J.J., 2000].

Heterogeneous fuel types such as the CONFU assembly concept offer additional flexibility with respect to the choice of an optimal fuel reprocessing option. In the CONFU concept, the UO_2 fuel pins have standard design and typical PWR fuel burnups. Therefore, their reprocessing can be handled in conventional reprocessing facilities that were not originally designed to operate at high radiation fields. Both aqueous and pyrochemical options can be applied to reprocessing of a standard UO_2 fuel depending on their availability and economic potential.

The reprocessing of spent FFF pins, although more challenging due to the high levels of radiation, can be significantly simplified as it does not require uranium separation from the rest of the actinides. Uranium separation is one of the major steps in the separation process which involves the largest volume of materials. Therefore, avoiding the uranium separation step would potentially allow significant reduction in the reprocessing costs and waste volumes. However, an inert oxide (e.g. ZrO_2) is typically mixed with the fuel and that will require separation.

8.2. TRU Multi-recycling Feasibility Evaluation

Apart from the availability and costs of the TRU separation technologies, the feasibility of a closed sustainable fuel cycle also depends on the complexity of fuel fabrication and handling. The fuel handling and fabrication are likely to require completely remote operation and extensive shielding as the radiation doses from the reprocessed TRU fuel are too high. Consideration of MA as part of the fuel cycle in addition to Pu is expected to increase significantly the levels of radiation from the reprocessed and re-fabricated fuel in comparison with conventional MOX fuel even during the first few recycle stages. In the case of multi-recycling, the very long saturation times for Cm246, Cm248 and Cf252 isotopes (Figure 5.1.6, Chapter 5) will result in continuous increases in the neutron dose rates from spontaneous fissions in these isotopes. Moreover, as mentioned earlier, the increased levels of radiation and heat generation will also complicate the fuel reprocessing causing degradation of organic extractants and increasing the volume of materials involved in the reprocessing as well as the volume of the reprocessing waste stream. The above comment however refers only to the aqueous reprocessing techniques. The impact of high radiation level environments on pyrochemical reprocessing is expected to be minimal.

The total radioactivity, decay power, spontaneous fission (SF) source and dose rates from the reprocessed TRU containing fuel were calculated for different recycle stages to evaluate the effect of changing TRU composition on these fuel characteristics. The comparison of calculated values with the corresponding data of conventional MOX fuel would indicate feasibility and potential limitations of TRU multi-recycling in LWRs.

Assumptions and Methodology

The materials mass flows used in this chapter are obtained from the assembly based neutronic evaluation of the CONFU assembly reported in Chapter 5. The radiotoxicity, decay heat, neutron and γ sources were calculated with the ORIGEN2.2 [ORNL, 2002] computer code. The SF neutron and γ dose rates were calculated with MCNP4C [Briesmeister, 2000] using ANSI/ANS-6.1.1-1977 flux-to-dose conversion factors [Battat M. E., 1977]. The photon energy spectrum for the dose rate calculations was obtained from ORIGEN2.2. Spontaneous fission neutron energy spectra were constructed from Watt spectrum parameters for individual nuclides provided in Appendix H of the MCNP4C users manual [Briesmeister, 2000]. For the isotopes for

which no SF energy spectrum data was available, the data for the next closest isotope of the same element was used.

The SF neutrons and γ dose rates were evaluated at the surface of an FFF pellet and at 1 m distance from the clad FFF pin. These two configurations were chosen for the analysis because the fuel pellet and the fuel pin represent two basic manufacturing units that must be handled in the fuel fabrication process. The medium surrounding a fuel pin was assumed to be dry air at atmospheric pressure.

The (α,n) reaction neutron source was not considered in the dose rate calculations because no data regarding its energy spectrum was available. In addition, the (α,n) reaction neutrons have very small contribution to the total neutron source (typically less than 2%). Instead, the (α,n) neutron source was added to the SF source value which was then used for the MCNP dose rate calculations. Considering (α,n) neutrons as SF neutrons is a conservative assumption because (α,n) reaction neutrons typically have a softer spectrum than SF neutrons and therefore lower biological quality factors.

Results and Discussion

The environmental hazard characteristics of the fuel materials circulating in the sustainable fuel cycle based on the CONFU concept are summarized in Table 8.2.I and Figures 8.2.1 - 8.2.4. All values in the Table 8.2.I and in Figures 8.2.1 - 8.2.4 are normalized per unit cycle energy (in GWe Years) The CONFU fuel cycle environmental hazard characteristics were calculated at two time points between the recycles: at 5 years after discharge (fuel reprocessing) and at 7 years after discharge (new fuel fabrication). Only the actinide contributions to the fuel characteristics were considered. Thus, the effects of the fission products are ignored here. As can be observed from Table 8.2.I and Figures 8.2.1 - 8.2.4, the activity, decay heat load and radiotoxicity of the materials within the fuel cycle are converging to equilibrium values after 3 to 5 recycles. The SF source is the only parameter that does not converge within the 5 cycles analyzed. As mentioned above, the SF source is one of the factors that limit the number of successive TRU recycles.

Table 8.2.I. CONFU Assembly: Environmental Hazard Characteristics of the Actinides at the Time of Separation and Fabrication. (Normalized per 1 GWeYear)

		Recycle Stage				
		1	2	3	4	5
Separation Stage, 5 years after discharge	HM mass flow, kg	15018	17560	18197	18320	18436
	Radioactivity, Ci	7.73E+06	9.71E+06	9.97E+06	9.90E+06	9.86E+06
	Thermal Power, W	5.99E+04	1.04E+05	1.26E+05	1.37E+05	1.44E+05
	Ingestion Radiotoxicity, Sv	1.09E+10	1.75E+10	2.00E+10	2.08E+10	2.11E+10
	Total Neutron Source, #/sec	1.31E+11	3.45E+11	8.11E+11	1.77E+12	3.25E+12
Fabrication Stage, 7 years after discharge	TRU mass flow, kg	495	629	665	676	686
	Radioactivity, Ci	7.06E+06	8.89E+06	9.14E+06	9.08E+06	9.05E+06
	Thermal Power, W	5.61E+04	9.73E+04	1.18E+05	1.28E+05	1.34E+05
	Ingestion Radiotoxicity, Sv	1.03E+10	1.64E+10	1.88E+10	1.95E+10	1.98E+10
	Total Neutron Source, #/sec	1.20E+11	2.92E+11	6.02E+11	1.20E+12	2.10E+12

Figures 8.2.5 and 8.2.6 show the effect of longer cooling time between recycles at the fuel fabrication stage on SF source and the decay heat load respectively. The values of the first-time-reprocessed UO_2 fuel and once recycled as MOX are also shown for comparison purposes. The SF source and decay heat load from TRU in irradiated UO_2 and MOX fuel were evaluated at 10 years after discharge.

Increasing the cooling time from 7 to 20 years substantially reduces the SF problem which can potentially increase the number of practically feasible recycles and reduce the cost of fuel reprocessing and handling. The SF source after 5 recycles is about twice that of the once reprocessed MOX fuel. The effect of cooling time on the TRU heat generation is also significant. The heat source from 20 years cooled TRU saturates after fewer recycle stages and at about 50% lower level than TRU recycled after 7 years of decay. The level of equilibrium 20 years cooled TRU heat load is only about 20% higher than first time reprocessed MOX after 10 years of cooling. The value of the SF source for the 5^{th} recycle and 20 years cooling time of the CONFU fuel corresponds to 12.8×10^6 n/s per kg of HM in the fuel assembly or 391×10^6 n/s per kg of HM in the FFF pins. Both values are substantially lower than those reported for ADS TRU burners (670×10^6 n/s-kgHM) or ADS MA burners (1992×10^6 n/s-kgHM) [OECD/NEA, 2002a].

Figures 8.2.7 and 8.2.8 show the SF neutrons, γ, and total dose rates at the FFF pellet surface and at 1 meter from the clad fuel pin respectively. The approximate values of the γ radiation dose rates at the fuel pellet surface for conventional MOX fuel are represented by the shaded band on Figure 8.2.7. The values for MOX fuel are both calculated and obtained from references ([Bairiot H. et al., 1989], [Taiwo T. A. et al., 2002]). The wide range of the MOX values is due to differences in Pu loading, Pu isotopic composition, and the time since Am separation.

During the first few early recycle stages, the dose rate from the fuel is dominated by the photon component. Only after 18-20 recycles, the photon and SF neutron doses become comparable. The initial photon dose rate is significantly higher (by a factor of 5 to 10) than that of the first time recycled typical MOX fuel. However, relatively simple shielding such as a few mm thick lead wall can significantly reduce the γ-photon dose rate to acceptable levels. Additionally, the photon dose rate increases substantially between the first and the 3rd recycle stages as a result of rapidly increasing concentrations of Pu238, Am241, and Cm243 and 244 (Figures 5.1.6 – 5.1.8, Chapter 5) with relatively short half lives and high energy γ-photons associated with their decay. The slight decrease in the γ-photon dose rate after the 3rd recycle stage is again due to the slow decrease in the concentrations of the same isotopes. The γ dose rate becomes practically constant from about the 5th recycle and beyond. The moderate increase in the γ dose rate between 5th and 20th recycle is due to the slow buildup of Cm isotopes which do not increase the γ source but slightly harden the γ-photon spectrum as illustrated in Figure 8.2.9. Otherwise, the γ-photon spectrum remains practically unchanged with the number of TRU recycles.

The SF neutron dose rate increases monotonically with the number of recycles in the range up to 20 recycles (Figure 8.2.7 – 8.2.8). Initially, the Cm244 isotope is the major contributor to the neutron dose as illustrated in Figure 8.2.10. The contribution of Cf252 to the neutron dose becomes comparable to that of Cm244 only after about 10 recycles. After 20 recycle stages, Cf252 dominates the SF source and therefore the neutron dose rate from the fuel. Note that in this analysis, 20 years cooling time between recycles was assumed as was suggested by the results presented in Figures 8.2.5 and 8.2.6. If 20 years cooling time between recycles is adopted, the dose from SF neutrons is less of an issue for at least the first 10 TRU recycles. At the 10th recycle stage, the neutron dose rate becomes comparable to the 1st recycle stage γ dose rate. If γ doses at the first three recycle stages can be managed by the fuel fabrication facilities, the additional relatively small neutron dose contribution is likely to be possible to tolerate with simple shielding arrangements and therefore moderate increase in fuel fabrication cost.

An dditional matter of concern is the production of He gas in the fuel pins containing TRU as pointed out in [Taiwo T. A. et al., 2002]. The presence of relatively short lived isotopes Am241, Cm242,244, Pu238 that decay through emission of an α particle results in buildup and partial release of He gas to the fuel free volume. Increased gas pressure inside the pin may significantly affect the fuel performance especially under accident conditions.

Taiwo T. A. et al. [2002] report however, that He generation in the CORAIL fuel (TRU-MOX type) constitutes a relatively small addition (up to 20%) to the typical fission gas production and therefore is expected to have limited overall effect.

For the fertile free fuel types, the important issue of fission gas retention is largely uncertain and it is currently being actively investigated. Thus, the particular problem of additional gas generation within the fuel due to TRU α decay should be carefully addressed in these studies.

8.3. Chapter Summary

In this chapter, the feasibility of a sustainable PWR fuel cycle was evaluated with respect to the ex-core aspects of the cycle. A brief review of the fuel reprocessing options is presented with the main focus on two reprocessing techniques: aqueous, based on a conventional PUREX solvent extraction process, and non-aqueous pyrochemical reprocessing.

Generally, aqueous processes have a relatively higher level of technology maturity than the pyrochemical processes. However, the high sensitivity of organic extractants to radiation and TRU decay heat makes aqueous reprocessing less attractive in a multi-recycle mode.

The elevated radiation field is not an issue of concern for the non-aqueous reprocessing. It can be implemented economically on a relatively small scale which can eliminate the need for spent fuel transportation over long distances. Moreover, simultaneous Pu and MA extraction enhances proliferation resistance of the cycle.

The two types of reprocessing can be combined to achieve better economic performance. The heterogeneous structure of the CONFU assembly concept can provide additional flexibility in choice of the TRU separation option. For example, UO_2 pins can be treated by a conventional

PUREX type process while FFF pins, where the main bulk of the assembly TRU is concentrated, can be processed by the advanced pyrochemical techniques. Furthermore, the uranium separation step is not required for the FFF pins which can potentially reduce the reprocessing costs. However, a reduction of TRU oxides to a metallic state and chemical separation of TRU from the inert matrix are required additional steps for pyroprocessing of FFF.

The radiation and TRU decay heat power is likely to limit the practically feasible number of TRU recycle stages in the sustainable CONFU based fuel cycle. Therefore, the decay heat load, SF source and radiation dose rates were evaluated for different numbers of recycle stages and compared with corresponding data of the conventional 1st generation MOX fuel.

The results demonstrate that the heat load and total radioactivity of the spent fuel saturates within 3 to 5 recycles at a constant equilibrium value which is up to a factor of 2 higher than the corresponding values after the 1st recycle. The SF source, however, monotonically increases due to slow buildup of the Cm and Cf isotopes.

Increasing the cooling down period between the fuel discharge and its reprocessing from 7 to 20 years may substantially mitigate the SF source growth problem. The value of SF source for the 5 times recycled TRU in the CONFU assembly with 20 years cooling time is comparable to that of conventional MOX fuel. The increased cooling time also results in saturation of the decay power at significantly lower level which is also comparable to the typical MOX value and implies the potential feasibility of conventional aqueous reprocessing.

The evaluation of radiation dose rates revealed that the photon dose dominates the total dose rate for the first 10 recycle stages if a 20 year cooling period is adopted. The photon dose rate saturates at a constant level which is about a factor of 2 higher than that of the TRU fuel after the 1st recycle. The radiation dose values obtained are such that relatively simple shielding arrangements can be implemented to reduce the dose rates to the safe levels without substantial increase in the cost of fuel handling and fabrication facilities. The dose from SF neutrons however, increases monotonically with the number of recycle stages, and it reaches the equivalent photon dose rate level only after about 20 recycles. It was concluded therefore that at least 10 TRU recycles are possible with only minor changes in fuel handling and fabrication procedures.

The reprocessing and fabrication of the CONFU fuel after more than 20 recycles with equilibrium TRU composition are likely to require completely remote operation. The pyrochemical reprocessing and vibro-packing fuel fabrication techniques as suggested in [Bychkov et al., 1997] are potential candidates for the fuel treatment at these advanced stages of the sustainable fuel cycle.

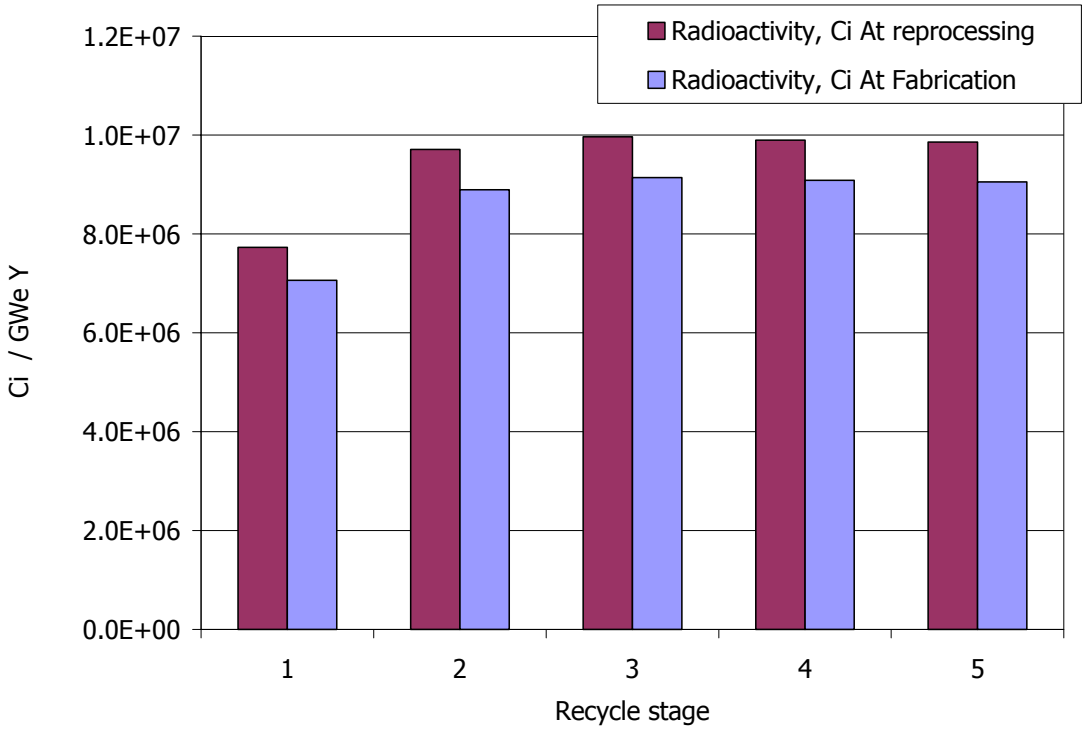

Figure 8.2.1. Radioactivity of the CONFU Fuel Assembly

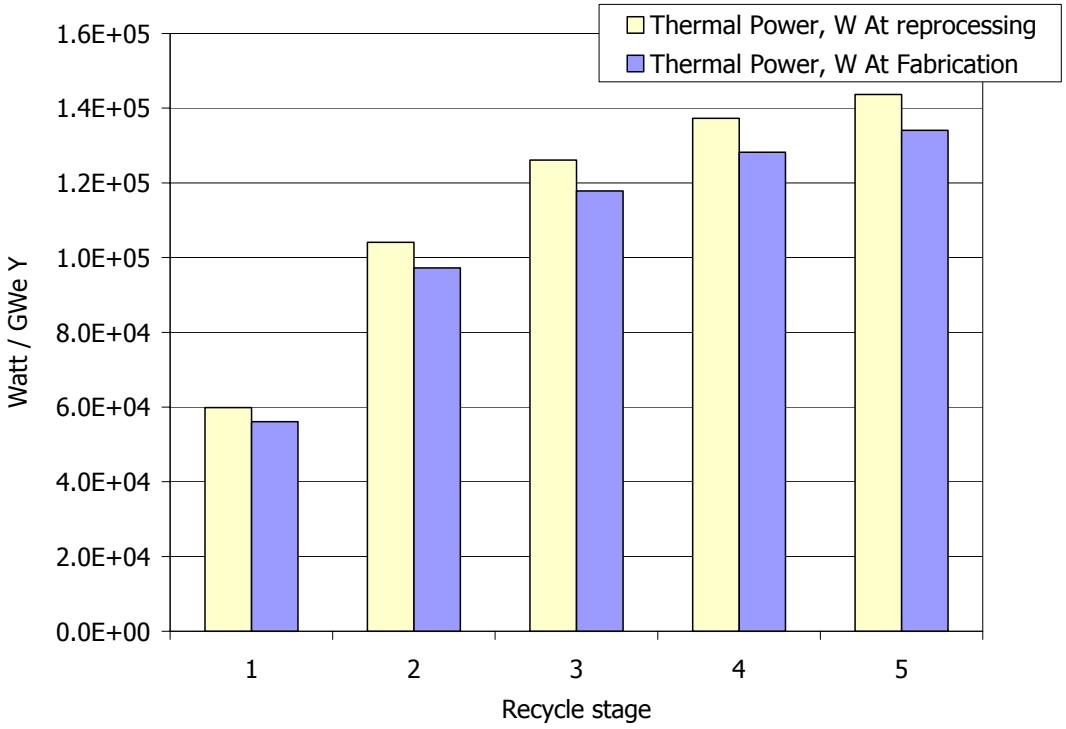

Figure 8.2.2. Decay Heat Generation of the CONFU Fuel Assembly

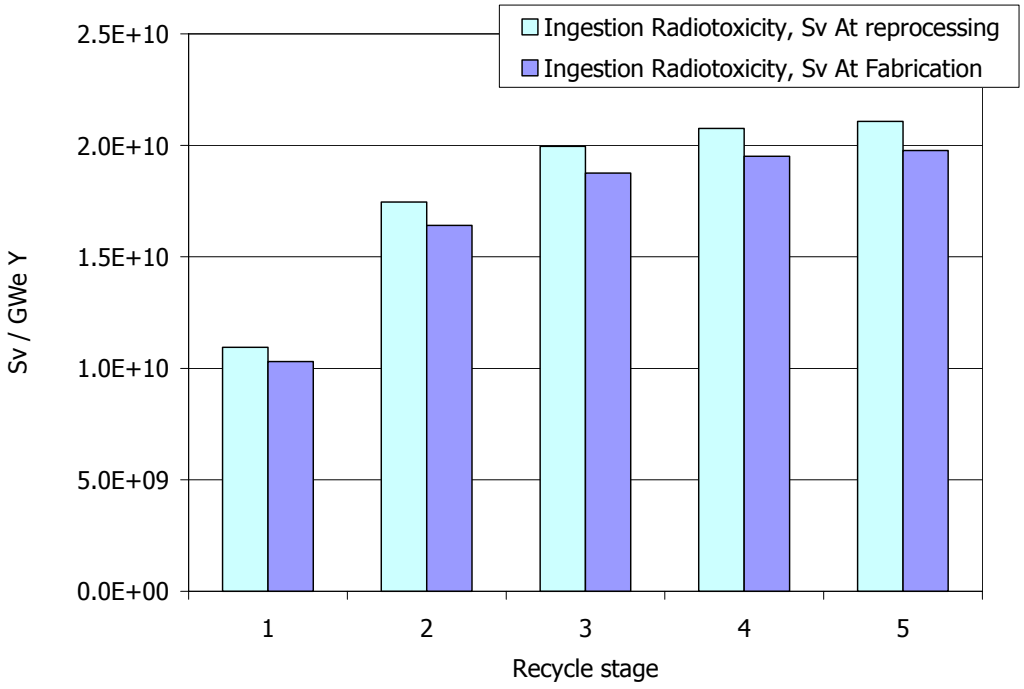

Figure 8.2.3. Ingestion Radiotoxicity of the CONFU Fuel Assembly

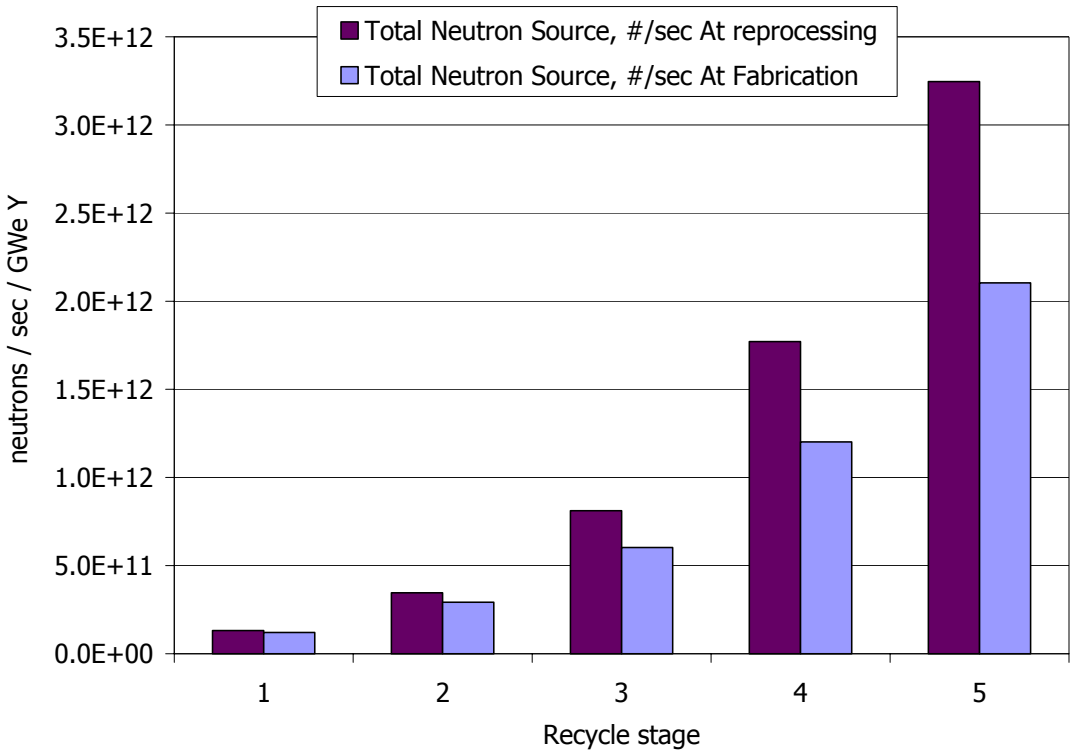

Figure 8.2.4. Total SF and (α,n) Neutron Source of the CONFU Fuel Assembly

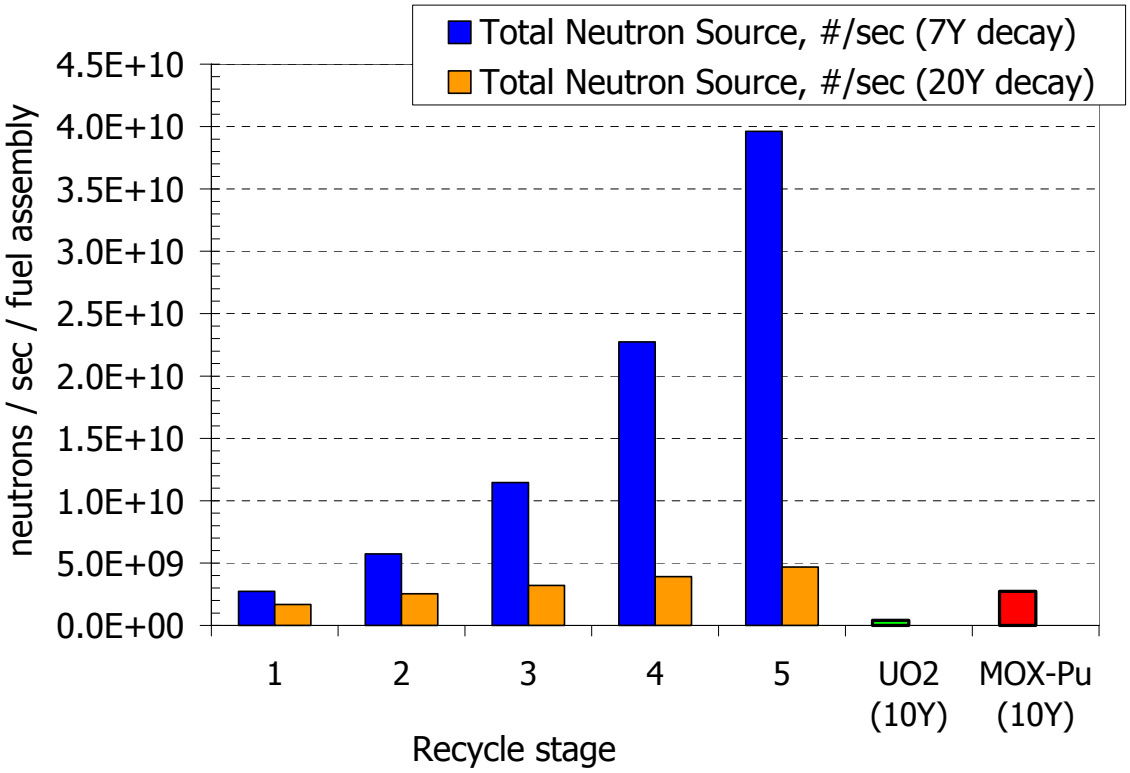

Figure 8.2.5 SFS per fuel assembly: 7y vs. 20y decay comparison

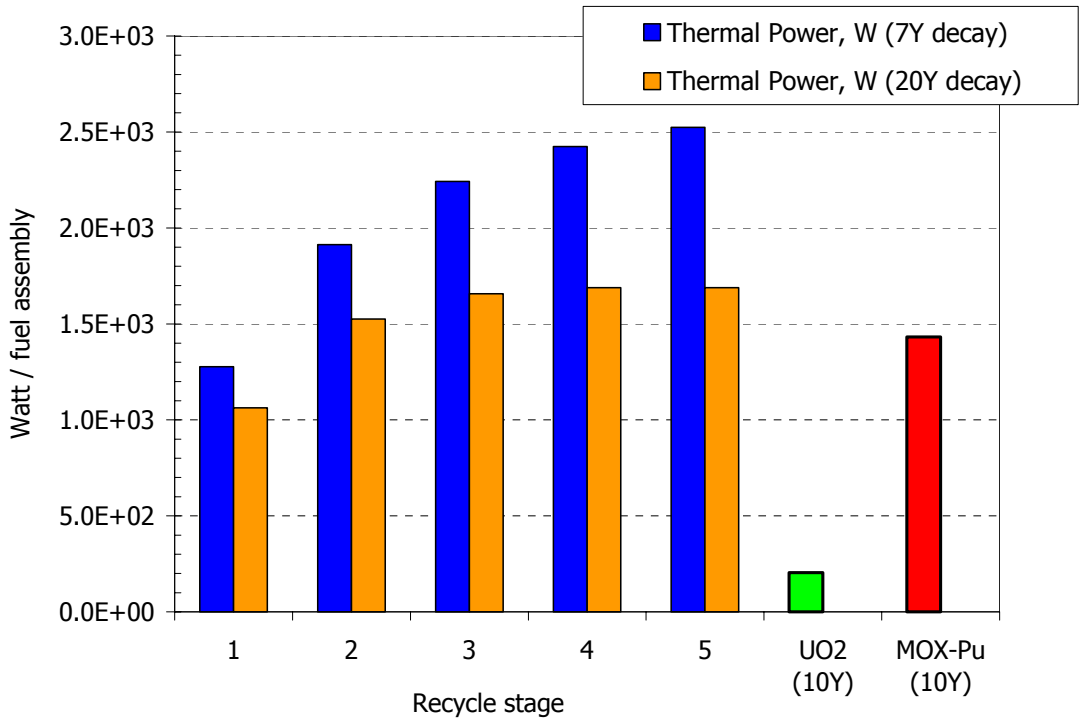

Figure 8.2.6 Heat load per fuel assembly: 7y vs. 20y decay comparison

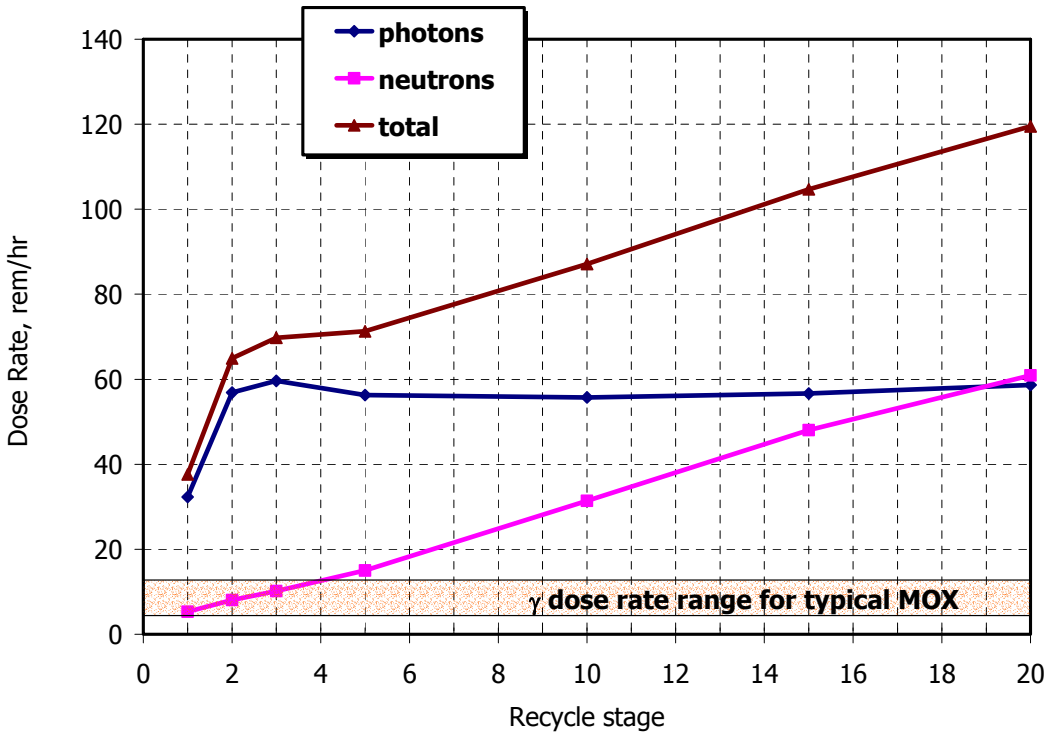

Figure 8.2.7. Dose rates at fuel pellet surface

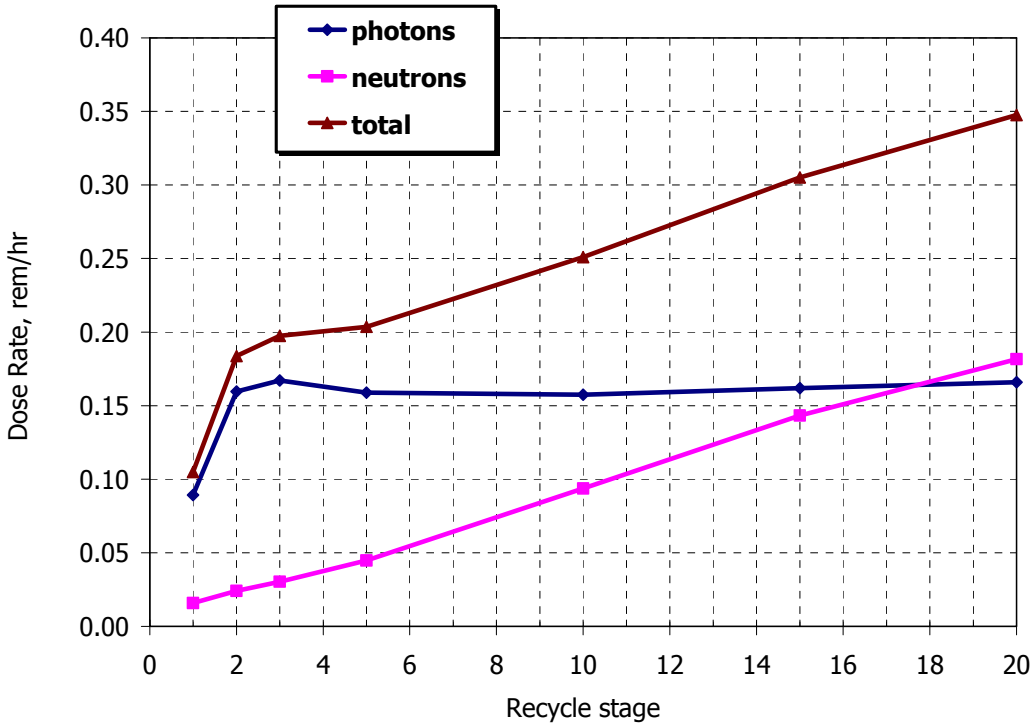

Figure 8.2.8. Dose rates at 1 m from the fuel cladding surface

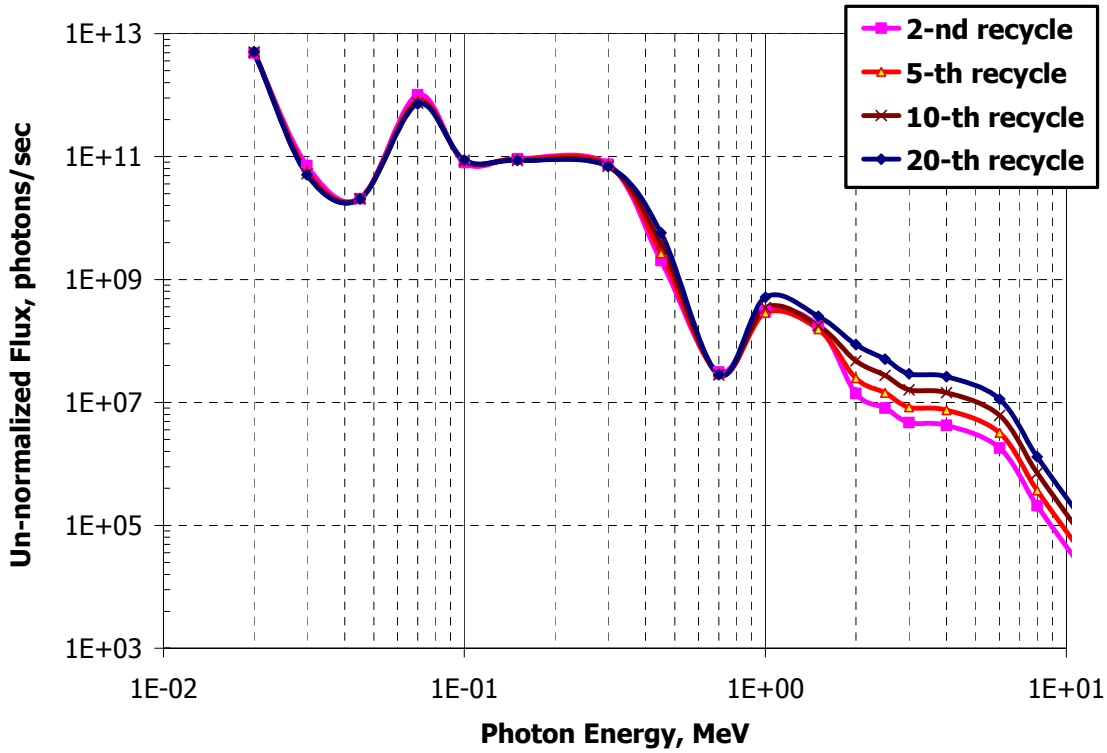

Figure 8.2.9. Photon energy spectra

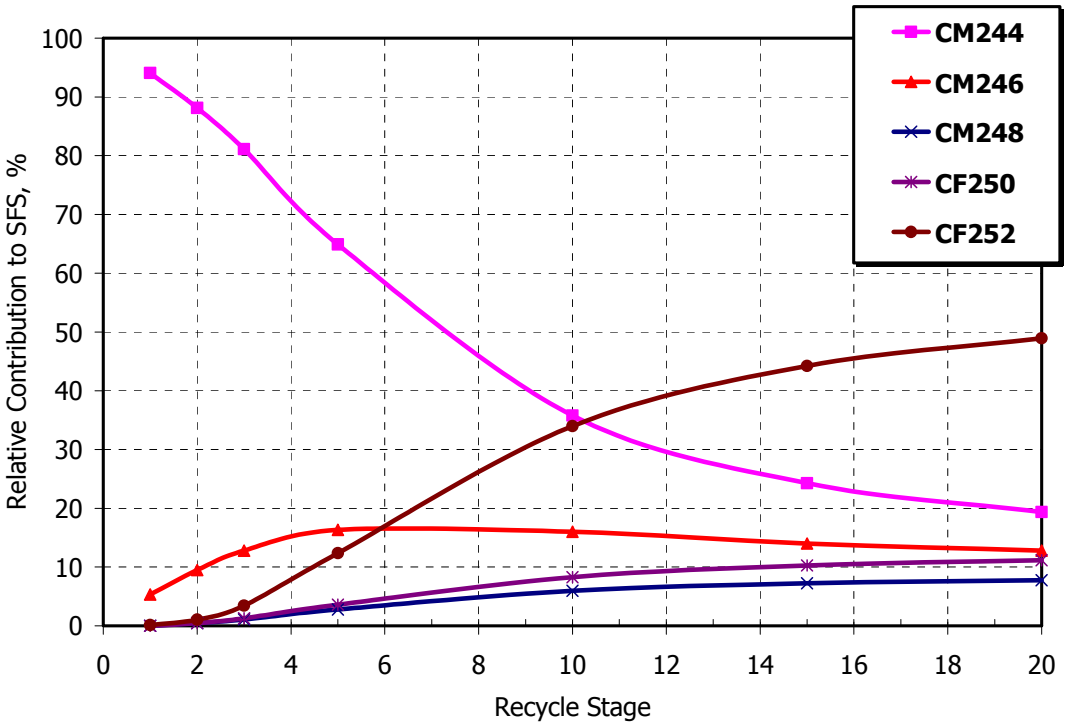

Figure 8.2.10. Major contributors to SF source

Chapter 9. Sustainable Fuel Cycle: Economics Assessment

Economic viability is crucial for any technological innovation. Therefore, the objective of reducing or eliminating the nuclear waste burden cannot be achieved unless the solution is cost competitive with the existing alternatives. Many of the proposed nuclear waste transmutation systems and their associated fuel cycles rely on innovative technologies whose economic performance is largely uncertain.

Since LWRs are likely to remain dominant in the global energy market for at least the next few decades, development of LWR spent fuel reprocessing technologies would be required regardless of the particular waste transmutation scenario. Therefore, any sustainable fuel cycle option would equally benefit from technical improvements and cost reduction of LWR spent fuel reprocessing.

The reprocessing of the TRU burner fuel is also a common challenge for all proposed transmutation concepts, since it is impractical to achieve in one transmutation path TRU burnup high enough to satisfy the environmental goal of radiotoxicity level below the original natural uranium ore level in less than 1000 years.

A major difference among the various transmutation systems comes from their economic performance. As a result, utilization of proven LWR technology, particularly with already installed capacity, will provide maximum economic certainty and benefit as a transmutation option. The LWR is a proven technology and is the least expensive nuclear plant to build and to operate today. Moreover, the advanced dedicated transmutation systems would require large initial capital investment. In that respect, transition of the existing LWR plants to the sustainable CONFU based fuel cycle might be even more economically attractive because many of the existing nuclear plants have already paid off their initial capital investments.

It is important to note, however, that the current market prices of natural uranium and uranium enrichment do not justify spent fuel reprocessing for the purposes of improved natural resources utilization. The closed fuel cycle therefore is mainly viewed as an alternative to direct geological disposal of the spent fuel which allows better management of the radioactive materials instead of leaving the nuclear waste in a repository to future generations with all the associated uncertainties. Although the transmutation of nuclear waste is a more responsible option for the

society than direct geological disposal, it can only be implemented if these two options are economically competitive.

In this chapter, a simplified economic analysis of the sustainable PWR fuel cycle is presented. The fuel cycle and total electricity costs are calculated for the conventional once-through fuel cycle and compared with those of the alternative sustainable PWR cycle based on the CONFU assembly concept as well as with the sustainable 1-tier fuel cycle based on an advanced fast spectrum TRU burning system [Romano A., 2003]. A single tier fuel cycle scheme assumes that all TRUs from the once through LWR fuel cycle are directed to a single type critical reactor where TRU are burned and recycled. Such a fuel cycle scheme was found to be the most economically attractive among other considered alternatives according to the results of a recent OECD waste transmutation study [OECD/NEA, 2002a].

9.1. Analysis Assumptions and Methodology

The fuel cycle steps considered for the three fuel cycle options mentioned above are schematically presented in Figures 9.1.1 through 9.1.3 respectively.

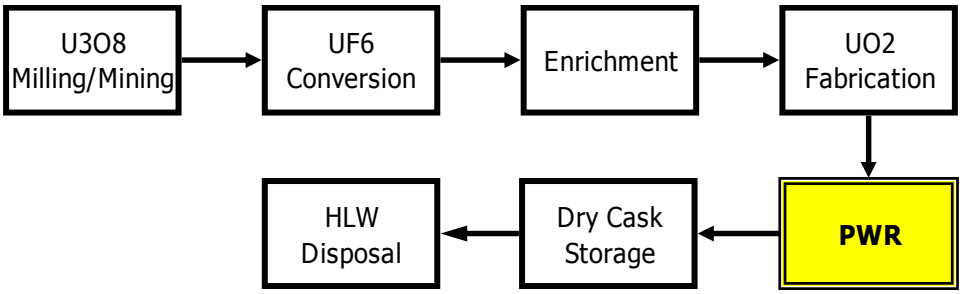

Figure 9.1.1. Once-through fuel cycle flowchart

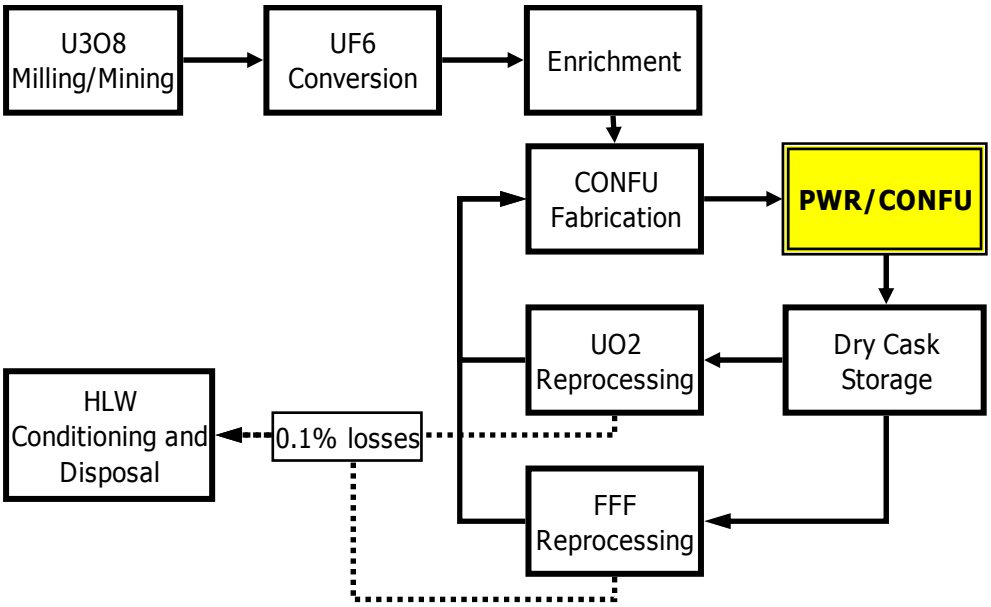

Figure 9.1.2. Sustainable CONFU assembly PWR based fuel cycle flowchart

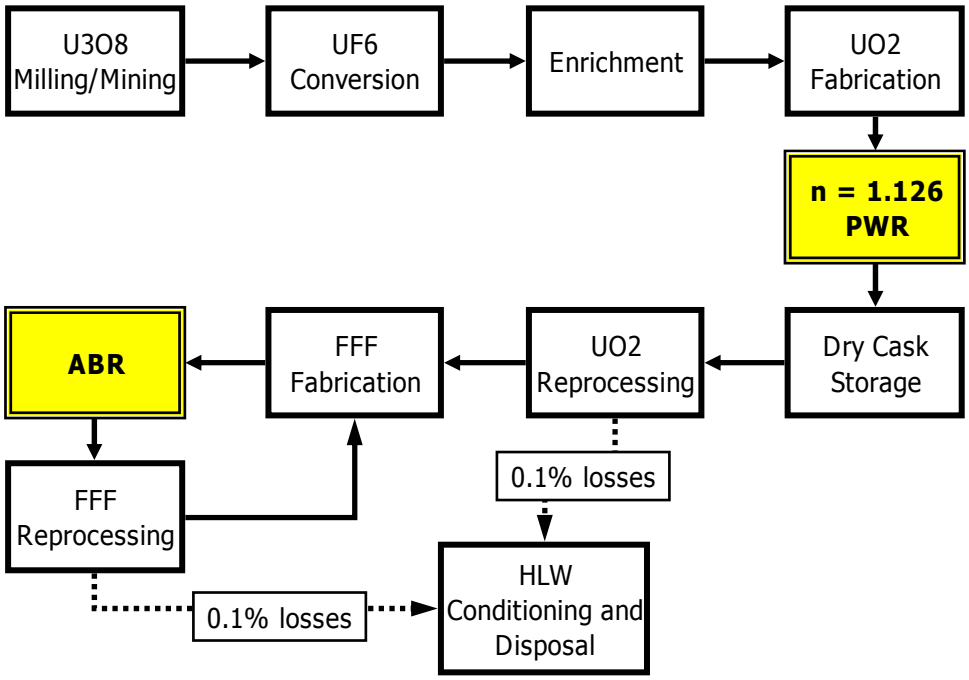

Figure 9.1.3. Sustainable PWR – advanced Actinide Burner Reactor (ABR) fuel cycle flowchart [Romano A., 2003].

The unit costs for the considered fuel cycle steps were primarily adopted from a comprehensive transmutation systems assessment by the OECD [OECD/NEA, 2002a]. The unit costs and time schedule for each fuel cycle step considered are summarized in Table 9.1.I. The waste disposal charges were calculated on the basis of 1 mill/kWh which is the current practice in the United States. The 1 mill/kW-h waste disposal fee was uniformly applied to the once through UO_2 fuel cycle. The 1 mill/kW-h value corresponds to about 412 $/kgHM for the current fuel burnup of 50 MWd/kgHM. The waste disposal charges vary significantly from country to country depending on the local conditions and repository size and may range between 200 to over 1000 $/kgHM [OECD/NEA, 2002a], [Bunn M. et al., 2003].

For the closed fuel cycles, 0.18 mills/kWh HLW conditioning and disposal costs were estimated by the OECD study [OECD/NEA, 2002a]. This includes the cost of vitrification and storage of short lived fission products. The 0.18 mills/kWh value assumes that constant amount of short lived fission products is produced per unit energy.

The cost of dry cask spent fuel storage was calculated on the basis of $1.2 M cost of a single cask that holds 24 standard PWR fuel assemblies which translates to about 100 $/kgHM. This value is consistent with a recent interim storage of spent nuclear fuel assessment by Bunn *et al.* [2001]. Since the design of a dry cask is driven by the decay power generated in the spent fuel and because the FFF contains considerably smaller quantities of HM than conventional UO_2 fuel, it is more logical to assume the dry cask storage cost in $ per unit decay heat load which is roughly proportional to the fission products inventory. In fuel assemblies which produced the same amount of energy, the fission product inventory will be similar. The discrepancy may arise from the difference in fission product yields for different actinides.

The fission product inventory is not directly proportional to fuel burnup because some of the fission products saturate during fuel irradiation. The effects of fuel burnup on the decay heat after discharge is discussed by Xu Zh. [2003]. It was shown, however, that in the period between 3 and 5 years after discharge, when a dry cask loading is expected to takes place, the decay heat power of UO_2 fuel is roughly proportional to its burnup (Figure 9.1.4). Although relative deviation from proportionality between burnup and decay heat increases with time between about 5 and 30 years after discharge, the absolute magnitude of the decay power decreases more rapidly.

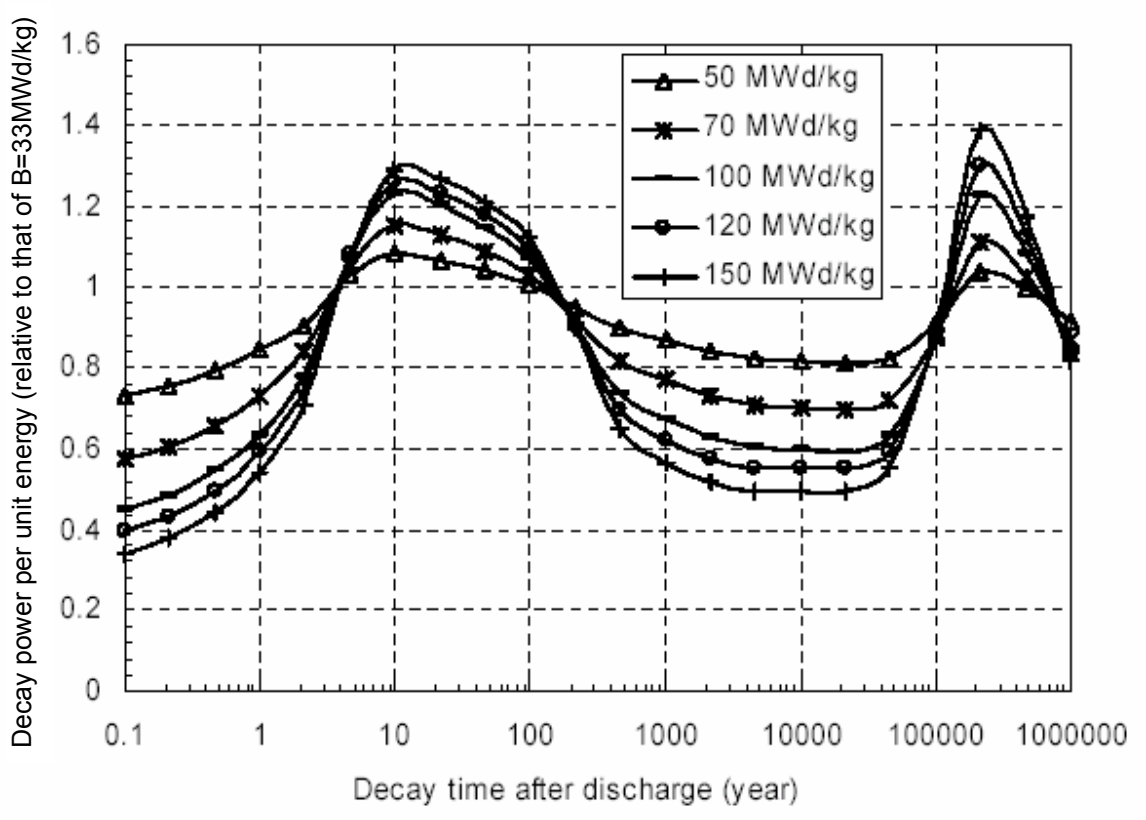

Figure 9.1.4. Relative magnitude of UO_2 fuel decay power per GWe-Year after discharge from [Xu Zh., 2003].

Additionally, the energy generated during the cycle per unit fuel volume for all fuel types considered in this study is similar (the equivalent 18 month fuel cycle length was an initial constraint of the analysis). Therefore, the FP concentrations should be comparable for all fuel cycle options and the assumption of decay heat proportionality to the total energy produced by the fuel should not introduce significant error into the final fuel cycle cost calculation results. Consequently, the dry cask storage charges were calculated in the units of $ per energy generated by the fuel based on the reference UO_2 fuel burnup of 50 MWd/kgHM (Table 9.1.I).

The expenses associated with dry cask storage were assumed to occur at fuel discharge. The situation is likely if the reactors' on-site storage pool capacity is reached. In this case, for each assembly discharged from the reactor to the storage pool, one assembly must be moved from the pool to the dry cask. The expenses associated with interim storage of spent ABR fuel were neglected.

In the fuel cycle scenario which combines a standard PWR operating in a once-through UO_2 fuel cycle mode and an advanced fast spectrum actinide burner reactor (ABR), the installed capacity of ABR is enough to consume TRU at a rate which corresponds to TRU production rate of about 1.12 PWRs [Romano A., 2003]. Namely, the sustainable fuel cycle with zero net TRU generation can be maintained for the 1 ABR + 1.12 PWRs system.

The unit cost of spent UO_2 fuel reprocessing was based on reported contract prices of the existing reprocessing plants and assumptions made in [National Research Council, 1996] and [OECD/NEA, 2001]. The reprocessing costs on the order of 800 $/kgHM were estimated for the government owned reprocessing plant with annual throughput of 900 MTHM [National Research Council, 1996].

Table 9.1.I. Fuel cycle steps, unit costs summary, and schedule.

Fuel cycle step	Cost	Unit	Lead time to beginning of irradiation
Natural Uranium	30.00	$/kg HM	12 months
Conversion	5.00	$/kg HM	6 months
Enrichment	80.00	$/kg HM	6 months
Fabrication UO_2	250.00	$/kg HM	3 months
Fabrication FFF	11000	$/kg HM	3 months
Reprocessing UO_2	800	$/kg HM	24 months
Reprocessing FFF	7000	$/kg HM	24 months
Dry Cask storage	2.18	$/MWd	at discharge
HLW Disposal (*Once through cycle*)	1.00	mill/kWh_e	added uniformly to FCC
HLW Conditioning and disposal (*Closed cycles*)	0.18	mill/kWh_e	

The reference data for the PWR and ABR used for the fuel cycle cost calculations is summarized in Table 9.1.II. ABR is a recent concept developed at MIT. It is a fast spectrum reactor using fertile free fuel. Its fuel cycle is optimized for the superior TRU destruction and economic performance. The ABR design utilizes a super-critical CO_2 power conversion cycle with up to 45% thermal efficiency. However, the costs of ABR technologies are more uncertain. Hence, a few of its parameters will be varied as a sensitivity analysis.

The same costs of FFF reprocessing and fabrication were assumed for the fertile free ABR fuel and FFF pins in the CONFU assembly.

The levelized fuel cycle cost calculation methodology described in [OECD/NEA, 1994] and in [Handwerk C.S. et al., 1998] was used in this study. The levelized fuel cycle cost (FCC) is calculated as the ratio of present valued front-end and back-end fuel cycle expenses for equilibrium fuel batch to the present valued energy generated by the same batch. Equation 9.1 gives a general expression for the FCC calculations.

$$FCC = \frac{\sum_i C_i e^{x\Delta t_i}}{E \times \frac{1-e^{-xT}}{xT}} \tag{9.1.1}$$

where C_i is the direct cost of transaction *i*, Δt_i is the time between the transaction occurrence and the reference point (beginning of batch irradiation), T is the fuel batch in-core residence time, and x is continuous discount rate. No escalation of costs due to inflation was assumed. Annual continuous compounding discount rate of 10% was used.

The data for capital and operation and maintenance (O&M) costs for ABR and PWR was obtained from [OECD/NEA, 2002a]. The total cost of electricity (COE) associated with fuel cycle, capital, O&M and decommissioning and dispostal (D&D) costs was also calculated as suggested in [OECD/NEA, 2002a] and given by the expression 9.1.2.

$$COE\left[\frac{mill}{kWh}\right] = FCC + \frac{UTC\left[\frac{\$}{kWe}\right] \times \left(\psi \times \left[1 + f_{D\&D}\right] + f_{O\&M}\right)}{CF \times 8766\left[\frac{h}{year}\right] \times 10^{-3}\left[\frac{\$}{mill}\right]} \tag{9.1.2}$$

where
- UTC – unit (total) capital cost
- CF – capacity factor
- ψ – fixed annual discount rate
- $f_{D\&D}$ – decommissioning and decontamination annual charge as a fraction of capital cost
- $f_{O\&M}$ – O&M annual charge as fraction of capital cost

Table 9.1.II. Reference PWR and ABR parameters

ABR [Romano A., 2003]		
Fuel in-core residence time	2.66	years
Average fuel burnup	200	MWd/kgHM
Annual TRU consumption	259	kg
Annual TRU loading	1231	kg
Thermal power	700	MW
Average capacity factor	0.90	
Thermal efficiency (Advanced SC CO_2 cycle)	0.45	
Capital cost	2100	$/kWe
PWR		
Fuel in-core residence time	4.5	years
Annual TRU generation	230	kg
Thermal power	3400	MW
Average capacity factor	0.90	
Thermal efficiency	0.337	
Capital cost	1700	$/kWe
Additional assumptions		
Annual discount rate	10	% / year
O&M annual charge as fraction of capital cost	4	% / year
Decommissioning annual charge as fraction of capital cost	8	% / year

9.2. Fuel Cycle Cost Estimates

The results of the FCC and COE calculations are presented in Table 9.2.I. The CONFU-1 FCC with first time recycled TRU is about 28% higher than the reference once through UO_2 cycle. The equilibrium TRU (CONFU-EQ) cycle is more expensive than the reference UO_2 cycle by about 60% due to increased uranium enrichment required to sustain a cycle length comparable to the reference UO_2 cycle as well as relatively high costs of the steps associated with TRU recycling.

The FCC of this macro-heterogeneous equilibrium CONFU is somewhat higher than micro-heterogeneous CONFU option due to slightly superior burnup performance of the latter.

The total cost of electricity for the CONFU-EQ and PWR-ABR cycle are comparable. Higher capital cost of ABR is offset by the neutronic advantages of fast spectrum with respect to TRU destruction. Changes in TRU isotopic composition does not significantly affect burnup performance of the ABR. In the CONFU cycle, on the other hand, the degradation of TRU isotopic vector results in a requirement for higher uranium enrichment which impairs the fuel cycle economics. Table 9.2.I also shows the FCC and COE for PWR and ABR parts of the ABR-PWR fuel cycle. The UO_2 fuel reprocessing expenses are attributed to the ABR fuel cycle. Therefore, the FCC of PWR in PWR-ABR system is lower than that of the once through PWR cycle.

Although the FCC for the CONFU-EQ cycle is higher than the once through cycle, the total COE for the CONFU-EQ is higher by only about 8%.

Figure 9.2.1 shows individual contributions of the considered fuel cycle transactions for the cases analyzed. Reprocessing of the spent UO_2 fuel represents the largest expense for the closed fuel cycles. The next largest contribution to the cost of the closed fuel cycles is from fabrication the FFF fabrication and reprocessing. The cost of FFF reprocessing and fabrication in the CONFU-EQ case is lower than in ABR-PWR case because of the lower TRU inventory in the former system as a result of higher actinide cross-sections in thermal spectrum. However, the PWR-ABR system does not require higher UO_2 enrichment because of the fast spectrum in ABR and its transmutation performance is not sensitive to TRU isotopic composition. As a result, the contribution of UO_2 enrichment to the fuel cycle cost is substantially lower in PWR-ABR case.

Table 9.2.I Fuel Cycle and Total Electricity Cost Summary (mills/kW$_e$h)

	FCC	Capital + O&M Cost	Total COE
Once-through UO_2	4.52	31.91	36.44
CONFU-1	5.80	31.91	37.72
CONFU-EQ	7.33	31.91	39.24
M-CONFU-EQ	7.69	31.91	39.61
PWR - ABR	7.48	33.38	40.86
PWR – 3400 MW_{th}	*3.70*	*31.91*	*35.62*
ABR – 700 MW_{th}	*22.81*	*39.42*	*62.23*

Nevertheless, the major advantage of the CONFU concept is the possibility of TRU transmutation in a sustainable mode without the introduction of new reactor concepts. The implementation of the CONFU based TRU transmutation strategy will allow to address the nuclear waste issue earlier. It will also provide extra time for the research and development effort on more advanced transmutation concepts without accumulation of TRU from the existing reactors. In addition, the 1-tier system considered here is based on critical TRU burner reactor [Romano A., 2003]. In comparison with ADS, which are currently preferred choice for transmutation systems in Europe [Rubbia C. et al., 1997], the economic advantages of CONFU are projected to be significantly more pronounced than in the case of critical TRU burning systems.

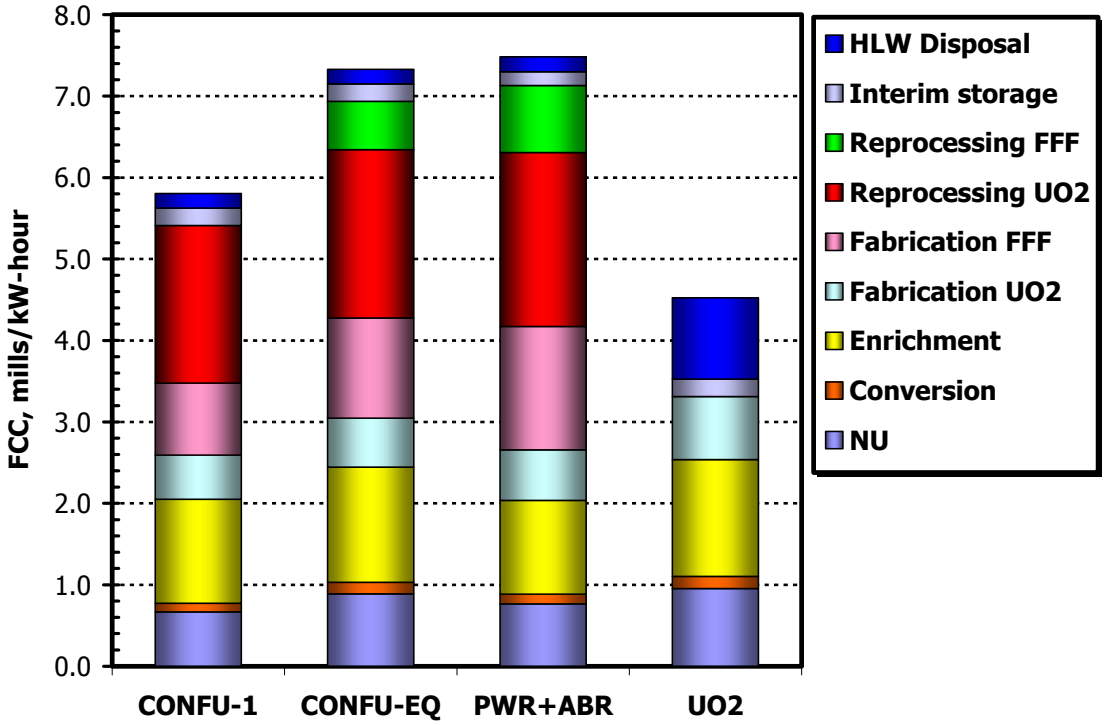

Figure 9.2.1. Breakdown of FCC components

A number of alternative fuel cycles were compared in OECD study mentioned earlier [OECD/NEA, 2002a] in terms of there economic performance and environmental impact. Figure 9.2.2 shows the results of this comparison. Index RLOSS is defined as TRU losses to the repository relative to once through fuel cycle, while quantity RCOST represents total cost of electricity relative to that of the once through fuel cycle. Since both indices are relative parameters and the OECD/NEA [2002a] report was the main reference source of unit costs for the

current analysis, the corresponding values of RLOSS and RCOST for the CONFU and PWR-ABR fuel cycles are also plotted in Figure 9.2.2. Both, the CONFU and PWR-ABR fuel cycles exhibit superior performance to any of the fuel cycles considered in OECD study primarily because both systems employ fertile free fuel technology which allows minimization of TRU inventory within the cycle.

Two-tier systems considered in OECD study relied on conventional MOX technologies for burning Pu in the first-tier LWRs while residual Pu and MA from the first-tier are burned and recycled in the second-tier accelerator driven system. Such two-tier fuel cycles are not very effective economically due to a relatively poor Pu destruction efficiency in MOX fuel and high costs of development and deployment of accelerator technologies. However, the economics of 2-tier fuel cycles can be significantly improved if FFF based LWRs or gas cooled reactors are used in the first-tier as Pu or TRU burners and critical fast spectrum reactors with fertile free fuel in the second tier as was demonstrated by Romano A. [2003].

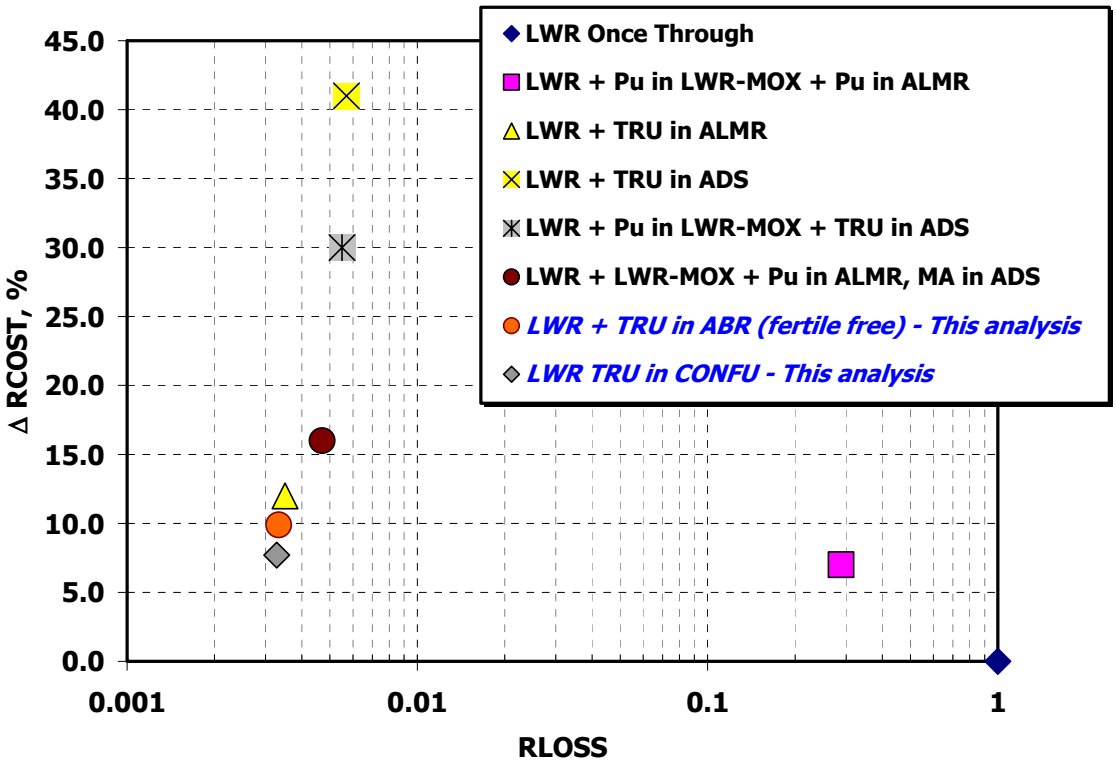

Figure 9.2.2. TRU loss vs. COE comparison of CONFU and PWR-ABR cycles with [OECD/NEA, 2002a] results.

9.3. Fuel Cycle Cost Sensitivities

As mentioned earlier, the uncertainty in costs of spent fuel reprocessing and TRU target fuel fabrication is significant. However, development of innovative technologies can considerably reduce the cost of TRU recycling [OECD/NEA, 2002a]. A series of sensitivity calculations of the FCC to various fuel cycle stage unit costs was performed to evaluate the potential of the CONFU based fuel cycle to achieve an economic performance comparable to that of the once-through fuel cycle. Additionally, some assumptions regarding ABR technology have large uncertainties for example: its capital cost and feasibility of high thermal efficiency supercritical CO_2 (SC CO_2) power conversion cycle, which is currently being studied at MIT [Dostal V., et al., 2002]. Therefore, the PWR-ABR fuel cycle cost sensitivity to ABR capital cost and thermal efficiency was also investigated.

Figure 9.3.1 shows the FCC of equilibrium CONFU relative to the reference once through UO_2 cycle as a function of fractional change in unit costs of UO_2 fuel reprocessing, FFF reprocessing and FFF fabrication. As expected, the CONFU FCC exhibits greatest sensitivity to the UO_2 fuel reprocessing cost. Although UO_2 fuel reprocessing has the lowest cost per kg of feed, it has a major contribution to the FCC because of the volume of material to be reprocessed. Therefore, superior priority should be given to the development of conventional UO_2 fuel reprocessing technologies. The data presented in Figure 9.3.1 also suggests that the CONFU concept can be economically competitive with the conventional once through fuel cycle if all three transaction unit costs are reduced by at least a factor of two which is somewhat lower than the most optimistic unit cost estimates reported in [OECD/NEA, 2002a].

Another change in the relative economic performance of the sustainable CONFU and conventional UO_2 cycles may arise from the change in the federal waste disposal fee policy. It is still a matter of considerable debate whether 1 mill/kWh fee is sufficient for the financing of permanent repository construction at Youcca Mountain site especially if second repository will be required at some point. As an example, the cost of waste disposal in Japan is estimated to be eight times higher than in France and 13 times higher than in the UK [Saegusa A., 1999]. Higher waste disposal charges will increase economic attractiveness of the sustainable fuel cycle.

Figure 9.3.2 depicts the FCC as a function of relative increase of the waste disposal cost for the CONFU-1, CONFU-EQ and once through fuel cycles. For the once through fuel cycle, the

waste disposal fee was increased up to eight times of its nominal value. Similarly, the cost of HLW conditioning and disposal for the closed cycles (0.18 mills/kWh) was increased by the same factor. The CONFU-1 FCC becomes even with UO_2 cycle if the waste disposal costs are increased by a factor of 2.5 relative to the respective nominal values of the once through and CONFU-1 cycles. The single stage UO_2 fuel reprocessing and TRU recycling in the form of CONFU-1 fuel, although not capable of major radiotoxicity reduction, can substantially reduce the volume of spent fuel intended for geological disposal. Therefore, the implementation of just a first stage of the CONFU cycle can postpone the need for additional repository capacity. The equilibrium CONFU cycle becomes economically competitive with the once through only for the waste disposal costs which are higher than nominal values by about a factor of 4.5 (1850 $/kgHM for once through cycle) which is higher than any current estimates.

Although the price of natural uranium was relatively stable within the past decade, in a possible scenario of rapidly growing world nuclear generation capacity, the prices of natural uranium could increase. Higher natural uranium price would also encourage fuel reprocessing and recycling.

Figure 9.3.3 shows the difference in FCC between CONFU and once through fuel cycles as a function of natural uranium unit cost. The CONFU-1 FCC reaches breakeven value with that of the UO_2 cycle if natural uranium recovery becomes economical at a price of 150 $/kgHM. The difference between the equilibrium CONFU cycle and the once through is reduced from 60% to about 30% when the uranium price is increased to 150 $/kg/HM.

The enrichment prices, on the other hand, are likely to fall as a consequence of new enrichment technologies or improvements in the existing ones. However, less expensive enrichment would increase the gap between the once-through and closed fuel cycle costs as illustrated by Figure 9.3.4.

A nominal thermal efficiency of 45% was assumed for the SC CO_2 power conversion cycle of ABR. Main advantage of the SC CO_2 cycle is that such a high efficiency can be achieved at a relatively low reactor coolant outlet temperature on the order of 600 ºC MIT [Dostal V., et al., 2002]. In order to achieve a similar efficiency with the more conventional He coolant, the reactor coolant temperature has to be increased by over 200 ºC challenging the performance of reactor

core materials. Conversely, a He cycle would provide only about 35% power conversion efficiency for the same core outlet temperature as in the SC CO_2 case.

The sensitivity of ABR fuel cycle cost to the power conversion efficiency is shown in Figure 9.3.5. The fuel cycle cost of ABR is increased by almost 30% when the power conversion efficiency is dropped to 35%. However, an increase in the total cost of electricity of ABR is more moderate (about 10%) because the ABR FCC is smaller than its capital and O&M costs by about a factor of two. Furthermore, the COE of the PWR-ABR system is practically insensitive to the ABR conversion efficiency. Lower efficiency increases the ABR COE but it also reduces the relative ABR electric power fraction of the total PWR-ABR power so that overall effect is small. It should also be noted that thermal efficiency does not affect the efficiency of TRU destruction in ABR since the rate of TRU destruction is proportional to the thermal power of ABR.

Figure 9.3.6 shows the PWR-ABR system FCC and COE relative to those of the CONFU-EQ cycle. As discussed above, the variation of ABR thermal efficiency does not practically affect the relative COE of the CONFU-EQ and PWR-ABR systems. However, the fuel cycle cost of PWR-ABR at 45% thermal efficiency is higher than that of the CONFU-EQ by only about 2%, however, the difference in the FCC between the CONFU-EQ and PWR-ABR cycles increases to about 8% if the ABR thermal efficiency is 35%. Overall, the observed effect of ABR thermal efficiency on the relative performance of the considered fuel cycles is small.

Figures 9.3.6 and 9.3.7 show the total cost of electricity for the PWR-ABR system as a function of ABR capital cost relative to the nominal PWR-ABR COE and to the CONFU-EQ cycle COE respectively. The variation of ABR capital cost by ± 400 $/kWe results in about 13% change of ABR COE and about 4% variation of PWR-ABR COE. The COE of ABR remains much higher than CONFU-EQ COE even if the capital cost of ABR is the same as for PWR. This is due to significantly higher FCC of ABR (Figure 9.3.7). However, the PWR-ABR system COE reaches break even with that of the CONFU-EQ cycle as the capital cost of ABR approaches the PWR nominal value. Application of super-critical CO_2 power conversion cycle may substantially reduce a footprint of Balance of Plant (BOP) of ABR type reactor and therefore ABR capital costs by up to 40% in comparison with capital costs of a more conventional ALMR [Hejzlar P. et al., 2003]. The PWR-ABR system COE can be lower than that of the CONFU-EQ system by about 5% if capital cost of ABR on the order of 1200 $/kWe can be achieved.

In general, the dependence of total cost of electricity of PWR-ABR system on the capital cost of ABR is also relatively weak because of the small ABR contribution to the total system power (see Table 9.1.II).

Substantial capital cost reduction is also predicted for many advanced LWR systems such as AP-1000, EPR, SWR-1000, APWR and others. Figure 9.3.8 shows PWR-ABR and CONFU-EQ cycles COE as a function of PWR capital cost. Although all fuel cycles would benefit from PWR capital cost reduction, lower capital cost of PWR would result in higher relative to once through fuel cycle COE for both PWR-ABR and CONFU-EQ cycles. However, the sensitivity of PWR-ABR system to PWR capital cost reduction is substantially greater than that of the CONFU system because of the relatively high capital cost of ABR which remains unaffected.

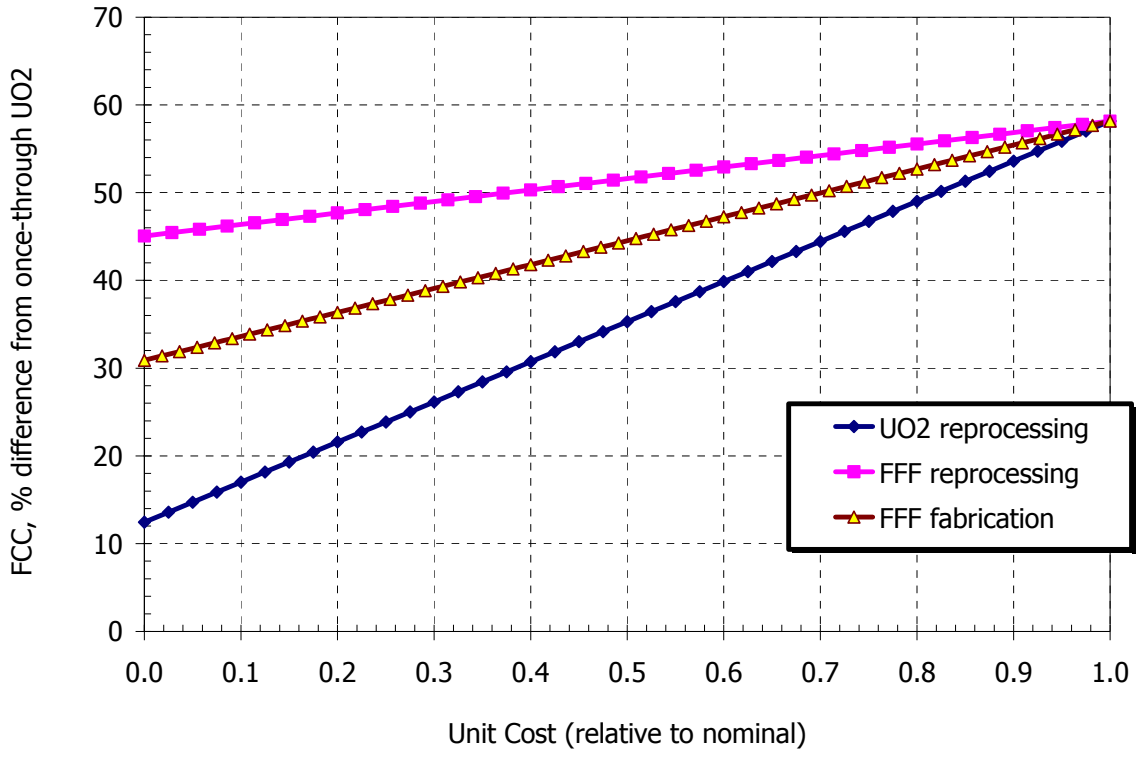

Figure 9.3.1 Sensitivity of FCC to changes in fuel reprocessing and fabrication costs

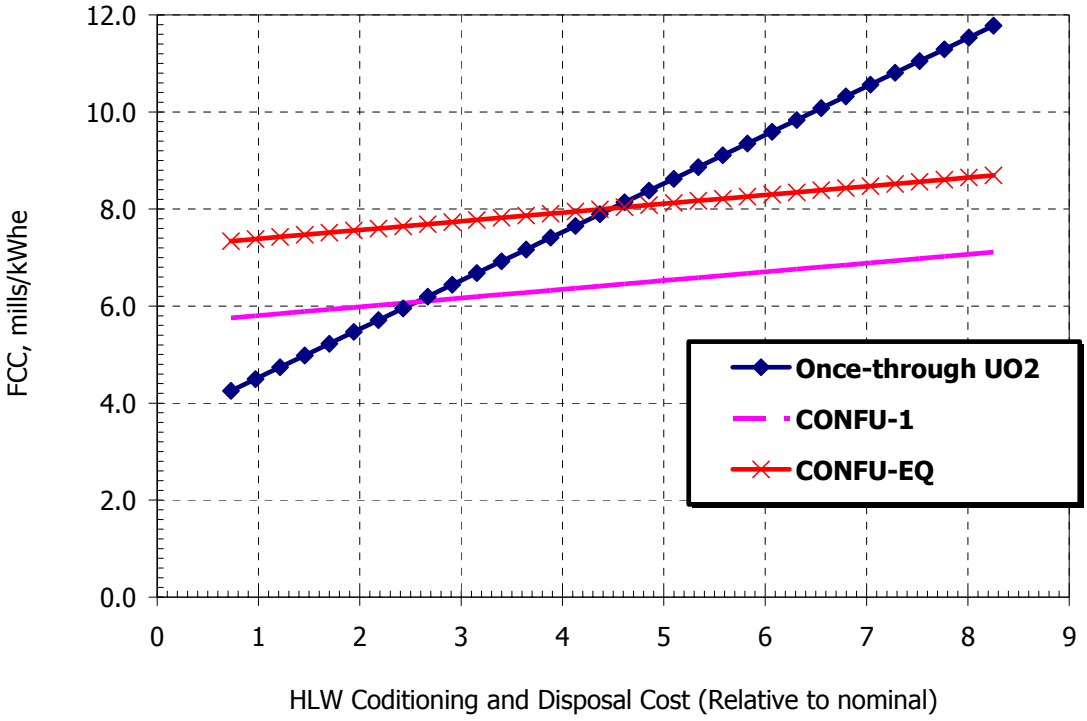

Figure 9.3.2. FCC Sensitivity to waste disposal cost

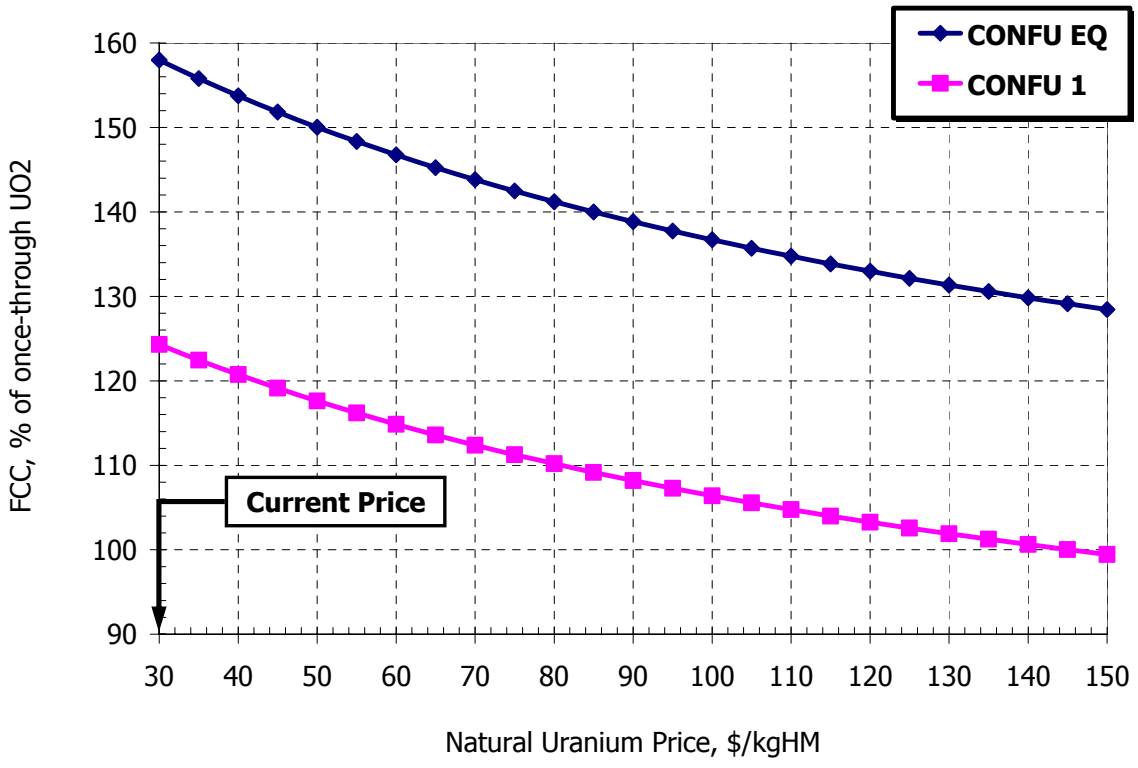

Figure 9.3.3. CONFU FCC Sensitivity to natural uranium price

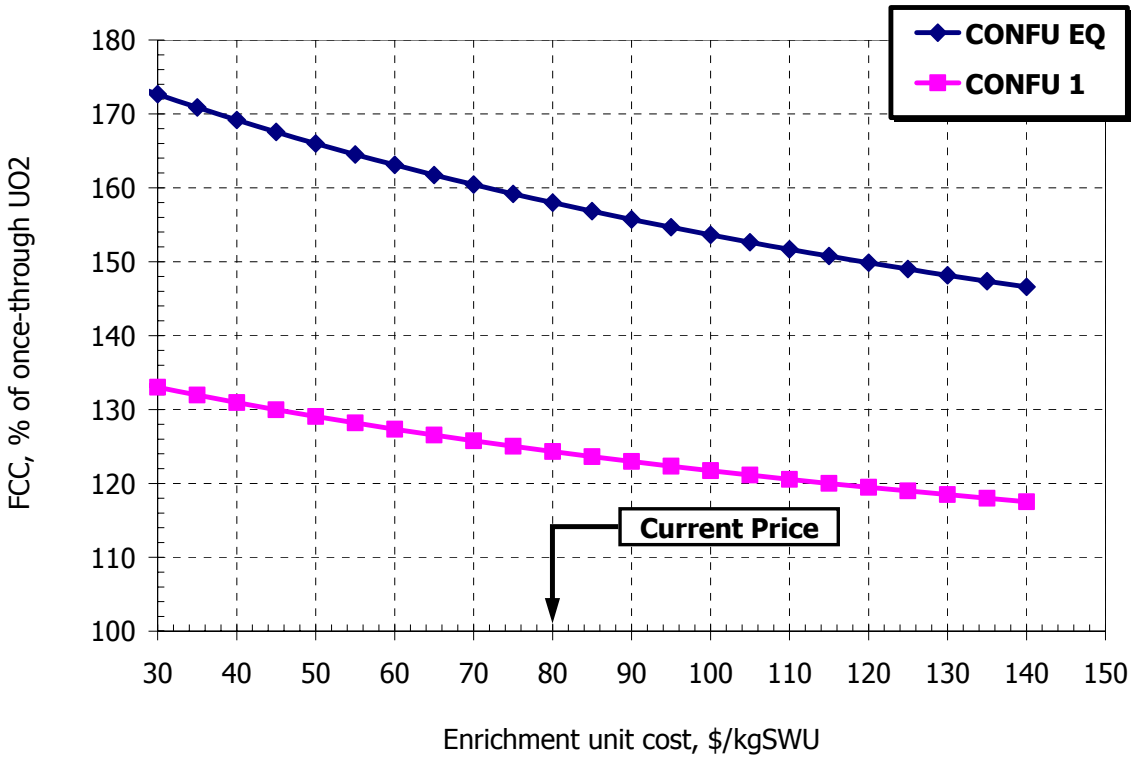

Figure 9.3.4. CONFU FCC sensitivity to SWU price

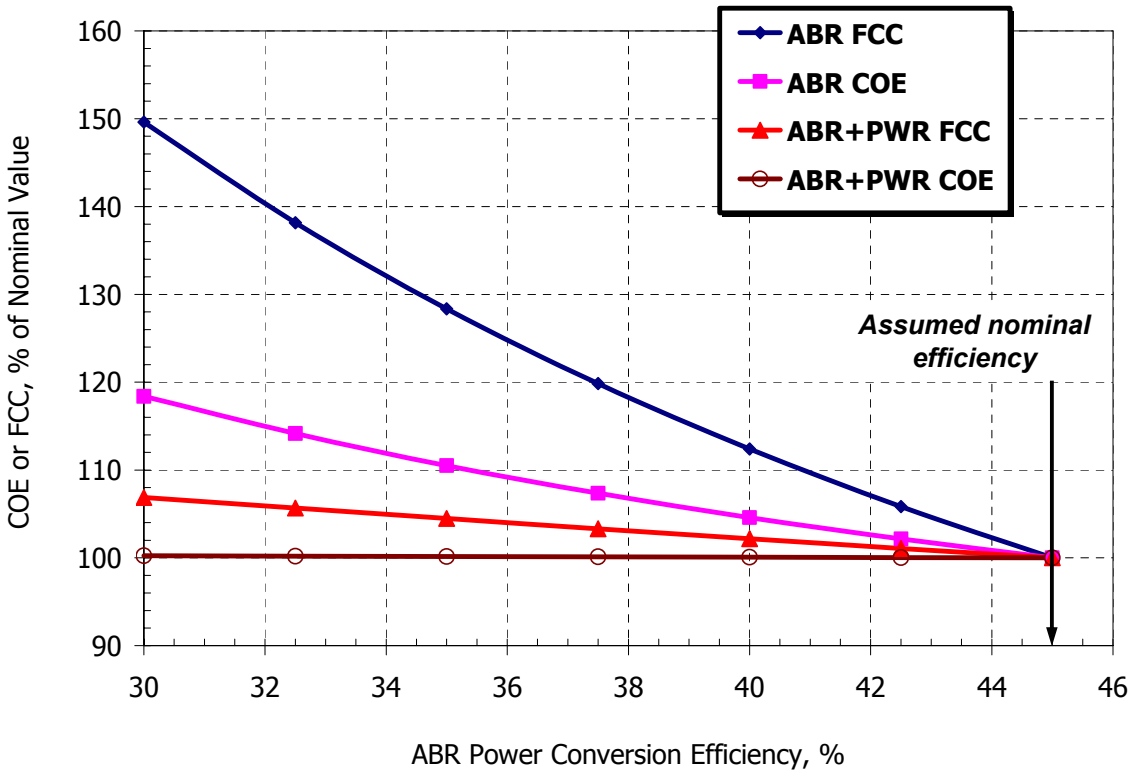

Figure 9.3.5. Sensitivity of ABR COE and FCC to ABR power conversion efficiency

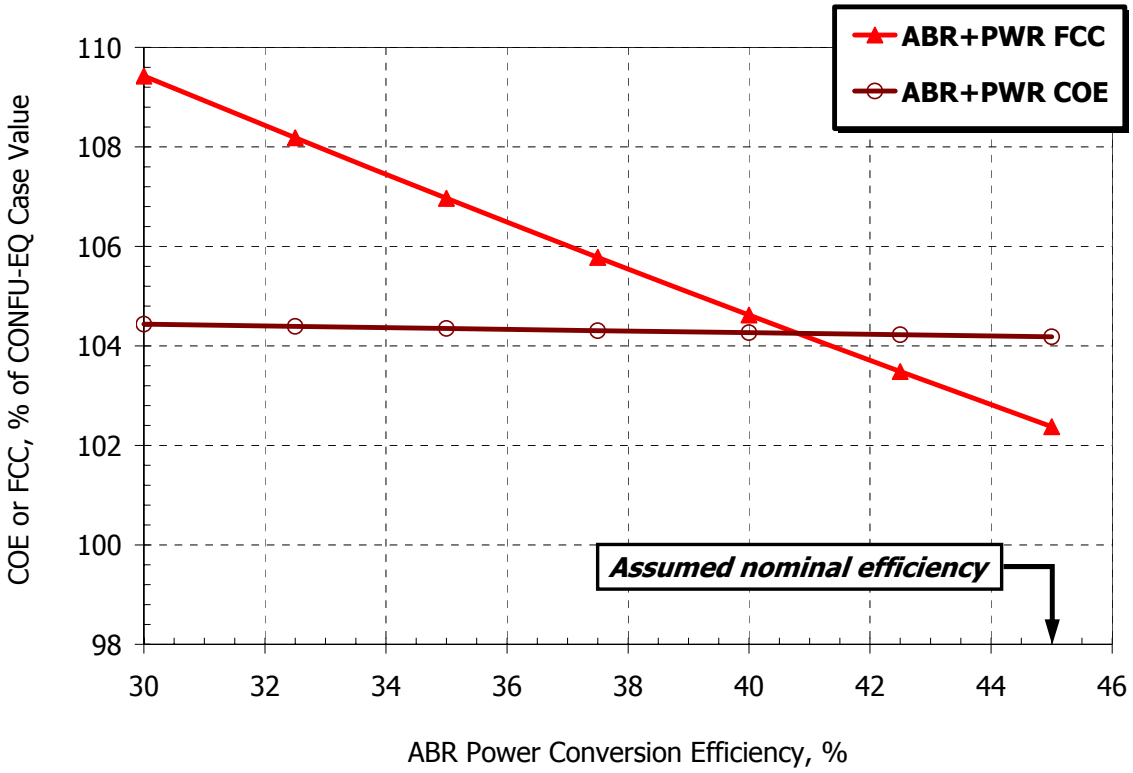

Figure 9.3.6. Sensitivity of ABR COE and FCC to ABR power conversion efficiency

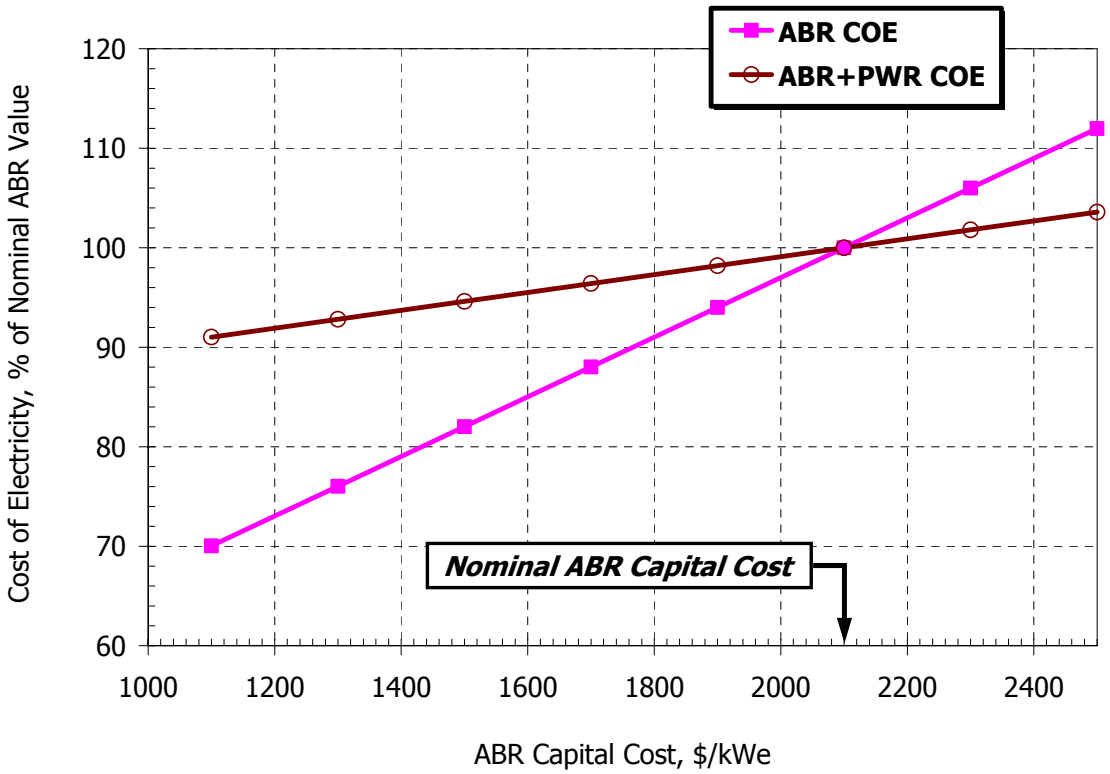

Figure 9.3.7. ABR and PWR-ABR COE as a function of ABR capital cost

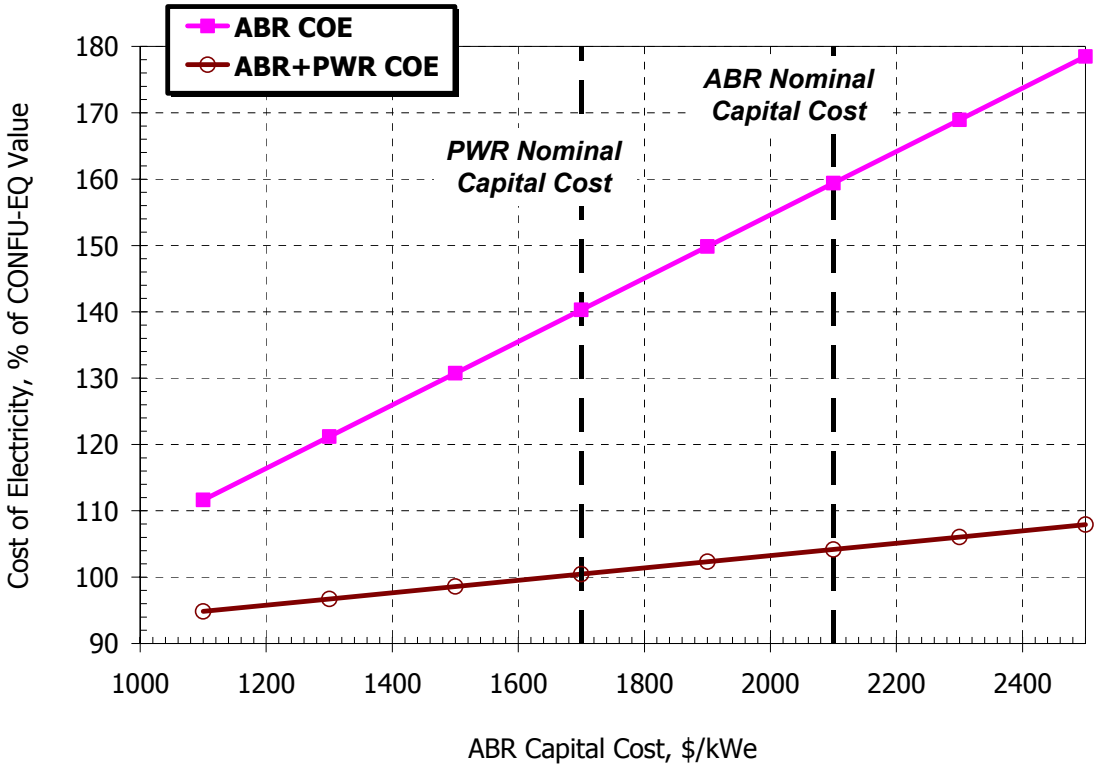

Figure 9.3.8. ABR and PWR-ABR to CONFU-EQ COE ratio as a function of ABR capital cost

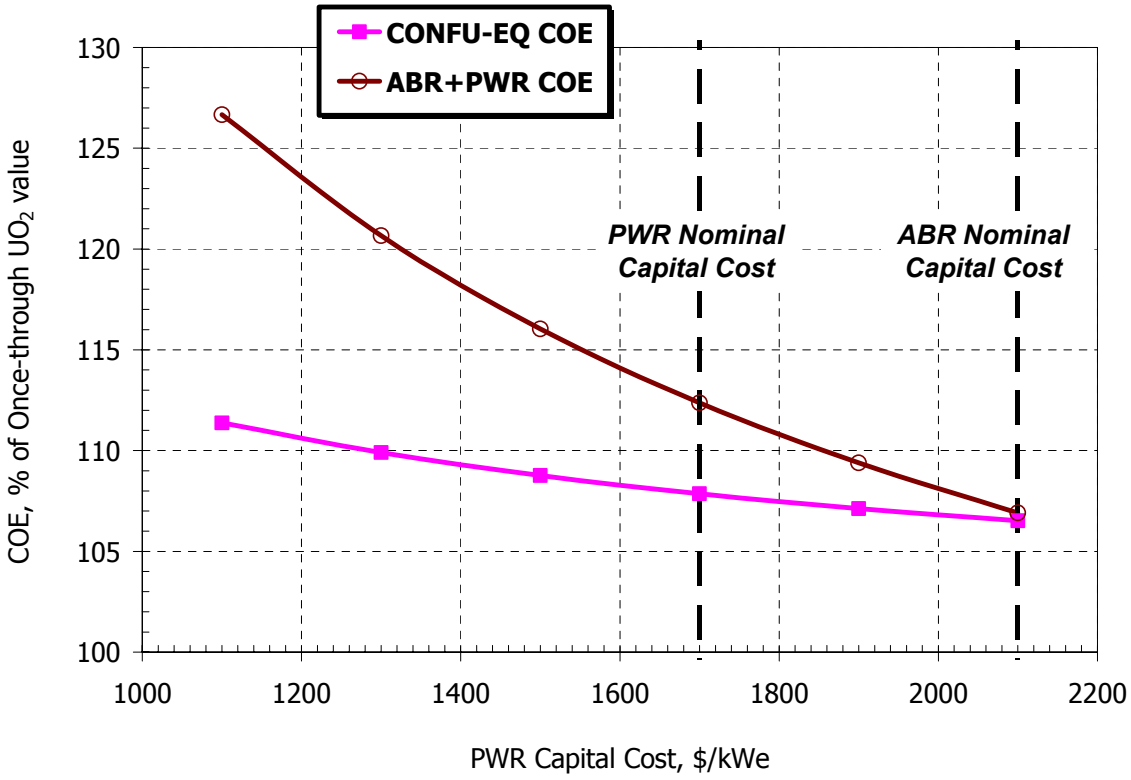

Figure 9.3.8. Relative PWR-ABR and CONFU-EQ COE as a function of PWR capital cost

Additional illustration of sensitivity of FCC and COE to various fuel cycle parameters for the once through PWR, CONFU-EQ, and PWR-ABR fuel cycles is presented in Table 9.3.I. All fuel cycle parameters in Table 9.3.I were perturbed by a constant fraction (10%) relative to their nominal values. As discussed earlier, the CONFU-EQ and PWR-ABR fuel cycle costs are most sensitive to the cost of UO_2 fuel reprocessing. The second most sensitive parameter for the CONFU cycle is the enrichment cost while for PWR-ABR fuel cycle the FFF fabrication is more important. This is due to the fact that equilibrium CONFU cycle requires higher UO_2 enrichment than in PWR-ABR cycle. However, TRU inventory is larger in PWR-ABR system. Therefore, FFF reprocessing and fabrication have larger contribution to FCC of PWR-ABR than in the CONFU-EQ case. As expected, the COE of all fuel cycles exhibit the strongest dependence on the capital cost of PWR because capital and O&M costs constitute over 80% of total cost of electricity for all fuel cycles considered.

Table 9.3.I. Sensitivity of CONFU-EQ and PWR-ABR cycle costs to various parameters

	FCC, mills/kWh			COE, mills/kWh		
Parameter	PWR	CONFU-EQ	PWR-ABR	PWR	CONFU-EQ	PWR-ABR
All nominal values	4.52	7.33	7.48	36.44	39.24	40.86
NU price +10%	4.62	7.42	7.56	36.53	39.33	40.94
SWU price + 10%	4.67	7.47	7.60	36.58	39.38	40.98
HLW disposal + 10%	4.62	7.35	7.50	36.54	39.26	40.88
LWR Capital cost + 10%	4.52	7.33	7.48	39.63	42.43	43.43
ABR Capital cost + 10%	4.52	7.33	7.48	36.44	39.24	41.63
UO_2 reprocessing + 10%	4.52	7.54	7.70	36.44	39.45	41.07
FFF fabrication + 10%	4.52	7.45	7.63	36.44	39.36	41.01
FFF reprocessing + 10%	4.52	7.39	7.56	36.44	39.30	40.94

9.4. Chapter Summary

The economic performance of the sustainable CONFU fuel cycle is analyzed and compared with conventional UO_2 once through fuel cycle. The fuel cycle cost calculations indicate inferior economics of the CONFU based versus conventional UO_2 cycle. The difference in the FCC between the two fuel cycle options is about 60%. The total cost of electricity, however, is higher for the CONFU cycle by only 8%. The higher costs of the sustainable CONFU cycle are due to higher enrichment requirements as a result of the TRU isotopics degradation and relatively high costs associated with fuel reprocessing and re-fabrication. The UO_2 fuel reprocessing has the largest contribution to the sustainable FCC. Reduction of reprocessing and FFF fabrication costs by a factor of two would result in comparable economic performance of UO_2 and CONFU fuel cycles.

The total COE of the CONFU based cycle and the combined PWR and advanced fast spectrum Actinide Burner Reactor (ABR) are similar. The neutronic superiority of the fast spectrum for TRU transmutation results in lower uranium enrichment requirements for PWR-ABR cycle than for the equilibrium CONFU cycle which offsets the effect of considerably higher capital cost of ABR. The CONFU fuel cycle is expected to be significantly more economical than PWR-ABR cycle if financial risks associated with large capital investments for new nuclear power plants are considered. This is because the CONFU fuel cycle relies mostly on conventional LWR technologies with vast operating experience while the uncertainty in costs of fast reactor technologies is considerably higher. The COE of the equilibrium CONFU and single-tier PWR-ABR systems is lower than that of the two-tier system with MOX LWR and ADS as a first and second tier respectively. However, two-tier system with FFF LWR and critical ABR as a first and second tier may prove to be more economical.

The effect of ABR thermal efficiency and capital cost on PWR-ABR total cost of electricity is moderate due to a relatively small contribution of ABR to total PWR-ABR system power. Nevertheless, an additional and ultimate advantage of the CONFU cycle is the possibility of its application to the existing fleet of reactors with immediate environmental effect on the repository.

Rethinking of the federal nuclear waste disposal fee and increase in natural uranium prices may improve economic performance of the CONFU fuel cycle in comparison with conventional once through cycle and may consequently facilitate its implementation.

Chapter 10. Summary and Recommendations

The current US nuclear energy depends on a once through fuel cycle that is economic but raises a number of public concerns which retard the exploitation of the full potential of nuclear power to contribute to a sustainable development of human society. An issue of superior importance is the accumulation of long lived radioactive wastes in the environment which will require isolation for hundreds of thousands of years. Currently, the economic and environmental benefits of the long term geological storage of the nuclear waste are a matter of considerable uncertainty and debate throughout the scientific and political community.

Partitioning and transmutation of spent fuel can greatly diminish the need for long term geological storage, improve utilization of natural resources, and enhance proliferation resistance of the nuclear fuel cycle. Numerous transmutation systems and closed fuel cycle concepts capable of achieving the nuclear waste transmutation goals have been proposed and investigated throughout the world. Implementation of such innovative fuel cycle approaches is not anticipated in the near future primarily because of the costs, as well as large uncertainty in costs, associated with the development of necessary transmutation technologies.

Two categories of nuclear waste treatment technologies can be distinguished. The first category is related to the fuel cycle infrastructure and it includes the development of innovative techniques for the spent fuel reprocessing, partitioning of the actinides and fission products, and the transmuter system fuel fabrication and handling. These technologies must be an integral part of any fuel cycle option with no requirement for the long term geological repository regardless of the waste transmutation system type assumed. Another category of technologies that requires significant amount of research and development effort is the waste transmutation systems themselves. Fast spectrum critical or accelerator driven systems (ADS) are believed to be beneficial with respect to the TRU waste transmutation capabilities. However, such systems do not exist yet and their effective deployment and economic performance remains to be demonstrated.

On the other hand, the possibility of utilization of the LWR for transmutation offers significant fuel cycle advantages. The application of TRU recycling within the existing LWRs would yield immediate results in the form of radioactive waste burden reduction and would eliminate the need for a relatively large waste repository capacity. Furthermore, the accumulation

of TRU can be already constrained during the time needed for the development and deployment of advanced ADS and fast reactor transmutation systems.

In this thesis, the use of the PWR, as the most common reactor type, was evaluated with respect to its capabilities to operate in a sustainable mode with orders of magnitude reduction in the generation of TRU waste. Technical feasibility of such a fuel cycle was judged to be highly probable. The environmental impact of a single path TRU burndown scenario, in which TRU from the spent UO_2 fuel are separated and burned once in PWRs, was also evaluated.

10.1. Choice of Fuel for Transmutation of TRU in LWRs

Thorium and fertile free fuel matrices were identified as the most promising candidates for TRU transmutation in LWRs due to the limited or absence of additional TRU generation in contrast to conventional mixed oxide (MOX) fuel.

The rate of TRU destruction and fractional TRU burnup were evaluated for both fuel matrix types and various PWR assembly lattice geometries. The TRU destruction rate for fertile free fuel is limited solely by the specific power. A typical PWR can eliminate TRU via utilization of FFF at a rate of about 1140 kg/GWe-Year. TRU destruction rate in ThO_2 matrix is about 900 kg/GWe-Year and can be slightly improved by increasing the fuel lattice H/HM ratio. Breeding of fissile U233 slows down the TRU destruction due to the competition of TRU and U233 for neutron absorption. In addition, if the once through burndown scenario is considered, U233 as a potentially weapons usable material must be isotopically diluted (denatured) by U238 to eliminate the proliferation concerns. Addition of U238 further degrades TRU destruction rate in a ThO_2 matrix.

The residual TRU fraction in the discharged fuel is a primary indicator of the TRU destruction efficiency. Higher TRU fractional burnup ultimately implies economic benefits from smaller amount of material to handle in recycling. Although both ThO_2 and FFF matrices can achieve about 50% of TRU destruction per path through the reactor core, ThO_2 fuel requires much higher fuel lattice H/HM ratio than that of the reference PWR, while a destruction rate of over 50% can be achieved in FFF already with the reference fuel lattice geometry (Figure 10.1.1). Minimal requirements for changes in PWR assembly geometry to accommodate TRU hosting

fuel is a desirable feature. The TRU loading in the two fuel options shown in Figure 10.1.1 is sufficient to provide a comparable fuel cycle length of 18 month in the reference PWR fuel geometry.

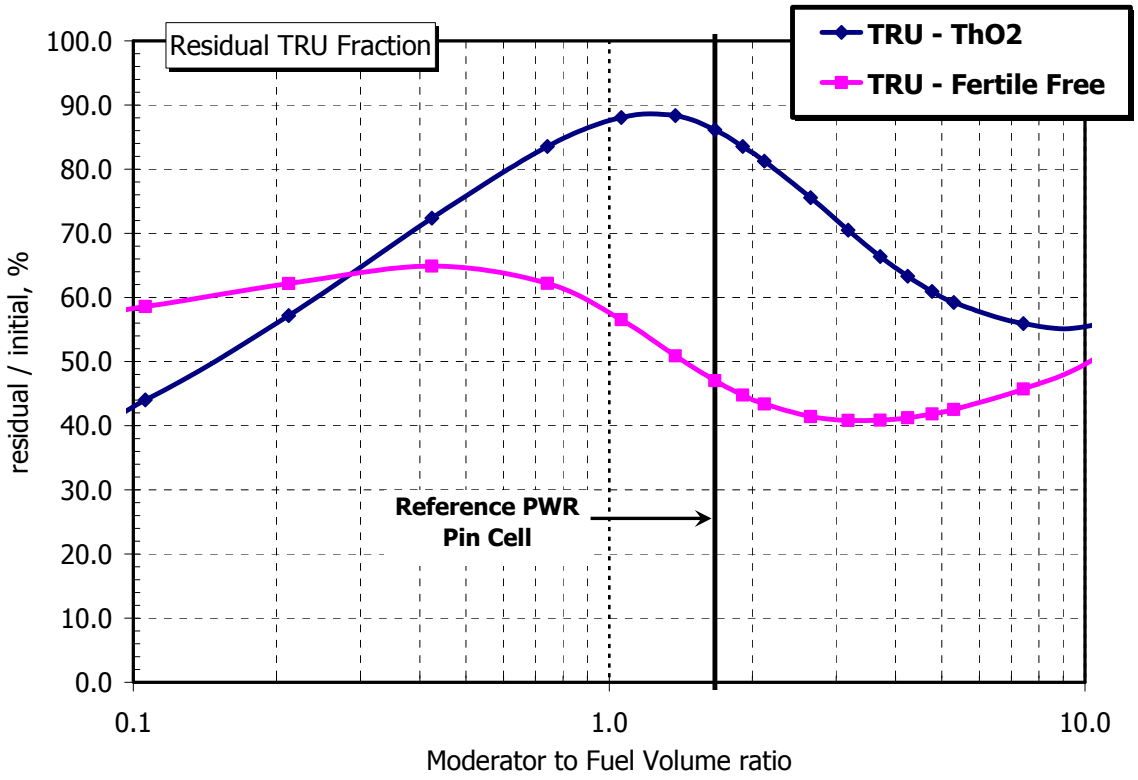

Figure 10.1.1. TRU residual fraction in discharge fuel of a PWR transmuter core

The feasibility of practical designs for thorium and FFF based PWR transmuter was assessed through comparison of reactivity feedback coefficients and soluble boron worth for the two fuel matrix options with those of the conventional MOX and reference PWR fuel. A brief summary of the comparison is presented in Table 10.1.I. All TRU containing fuels exhibit significantly reduced control materials reactivity worth due to the harder spectrum in comparison with UO_2 fuel which may require a redesign of the core reactivity control features. Reduced effective delayed neutron fraction may result in inferior reactor response to fast reactivity transients. In the FFF case, this problem is aggravated by significantly reduced fuel temperature feedback due to the reduced concentrations of fertile resonance nuclides. The high loading of TRU required to sustain a standard 18 month fuel cycle length in the case of TRU-MOX and TRU-ThO_2 fuel

results in a less negative, or even positive, void coefficient. A positive void coefficient is the limiting factor on the maximum TRU loading in ThO_2 or TRU-MOX cores.

Table 10.1.I. Safety and control parameters of transmuter PWR core

	DC, pcm/K		MTC, pcm/K		BW, pcm/ppm		$\beta_{eff} \times 10^3$	
	BOL	EOL	BOL	EOL	BOL	EOL	BOL	EOL
All – U	-2.20	-3.33	-22.2	-78.8	-4.80	-6.23	7.2	4.8
TRU – MOX	-2.19	-2.32	-0.86	+0.40	-1.64	-1.96	3.4	3.7
TRU – Th	-2.98	-3.15	-18.5	-23.4	-1.05	-1.24	2.6	2.5
FFF – TRU	-0.63	-1.04	-21.9	-51.8	-2.34	-8.02	2.7	3.9

Nuclear waste characteristics were compared for different fuel options for the once through burndown fuel cycle scenario applied to PWRs. Such scenario assumes reprocessing of the conventional LWR spent fuel and single path recycling of TRU in the same system followed by permanent geological disposal. It was concluded that no major environmental benefits can be achieved by means of a once through TRU burndown strategy. The reduction in the spent fuel radiotoxicity in the repository is marginal or in some cases it is even non-existent compared to the conventional once through fuel cycle for the first 100 to 1000 years due to buildup of additional minor actinides (Figure 10.1.2). The radiotoxicity data presented in Figure 10.1.2 is normalized per unit energy produced by each fuel type accounting for the energy of the reprocessed fuel from which the TRU were originally obtained.

The release of TRU to the environment must be restricted to about 0.1% of their inventory in the fuel cycle in order to reduce the waste radiotoxicity below that of the original natural uranium ore in less than 1000 years. Such deep burnup of TRU with a residual fraction of less than 0.1% is impossible in any of the existing or proposed transmutation systems or fuel designs. Therefore, recycling of TRU is necessary in order to meet the environmental goals of transmutation. The recovery of TRU from the spent fuel with the efficiency of at least 99.9% becomes a major technological challenge.

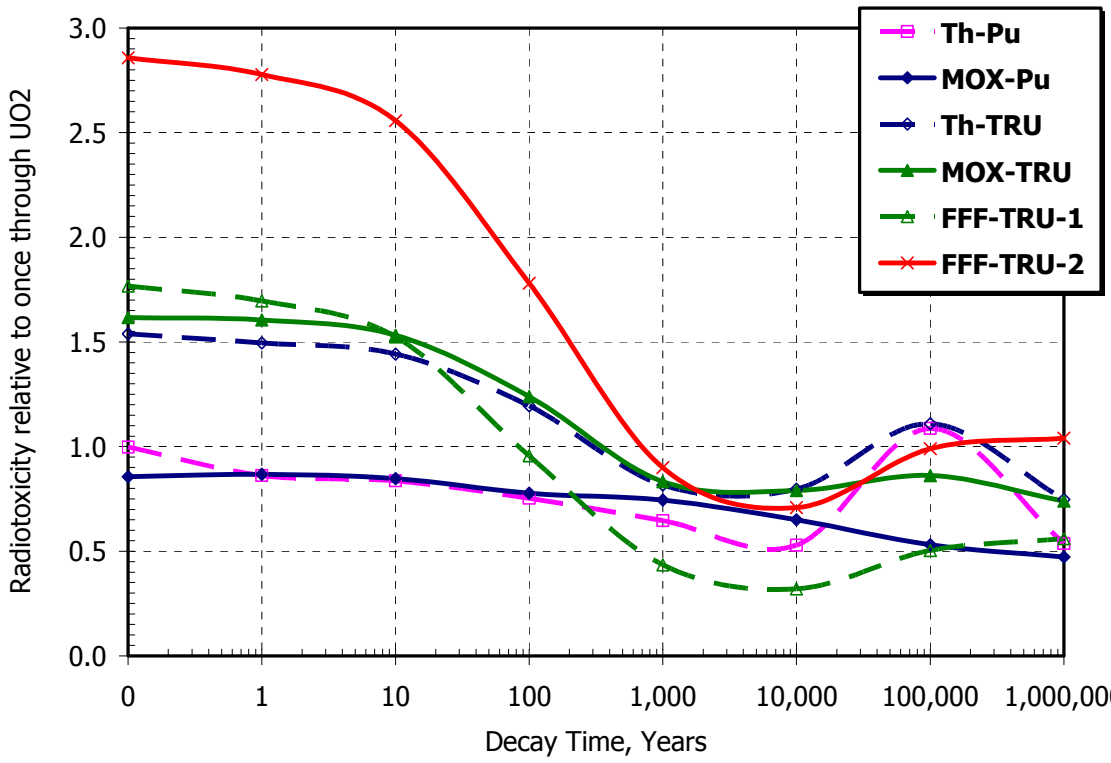

Figure 10.1.2. Spent fuel radiotoxicity relative to once trough UO_2 fuel cycle.

10.2. Evaluation of a Sustainable Fuel Cycle

The Combined Non-Fertile and UO_2 (CONFU) assembly concept is proposed for multi-recycling of TRU in existing PWRs (Figure 10.2.1). The assembly assumes a heterogeneous structure where only about 20% of conventional UO_2 fuel pins on the assembly periphery are replaced with FFF pins hosting TRU generated in the previous cycle.

Possibility of achieving a zero TRU generation on the net balance is demonstrated. Three to five TRU recycles are required to achieve an equilibrium fuel cycle length and TRU generation and destruction balance. Majority of TRU nuclides reach their equilibrium concentration levels in less than 20 recycles. The exceptions are Cm246, Cm248, and Cf252. Extremely small absorption cross-sections for these nuclides, even in a thermal spectrum, require relatively high equilibrium concentrations. Accumulation of these isotopes is highly undesirable with regards to TRU fuel fabrication and handling because they are very strong sources of spontaneous fission (SF) neutrons. The shielding of neutron radiation is more challenging than γ radiation which may lead

to increased fuel reprocessing and fabrication costs. Allowing longer cooling down of the spent fuel before reprocessing can drastically reduce the SF neutron radiation problem due to decay of Cm244 and Cf252 isotopes with particularly high SF source. However, longer cooling time also allows a valuable fissile nuclide Pu241 to decay to Am241 with the half life of about 14.4 years. Am241 is hard to transmute because of the fast decay of daughter nuclide Am242 to Cm242 and then to Pu238. In addition, Am241 is a source of high energy γ-photons which are also difficult to shield.

Accumulation of He gas as a result of α – decay of some short lived actinides (primarily Cm242) may lead to internal pressurization of TRU containing fuel pins challenging the fuel performance especially under accident conditions.

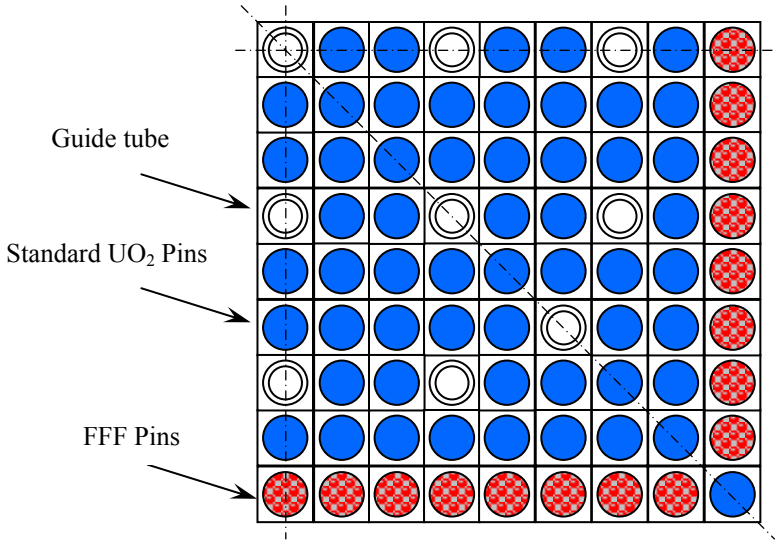

Figure 10.2.1. CONFU Assembly Configuration

The relative fraction of fissile isotopes in the TRU vector is reduced from about 60% in the initial spent UO_2 to about 25% at equilibrium. As a result, the fuel cycle length is reduced by about 30%. An increase in the enrichment of UO_2 pins from 4.2 to at least 5% is required to compensate for the TRU isotopics degradation.

The environmental impact of the cycle with recycling of TRU is limited by the efficiency of TRU recovery in the spent fuel reprocessing. Figure 10.2.2 compares the radiotoxicity of the actinides in a conventional UO_2 once through fuel cycle with that of the reprocessing waste

stream losses of 0.1% in the sustainable CONFU based fuel cycle. The achievable reduction in decay heat and radiotoxicity is up to a factor of 1000 compared to direct disposal of spent fuel in the once through fuel cycle.

3-dimensional whole core neutronic simulations were performed in order to demonstrate the feasibility of CONFU concept. A number of potential CONFU candidate approaches for the whole PWR core design were simulated and compared to the reference UO_2 and 100% fertile free TRU containing cores. The CONFU cases included micro-heterogeneous configuration where FFF pins are located in the periphery of each assembly (Figure 10.2.1) and macro-heterogeneous configurations where FFF pins occupy the whole assembly region. On average, the macro-heterogeneous PWR core contains about 20% of FFF assemblies while the remainder is occupied by the conventional UO_2 assemblies. For each of the core geometries, the first time recycled and equilibrium TRU compositions were considered as the two limiting cases.

The results confirmed technical feasibility of the CONFU based sustainable fuel cycle. The burnup achieved by the UO_2 fuel and FFF in both micro and macro heterogeneous configurations indicate the possibility of maintaining zero net balance of TRU in the closed fuel cycle. The neutronic characteristics e.g. power peaking factors and reactivity feedback coefficients of the CONFU cores are close to those of the reference UO_2 core (Table 10.2.I). The presence of TRU leads to the hardening of neutron spectrum and results in somewhat reduced soluble boron worth. The extent of this effect is directly related to the total TRU inventory in the core. As a result, operation of all-FFF core, evaluated for the comparison purposes, is particularly challenging and requires high burnable poison loading to maintain soluble boron concentration within allowable range. The Doppler coefficient is also less negative than in all-UO_2 core due to displacement of fertile U238 with fertile free matrix.

The effect of heterogeneous assembly structure and higher than typical power peaking factors on the Minimum Departure from Nucleate Boiling Ratio (MDNBR) margin was also studied. A single assembly based analysis performed for all the considered CONFU assembly options, with conservative assumptions regarding the core power peaking factors, showed a moderate deterioration of the MDNBR margin (by about 10 to 15%) in comparison with all-UO_2 fuel. The detailed whole core thermal hydraulic simulation of the most limiting micro heterogeneous CONFU case with first generation of TRU and simulation of the reference UO_2

core yielded MDNBR values of 1.43 and 1.71 respectively which is a reduction of about 20%. Both values however are higher than the W3-L correlation MDNBR limit of 1.3.

Table 10.2.I. Summary of 3-Dimensional core analysis results

Case	Distributed DC, HFP, pcm/F		MTC, HFP, pcm/F		Soluble BW, pcm/ppm		3D max. nodal power peaking factor
	BOC	EOC	BOC	EOC	BOC	EOC	
UO_2	-1.80	-1.82	-22.7	-41.6	-6.88	-8.86	2.03
FFF	-0.43	-0.51	-10.3	-32.8	-3.03	-4.70	1.91
CONFU-1	-1.42	-1.44	-19.2	-37.6	-5.70	-7.27	1.95
CONFU-E	-1.60	-1.53	-20.5	-40.9	-5.06	-6.41	1.88
M-CONFU-1	-1.60	-1.61	-21.4	-40.0	-6.06	-7.98	1.88
M-CONFU-E	-1.63	-1.60	-25.5	-39.6	-5.45	-6.56	1.86

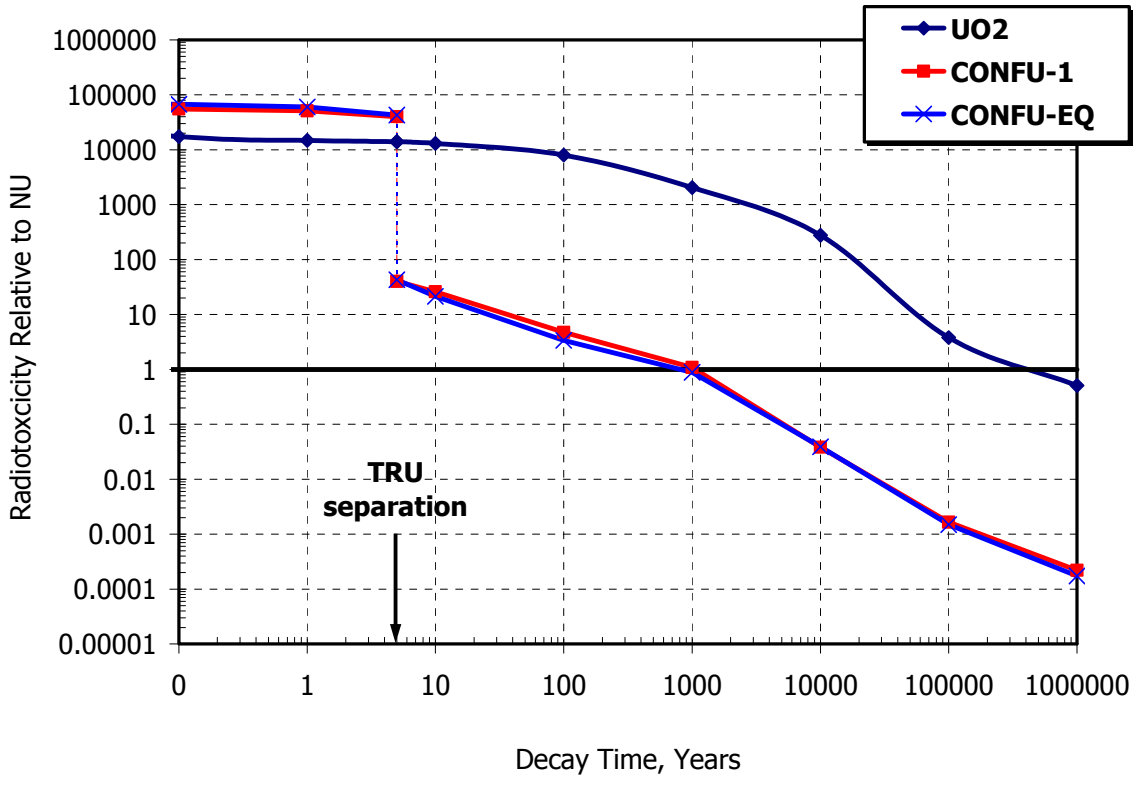

Figure 10.2.2. Actinide radiotoxicity of the sustainable CONFU fuel based cycle

10.3. Consideration of Accidents

The reduced delayed neutron fraction and Doppler coefficient for the TRU containing CONFU cores may result in inferior core response to fast reactivity transients such as a Control Rod Ejection (CRE) accident. Additionally, the fuel material properties such as melting temperature, thermal conductivity, and heat capacity are very different for the UO_2 and fertile free fuels. A simple computer model simulating the core response to a CRE accident was developed to assess these effects.

The simulation approach is based on the point kinetics model for neutronics with thermal reactivity feedback and accounts for the differences in materials thermal properties. The reactor kinetics data and reactivity worth of individual control rods were obtained from the 3-dimensional whole core analysis. The simulation results of the CONFU and all-FFF cases were compared with those of the reference all-UO_2 case.

The CONFU fuel exhibits similar characteristics to all-UO_2 fuel dynamic behavior because of the fact that the CONFU core physics is still dominated by the UO_2 fuel. Efficient TRU destruction in FFF pins allows for the small TRU inventory and mitigates the negative effects of TRU presence in the core. Higher than UO_2 thermal conductivity of FFF matrix does not offset the effect of lower FFF melting point. FFF pins in the CONFU assembly exhibit more limiting than UO_2 pins performance in CRE accident due to larger relative degradation of margin to the fuel melting temperature.

However, larger than UO_2 heat capacity of the fertile free fuel matrix implies higher thermal inertia and slower response to transients which is a desirable feature. In the Loss of Coolant Accident (LOCA), the fuel melting temperature is reached at about the same time for the UO_2 and FFF assuming instantaneous loss of all cooling capabilities and identical decay heat power evolution for both fuel types. Identical fuel pin geometries for FFF and UO_2 pins in the CONFU assembly and in typical PWR assembly suggest similar behavior to all-UO_2 fuel during LOCA with regards to re-flood capabilities. However, higher power peaking in FFF pins diminishes this potential advantage of FFF matrix. Additionally, the maximum cladding temperature during blowdown phase of LOCA is related to fuel stored energy rather than thermal inertia. At a comparable power level, the stored energy in UO_2 and FFF pins is about the same despite higher Cp of the FFF due to its better thermal conductivity and therefore slightly lower temperature. The

stored energy is about 13% higher in FFF pins than in UO2 pins if local power peaking is considered.

All-FFF, TRU-MOX, and TRU-ThO_2 fuel have the potential for positive void coefficients during a LOCA without scram accident or in the case of substantial local voiding in the core. The positive void coefficient is a result of high TRU loading required to achieve a desired fuel cycle length. The CONFU core, similarly to the reference UO_2 core, exhibits monotonic reactivity decrease with increasing coolant void fraction because of the high efficiency of TRU destruction in FFF pins and therefore minimal required TRU inventory.

10.4. Feasibility of TRU Multi-recycling

Multi-recycling of TRU was proven to be feasible with respect achieving an equilibrium state with zero net balance of TRU. However, the equilibrium TRU isotopic vector has a larger fraction of MA than the first time reprocessed UO2 fuel. Furthermore, some MA isotopes do not reach their equilibrium concentrations within 20 recycle stages. The buildup of these isotopes does not affect the core physics but it has a significant effect on the feasibility of fuel handling and reprocessing.

Two major issues associated with an increased MA fraction in the TRU vector and buildup of non-saturating MA nuclides can be distinguished. First, reprocessing of the spent TRU containing fuel with conventional aqueous solvent extraction based methods may prove to be impossible due to the high levels of radiation resulting from increased MA content. The organic solvent agents rapidly degrade in the high radiation environment. This may limit the TRU fuel reprocessing options to the more advanced non-aqueous pyrochemical or pyrometallurgical techniques. Non-aqueous reprocessing can be potentially more economical than conventional aqueous reprocessing. Therefore, it can be implemented on a small scale close to the nuclear power generation units eliminating the requirement for spent fuel transportation over long distances.

The second issue is related to manufacturing of TRU containing fuel. Increased radiation, especially from spontaneous fission (SF) neutrons, will require significant shielding and completely remote fuel fabrication and handling. The buildup of SF neutrons emitting MA is

likely to be the limiting factor with respect to the number of practically feasible number of TRU recycles.

Evaluation of TRU characteristics at the fuel reprocessing and fabrication stages indicate that the TRU activity and decay heat power approach their equilibrium values within 3 to 5 recycles. The activity saturates at a level about 30% higher than that of the first time recycled TRU, while the decay heat saturates at the level which is higher by about a factor of two than that of the first time recycled TRU.

Monotonic increase of the SF source with the number of recycles can be significantly slowed down by extension of the cooling time between fuel discharge and its reprocessing. In case that the 7 years cooling time is extended to 20 years, the SF source for the 5 times recycled TRU in the CONFU fuel cycle would be comparable to that of the once recycled Pu in a typical PuO_2-UO_2 MOX fuel (Figure 10.4.1). Moreover, decay heat generation saturates within a fewer number of recycles at about 50% lower level than in the case of 7 years cooling time. The equilibrium decay heat value with 20 years cooling is also comparable to the once recycled MOX fuel after 10 year decay. The 20 years of cooling is possible if a large number of reactors would adopt the CONFU fuel with TRU recycling. In this case, the long time between recycles would not necessarily delay the attainment of an equilibrium state, as the spent fuel of one reactor could be recycled in the cores of other reactors.

The total dose rate from TRU in re-fabricated "fresh" fertile free fuel is dominated by γ radiation for the first 10 recycles if the 20 years cooling time is adopted. The γ dose rate saturates within 3 to 5 recycles at an equilibrium value about twice as high as that of the first time recycled TRU. The SF neutron dose rate increases monotonically primarily due to the buildup of Cf250 and Cf252 isotopes which results in an increase of SF source. However, the γ and SF neutron dose rates become comparable only after about 20 recycles. It was concluded that at least 10 TRU recycles should be feasible by implementation of relatively straightforward shielding arrangements to reduce the radiation dose rates during fuel fabrication to safe levels.

Management of the CONFU fuel containing more than 20 times recycled TRU is likely to require completely remote handling and pyrochemical reprocessing. Advanced fuel fabrication techniques such as vibro-packing may be found particularly beneficial. Cm separation and storage

to reduce the radiation dose from TRU may be challenging because of the difficulties associated with separated Cm handling and potential criticality accidents.

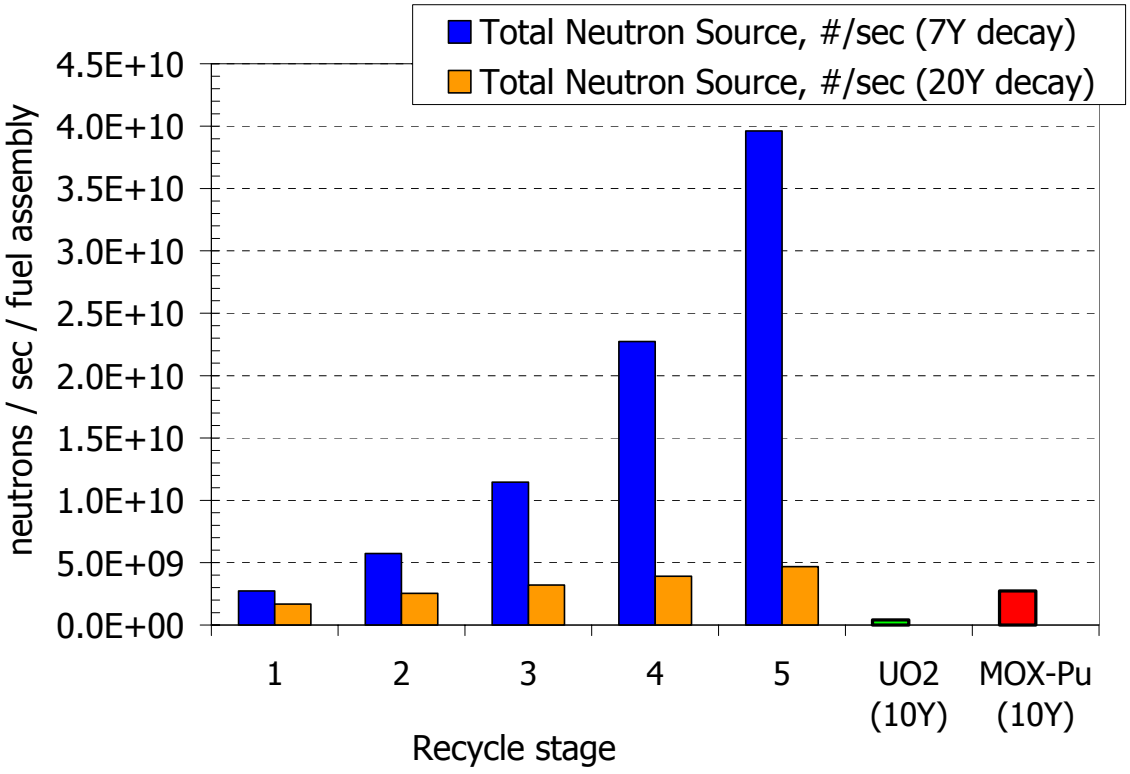

Figure 10.4.1 SFS per fuel assembly: 7y vs. 20y decay comparison

10.5. Sustainable Fuel Cycle Economics

The uncertainty in cost estimation of the fuel reprocessing and TRU containing fuel fabrication represents the main difficulty in the evaluation of the sustainable fuel cycle economic performance. Median values for the unit costs reported in a comprehensive waste transmutation study [OECD/NEA, 2002] were adopted for the current analysis.

Sixty percent increase in fuel cycle cost relative to conventional once through fuel cycle was estimated by a simple economic analysis of the sustainable PWR fuel cycle based on CONFU assembly concept. The increase in total cost of electricity (COE) however is only 8%.

The higher fuel cycle cost is a result of higher uranium enrichment in a CONFU assembly required to compensate for the degradation of TRU isotopics. The major expense in the sustainable CONFU fuel cycle is associated with the reprocessing of UO_2 fuel. Although reprocessing and fabrication of FFF pins have relatively high unit costs, their contribution to the fuel cycle cost is marginal as a result of the small TRU inventory. A reduction in the unit costs of UO_2 reprocessing and FFF fabrication by a factor of two would result in comparable fuel cycle costs for the CONFU and conventional once through cycle. An increase in natural uranium prices and waste disposal fees will also reduce the gap between the costs of the once through and closed fuel cycles.

The economic performance of an alternative to CONFU closed fuel cycle was also evaluated. The system assumes once through fuel cycle operation of conventional LWR which provides TRU for a fast spectrum Actinide Burner Reactor (ABR) operating in a closed fuel cycle. The ABR is an innovative design which utilizes 700 MW_{th} capacity and 45% efficient power conversion cycle. The ratio of LWRs to ABRs in the system is such that it provides zero net TRU generation. The total COE for the CONFU and LWR-ABR cycle are similar for the assumed set of operational characteristics of both systems. Neutronic superiority of the fast spectrum allows operation of PWR without requirements for UO_2 enrichment increase. Lower uranium enrichment cost in PWR-ABR cycle offsets its higher capital and O&M costs in comparison with LWR CONFU based cycle. Nevertheless, the major advantage of the CONFU concept is the possibility of its application to the existing fleet of reactors with immediate realization of all the sustainable fuel cycle benefits.

A number of alternative fuel cycles were compared in a comprehensive transmutation systems assessment by the OECD [OECD/NEA, 2002a] in terms of there economic performance and environmental impact. Figure 10.5.1 shows the results of this assessment. Index RLOSS is defined as TRU losses to the repository relative to once through fuel cycle, while quantity RCOST represents total cost of electricity relative to that of the once through fuel cycle. The results of the current analysis for the CONFU and PWR-ABR fuel cycles are also plotted in Figure 10.5.1 for the comparison. Both, the CONFU and PWR-ABR fuel cycles exhibit superior performance to any of the fuel cycles considered in OECD study primarily because both systems employ fertile free fuel technology which allows minimization of TRU inventory within the cycle.

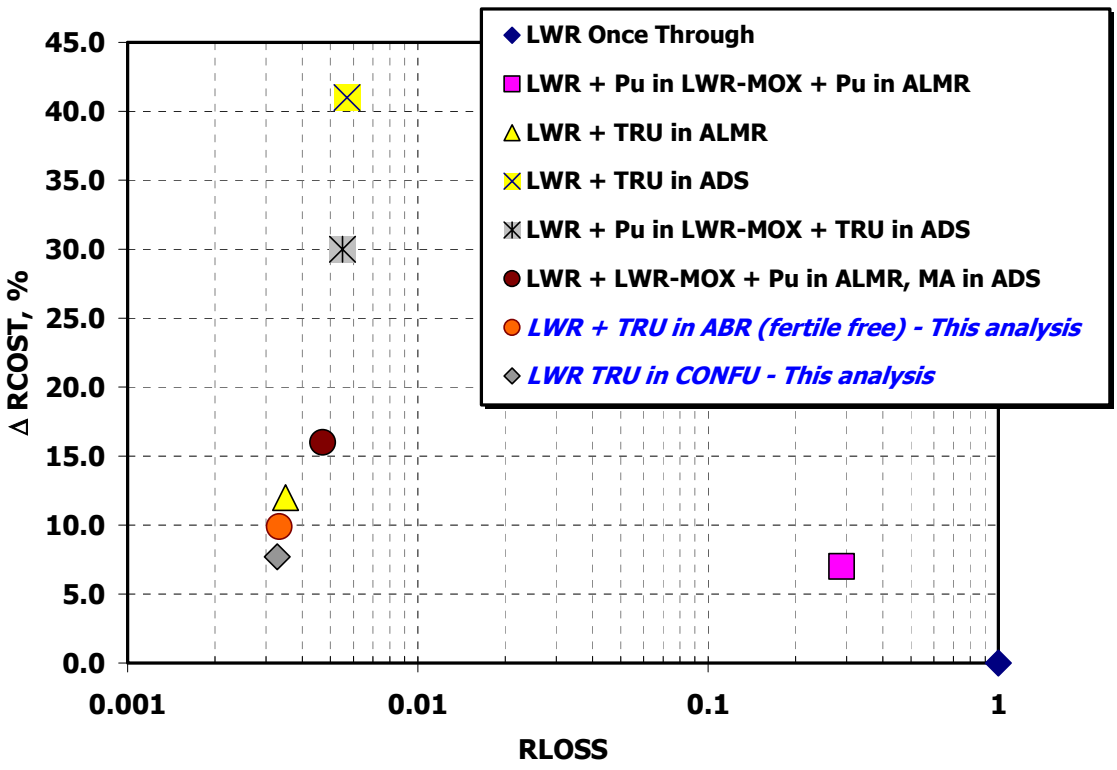

Figure 10.5.1. TRU loss vs. COE comparison of CONFU and PWR-ABR cycles with [OECD/NEA, 2002a] results.

10.6. Recommendations for Future Work

The sustainable fuel cycle cannot be implemented unless it is economically competitive with the existing alternatives. Therefore, a major research effort should be directed to the development of UO_2 fuel reprocessing and TRU containing fuel fabrication technologies aiming at reduction of their costs.

The possibility of TRU recovery with the efficiency required to meet the environmental goals of the waste transmutation on a large industrial scale has yet to be demonstrated. The focus should be on the non-aqueous fuel reprocessing technologies as they offer significant advantages in proliferation resistance, a potential for reprocessing cost reduction, the capability of operation in high radiation environment, and reduction of the waste volume.

Long term environmental and non-proliferation benefits of the closed fuel cycle must be carefully evaluated against increased risks of radiation exposure and diversion of weapons usable materials during spent fuel reprocessing, fabrication and handling.

The development of TRU hosting fuels is the most cost and time demanding task due to the requirement of fuel irradiation testing to investigate the fuel behavior under normal operating conditions and during accidents. Although the fertile free fuel is the most attractive option among the candidates because of its TRU destruction capabilities, it is the least explored option and therefore also requires major R&D effort.

Strategies aiming at the reduction of the long term risks from the nuclear fuel cycle through application of the spent fuel partitioning and transmutation technologies have to be carefully evaluated against increased short term radiological and proliferation risks associated with additional spent fuel handling. Methodology development for the assessment of such tradeoffs is another important area of research.

Finally, the CONFU assembly concept can also be utilized for reduction of the already existing stockpile of TRU from over 40 years of LWRs operation in the once through fuel cycle mode. The number of TRU hosting FFF pins per assembly can be increased to achieve net TRU destruction rather than zero balance while still maintaining acceptable neutronic characteristics. In contrast to the once through burndown scenario, the residual TRU can be recycled and refabricated to “fresh” FFF pins for the next CONFU cycle. The performance and technical feasibility of such a design as well as the operational and safety limits on TRU inventory are suggested as subjects for future investigation.

References

AECL Technologies Inc., "Optimization and Implementation Study of Plutonium Disposition Using Existing CANDU Reactors", Final Report, (1996).

Akie H., Takano H., Anoda Y., " Core Design Study on Rock-like Oxide Fuel Light Water Reactor and Improvements of Core Characteristics", *Journal of Nuclear Materials*, **274,** pp. 139-145, (1999).

Albright D., Berkhout F., Walker W., "*Plutonium and Highly Enriched Uranium 1996. World Inventories, Capabilities and Policies"*, Oxford University Press, (1997).

Aniel S., Puill A., Bergeron J., Rohart M., "Plutonium Multirecycleing in PWR. The CORAIL Concept", *Proc. of ICONE-8, 8th International Conference on Nuclear Engineering*, Baltimore, USA, April, (2000).

Bairiot H., Vandenberg C., "Use of MOX Fuels" *Nuclear Fuel Cycle in the 1990's and Beyond the Century: Some Trends and Foreseeable Problems*, Technical Reports Series No. 305, page 73, IAEA, Vienna, (1989).

Battat M. E. (Chairman), ANS-6.1.1 Working Group, ''American National Standard Neutron and Gamma-Ray Flux-to-Dose Rate Factors,'' ANSI/ANS-6.1.1-1977 (N666), American Nuclear Society, LaGrange Park, Illinois, (1977).

Belle J., Berman R. M. (Editors), "Thorium Dioxide: Properties and Nuclear Applications." *DOE/NE-0060*, Naval Reactors Office, USDOE, August 1984.

Beller D.E. et. al., "The U.S. Accelerator Transmutation of Waste Program", *Nuclear Instruments and Methods in Physics Research*, **A 463,** pp. 468-486, (2001).

Berna G.A., Beyer C.E., Davis K.L., Lanning D.D., "FRAPCON-3: A Computer Code for the Calculation of Steady State Thermal-Mechanical Bahavior of Oxide Fuel Rods for High Burnup", NUREG/CR-6534, Vol. 2, PNNL-11513, December (1997).

Boulilis B., Brossard P., "Assessment of Pyrochemical Processes for Separation/Transmutation Strategies: Proposed Areas of Research", *Proc. of International Workshop on Pyrochemical Separations*, OECD/NEA, Avignon, France, March 14-16, (2000).

Bowman C. D. et al., "Nuclear energy generation and waste transmutation using an accelerator-driven intense thermal neutron source", *Nuclear Instruments and Methods in Physics Research Section A*, **320**, pp. 336-367, (1992).

Bowman C. D., "Once-Through Thermal-Spectrum Accelerator-Driven LWR Waste Destruction without Reprocessing"*, Nuclear Technology,* **132**, 66 (2000).

Bowman C. D., "Once-Through Thermal-Spectrum Accelerator-Driven Waste Transmutation: Performance Calculations", Report ADNA/01-03, ADNA Corporation, Los Alamos, NM 87544 (2001).

Bresee J.C., "A roadmap for developing accelerator transmutation of waste (ATW) technology", A report to Congress, Review of national accelerator driven system programmes for partitioning and transmutation Proceedings of an Advisory Group meeting, Taejon, Republic of Korea, 1–4 November 1999, IAEA-TECDOC-1365, August (2003).

Briesmeister J. F. (editor), "MCNP^{TM} - A General Monte Carlo N-Particle Transport Code, Version 4C," LA-13709M, Los Alamos National Laboratory, April (2000).

Briesmeister J. F. Ed., "MCNP - A General Monte Carlo N-Particle Code, Version 4C, Appendix H", Los Alamos National Laboratory, LA-13709-M, March (2000).

Broeders C.H.M., Kiefhaber E., Wiese H.W., "Burning transuranium isotopes in thermal and fast reactors", *Nuclear Engineering and Design*, **202**, pp. 157–172, (2000).

Brusselaers P. *et al*., "Possible Transmutation of Long-lived Fission Products in Usual Reactors", *Proc. Int. Conf. on the Physics of Reactors: PHYSOR 96*, **3**, p. M-101, Mito, Japan, September 16-20, (1996).

Bunn M., Fetter S., Holdren J.P., Van der Zwaan B., "The Economics of Reprocessing vs. Direct Disposal of Spent Nuclear Fuel", DE-FG26-99FT4028, J.F. Kennedy School of Government, Harvard University, July (2003).

Bunn M., Holdren J. P., Macfarlane A., Pickett S. E., Suzuki A., Suzuki T., Weeks J., "Interim Storage of Spent Nuclear Fuel: A Safe, Flexible, and Cost-Effective Near-Term Approach to Spent Fuel Management", Harvard University Project on Managing the Atom, University of Tokyo Project on Sociotechnics of Nuclear Energy, June (2001).

Burghartz M., Matzke Hj., Leger C., Vambenepe G., Rome M., "Inert matrices for the transmutation of actinides: fabrication, thermal properties and radiation stability of ceramic materials", *Journal of Alloys and Compounds*, **271–273**, pp.544–548, (1998).

Bychkov A.V. et al., "Pyroelectrochemical Reprocessing of Irradiated FBR-MOX Fuel. III. Experiment on High Burn-up Fuel of the BOR-60 Reactor", *Proc. Int. Conf. on Future Nuclear Systems, Global'97*, p. 912, Yokohama, Japan, 5-10 October (1997).

Carbajo J.J., Gradyon L.Y., Popov S.G., Ivanov V.K., "A review of the Thermophysical Properties of MOX and UO2 Fuels", *Journal of Nuclear Materials*, **299**, pp 181-198, 2001.

Carminati F., Klapisch R., Revol J.P., Roche Ch., Rubio A.J. Rubbia C., "An Energy Amplifier for Cleaner and Inexhaustible Nuclear Energy Production Driven by a Particle Beam Accelerator," CERN/AT/93-47(ET), CERN, Geneva, November (1993).

Chang Y.I., "The Integral Fast Reactor", *Nuclear Technology*, 88, 129 (1989).

Chidester K., Ramsey K.B., Eaton S.L., "Disposition of Plutonium as Non-Fertile Fuel for Water Reactors", LA-UR-91-1879, LANL, (1998).

Chodak P., "Destruction of Plutonium Using Non-Uranium Fuel in Pressurized Water Reactor Peripheral Assemblies", Ph.D. Thesis, Department of Nuclear Engineering, Massachusetts Institute of Technology, (1996).

Combustion Engineering Inc., "Analysis of Existing CE-ABB Light Water Reactors for the Disposition of Weapons Grade Plutonium", Final Report, (1994).

CRC Press, "Properties of Inorganic Compounds", *CRC Handbook of Chemistry and Physics*, 3rd Electronic Edition, http://www.knovel.com (2000).

Croff A. G., "A User's Manual for the ORIGEN2 Computer Code," ORNL/TM-7175, Oak Ridge National Laboratory, July (1980).

Croff A. G., "ORIGEN2: A Versatile Computer Code for Calculating the Nuclide Compositions and Characteristics of Nuclear Materials" *Nuclear Technology*, September (1983).

Cronin J. T., Smith K. S., Ver Planck D. M., "SIMULATE-3 Methodology, Advanced Three-Dimensional Two-Group Reactor Analysis Code", Studsvik/SOA-95/18, Studsvik of America, Inc., (1995).

Cuta J. M., Koontz A. S., Stewart C. W., Montgomery S. D., Nomura K. K., "VIPRE-01: A Thermal-Hydraulic Code for Reactor Cores, Volume-2, User's Manual (Revision 2)", EPRI-NP-2511-CCM, Electric Power Research Institute (EPRI), July (1985).

Damen P.M.J, Kloosterman J.L., "Dynamic Aspects of Plutonium Burning in an Inert Matrix", *Pregress in Nuclear Energy*, **38**, No. 3-4, pp 371-374, 2001.

Damen P.M.J, Kloosterman J.L., "Reactor Physics Aspects of Plutonium Burning in Inert Matrix Fuels", *Journal of Nuclear Materials*, **274**, pp 112-119, 1999.

Degueldre C., Tissot P., Lartigue H., Pouchon M., "Specific Feat Capacity and Debye Temperature of Zirconia and its Solid Solution", *Thermochimica Acta,* **403**, 2, pp. 267-273, July (2003).

Diamond D.J., Bromley B.P., Aronson A.L., "Studies of the Rod Ejection Accident in a PWR", W-6382, Brookhaven National Laboratory, January 22, (2002).

DiGiovine A. S., Rhodes J. D., "SIMULATE-3 User's Manual", Studsvik/SOA-95/15, Studsvik of America, Inc., (1995).

DOE/Generation IV International Forum, "A Technology Roadmap for Generation IV Nuclear Energy Systems", GIF-002-00, *U.S. DOE Nuclear Energy Research Advisory Committee and the Generation IV International Forum*, December (2002).

DOE/NE, "Report to Congress on Advanced Fuel Cycle Initiative: The Future Path for Advanced Spent Fuel Treatment and Transmutation Research", US Department of Energy, Office of Nuclear Energy, January (2003).

Dostal V., Todreas N.E., Hejzlar P., and Kazimi M.S., "Power Conversion Cycle Selection for the LBE Cooled Reactor with Forced Circulation", MIT-ANP-TR-085, Massachusetts Institute of

Technology, Department of Nuclear Engineering, Center for Advanced Nuclear Energy Systems, February (2002).

Downar T., Kim C.H., Kim T.K., Xu Y., Takahashi H., Rohatgi K., "Feasibility Study of a Plutonium-Thorium Fuel Cycle for a High-Conversion Boiling Water Reator", *Trans. of the American Nucl. Soc.*, **83**, (2000).

Driscoll M.J., Downar T.J., Pilat E.E., *The Linear Reactivity Model for Nuclear Fuel Management*, American Nuclear Society, LaGrange Park, (1990).

Edenius M., Ekberg K, Forssen B.H., Knott D., "CASMO-4, A Fuel Assembly Burnup Program: User's Manual", STUDSVIK/SOA-95/1, Studsvik of America, Inc., (1995).

Edenius M., Ekberg K., Forssen B. H., Knott D., "CASMO-4, A Fuel Assembly Burnup Program, User's Manual", Studsvik/SOA-95/1, Studsvik of America, Inc., (1995).

Feinberg S.M., Kunegin E.P., "Proceedings of the Second United Nations International Conference on the Peaceful Uses of Atomic Energy", *Nuclear Power Plants*, **9**, Part 2, pp. 447-448, Record of Proceedings of Session B-10: Power Reactor Experiments, Discussion Comment, United Nations, Geneva, (1958).

Finck, P. J. "The Physics of transmutation systems: system capabilities and performances", Argonne National Laboratory, ANL/TD/CP-108527, (2002).

Fink J. K., Leibowitz L., "Thermal conductivity of zirconium"*, Journal of Nuclear Materials*, **226**, pp. 44-50, (1995).

Fink J.K., "Thermophysical properties of uranium dioxide", *Journal of Nuclear Materials*, **279**, pp. 1-18, (2000).

Fischer G.J. et al., "Physics and Feasibility Study of the Fast-Mixed-Spectrum Reactor Concept", Brookhaven National Laboratory, BNL-25598, January 1, (1979).

Forsberg C.W., Hopper C.M. and Vantine H.C., "What is Nonweapons-Usable U-233?" *Trans. Am. Nucl. Soc.*, **81**, p. 62, Long Beach, California, November 14-18, (1999).

Fuchs K., "Efficiency for very slow neutron assembly", LA-596, Los Alamos National Laboratory, (1946).

Galperin A., Segev M., Todosow M., "Pressurized water reactor plutonium incinerator based on thorium fuel and seed-blanket assembly geometry", *Nuclear Technology*, **132** (2), pages 214-226 Nov. (2000).

GE Nuclear Energy, "Study of Plutonium Disposition Using the GE Advanced Boiling Water Reactors (ABWR)", Final Report, (1994).

Gohar Y., Taiwo T. A., Cahalan J.E., Finck P. J., "Assessment of the General Atomics Accelerator Transmutation of Waste Concept Based on the Gas-Turbine-Modular Helium Cooled Reactor Technology", ANL/TD/TM01-16, Argonne National Laboratory, January (2001).

Handwerk C.S., Driscoll M.J., Todreas N.E., Mac Mahon M.V., "Economic Analysis of Extended Operating Cycles in Existing LWRs", *MIT-NFC-TR-007*, Massachusetts Institute of Technology, January, (1998).

Hejzlar P., Buongiorno J., Mac Donald P. E. and Todreas N.E., "Strategy for Actinide Burning in Medium Power Lead-alloy Cooled Concepts", *Nuclear Technology*, submitted (2003).

Hejzlar P., Driscoll M.J., Kazimi M.S., "Conceptual Neutronic Design of a Lead-Bismuth-Cooled Actinide Burning Reactor," *Nuclear Science and Engineering*, **139**, pp.1-18, (2001).

Hejzlar P., Driscoll M.J., Kazimi M.S., Todreas N.E., "Minor Actinide Burning in Dedicated Lead-Bismuth Cooled Fast Reactors," *Proc. of the ICONE-9, 9th International Conference on Nuclear Engineering*, Nice, France, April 8-12, (2001).

Hetrick D.L., "*Dynamics of Nuclear Reactors*", pp. 164-174, The University of Chicago Press, Ltd. Chicago, (1971).

Hidaka A., Nakamura J., Sugimoto J., "Influence of Thermal Properties of Zirconia Shroud on Analysis of PHEBUS FPT0 Bundle Degradation Test with ICARE2 Code", *Nuclear Engineering and Design,* **168**, 1-3, pp. 361-371, May (1997).

Hill R. N., Taiwo T. A., Stillman J. A., Graziano D. J., Bennett D. R., Trellue H., Todosow M., Halsey W. G., Baxter A., "Multiple Tier Fuel Cycle Studies for Waste Transmutation", *ICONE-10: Tenth International Conference on Nuclear Engineering*, Arlington, Virginia, USA, (2002).

Hill R.N., Wade D.C., Liaw J.R., Fujita E.K., "Physics Studies of Weapons Plutonium Disposition in the Integral Fast Reactor Closed Fuel Cycle", *Nuclear Science and Engineering*, **121**, pp. 17-31, (1995).

IAEA, "Accelerator Driven Systems: Energy Generation and Transmutation of Nuclear Waste", Status Report, IAEA-TECDOC-985, November, (1997).

ICRP (Edited), "ICRP Publication 68: Dose Coefficients for Intakes of Radionuclides by Workers: A report of a Task Group of Committee 2 of the International Commission on Radiological Protection", 0-08-042651-4, (1995).

Inoue T. and Tanaka H., "Recycling of Actinides Produced in LWR and FBR Fuel Cycles by Applying Pyrometallurgical Process", *Proc. Int. Conf. on Future Nuclear Systems, Global'97*, p. 646, Yokohama, Japan, 5-10 October (1997).

INSC - International Nuclear Safety Center, Material Properties Database, "Zircaloy Heat Capacity", http://www.insc.anl.gov.

Joo H.G. et al., "PARCS: A Multi-Dimensional Two-Group Reactor Kinetics Code Based on the Nonlinear Analytic Nodal Method," PU/NE-98-26, Purdue University, School of Nuclear Engineering, September (1998).

Kasemeyer U., Paratte J.M., Grimm P., Chawla R., "Comparison of Pressurized Water Reactor Core Characteristics for 100% Plutonium-Containing Loadings," *Nuclear Technology*, **122**, pp. 52–63, April (1998).

Kazimi M.S., Czerwinski K. R., Driscoll M.J., Hejzlar P., Meyer J.E., "On The Use of Thorium in Light Water Reactors", MIT-NFC-TR-016, Department of Nuclear Engineering, Massachusetts Institute of Technology, April (1999).

Kim D., Kazimi M.S., Todreas N.E., Driscoll M.J., "Economic Analysis of the Fuel Cycle of Actinide Burning Systems", ", *MIT-NFC-TR-019*, Massachusetts Institute of Technology, February, (2000).

Kloosterman J.L., "Dynamics Aspects of Plutonium Recycling in PWRs: Influence of the Moderator to Fuel Ratio", *Proc. PHYSOR 2000*, Pittsburgh, USA, May 7-11, (2000).

Knott D., Forssen B. H., Edenius M., “CASMO-4, “A Fuel Assembly Burnup Program, Methodology”, Studsvik/SOA-95/2, Studsvik of America, Inc., (1995).

Koch L., “Role of Pyrochemistry in Advanced Nuclear Energy Generating Systems”, *Proc. of International Workshop on Pyrochemical Separations*, OECD/NEA, Avignon, France, March 14-16, (2000).

Koch L., Glatz J.P., Konings M.J.R., Magill J., “Partitioning and Transmutation Studies at ITU”, *EUR 19054* (1999).

Kodochigov N., Sukharev Yu., Marova E., Ponomarev-Stepnoy N., Glushkov E., Fomichenko P., “Neutronic Features of the GT-MHR Reactor”, *Proc. of ICONE-10, 10th International Conference on Nuclear Engineering*, Arlington, VA, April 14-18, (2002).

Koster A., Matzner H.D., Nicholsi D.R., “PBMR design for the future”, *Nuclear Engineering and Design*, **222**, pp. 231–245, (2003).

Krivitski I. Y., Kochetkov A. L., “Actinide and Fission Product Burning in Fast Reactors with a Moderator”, *Actinide and Fission Product Partitioning and Transmutation*, 6th Information Exchange Meeting, OECD/NEA EUR 19783, Madrid, Spain, 11-13 December (2000).

Kuraishi H., Sawada T., Ninokata H., "Inherent and Passive Safety Sodium-Cooled Fast Reactor Core Design with Minor Actinide and Fission Product Incineration," *Nucl. Sci.Eng*., **138**, pp. 205-232, (2001).

Kuznetsov V.V., Sekimoto H., “Radioactive Waste Transmutation and Safety Potentials of the Lead-Cooled Fast Reactor in the Equilibrium State”, *Journal of Nuclear Science and Technology*, **32**, 6, pp. 507-516, June (1995).

LaBar M. P., “The Gas Turbine – Modular Helium Reactor: A Promising Option for Near Term Deployment”, General Atomics, GA-A23952, April (2002).

Laidler J.J., “Pyrochemical Separation Technologies Envisioned for the US Accelerator Transmutation of Waste System”, *Proc. of International Workshop on Pyrochemical Separations*, OECD/NEA, Avignon, France, March 14-16, (2000).

Laughter M., Hejzlar P., Kazimi M.S., "Self-Protection Characteristics of Uranium-233 in the ThO2-UO2 PWR Fuel Cycle", MIT-NFC-TR-045, MIT, Nuclear Engineering Department, Cambridge, MA, (2002).

Lebenhaft J. R., Driscoll M. J., "Monte Carlo Simulation of Pebble Bed HTGR Criticals", *Tran. Am. Nucl. Soc.*, **86**, Hollywood, Florida, June 9–13, (2002).

Lombardi C., Mazzola A., "Exploiting the Plutonium Stockpiles in PWRs by Using Inert Matrix Fuel", *Annals of Nuclear Energy*, **23**, 14**,** pp. 1117-1126, (1996).

Lombardi C., Mazzola A., Padovani E., Ricotti M.E., "Neutronic analysis of U-free inert matrix and thoria fuels for plutonium disposition in pressurised water reactors", *Journal of Nuclear Materials*, **274**, pp. 181-188, (1999).

Lombardi C., Padovani E., Ricotti M. E., Vettraino F., "Plutonia-Thoria Fuel Cycle As Starting Solution for a Wider Thorium Use", *Proc. International Conference on Future Nuclear Systems (GLOBAL '99)*, Jackson Hole, WY, (1999).

Long Y., Monnier P., Schultz S.P. and Kazimi M.S., "Modeling the Rim Effect and Fission Gas Release Performance in Thoria Fuel," *Proc. of International Topical Meeting on LWR fuel Performance*, Park City, Utah, April (2000).

Long Y., Zhang Y., Kazimi M.S., "A Survey of Inert Matrix Materials as Hosts of Actinide Nuclear Fuels", MIT-NFC-TR-055, Department of Nuclear Engineering, Massachusetts Institute of Technology, March (2003).

Lowenthal M.D., "Transmutation in the Nuclear Fuel Cycle: Approaches and Impacts", *Nuclear Technology*, **138**, 284-299, June (2002).

Lung M., "A Present Review of the Thorium Nuclear Fuel Cycles", European Commission, Nuclear Science and Technology Series, EUR 17771, 1997.

Nakamura T. , Kusagaya K., Yoshinaga M., Uetsuka H., Yamashita T., "Rock-like oxide fuel behavior under reactivity initiated accident conditions", *Progress in Nuclear Energy*, **38**, No. 3-4, pp. 379-382, (2001).

Nakamura T., Kusagaya K., Sasajima H., Yamashita T., Uetsuka H., "Behavior of YSZ based Rock-Like Oxide Fuels under Simulated RIA Conditions"**,** *Journal of Nuclear Science and Technology*, **40**, No. 1, pp. 30–38, January (2003).

National Research Council, *"Nuclear Wastes: Technologies for Separation and Transmutation"*, National Academy Press, Washington D.C. (1996).

Nitani N., Yamashita T., Matsuda T., Kobayashi S.-I., Ohmichi T., "Thermophysical Properties of Rock-Like Oxide Fuel With Spinel-Yttria Stabilized Zirconia System", *Journal of Nuclear Materials*, **274,** pp 15-22, (1999).

Nordheim L.W., "Pile kinetics", MDDC-35, (1946).

Nuclear News, "World List of Nuclear Power Plants", American Nuclear Society, March (2003).

Oak Ridge National Laboratory, RSICC Computer Code Collection, "ORIGEN 2.1, Isotope Generation and Depletion Code Matrix Exponential Method", CCC-371, Oak Ridge, Tennessee, Revised version, May (2002).

OECD/NEA, *1st Phase P&T Systems Study: Status and Assessment Report on Actinide and Fission Product Partitioning and Transmutation*, May (1999).

OECD/NEA, *Accelerator-Driven Systems (ADS) and Fast reactors (FR) in Advanced Nuclear Fuel Cycles: A Comparative Study*, Paris, France, (2002a).

OECD/NEA, *Nuclear Fuel Safety Criteria Technical Review*, Paris, France (2001).

OECD/NEA, *The Economics of the Nuclear Fuel Cycle*, (1994).

OECD/NEA, *Trends in the Nuclear Fuel Cycle: Economic, Environmental and Social Aspects*, Paris, France, (2001).

OECD/NEA, *Uranium 2001: Resources, Production and Demand*, Paris, France, (2002b).

Oggianu S. M., Kazimi M. S., "A Review of Properties of Advanced Nuclear Fuels", MIT-NFC-TR-021, Department of Nuclear Engineering, Massachusetts Institute of Technology, February (2000).

Okonogi K., Nakamura T., Yoshinaga M., Ishijima K., Akie H., Takano H., "Pulse irradiation tests of rock-like oxide fuel", *Journal of Nuclear Materials*, **274,** pp. 167-173, (1999).

Olson G.L., McCardell R.K., Illum D.B., "Fuel Summary Report: Shippingport Light Water Breeder Reactor", INEL/EXT-98-00799, Rev.1, January (1999).

Orlov V.V., "Evolution of the technical concepts of fast reactors: The concept of BREST", AEA-TECDOC-1365, *Review of national accelerator driven system programmes for partitioning and transmutation, Proceedings of an Advisory Group meeting*, Taejon, Republic of Korea, 1–4 November 1999, IAEA, (2003).

Ott K.O., Neuhold R.J., "*Introductory Nuclear Reactor Dynamics*", American Nuclear Society, La Grange Park, IL, USA, (1985).

Pellaud B., "Proliferation aspects of plutonium recycling", *C. R. Physique 3* 1067–1079, (2002).

Peryoga Y., Saito M., Artisyuk V., Shmelev A., "Effect of Transplutonium Doping on Approach to Long-life Core in Uranium-fueled PWR", *Journal of Nuclear Science and Technology*, **39**, No. 8, p. 838–844, August (2002).

Phlippen P.W., Neuhaus I., "Thorium Assisted Pu Burning in PWRs", H. Gruppelaar, J.P. Schapira (Editors), *Thorium as a Waste Management Option*, Final Report EUR 19142EN, European Commission, (2000).

Puill A., Bergeron J., Rohart M., Aniel-Buchheit S., Bergeron A., Matheron P., "Progress in the studies of the Advanced Plutonium fuel Assembly", *Progress in Nuclear Energy,* **38**, No. 3-4, pp. 403-406, (2001).

Rempe K. R., Smith K. S., "SIMULATE-3 Pin Power Reconstruction: Methodology and Benchmarking," *Nuclear Science and Engineering*, **103**, pp. 334-342, (1989).

Romano A. "Optimization of Actinide Transmutation in Innovative Lead-Cooled Fast Reactors" PhD Thesis, Massachusetts Institute of Technology, Department of Nuclear Engineering, May, (2003).

Romano A., Hejzlar P., Todreas N. E., "Dedicated Fast Reactors for Efficient Minor Actinides Incineration: Neutronic Design of a Pb-Bi Cooled Concept," AAA Program Report, MIT-NFC-TR-050, October (2002).

RSICC Computer Code Collection, "ORIGEN 2.1, Isotope Generation and Depletion Code Matrix Exponential Method", CCC-371, Oak Ridge National Laboratory, Oak Ridge, Tennessee, Revised version, May (2002).

Rubbia C., Bruno S., Kadi Y., Rubio J. A., "Fast Neutron Incineration in the Energy Amplifier as Alternative to Geologic Storage: The Case of Spain," European Organization for Nuclear Research, Report CERN/LHC/97-01 (EET), (1997).

Rütten H. J., Haas K. A., **"**Research on the incineration of plutonium in a modular HTR using thorium-based fuel"**,** *Nuclear Engineering and Design,* **195**, (3), Pages 353-360, February (2000a).

Rütten H.-J. et al., "Potential of Thorium-based Fuel Cycles to Constrain Plutonium and to Reduce the Long-lived Waste Toxicity", Final Report on the Coordinated Research Program, Reg. No. I3.30.08, (2000b). *In Press*

Saegusa A., "Geological Problems Drive up Cost of Nuclear Waste Dump in Japan", *Nature*, **398**, p. 357, April (1999).

Salvatores M., "The physics of transmutation in critical or subcritical reactors", *C. R. Physique 3*, 999–1012, (2002).

Salvatores M., *Private Communication* (2002).

Seitz F., "*The Modern Theory of Solids*", McGraw-Hill, New York, pp. 38-39 (1940).

Taiwo T. A., Kim T. K., Salvatores M., "Feasibility Study of a Proliferation Resistant Fuel Cycle for LWR-Based Transmutation of Transuranics", ANL-AAA-027, Argonne National Laboratory, September (2002).

Todosow M. et al., "LWR-Based Transmutation of Nuclear Waste an Evaluation of Feasibility of Light Water Reactor (LWR) Based Actinide Transmutation Concepts: Thorium-Based Fuel Cycle Options", BNL-AAA-2002-001, Brookhaven National Laboratory, October 14, (2002).

Todreas N.E., Kazimi M.S., "*Nuclear Systems I: Thermal Hydraulic Fundamentals*", Hemisphere Publishing Co., (1990).

Tommasi J., Puill A., Lee Y.K., "Reactors with Th/Pu Fuels", *Advanced Reactors with Innovative Fuels, Workshop Proceedings*, Villigen, Switzerland, 21-23 October, (1998).

Tong L.S., Weisman J., "*Thermal Analysis of Pressurized Water Reactors*", 3rd Edition, American Nuclear Society, La Grange Park, IL, USA, (1996).

US NRC, "Assumptions Used for Evaluating a Control Rod Ejection Accident for Pressurized Water Reactors", Regulatory Guide for Power Reactors 1.77, May (1974).

Van Tuyle G.J., "Candidate Approaches for an Integrated Nuclear Waste Management Strategy - Scoping Evaluations", Los Alamos National Laboratory, LA-UR-01-5572, November, (2001).

Ver Planck D. M., "TABLES-3 User's Manual", Studsvik/SOA-95/16, Studsvik of America, Inc., (1995).

Vergnes J., Lecarpentier D., "The AMSTER concept (Actinides Molten Salt TransmutER)", *Nuclear Engineering and Design*, **216**, 43–67, (2002).

Wade D.C., Chang Y.I., "The Integral Fast Reactor Concept: Physics of Operation and Safety", *Nuclear Science and Engineering*, **100**, pp. 507-524, (1988).

Wang D., "Optimization of a Seed and Blanket Thorium-Uranium Fuel Cycle for Pressurized Water Reactors", Ph.D. Thesis, Department of Nuclear Engineering, Massachusetts Institute of Technology, July (2003).

Westinghouse Electric Co., "Plutonium Disposition in Existing Pressurized Water Reactors", US DOE, DOE/SF/19683-6, June, (1994).

Wiese H.W., "Actinide Transmutation Properties of Thermal and Fast Fission Reactors Including Multiple Recycling", *Journal of Alloys and Compounds*, **271–273,** 522–529, (1998).

Wilson P.D., Ainsworht K.F., "Potential Advantages and Drawbacks of the Thorium Fuel Cycle in Relation to Current Practice: a BNFL View", IAEA-TECDOC-1319, Thorium Fuel Utilization: Options and Trends, Proceedings of three IAEA meetings held in Vienna in 1997, 1998 and 1999, IAEA, November, (2002).

Wolfram S., *The Mathematica Book*, 4th ed., Wolfram Media/Cambridge University Press, (1999).

Xu Z., Hejzlar P., Driscoll M.J., Kazimi M.S., "An Improved MCNP-ORIGEN Depletion Program (MCODE) and Its Verification for High burnup Applications," *Proc. of PHYSOR 2002*, Seoul, Korea, October 7-10, (2002).

Xu Zh., "Design Strategies for Optimizing High Burnup Fuel in Pressurized Water Reactors", Ph.D. Thesis, Department of Nuclear Engineering, Massachusetts Institute of Technology, December, (2003).

Yarsky P., "Neutronic Evaluation of GFR Breed and Burn Fuels", MIT-GFR-004, Massachusetts Institute of Technology, May (2003).

Yu K., M. J. Driscoll, Hejzlar P., "Neutronic Limits of Breed and Burn Fast Reactor Performance", *Trans. Am. Nucl. Soc.*, **86**, Hollywood, Fla., June 9–13, (2002).

Yuan Y., No H.C., Kazimi M.S., "A Preliminary Investigation of Performance of Rock-like Oxide Fuel for High Burnup in LWRs", MIT-NFC-TR-037, Massachusetts Institute of Technology, December (2001).

Zhang J., Bajorek S.M., Kemper R.M., Nissley M.E., Petkov N., Hochreiter L.E., "Application of the W6 COBRA: TRAC best-estimate methodology to the AP600 large-break LOCA analysis", *Nuclear Engineering and Design*, **186**, pp. 279–301, (1998).

Appendix A. Computational Tools

This chapter presents a concise summary of computational tools used for this thesis. The major areas of research in this thesis are evaluation of the feasibility of the neutronic and thermal hydraulic design of innovative PWR fuel cycles as well as evaluation of the impact of these fuel cycles on the repository, fuel cycle facilities and biological environment. Modern computer codes widely used by the nuclear industry, academic, and research institutions were adopted for the analysis of tasks identified by the scope of this thesis.

A.1. Neutronic Analysis

CMS

The Studsvik Core Management System (CMS) is a commercial computer code package developed for comprehensive neutronic analysis of PWR and BWR reactors. It is routinely used by utilities for fuel management calculations. The primary applications of the CMS code package include in-core fuel management and loading pattern optimization, evaluation of fuel cycle length, burnable poison design and requirements, various fuel and core licensing calculations e.g. reactivity coefficients and shutdown margin requirements. The CMS package consists of two-dimensional transport code CASMO-4 [Edenius M., et al., 1995] used to generate homogenized burnup dependent macroscopic cross-sections library which is subsequently used in two-group three-dimensional nodal diffusion code SIMULATE-3 for the whole core neutronic analysis. The link between the CASMO and SIMULATE is realized via the auxiliary utility code TABLES-3 which generates a binary macroscopic cross-sections library accessible to SIMULATE from the data generated by CASMO. The flow of CMS calculations is schematically presented in Figure A.1.1.

CASMO4 and CMS code were the primary computational tools used in this thesis for the neutronic analysis of various fuel designs and fuel cycle options.

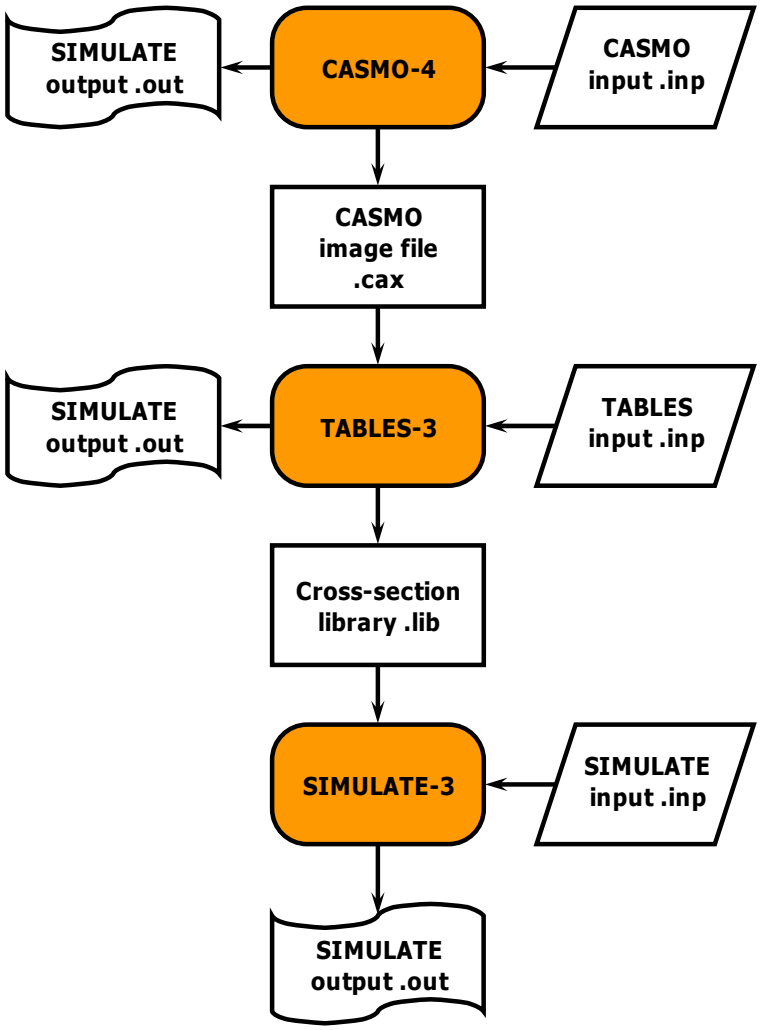

Figure A.1.1. CMS Calculations flow diagram

CASMO

CASMO-4 is a two-dimensional transport theory code used for burnup calculations of BWR and PWR fuel assemblies or simple fuel unit cells [Edenius M., et al., 1995]. It uses 70 energy groups cross-section library based on the ENDF/VI and JEF2-2 evaluated data files. The CASMO-4 code tracks the evolution of about 200 fission products and over 40 actinides ranging from Th232 to Cf252.

The code can handle generalized fuel assembly geometry with square or hexagonal pitch. Non symmetrical fuel assemblies with various burnable absorbers, control rod clusters, instrumentation channels, walls or water gaps can be modeled. Only cylindrical fuel rod geometry is allowed.

The CASMO calculation flow diagram is presented in Figure A.1.2. The effective absorption and fission cross-sections in a resonance energy region are calculated using resonance integrals obtained from equivalence theorem. The fuel lattice shadowing effect is accounted for through analytically calculated Dancoff factors.

The neutron energy spectrum is calculated by a collision probabilities method using prepared cross-sections. The spectrum is calculated for each individual fuel pin type, burnable absorber and water gap regions in the assembly. The spatial flux distribution and the eigenvalue are obtained from the two-dimensional transport theory calculation normally performed in a collapsed few energy group structure. In CASMO-4 version, the 2D Boltzmann transport equation is solved by the method of characteristics KRAM [Knott D., et al., 1995] in contrast to a more conventional collision probabilities method employed in earlier CASMO versions. The leakage effect is considered through adjustment of the results by performing the fundamental mode buckling calculation.

The burnup calculation is performed for each individual fuel pin and burnable absorber region. A predictor-corrector algorithm is used. In the predictor-corrector approach, the depletion is performed twice – using the spectrum at the beginning and at the end of the timestep. Average isotope number densities between these two calculations are then used as initial values for the subsequent burnup step.

The γ photon transport module calculates prompt and delayed γ sources and determines the γ detector responses.

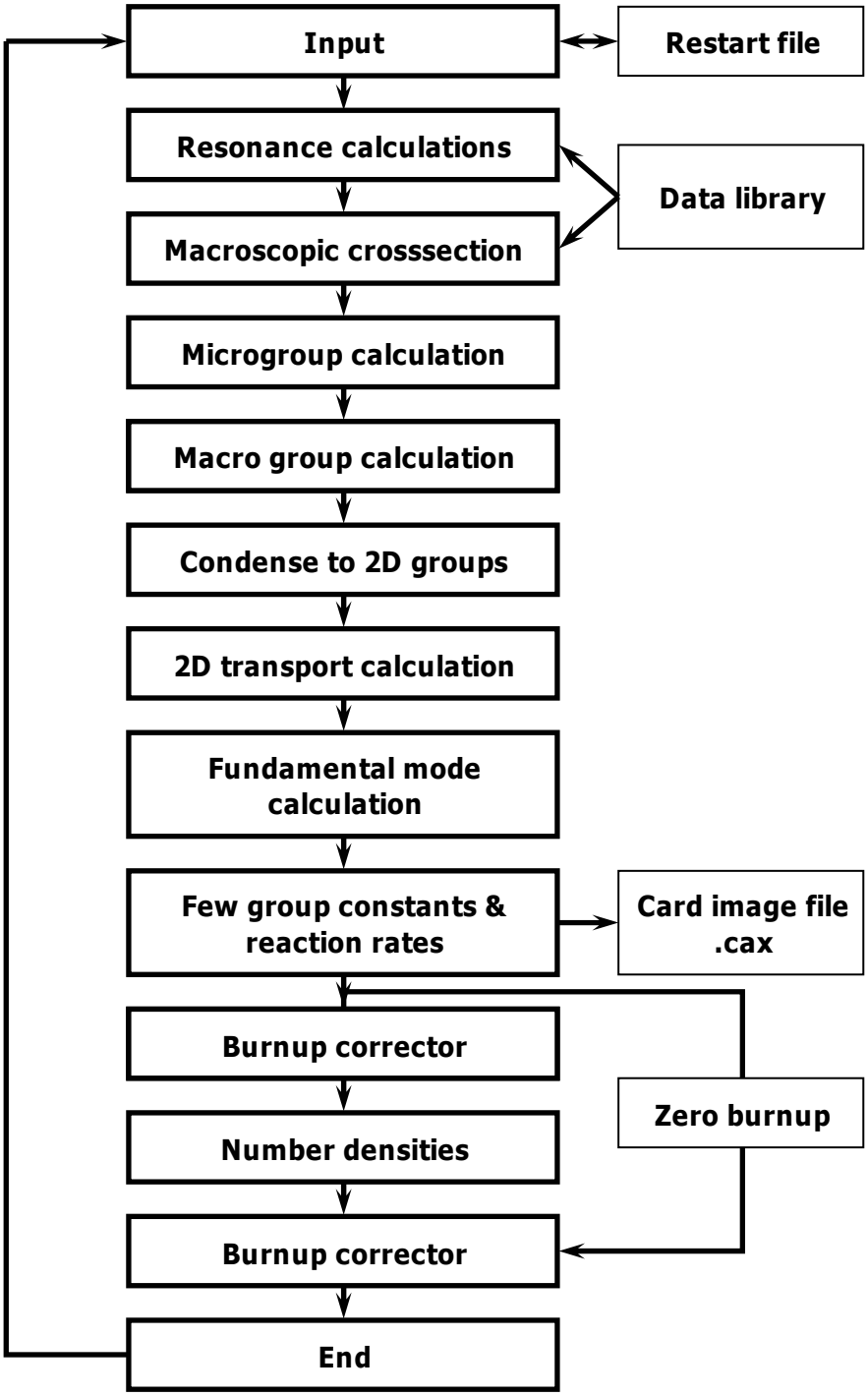

Figure A.1.2. CASMO Calculation flow diagram

TABLES

TABLES-3 code is used to generate a binary library of two-group burnup dependant multi dimensional cross-section tables for SIMULATE-3. In addition to cross-section data, discontinuity factors, fission product, detector, pin power reconstruction, kinetics, and isotopics data are processed by the TABLES code. TABLES can also be used to add or delete data from the SIMULATE library.

Each data type with exception of pin power reconstruction, kinetics, and isotopics data can be represented in the library as a function of up to three state variables defined by the user. The pin power reconstruction, kinetics, and isotopics data is expressed as a summation of one dimensional (in exposure) base table and additional one dimensional tables containing derivatives.

SIMULATE

SIMULATE-3 is three-dimensional two-group nodal diffusion code used for the licensing level whole core neutronic analysis of LWRs [DiGiovine A. S., et al., 1995]. It can perform calculations for fuel shuffling and reloading in 2 or 3 dimensions and in various core symmetries. Other uses of the code include reactivity coefficient calculations, control rod worth, shutdown margin, and dropped or ejected rod worth calculations as well as xenon transients and the core follow support for plant operations.

The code employs QPANDA neutronic calculation model with fourth order polynomial representation of intranodal flux distributions in two energy groups [Cronin J. T., et al., 1995]. Additional module provides pin power reconstruction capabilities.

Thermal hydraulic module provides fuel and coolant temperature values in each node for the reactivity feedback calculation. The node average fuel temperature is modeled by second degree polynomial with respect to nodal power with coefficients defined by the user. The linear term in the polynomial can also be a function of any two state variables (e.g. exposure, coolant

temperature, or boron concentration). The thermal hydraulic model assumes no flow communication between assembly channels and the inlet flow distribution is defined by the user.

MCNP

MCNP [Briesmeister J.F., 2000] is a general purpose Monte Carlo particles transport code developed at Los Alamos National Laboratory. It can be used in neutron, photon or electron transport mode as well as in a mode which is any combination of the above three. In the Monte Carlo approach, unlike in deterministic methods, the particles transport problem is solved by following the histories of individual particles. The average particle characteristics in the physical system are determined by average behavior of simulated particles. The major advantage of Monte Carlo method is its capabilities of solving a particle transport problem in complex generalized 3-D geometries which cannot be practically handled by deterministic methods. In principle, Monte Carlo simulation can yield the exact transport equation solution provided that physical models, nuclear data, and number of particle histories are sufficient. The major drawback of the Monte Carlo is considerably higher computation power requirements to achieve high accuracy of the results.

MNCP provides great flexibility in definition of particles source distributions, system geometries and tallied parameters. The energy deposition tally allows calculation of spatial power distribution in the modeled system. Dose rates can be calculated through surface flux or point detector tallies with provided flux-to-dose conversion factors. Calculation of k_{eff} eigenvalue is also a standard feature of MCNP.

ORIGEN

ORIGEN2 [Croff A.G., 1980] is a point depletion and radioactive decay computer code developed at Oak Ridge National Laboratory. It is used for the analysis of isotopic composition and characteristics of materials contained in the nuclear fuel (radiotoxicity, decay heat power, photon and neutron emission etc.). ORIGEN has a fairly complete representation of isotopes. It follows the evolution of some 1700 nuclides including 130 actinides, 850 fission products and

720 activation products. One group cross-sections are used for the burnup calculations. The cross-sections are obtained from the specified libraries compiled for various reactor types. The cross-sections for individual nuclides in the existing libraries can be substituted with those provided by the user. The matrix exponential method is used for solving the system of burnup and decay differential equations [Croff A.G., 1983]. Additional features of the ORIGEN code include power or flux normalization for the depletion calculations and possibility of modeling of continuous materials feed or removal.

MCODE

MCNP-ORIGEN Depletion program (MCODE) [Xu Z., et al., 2002] was developed at MIT to take advantage of MCNP capabilities to analyze generalized geometry systems and complete isotopics representation in ORIGEN2 depletion calculations for the analysis of various reactor systems. MCODE provides data exchange interface between MCNP and ORIGEN2. The MCNP is used to generate fluxes and one-group reaction rates for the most neutronically important nuclides in each burnup region defined by the user. The fluxes and reaction rates from MCNP are processed by the MCODE to update the ORIGEN2 libraries. The depletion is then performed by the ORIGEN using appropriate one-group cross-sections for the system analyzed which eliminates ambiguity of the results associated with the use of standard ORIGEN cross-section libraries.

MCODE offers greatly simplified user interface, extensive and flexible output processor, and optional predictor-corrector algorithm depletion. In this thesis, the MCODE was mainly used for benchmarking and verification of the results obtained with CASMO4 and SIMULATE3 computer codes.

A.2. Thermal Hydraulic Analysis

VIPRE

VIPRE-01 (Versatile Internals and Component Program for Reactors; EPRI) code is widely used for thermal hydraulic analysis of LWRs [Cuta J.M., et al., 1985]. The code is used for evaluation of various reactor core safety limits such as Minimum Departure from Nucleate Boiling Ratio (MDNBR), Critical Power Ratio (CPR), fuel and cladding temperatures under normal operating conditions and in assumed accidents.

The code solves finite difference equations for conservation of mass, energy, and momentum to predict three-dimensional velocity, pressure, and thermal energy fields as well as fuel temperatures for single and two-phase flow in PWR and BWR type cores. The equations are solved for an interconnected array of channels assuming incompressible thermally expandable homogeneous flow. No restrictions for stability are imposed on the time step or channel size. The code includes non-mechanistic models for sub-cooled boiling and vapor-liquid slip in two-phase flow despite general homogeneous formulation.

The core geometry modeling is very general and provides a great deal of flexibility as the code uses sub-channel analysis modeling structure. The modeled region is represented by an array of adjacent sub-channels with lateral communication. Sub-channels in a fuel rods array can be represented individually or can be lumped to larger regions. The shape and size of the channels as well as their interconnection are effectively arbitrary.

In this thesis, the VIPRE-01 computer code was used for the evaluation of MDNBR safety margins of innovative PWR fuel designs suggested for the analysis by the neutrinc feasibility studies.

Appendix B. Double-Heterogeneous Effect Evaluation and Codes Benchmarking

Evolution of Selected Actinides Number Densities with Burnup

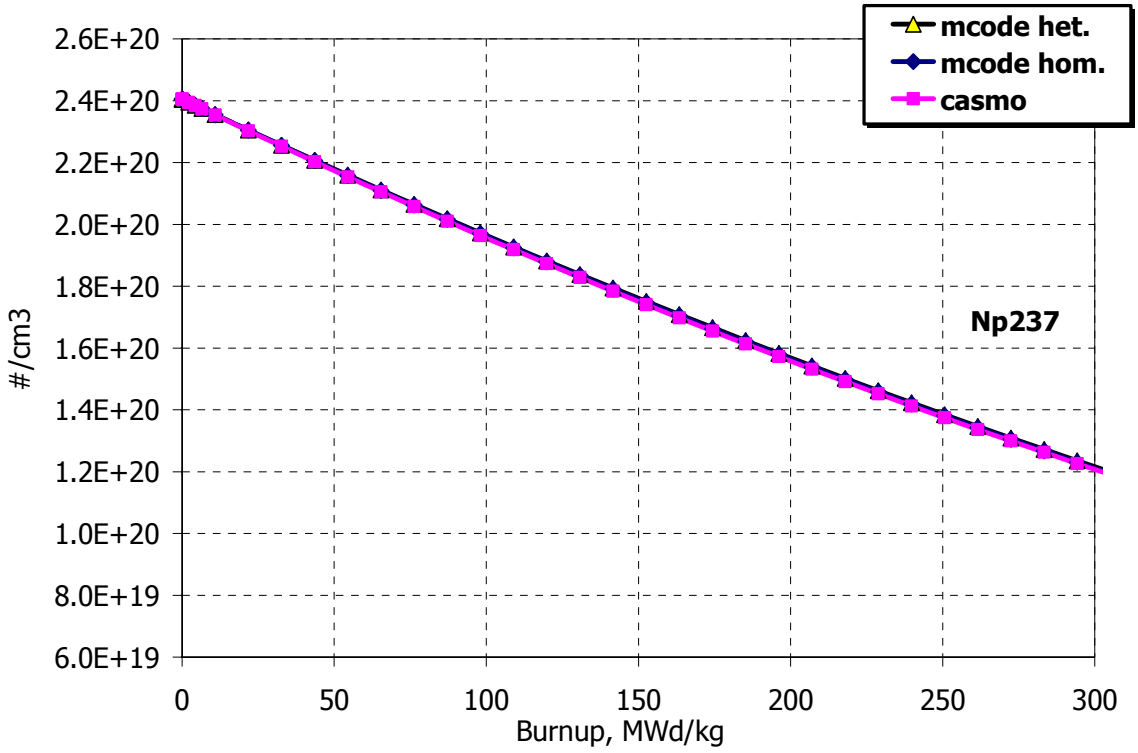

Figure B.1. Np237 Number Density vs. Burnup

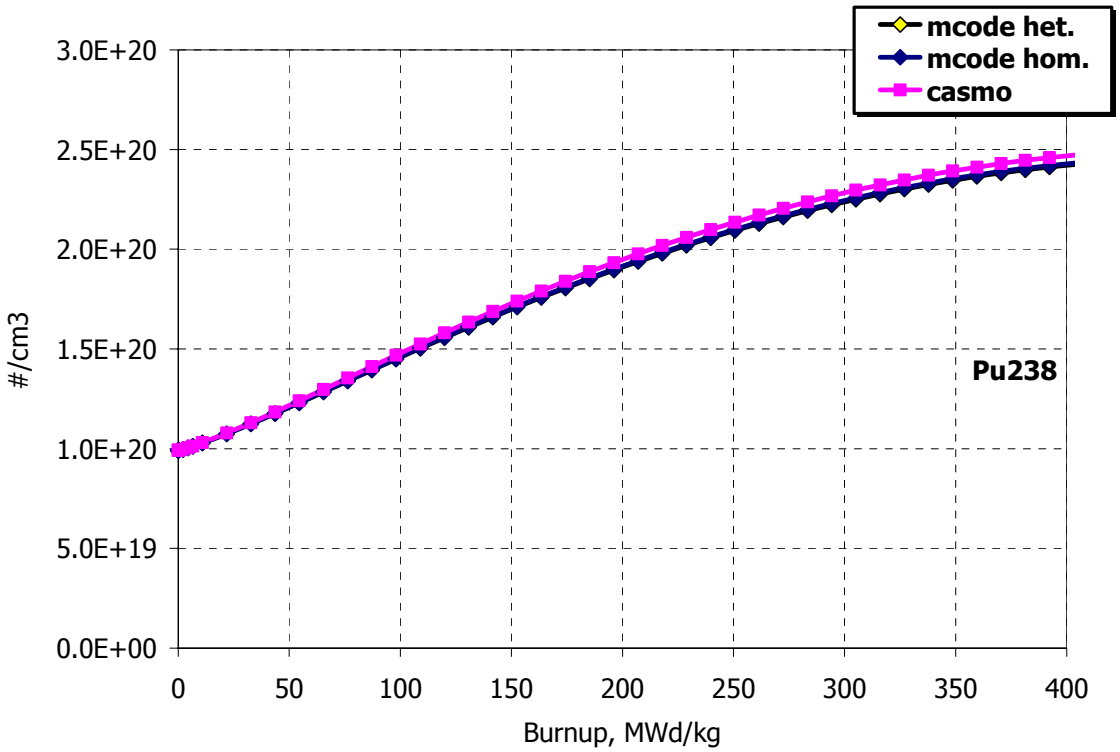

Figure B.2. Pu238 Number Density vs. Burnup

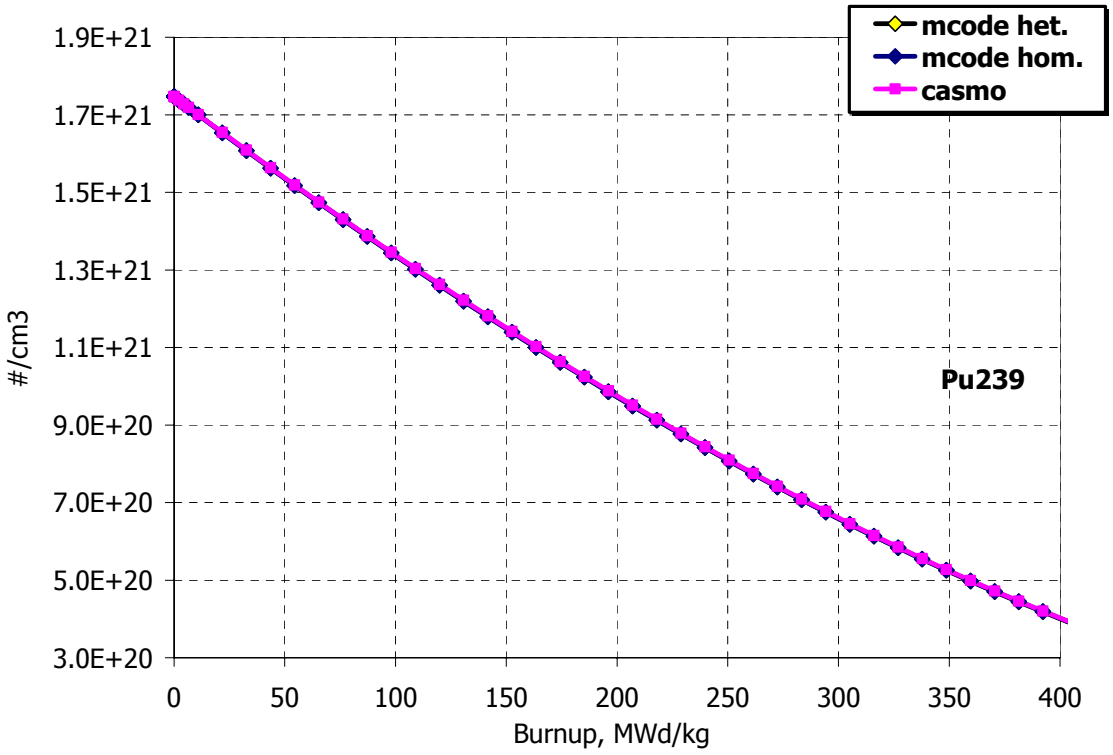

Figure B.3. Pu239 Number Density vs. Burnup

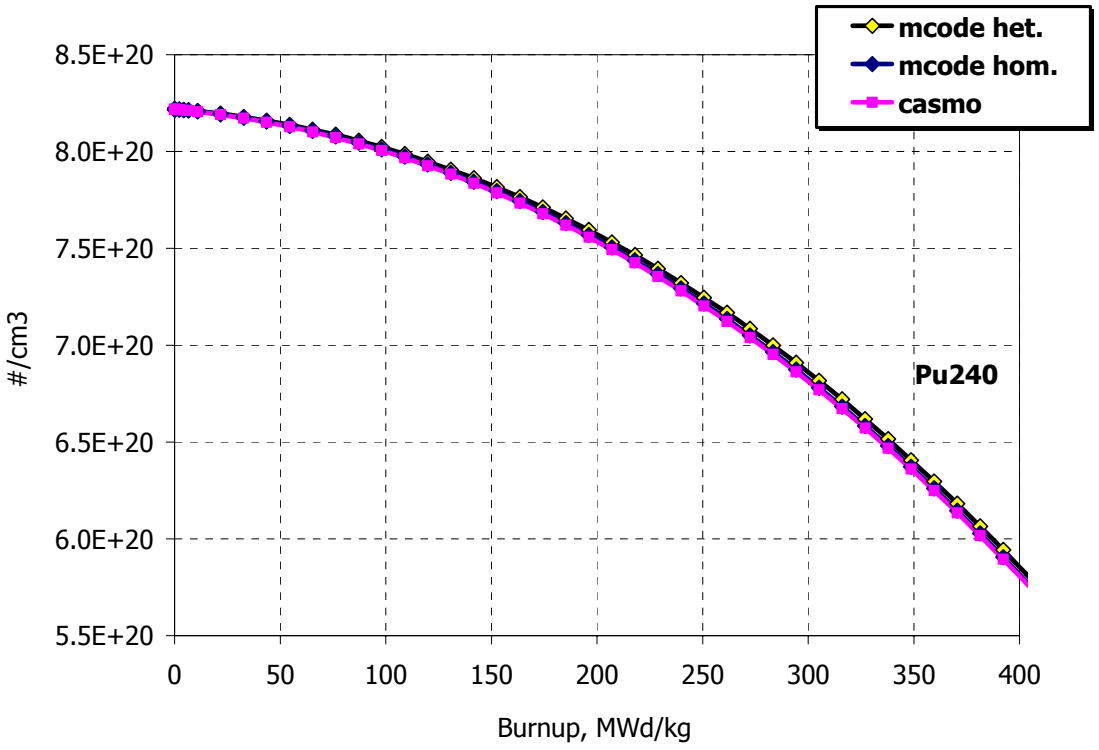

Figure B.4. Pu240 Number Density vs. Burnup

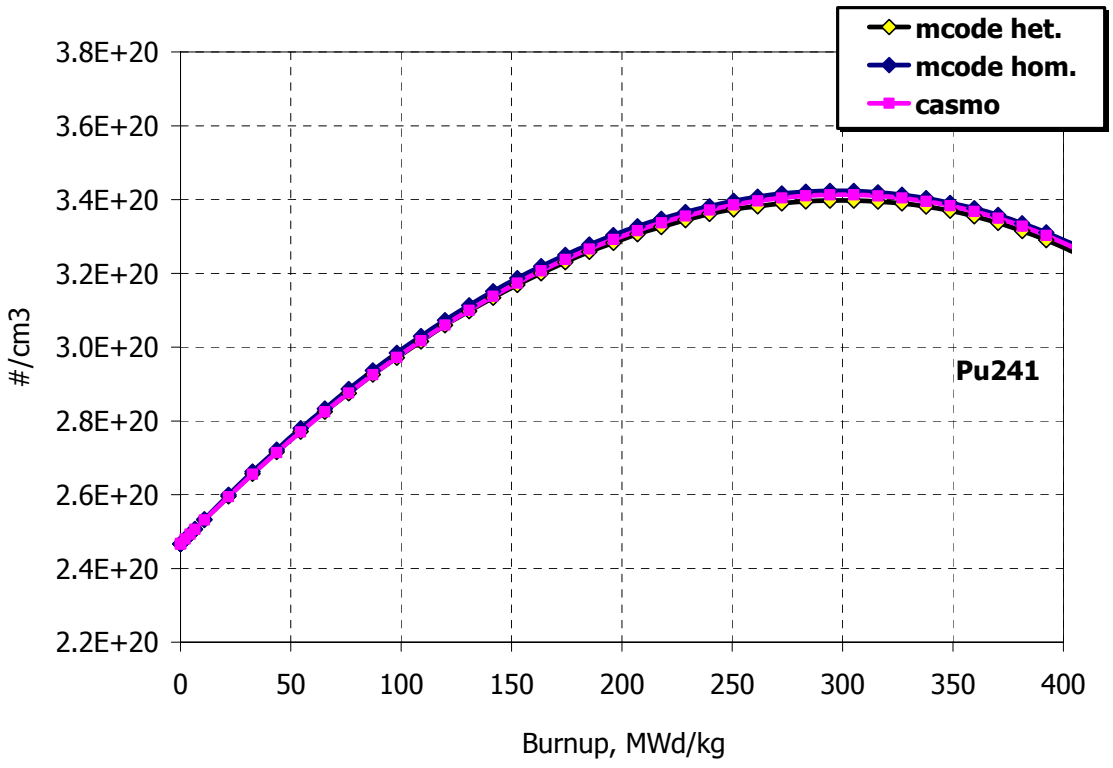

Figure B.5. Pu241 Number Density vs. Burnup

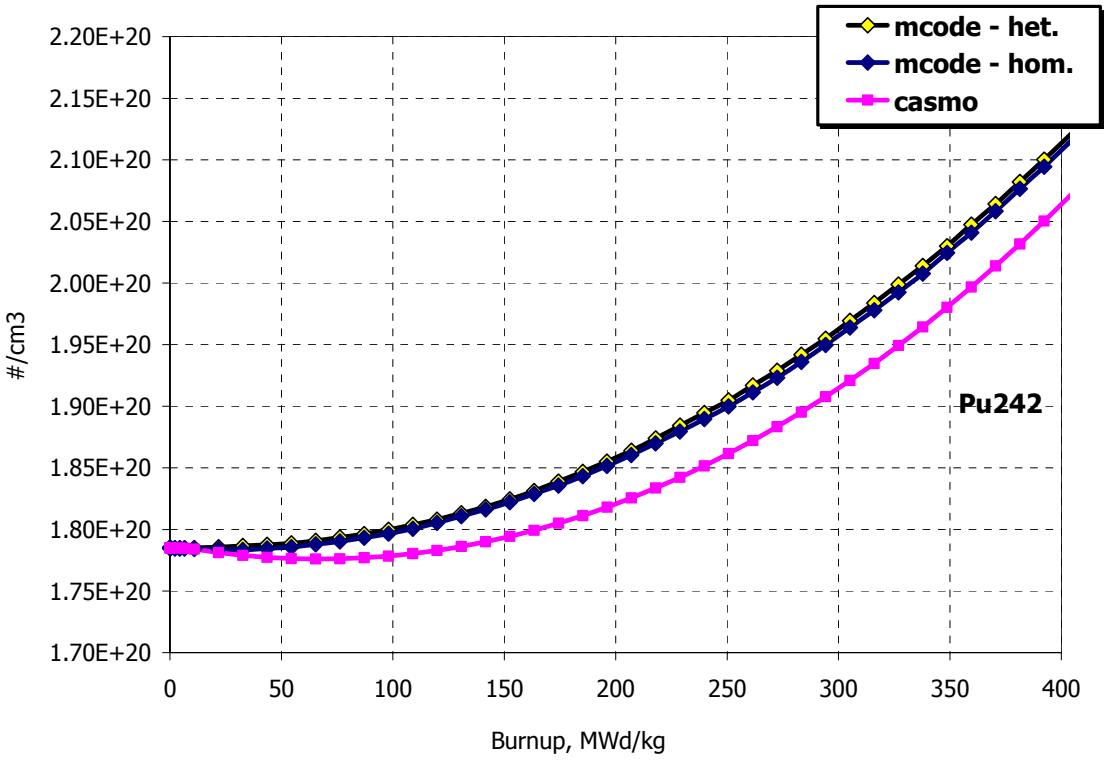

Figure B.6. Pu242 Number Density vs. Burnup

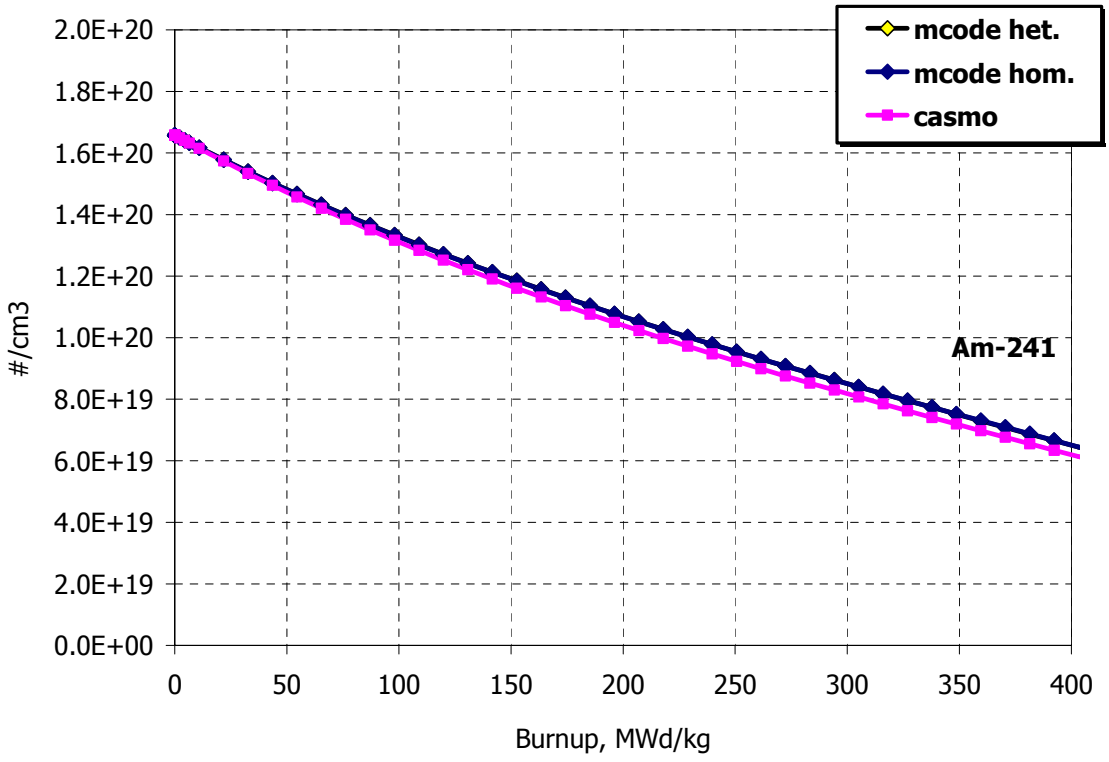

Figure B.7. Am241 Number Density vs. Burnup

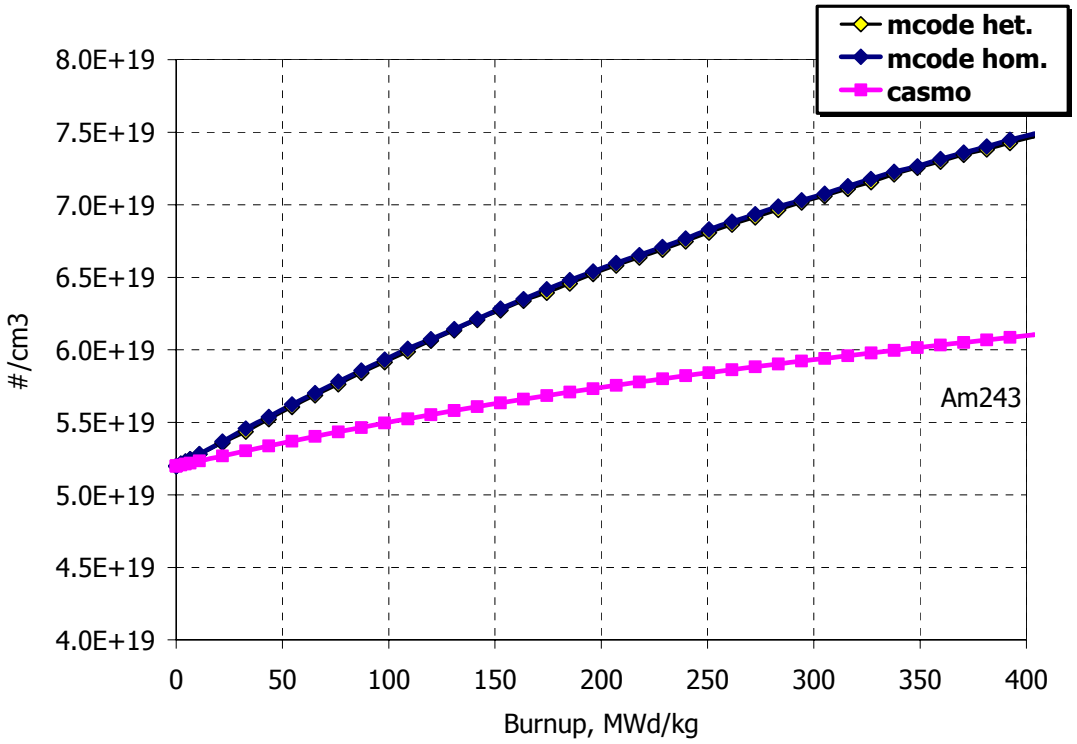

Figure B.8. Am243 Number Density vs. Burnup

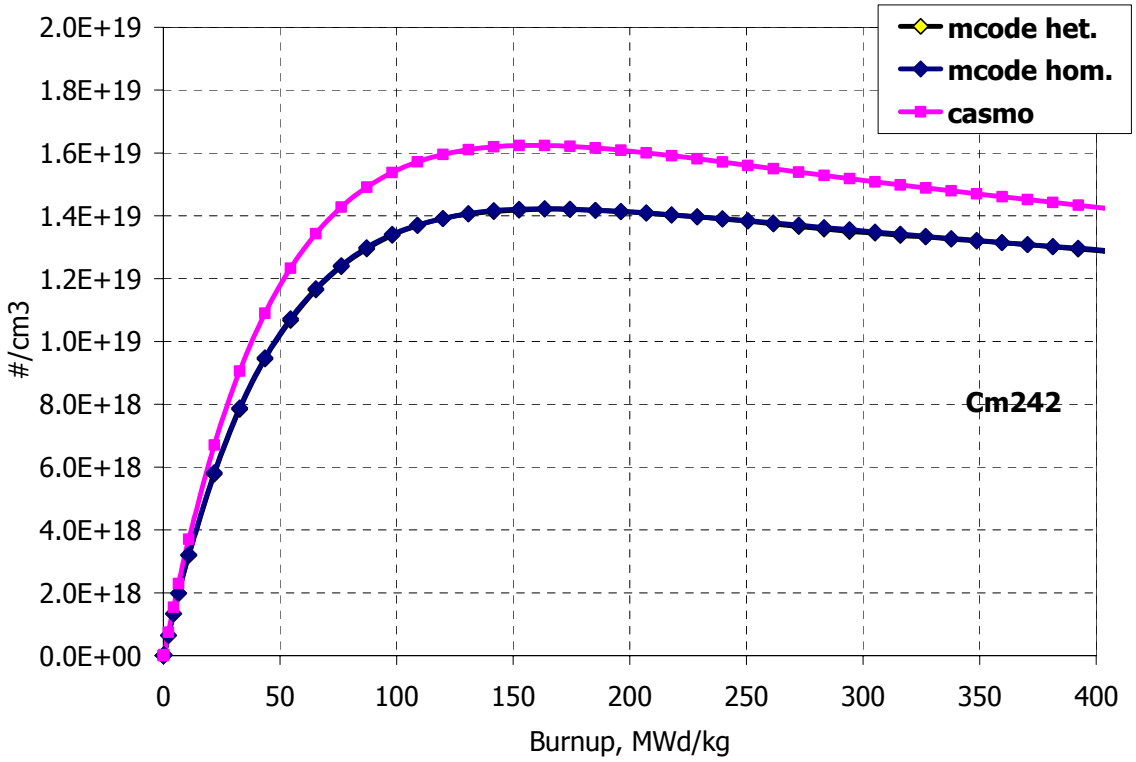

Figure B.9. Cm242 Number Density vs. Burnup

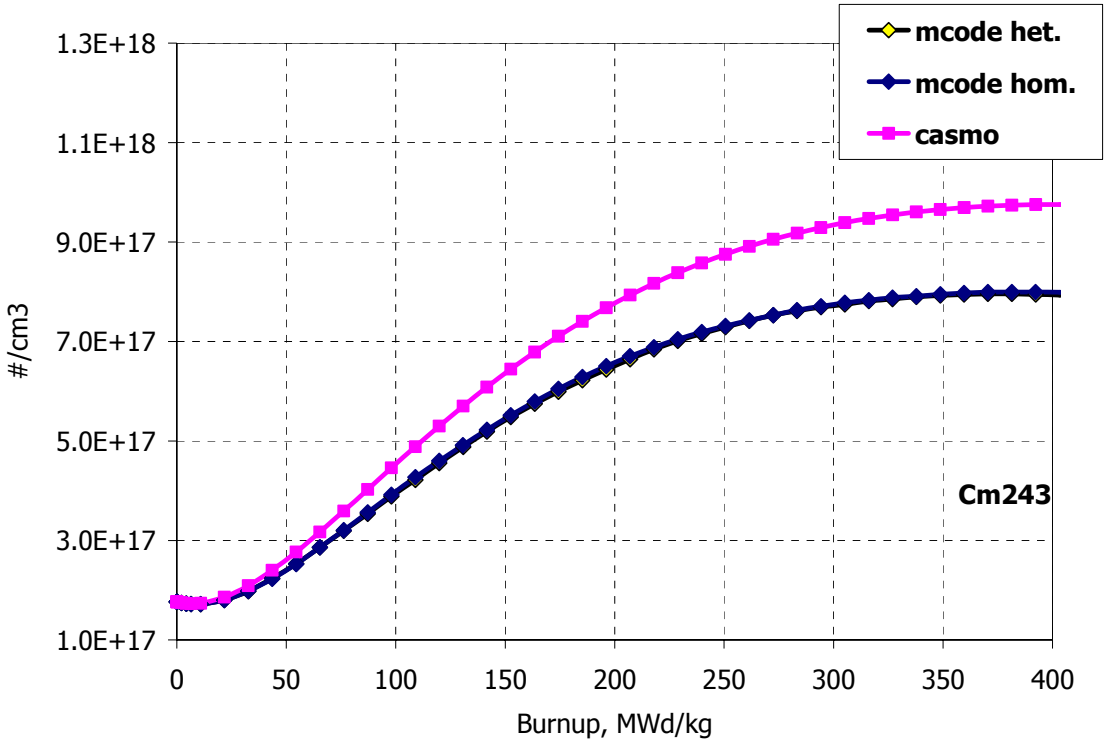

Figure B.10. Cm243 Number Density vs. Burnup

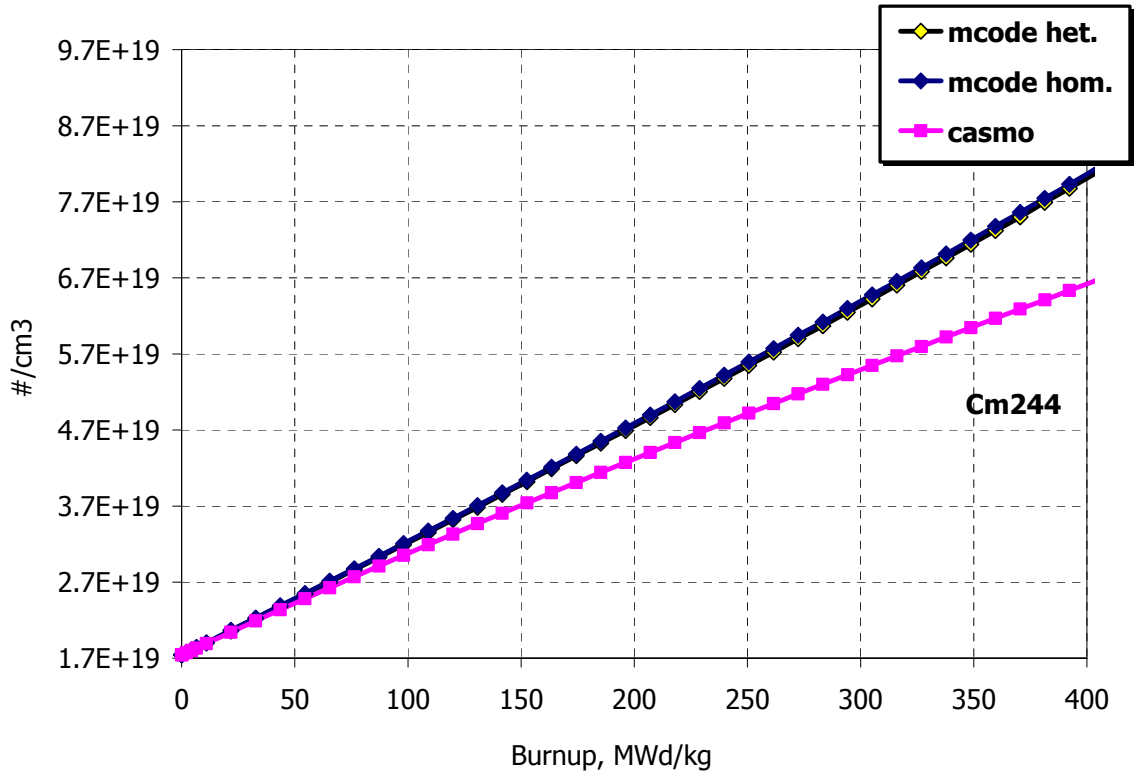

Figure B.11. Cm244 Number Density vs. Burnup

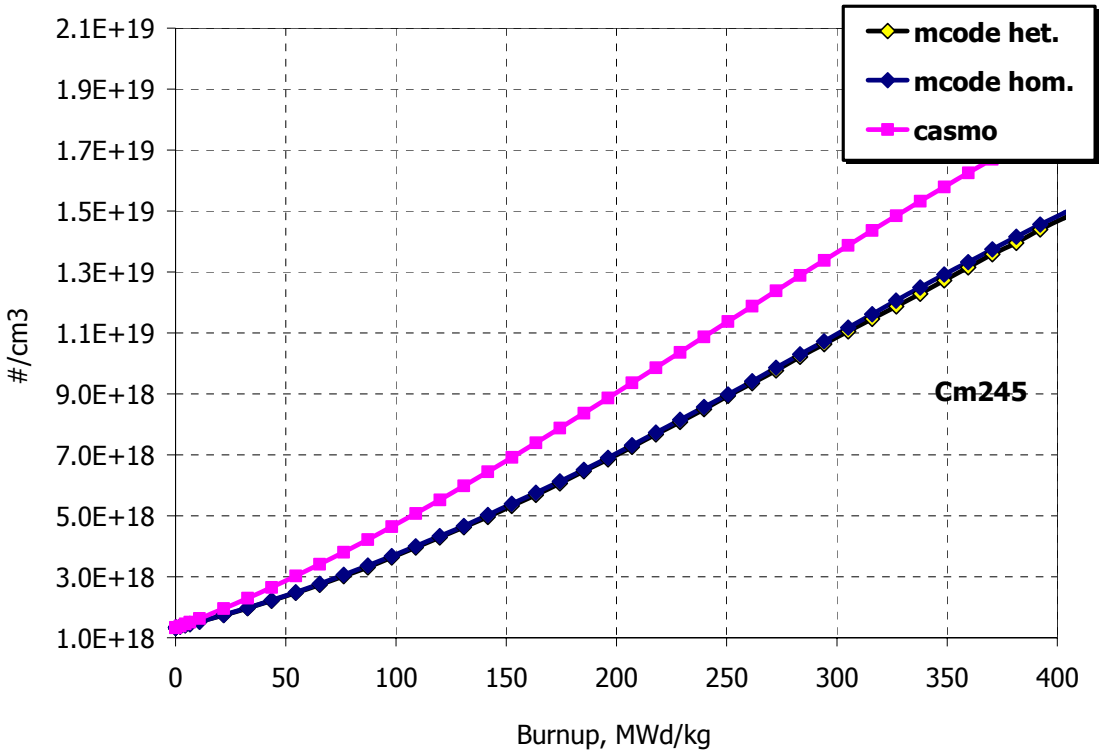

Figure B.12. Cm245 Number Density vs. Burnup

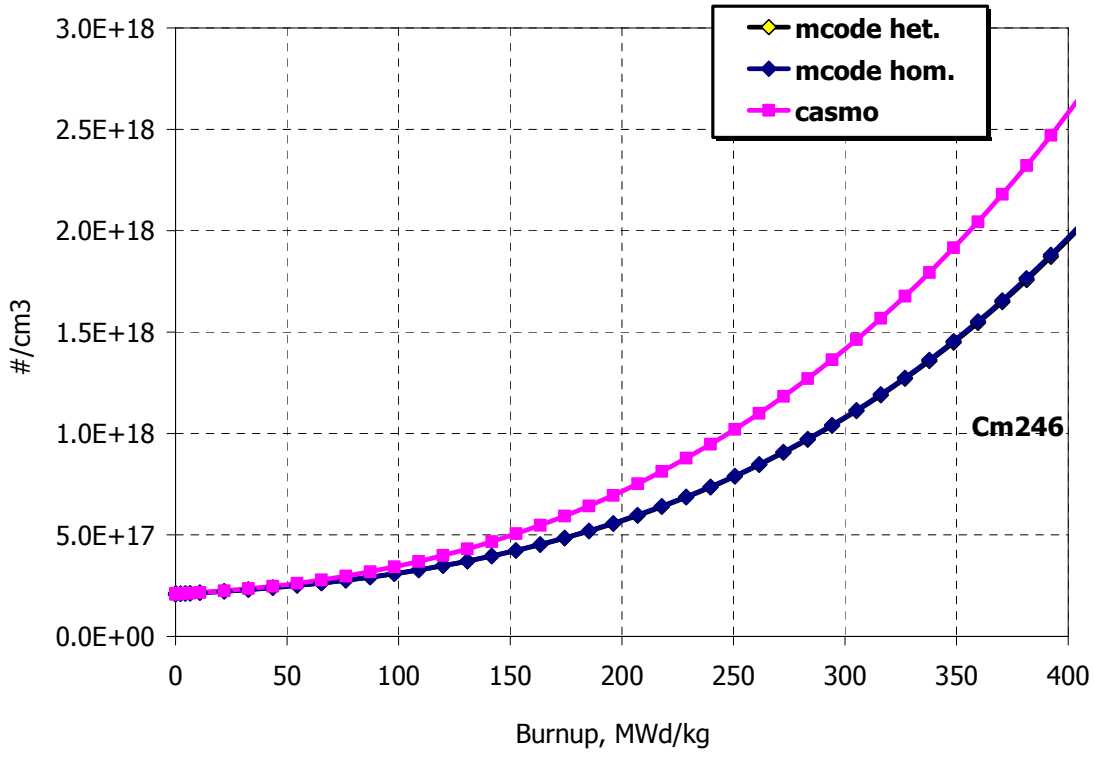

Figure B.13. Cm246 Number Density vs. Burnup

Appendix C. Loading maps for 3-Dimensional core analysis

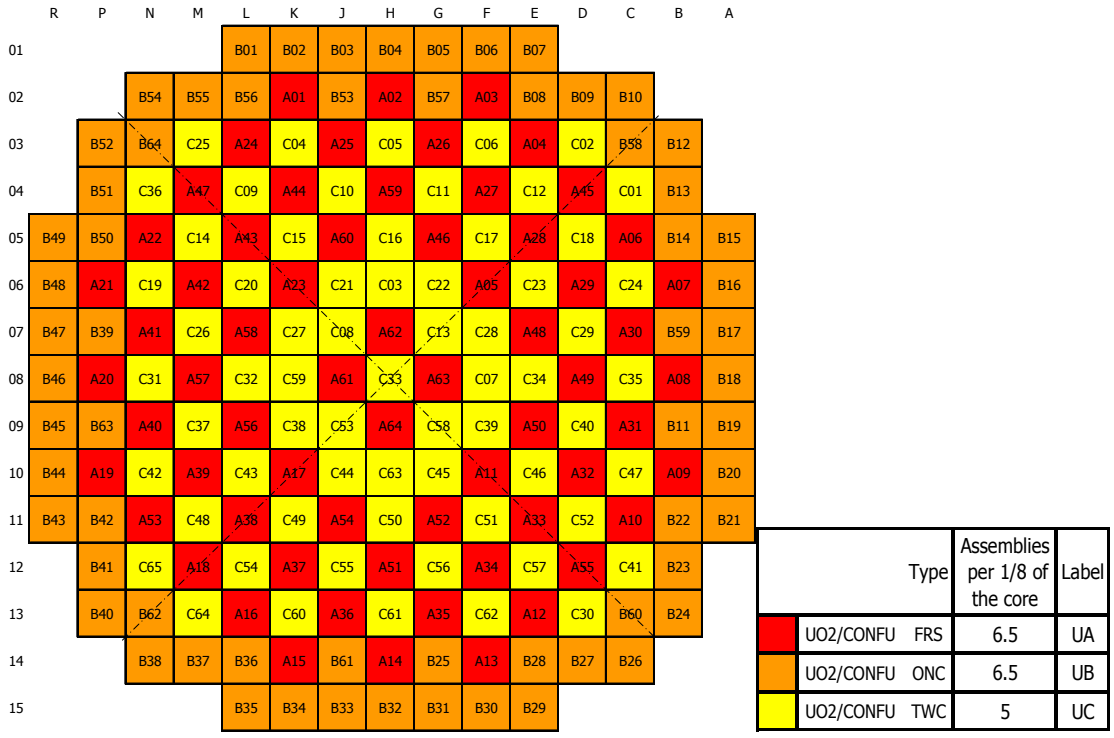

Type	Assemblies per 1/8 of the core	Label
UO2/CONFU FRS	6.5	UA
UO2/CONFU ONC	6.5	UB
UO2/CONFU TWC	5	UC

Figure C.1. Core loading map: Cases 1,3,4

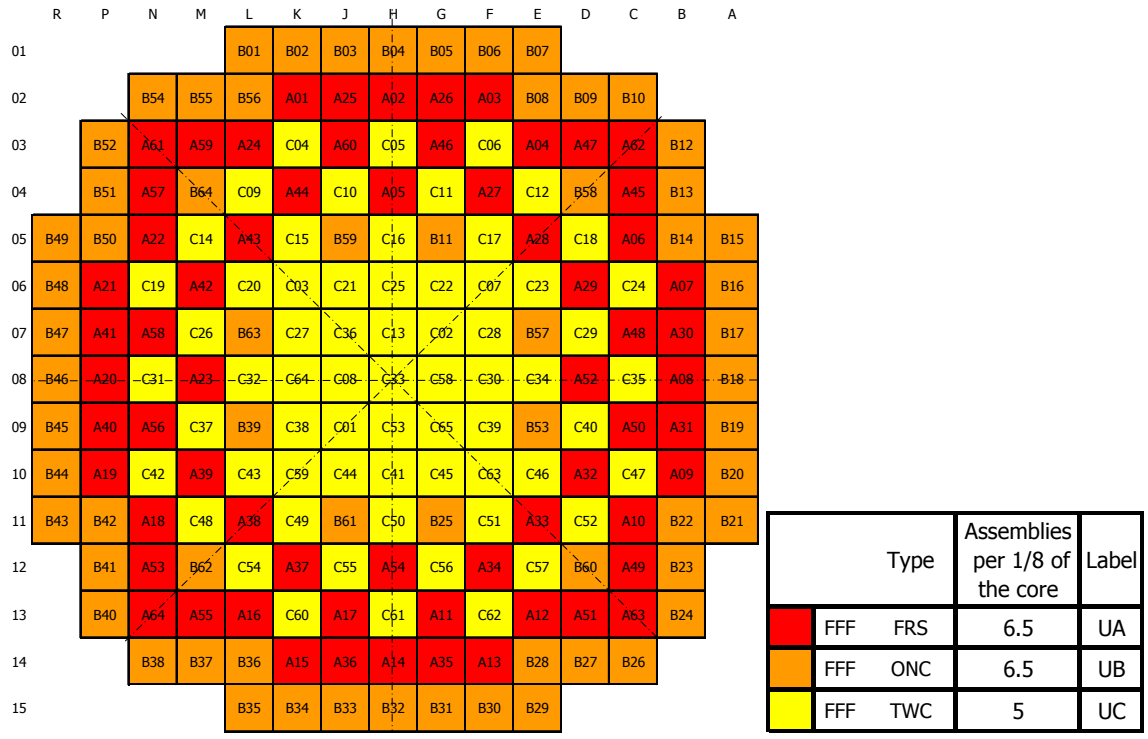

	Type		Assemblies per 1/8 of the core	Label
	FFF	FRS	6.5	UA
	FFF	ONC	6.5	UB
	FFF	TWC	5	UC

Figure C.2. Core loading map: Case 2

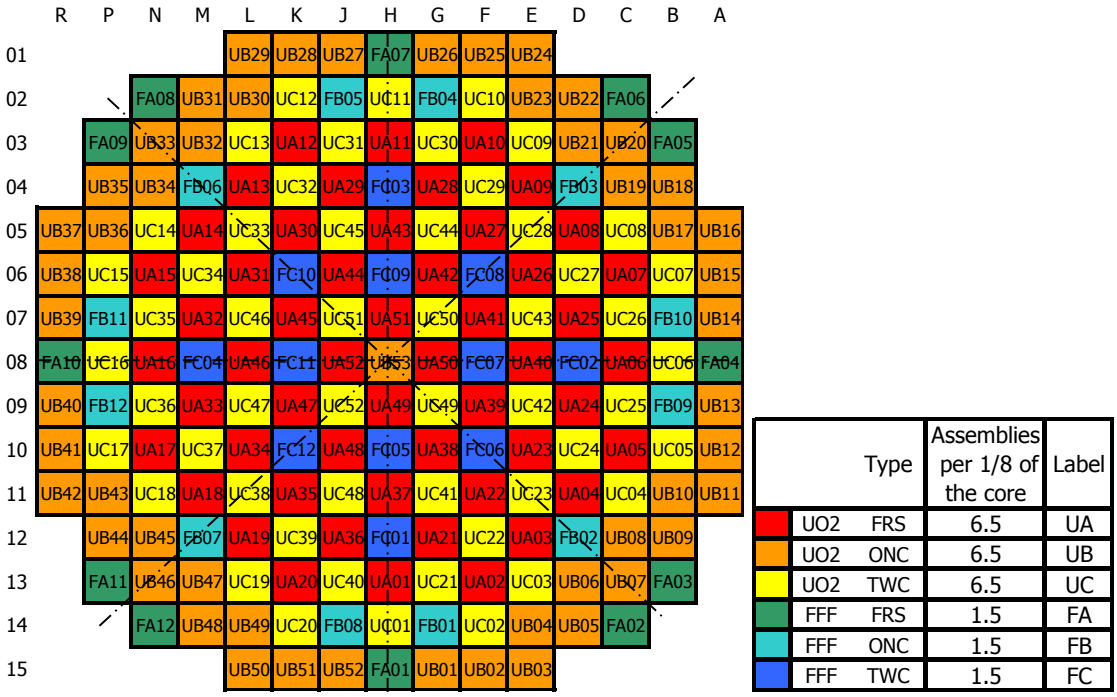

	Type		Assemblies per 1/8 of the core	Label
	UO2	FRS	6.5	UA
	UO2	ONC	6.5	UB
	UO2	TWC	6.5	UC
	FFF	FRS	1.5	FA
	FFF	ONC	1.5	FB
	FFF	TWC	1.5	FC

Figure C.3. Core loading map: Cases 5 and 6

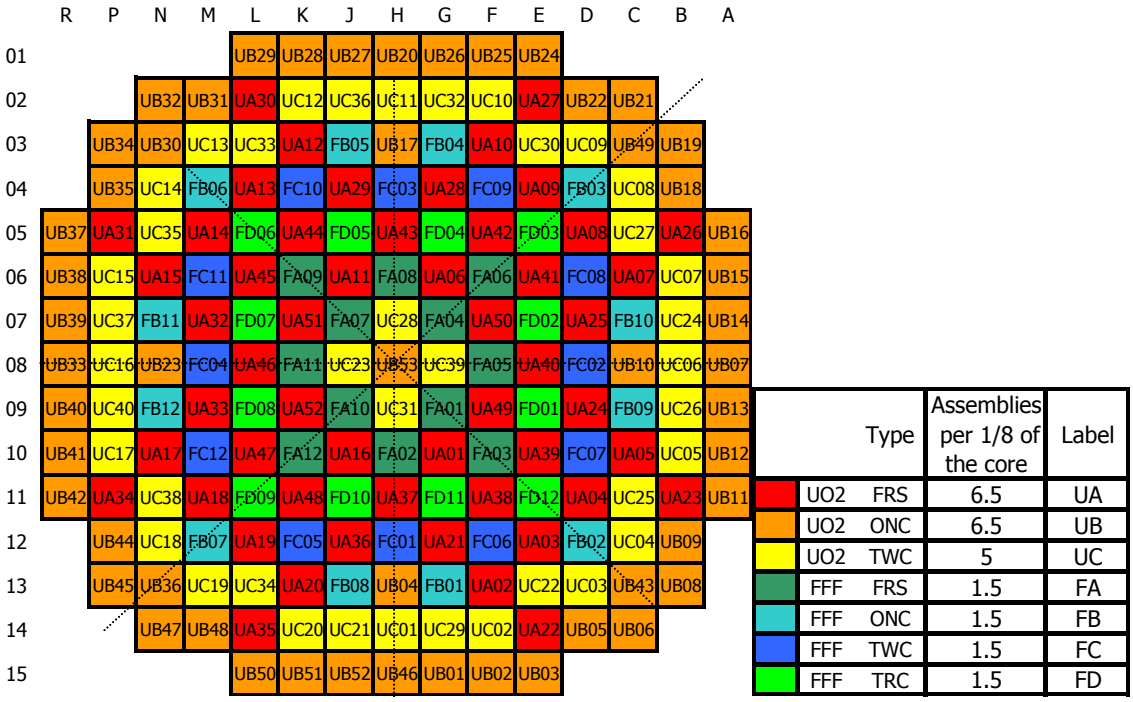

Type		Assemblies per 1/8 of the core	Label
UO2	FRS	6.5	UA
UO2	ONC	6.5	UB
UO2	TWC	5	UC
FFF	FRS	1.5	FA
FFF	ONC	1.5	FB
FFF	TWC	1.5	FC
FFF	TRC	1.5	FD

Figure C.4. Core loading map: Case 7

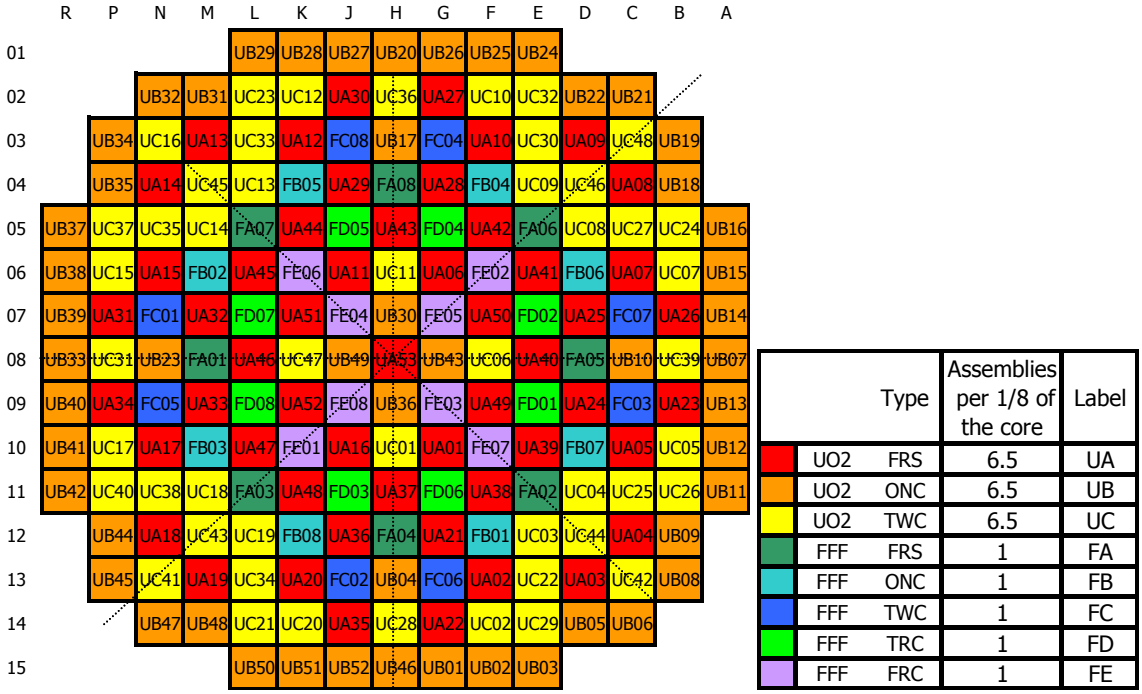

Type		Assemblies per 1/8 of the core	Label
UO2	FRS	6.5	UA
UO2	ONC	6.5	UB
UO2	TWC	6.5	UC
FFF	FRS	1	FA
FFF	ONC	1	FB
FFF	TWC	1	FC
FFF	TRC	1	FD
FFF	FRC	1	FE

Figure C.5. Core loading map: Case 8